Biochemistry of Human RecQ DNA Helicases and their Role in DNA Repair

Dissertation

zur

Erlangung der naturwissenschaftlichen Doktorwürde

(Dr. sc. nat.)

vorgelegt der

Mathematisch-naturwissenschaftlichen Fakultät

der

Universität Zürich

von

Kanagaraj Radhakrishnan

aus

Indien

Promotionskomitee

Prof. Dr. Josef Jiricny (vorsitz)

Prof. Dr. Ulrich Hübscher

Prof. Dr. Primo Schär

Dr. Pavel Janscak (Leitung der Dissertation)

Zürich, 2008

The End of Knowledge is Wisdom
The End of Culture is Perfection
The End of Wisdom is Freedom
The End of Education is Character

- BABA

Table of contents

1. Summary…… 7
2. Zusammenfassung…… 11
3. Introduction…….. 16
   3.1. Maintenance of genomic stability and cancer…… 16
   3.2. DNA damage and DNA repair Pathways…… 19
      3.2.1. Types of DNA damage…… 19
      3.2.2. DNA repair pathways…… 21
         3.2.2.1. Direct Reversal…… 21
         3.2.2.2. Base Excision Repair…… 23
         3.2.2.3. Nucleotide Excision Repair…….. 24
         3.2.2.4. Mismatch Repair…… 26
         3.2.2.5. Homologous Recombination…… 28
         3.2.2.6. Non-Homologous End Joining…….. 30
   3.3. Helicases……..... 32
      3.3.1. Classification……... 32
      3.3.2. Helicase motifs…… 33
      3.3.3. Mechanisms of nucleic acid translocation and unwinding by SF1 and SF2 helicases…… 35
      3.3.4. Helicase functions…… 38
   3.4. RecQ family of DNA helicases…….. 41
      3.4.1. Introduction…… 41
      3.4.2. The *Escherichia coli* RecQ…….. 45
         3.4.2.1. Domain organization and Structure…… 45
         3.4.2.2. Biochemical properties…… 47
         3.4.2.3. Cellular functions……... 48
      3.4.3. The yeast Sgs1…… 51
         3.4.3.1. Discovery…… 51
         3.4.3.2. Cellular pheotypes of Sgs1 deficiency……... 51
         3.4.3.3. Biochemical properties…… 51
         3.4.3.4. Interaction partners and cellular roles…… 52
      3.4.4. RECQ1……... 54
         3.4.4.1. *RECQ1* gene and phenotypic consequences of its dysfunction…… 54
         3.4.4.2. Biochemical properties…… 54
         3.4.4.3. Interaction partners and cellular roles…… 55
      3.4.5. The Bloom syndrome helicase…… 57
         3.4.5.1. Bloom syndrome…… 57
         3.4.5.2. Cellular phenotypes of BLM deficiency…….. 57

3.4.5.3. Biochemical properties…….. 58
3.4.5.4. Interaction partners and cellular roles…… 59
3.4.6. The Werner syndrome helicase……. 62
3.4.6.1. Werner syndrome…… 62
3.4.6.2. Cellular phenotypes of WRN deficiency…… 62
3.4.6.3. Domain structure…….. 63
3.4.6.4. Biochemical properties…… 63
3.4.6.5. Interacting partners and cellular roles…….. 64
3.4.7. RECQ4……. 66
3.4.7.1. RECQ4 and genetic diseases…… 66
3.4.7.2. Cellular phenotypes of RECQ4 deficiency…….. 67
3.4.7.3. Domain structure…… 68
3.4.7.4. Biochemical properties…….. 68
3.4.7.5. Interaction partners and cellular roles…….. 68
3.4.8. RECQ5……. 71
3.4.8.1. Cloning…….. 71
3.4.8.2. Cellular phenotypes of RECQ5 deficiency…….. 71
3.4.8.3. Domain structure…….. 72
3.4.8.4. Biochemical properties…… 72
3.4.8.5. Interaction partners and cellular roles…….. 74
4. Results…… 77
5. Conclusion and Future Perspectives…….. 86
6. References……..…. 94
7. Appendix……. 120
7.1. Appendix I: “Human RECQ5β helicase promotes strand exchange on synthetic DNA structures resembling a stalled replication fork”…….. 121
7.2. Appendix II: “The zinc-binding motif of human RECQ5β suppresses the intrinsic strand-annealing activity of its DExH helicase domain and is essential for the helicase activity of the enzyme”…….... 146
7.3. Appendix III: “The MRE11/RAD50/NBS1 complex links RECQ5 helicase to sites of DNA damage”……..... 158
7.4. Appendix IV: “Physical and functional interactions between Werner syndrome helicase and mismatch-repair initiation factors”…… 186
8. Acknowledgements……. 203
9. *Curriculum Vitae*…….. 206
10. List of publications……... 208
11. Abstracts presented in scientific meetings……... 210

1. Summary

Proteins belonging to the RecQ DNA helicase family are highly conserved from bacteria to man and are implicated in removing aberrant DNA structures arising during DNA replication and repair to prevent inappropriate DNA recombination events. While *E.coli* and yeast have only one RecQ-type helicase, humans have five of these named RECQ1, BLM, WRN, RECQ4 and RECQ5. Inherited defects in the genes encoding for BLM, WRN and RECQ4 have been found to give rise to Bloom's, Werner's and Rothmund-Thomson syndrome, respectively. These severe recessive disorders are associated with genomic instability, cancer predisposition and premature aging. Association of inherited defects in the *RECQ1* and *RECQ5* genes with human disease has not been reported. However, knockout studies in chicken DT40 cells and in mice suggested that these genes function as tumor suppressors through enforcing chromosomal stability. A numerous biochemical and cellular studies indicated that the multiple RecQ homologues in human cells have non-redundant biological roles. However, the exact DNA transactions mediated by these proteins remain elusive.

The goal of this thesis was to advance our understanding of the cellular functions of RECQ5 and WRN helicases. In the first project (**Kanagaraj *et al.*, 2006)**, we explored the possible role for RECQ5 in replication fork management. Earlier biochemical studies from our group have shown that RECQ5 functions as a 3'-5' DNA helicase and it has also an ability to promote DNA strand annealing. We analyzed the action of RECQ5 on various synthetic forked DNA structures containing either heterologous or homologous arms. We found that the mode of action of RECQ5 helicase on these structures was different as compared to other human RecQ helicases. For example, we found that on forked structures with heterologous arms, RECQ5 showed preference for unwinding of the lagging-strand arm, whereas BLM and WRN helicases displayed a strong preference for unwinding of the parental arm. We also showed that RECQ5 promoted strand exchange between homologous arms of a synthetic forked DNA structure in a reaction dependent on ATP hydrolysis and that human replication protein A (hRPA) stimulated this reaction. Further, we identified a domain located in the non-conserved C-terminal portion of RECQ5 (a region spanning amino acids 561-651) as being important for its ability to unwind the lagging-strand arm of the fork and to promote strand

exchange on hRPA-coated forked structures. Our cellular studies revealed that RECQ5 was associated with the DNA replication factories in S phase nuclei and persisted at the sites of stalled replication forks after exposure of cells to UV irradiation and cisplatin. Moreover, RECQ5 was found to physically interact with the polymerase processivity factor proliferating cell nuclear antigen *in vitro* and *in vivo*. Taken together, our findings suggested that RECQ5 might be involved in the reactivation of stalled replication forks.

In contrast to the other human RecQ homologues, RECQ5 exists in at least three different isoforms (named RECQ5α, RECQ5β and RECQ5γ) that result from alternative mRNA splicing. Although the RECQ5β isoform has been biochemically well characterized, no information was available for the other two isoforms. In the second project, we studied the biochemical properties of the two uncharacterized isoforms of RECQ5 in collaboration with Dr. Xi's laboratory (**Ren *et al.*, 2008**). This work clarified the function of the zinc (Zn^{2+})-binding motif that is present in the RECQ5β protein but not in the other two short isoforms. Our initial studies have shown that the short RECQ5 isoforms, RECQ5α and RECQ5γ, containing all conserved helicase motifs do not possess ATPase and DNA unwinding activities. Additional biochemical experiments with the RECQ5α protein revealed that this RECQ5 isoform was proficient in DNA strand annealing. Surprisingly, a fragment of RECQ5β (1-475 aa) containing an intact Zn^{2+}-binding motif did not exhibit any strand-annealing activity and was proficient in DNA unwinding. Further, our results demonstrated that Zn^{2+}-binding motif of the human RECQ5β protein negatively regulates the intrinsic DNA strand-annealing activity of the helicase domain and is essential for the ATPase and helicase activities of the enzyme. Moreover, quantitative kinetic measurements indicated that the regulatory role of the Zn^{2+}-binding motif was achieved by enhancing the DNA binding affinity of the enzyme. Taking into consideration that Zn^{2+}-binding motif is highly conserved among RecQ family DNA helicases, we believe that the novel intra-molecular regulation of RECQ5 catalytic activity mediated by the Zn^{2+}-binding motif (identified in this work) may represent a universal regulation mode for all RecQ family helicases.

To further explore the biological role of the human RECQ5 helicase, we employed a proteomic approach to identify proteins associated with RECQ5 *in vivo*. One of the RECQ5 binding partners we found in this analysis was the MRE11/RAD50/NBS1 (MRN) complex, a nuclease that functions in many aspects of

DNA metabolism including DNA double-strand breaks (DSBs). Accumulating evidence suggest that the MRN nuclease acts as a DSB sensor and activates the ATM-signalling pathway. Accordingly, defects in the genes encoding for the components of the MRN complex lead to severe DNA damage sensitivity, high genomic instability, shortening of telomeres and aberrant meiosis. In the third project (**Zheng *et al.*, manuscript to be submitted**), we investigated the biological significance of the association of RECQ5 with the MRN complex. We have demonstrated that RECQ5 binds directly to the MRE11 and NBS1 subunits of the MRN complex. The MRN complex and RECQ5 were found to co-localize at sites of stalled DNA replication forks and sites of DNA DSBs. Further, we showed that the MRN complex is required for the recruitment of RECQ5 to the sites of DNA damage. In addition, our biochemical experiments revealed that RECQ5 negatively regulates the MRN complex by attenuating its 3'-5' exonuclease activity. Collectively, these data establish a functional relationship between RECQ5 and the MRN complex in the cellular response to DNA damage.

In the last project, we characterized the interaction between the Werner syndrome protein (WRN) and the mismatch-repair (MMR) initiation factors (**Saydam *et al.*, 2007**). The MMR system maintains genomic integrity by correcting DNA replication errors and preventing recombination between divergent sequences. Werner syndrome (WS) is a severe recessive disorder characterized by premature aging, cancer predisposition and genomic instability. The gene mutated in WS encodes a bi-functional enzyme called WRN that acts as a 3'-5' DNA helicase and a 3′-5′ exonuclease, but its exact role in DNA metabolism is poorly understood. We found that WRN physically interacts with the MMR initiation factors, MutSα (heterodimer of MSH2/MSH6), MutSβ (heterodimer of MSH2/MSH3) and MutLα (heterodimer of MLH1/PMS2). Also, we found that the helicase activity of WRN on forked DNA structures containing a 3'-single-stranded arm was strongly stimulated by MutSα or MutSβ, but not by MutLα. Moreover, the stimulatory effect of MutSα on WRN-mediated unwinding was enhanced by presence of a G/T mismatch in the DNA duplex ahead of the fork. Collectively, these data are consistent with results of genetic experiments conducted in yeast suggesting that MMR factors act in conjunction with a RecQ-type helicase to reject recombination between divergent sequences.

2. Zusammenfassung

Proteine, die zur RecQ DNA Helikase Familie gehören, sind hoch konserviert vom Bakterium bis hin zum Menschen. RecQ Helikasen werden zum Entfernen von ungewöhnlicher DNA Strukturen benötigt, die während der DNA Replikation und Reparatur entstehen und verhindern daher eine übermässige DNA Rekombination (Bachrati & Hickson, 2003). Während *E.coli* und Hefe nur eine RecQ Helikase haben, gibt es beim Menschen fünf Mitglieder dieser Proteine, nämlich RECQ1, BLM, WRN, RECQ4 und RECQ5. Vererbte Defekte im BLM, WRN oder RECQ4 Gen werden in Patienten mit Bloom, Werner oder Rothmund-Thomson Syndrom gefunden. Dies sind schwere rezessive Erkrankungen, die mit genomischer Instabilität, Krebsprädisposition und beschleunigtem Alterungsprozess assoziiert sind. Vererbte Defekte im *RECQ1* und *RECQ5* Gen sind bis jetzt nicht in Verbindung gebracht worden mit Erkrankungen beim Menschen. Studien mit aviären DT40 knock-out Zellen und in Mäusen deuten jedoch darauf hin, dass diese Gene auch als Tumorsuppressoren agieren und die chromosomale Stabilität erhöhen. Eine Anzahl biochemischer und zellulärer Studien zeigen auf, dass die mehrfachen RecQ Homologe in der humanen Zelle nicht redundante biologische Funktionen haben. Die exakte DNA Transaktion, die von diesen Proteinen vermittelt wird, bleibt hingegen ungewiss.

Das Ziel dieser Dissertation war die zelluläre Funktion der RECQ5 und WRN Helikase besser zu definieren. Im ersten Projekt (**Kanagaraj *et al.*, 2006)**, untersuchten wir die mögliche Funktion von RECQ5 an der Replikationsgabel. Frühere biochemische Studien in unserer Gruppe haben gezeigt, dass RECQ5 eine 3'-5' DNA Helikase ist und das Zusammenlegen von einzelsträngiger DNA beschleunigen kann. Wir analysierten die Aktivität von RECQ5 mit verschiedenen synthetischen gabelförmiger DNA Strukturen, die entweder heterologe oder homologe Arme hatten. Wir fanden andere Aktivitätsmuster bei RECQ5 als bei anderen humanen RecQ Helikasen. Zum Beispiel zeigte RECQ5 eine Präferenz den Folgestrang zu entwinden, bei einer gabelförmiger Duplex-DNA mit heterologen Armen, während BLM und WRN Helikasen eine strarke Präferenz aufwiesen den parentalen Arm zu entwinden. Wir zeigten auch, dass RECQ5 eine Strangaustausch-Reaktion zwischen den homologen Armen einer synthetischen gabelförmigen DNA Struktur katalysiert. Diese Reaktion war abhängig von ATP

Hydrolyse und wurde stimuliert durch das humane Replikationsprotein (hRPA). Wir identifizierten weiter eine Domäne im nicht konservierten C-terminalen Bereich von RECQ5 (umfasst Aminosäuren 561 -651), die wichtig ist für das Entwinden des Folgestrangarms und die Strangaustausch-Reaktion an einer gabelförmigen Struktur mit gebundenem hRPA. Unsere Zellkulturexperimente zeigten auf, dass RECQ5 mit der DNA Replikationsmaschinerie im S-Phasenkern assoziiert ist und nach UV-Exposition und Cisplatin-Behandlung an Stellen mit blockierten Replikationsgabeln gebunden bleibt. Wir fanden zusätzlich eine direkte Interaktion zwischen RECQ5 und dem proliferating cell nuclear antigen, dem Prozessivitätsfaktor der Polymerase, *in vitro* und *in vivo*. Zusammenfassend deuten unsere Resultate darauf hin, dass RECQ5 an der Reaktivierung von blockierten Replikationsgabeln beteiligt sein könnte.

Im Unterschied zu den anderen humanen RecQ Homologen, existiert RECQ5 in mindestens drei Isoformen (nämlich RECQ5α, RECQ5β und RECQ5γ), die durch alternatives mRNA Spleissen hervorgehen. Die RECQ5β Isoform ist biochemisch gut charakterisiert, über die beiden anderen Isoformen waren hingegen keine Informationen vorhanden. In einem zweiten Projekt studierten wir die biochemischen Eigenschaften dieser uncharakterisierten RECQ5 Isoformen in Kollaboration mit Dr. Xis Labor **(Ren et al., 2008)**. In dieser Arbeit wurde die Funktion des Zink (Zn^{2+})-Bindungsmotifes aufgeklärt, das im RECQ5β Protein vorhanden ist, nicht aber in den beiden kurzen Isoformen. Unsere ersten Studien haben gezeigt, dass die kurzen RECQ5 Isoformen (RECQ5α und RECQ5γ), die alle konservierten Helikasemotife enthalten, keine ATPase und DNA-Entwindungs-Aktivität zeigen. Weitere biochemische Experimente mit RECQ5α zeigten, dass dieses Protein das Zusammenlegen von einzelsträngiger DNA katalysiert. Dieser Vorgang wurde erstaunlicherweise nicht beschleunigt vom RECQ5β Fragment (Aminosäure 1-475), das ein intaktes Zn^{2+}-Bindungsmotif enthält und DNA-Duplex entwinden kann. Unsere Resultate zeigen auf, dass das Zn^{2+}-Bindungsmotif des humanen RECQ5 Proteins die intrinsische Einzelstrangpaarungsaktivität der Helikasedomäne negativ reguliert und essentiell für die ATPase und Helikaseaktivität des Enzymes ist. Quantitative Kinetikmessungen zeigten weiter, dass die regulatorische Funktion des Zn^{2+}-Bindungsmotifes durch Stimulierung der DNA-Bindungsaffinität erreicht wird. Da das Zn^{2+}-Bindungsmotif unter RecQ DNA Helikasen hoch konserviert ist, glauben wir, dass die hier neu identifizierte intramolekulare Regulation der RECQ5

Aktivität durch dieses Motif auch bei andern Mitglieder der RecQ Proteinfamilie gefunden werden könnte und es sich hierbei um einen universalen Regulationsmechanismus handeln könnte.

Um die biologische Funktion der humanen RECQ5 Helikase weiter zu erforschen, führten wir eine Proteom-Analyse durch, mit dem Ziel Proteine, die *in vivo* mit RECQ5 assoziiert sind zu identifizieren. Ein identifizierter Bindungspartner ist der MRE11/RAD50/NBS1 (MRN) Komplex, eine Nuklease, die in den DNA Metabolismus involviert ist, unter anderem auch in die Reparatur von DNA Doppelstrangbrüchen (DSB). Mehrere Anhaltspunkte weisen darauf hin, dass die MRN Nuklease als DSB-Sensor funktioniert und den ATM Signalweg aktiviert. Defekte in den Genen, die für die Komponente des MRN Komplexes kodieren, führen erwartungsgemäss zu erhöhter Empfindlichkeit gegenüber DNA-Schäden, hohe genomische Instabilität, verkürzte Telomere und fehlerhafte Meiose. In einem dritten Projekt (**Zheng *et al.*, Manuskript noch nicht eingereicht**) untersuchten wir die biologische Signifikanz von der RECQ5-MRN Interaktion. Wir konnten demonstrieren, dass RECQ5 die Untereinheiten des MRN Komplexes, MRE11 und NBS1, direkt bindet. Der MRN Komplex und RECQ5 konnten an Stellen von blockierten DNA Replikationsgabeln und DNA DSB co-lokalisiert werden. Wir zeigten weiter, dass der MRN Komplex erforderlich ist, um RECQ5 zu den DNA Schäden zu rekrutieren. In unseren biochemischen Experimenten konnten wir zusätzlich zeigen, dass RECQ5 den MRN Komplex negativ reguliert, indem die 3'-5' Exonukleaseaktivität des MRN Komplexes abgeschwächt wird. Diese Daten weisen auf eine funktionelle Beziehung zwischen RECQ5 und dem MRN Komplex in der zellulären Antwort auf DNA Schäden hin.

In einem letzen Projekt (**Saydam *et al.*, 2007**) charakterisierten wir die Interaktion zwischen dem Werner Syndrom Protein (WRN) und den Mismatch-Reparatur (MMR) Initiationsfaktoren. Das MMR System trägt zur genomischen Integrität bei, indem es DNA Replikationsfehler korrigiert und Rekombination zwischen abweichenden Sequenzen verhindert. Werner Syndrom (WS) ist eine schwere rezessive Erkrankung, die durch einen beschleunigten Alterungsprozess, Krebsprädisposition und genomische Instabilität charakterisiert ist. Das Gen, das im WS mutiert ist, kodiert für ein bifunktionelles Enzym WRN, das als 3'-5' DNA Helikase und 3'-5' Exonuklease agiert. Die exakte Funktion von WRN im DNA Metabolismus wird bis

jetzt nur unvollständig verstanden. Wir fanden eine direkte Interaktion zwischen WRN und den MMR Initiationsfaktoren MutSα (Heterodimer zwischen MSH2/MSH6), MutSβ (Heterodimer zwischen MSH2/MSH3) und MutLα (Heterodimer zwischen MLH1/PMS2). Wir konnten auch zeigen, dass die Helikaseaktivität von WRN an einer gabelförmigen DNA Struktur mit einem 3'-einzelsträngigen Arm stark stimuliert wird durch MutSα oder MutSβ, nicht aber durch MutLα. Ausserdem wird der stimulatorische Effekt von MutSα auf die WRN Helikaseaktivität durch G/T Mismatch in der DNA Duplex vor der Replikationsgabel verstärkt. Insgesamt stimmen diese Daten mit genetischen Experimenten in Hefe überein und deuten darauf hin, dass MMR Faktoren gemeinsam mit RecQ Helikasen funktionieren, um die Rekombination zwischen abweichenden Sequenzen zu verhindern.

3. Introduction

3.1. Maintenance of genomic stability and cancer

Today's living environment poses continuous threat to our genetic material, i.e. DNA. Sources such as ionizing radiations, ultraviolet light from the sun, carcinogenic agents used in food materials and cigarette smoke cause alterations of DNA (Wogan *et al.*, 2004). In addition, cellular DNA is subjected to spontaneous damage that includes loss of bases, base modifications and changes in base sequence (Lindahl, 1996). If left unrepaired, DNA damage can halt cellular metabolic processes (replication, transcription etc.), arrests proliferation and trigger apoptosis (Hoeijmakers *et al.*, 2001). Such changes in the cells cause genetic mutations (permanent base changes) in the DNA sequence (Niida & Nakanishi, 2006). Indeed, the accumulation of mutations over time in critical genes contributes to oncogenesis and aging process (Jackson & Loeb, 1998). Hence, maintenance of the integrity of the genome is paramount to the survival and propagation of a living organism. To that end, cells have evolved complex molecular pathways to detect and repair the DNA damage (Hoeijmakers *et al.*, 2001). The fact that most of these pathways are conserved through evolution from bacteria to human, emphasize the biological importance of these pathways (Kennedy & D'Andrea, 2006). It had been reported that even the lower organisms contain more than 100 genes that are known to be involved in the DNA damage recognition and repair (Kennedy & D'Andrea, 2006). In humans, approximately 150 DNA repair genes have been identified so far (Wood *et al.*, 2005).

The five major pathways of DNA repair are: i) direct repair (Lindahl *et al.*, 1988; Goosen & Moolenaar, 2007), ii) nucleotide excision repair (NER) (Costa *et al.*, 2003; Reardon & Sancar, 2005; Scharer, 2008), iii) base excision repair (BER) (Fortini *et al.*, 2003), iv) mismatch repair (MMR) (Kunkel & Erie, 2005; Iyer *et al.*, 2006; Jiricny, 2006) and v) recombinational repair (RR) (van Gent *et al.*, 2001; Thompson & Schild, 2002; Helleday, 2005). The two common steps involved in correction of different lesions by these repair pathways are the following: i) recognition of damaged DNA by cellular sensor proteins, and ii) recruitment of other repair enzymes working in a pathway to correct the DNA lesion (Zhou & Elledge, 2000). Despite these repair mechanisms, sometimes DNA damage may persist. In such cases, cells can make use of specialized

DNA polymerases that are able to bypass specific types of DNA damage, a process called translesion synthesis (TLS) (Lehmann *et al.*, 2007). Detailed description of molecular mechanisms of all these repair pathways are presented in the chapter 3.2.

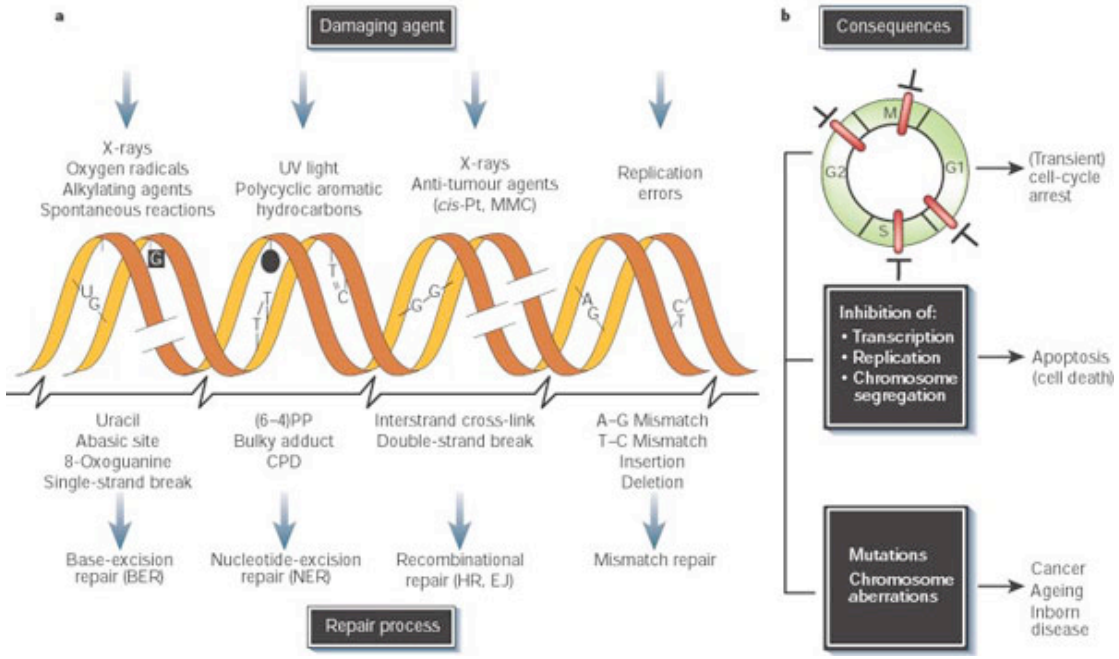

Figure 1. Causes (a) and consequences (b) of DNA damage induced by exogenous and endogenous sources. DNA repair pathways that are involved in the repair of specific DNA lesions are also shown in (a). Adapted from Hoeijmakers *et al.*, 2001.

Inherited mutations in various DNA repair genes lead to disease as a consequence of loss of genome stability and high rate of mutagenesis (Spry *et al.*, 2007). A variety of cancer prone and/or premature aging syndromes have been linked to various loss-of-function mutations in these genes (Heinen *et al.*, 2002; Thoms *et al.*, 2007) (see Table 1). The systematic study of these rare diseases has helped to a better understanding of the genes and proteins involved in the major DNA repair pathways. It is now known that defects in specific repair pathways cause syndrome(s) with unique and defined clinical characteristics (Lynch *et al.*, 2004) (Table 1). Hence, the knowledge of the molecular mechanisms of various DNA repair pathways is essential to provide clues about the occurrence of different types of cancer and may help to design a better cancer therapy. One group of DNA repair genes that function to guard and maintain genomic stability includes RecQ-type helicases (Bachrati & Hickson, 2008). Understanding the biological importance of these DNA processing enzymes are the

focus of the studies presented in this thesis. More details on helicases and RecQ-type helicases are described in the Chapters 3.3. and 3.4.

Clinical classification	Genes	Protective function	Molecular/cellular function	Neoplasia
Skin cancer group				
Xeroderma pigmentosum	XPA-XPG	UV light	Nucleotide excision repair (NER)	Skin carcinoma
Progeria group				
Without tumors				
Cockayne syndrome	XPD, XPG	UV light	Helicase/Replication-coupled repair	–
Trichothiodystrophy	XPB	UV light		
Niedernhofer syndrome	XPF-ERCC1	Crosslinking agents	Endonuclease (Crosslink repair)	
Progeria group				
With tumors				
Werner syndrome	WRN	4-NQO	Helicase/Exonuclease (NER)	Sarcoma, etc
Bloom syndrome	BLM	UV light	Helicase (HDR)	All tumors
Rothmund-Thompson	RecQ4	BrdUrd, UV	Helicase	Sarcoma
Rapadilino syndrome	RecQ4			
Lymphoma group				
Ataxia telangiectasia	ATM	Ionizing radiation (IR)	DSB-recognition and repair (NHEJ)	Lymphoma
Nijmegen Breakage syndrome	Nibrin			Lymphoma
AT-like syndromes (ATLD)	Mre11, Rad50	Ionizing radiation (IR)	DSB-recognition and repair (NHEJ)	Lymphoma
Primary Immunodeficiency group				
(SCID)	LIG4 Artemis Cerunnos-XLF	Ionizing radiation (IR)	DSB-repair (NHEJ)	EBV-associated lymphoma
Microcephaly group				
ATR-Seckel syndr.	ATR	Ionizing radiation (IR)	ATR-BRCA1-Chk1 signalling Mitosis	–
Primary microcephaly	BRIT1/MCPH1			
Dyskeratosis congenita group	Dyskerin, TERC	Unknown	Telomere maintenance	MDS, AML
Fanconi anemia group	FANC-A, B, C, D1,D2, E, F, G, I, J, L, M, N	Alkylating/cross-linking agents Reactive oxygen species (ROS)	DSB-recognition and homology-directed recombinational repair (HDR)	AML, squamous cell carcinomas
Breast/ovarian cancer group	BRCA1, BRCA2	Reactive oxygen species (ROS)	Rekombinational repair (HDR)	Mamma Ca Ovarian Ca
Colon carcinoma group	MSH2, MSH6, MLH1, PMS1,2	Reactive oxygen species (ROS)	Mismatch-repair (MMR)	Non-polyposis Colon cancer
Li-Fraumeni group	p53	IR, chemicals (?)	Cell cycle arrest	All tumors

Table 1. Human hereditary syndromes with defects in DNA-maintenance systems. Adapted from Neveling *et al.*, 2007.

3.2. DNA damage and DNA repair pathways

3.2.1. Types of DNA damage

DNA molecules can be damaged in numerous ways. This includes spontaneous damage such as deamination, depurination, oxidation and errors occurring during replication (Spry et al., 2007). In addition, radiation and environmental chemicals also chemically modify DNA bases (Spry et al., 2007). Further, these modifications result in abnormal molecular interactions (hydrogen bonding, etc.) between complementary bases of the double-stranded DNA. DNA modifications that occur commonly in the cells are listed below (see Figure 2).

i) *Base loss* - This kind of damage is created by the breakage of glycosyl bond linking DNA bases and sugar-phosphate backbone. As a result, the base is released and the strand remains intact (abasic site; see Figure 2B). In mammals, it is estimated that several thousand purines and several hundreds pyrimidines are spontaneously lost every day (De la Torre et al., 2003). Loss of a purine or pyrimidine base creates an apurinic/apyrimidinic (AP) site.

ii) *Base modifications* – The functional groups of the bases are somewhat unstable. For example, the amino groups of nucleic acid bases can be spontaneously converted into keto groups. In particular, uracil is frequently generated in the cells by spontaneous deamination of cytosine (Figure 2C). The other base changes that occur frequently in the cells are adenine to hypoxanthine, guanine to xanthine, and 5-methyl cytosine to thymine conversions. In addition, methyl or alkyl groups present in the environmental chemicals can be added to nucleotide bases. For example, it has been shown that S-adenosylmethionine, the normal biological methyl group donor, reacts with DNA to produce alkylated bases like 3-methyladenine (Figure 2D). It is estimated that several thousands of these modifications are generated each day per mammalian genome (Friedberg, 2003). Also, several hyper-reactive oxygen species [generally called Reactive oxygen species (ROS)] that are generated as byproducts of normal oxidative DNA metabolism can modify DNA bases. The formation of thymine glycol by the oxidation of thymine is the best example of oxidative modifications of DNA bases (Figure 2E). Some other oxidative modifications that frequently occur in DNA are 8-

hydroxyguanine, 2,6-diamino-4-hydroxy-5-formamidopyrimidine, 8-hydroxyadenine, 5-hydroxy uracil and 5-hydroxy-cytosine (Wiseman & Halliwell, 1996).

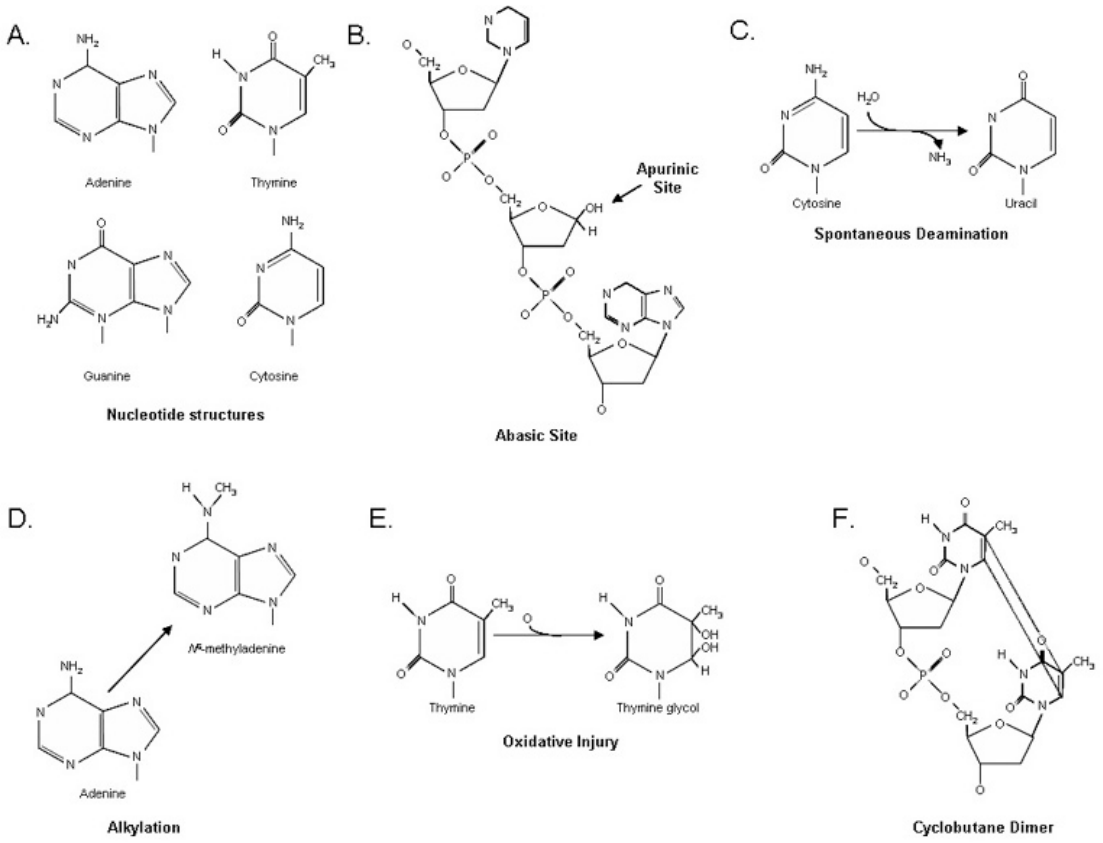

Figure 2. Examples of potentially mutagenic DNA lesions. A) Structure of the four bases present in DNA. B) Generation of abasic (apurinic) site by nucleotide base loss. C) Spontaneous deamination. D) Alkylation of DNA. E) Base modification by oxidative injury, F) Structure of cyclobutane pyrimidine dimer. Adapted from Spry *et al.*, 2007.

iii) *Photodamage* – The double bond between the C5 and C6 atoms of pyrimidine ring is sensitive to the UV-B (290-320 nm) or UV-C (100-280 nm) light. Upon exposure to UV light, these bonds break leading to abnormal covalent interactions between neighbouring pyrimidines that significantly alter the 3D structure of the double helical DNA (Hussein, 2005). The majority of such DNA lesions that are formed upon UV exposure are cyclobutane dimers (Figure 2F) (Daya-Grosjean & Sarasin, 2005). In addition, pyrimidine (6,4)-pyrimidone photoproducts are also formed in lesser amount (Cleaver & Crowley, 2002).

iv) *Mismatched bases* – Such damage to the DNA may occur during normal replication due to nucleotide misincorporation by DNA polymerases.

v) *Strand breakage* – This kind of damage to the DNA is generated either by the action of DNA topoisomerases during normal DNA replication or after exposure of cells to ionizing radiation. Strand breakage occuring only on one DNA strand is called single-stranded break. Breakage of both strands in the same location is referred as double-stranded break.

vi) *DNA crosslinks* – DNA crosslinks can be created by bifunctional alkylating agents, such as psoralens, that chemically attach to nucleotide bases on both strands to form an interstrand crosslinks. DNA damaging agents such as UV and ionizing radiation are also capable of generating DNA interstrand cross-links.

3.2.2. DNA repair pathways

Different DNA repair pathways are involved in the repair of different kinds of lesions. A simple scheme of DNA repair pathways is presented in Figure 3.

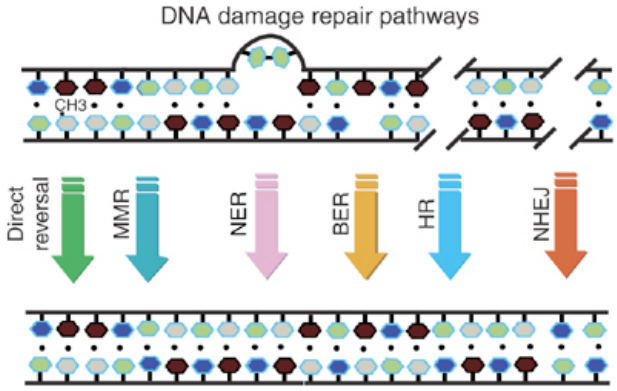

Figure 3. A simple scheme of DNA repair by different pathways. MMR – **Mis**Match **R**epair, NER – **N**ucleotide **E**xcision **R**epair, BER – **B**ase **E**xcision **R**epair, HR – **H**omologous **R**ecombination, NHEJ – **N**on-**H**omologous **E**nd **J**oining. Adapted from Hakem, 2008.

3.2.2.1. Direct reversal

Direct reversal of DNA damage is the simplest mechanism among all DNA repair pathways described so far. The best example for the direct reversal pathway is the conversion of highly mutagenic alkylation lesion O^6-methylguanine (O^6-meG) to its prototype guanine (Margison & Santibanez-Koref, 2002). The O^6-meG adducts are formed at lower levels in the cell by reaction of cellular catabolites with the guanine residues in the DNA (Sedgwick, 1997). The reversal reaction is catalyzed by enzyme

called MGMT (O^6-methylguanine DNA methyltransferase). In this direct reversal pathway, correction of the lesion occurs by direct transfer of the alkyl group on guanine to a cysteine residue in the active site of MGMT. The inactive alkyl-MGMT protein formed is then degraded by the ubiquitin proteosome pathway (Srivenugopal et al., 1996). The crystal structure of human MGMT has been established now and it has revealed that an O^6-meG residue in DNA is flipped out to access the acceptor cysteine residue (Daniels et al., 2004). Also, structural studies revealed that the enzyme contains two subdomains that are inactive when separated but regain activity when mixed together (Fang et al., 2005).

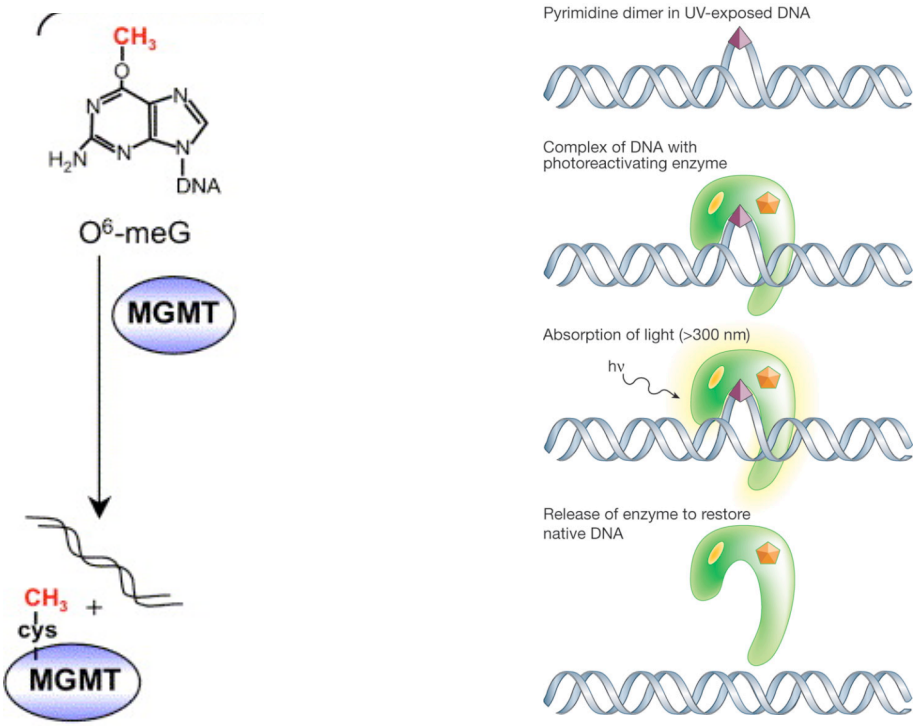

Figure 4. Left panel: Repair of O^6-methylguanine in DNA. See text for details. Adapted from Sedgwick et al., 2007. Right panel: Photoreactivation reverses UV-induced DNA damage. See text for details. Adapted from Friedberg, 2003.

UV lesions can be also removed by direct repair. The repair mechanism is termed photoreactivation and the enzymes that catalyzed this reaction are called photolyases. Photoreactivation was the first DNA repair mechanism discovered (Dulbecco, 1949). By using blue light photons as an energy source, photolyases with two chromophore cofactors resolve these aberrant structures. Briefly, DNA lesions are recognized by a photolyase enzyme, which absorbs light at wavelengths >300nm and

facilitates a series of photochemical reactions that help convert the dimerized pyrimidines to their native form (Figure 4B).

3.2.2.2. Base excision repair

Base excision repair (BER) is a multi-step process that is involved in correcting non-bulky DNA lesions caused by oxidation, methylation, deamination and/or spontaneous loss of the DNA bases (Memisoglu & Samson, 2000). These alterations are highly mutagenic and, if left unrepaired, pose a significant threat to genome stability (Friedberg, 1995).

BER has two subpathways namely Long-Patch BER (LP-BER) and Short-Patch BER (SP-BER) (Figure 5). In both pathways, the N-glycosidic bond between the damaged base and the sugar phosphate backbone of the DNA is cleaved, generating an apyrimidinic/apurinic (abasic or AP) site. This reaction is carried out by an enzyme called DNA glycosylase. Currently, there are eight DNA glycosylases identified in humans that share partially overlapping substrate specificity (Scharer & Jiricny, 2001). Sometimes, AP sites are also formed by the spontaneous hydrolysis of the N-glycosidic bond. In either case, the AP site is subsequently processed by the action of AP endonuclease 1 (APE1) that cleaves the phosphodiester backbone 5' to the AP site. As a result, a 3' hydroxyl group and a transient 5' abasic deoxyribose phosphate (dRP) are formed in the DNA. Removal of the dRP can be accomplished by the action of DNA polymerase β (pol β), which adds one nucleotide to the 3' end of the nick and removes the dRP moiety using its associated AP lyase activity (Matsumoto & Kim, 1995). The nicked DNA strand is finally sealed by the action of DNA ligase. SP-BER constitutes approximately 80 - 90% of the BER reaction happen in the cells.

LP-BER is used when the damaged base is resistant to the AP lyase activity of pol β (Matsumoto et al., 1994). Hence, LP-BER results in the replacement of approximately 2-10 nucleotides including the damaged base. LP-BER essentially utilizes the same factors as SP-BER; e.g. a DNA glycosylase, APE1 and pol β. However, unlike SP-BER, LP-BER is a PCNA-dependent pathway, and the participation of other DNA polymerases is necessary to add several nucleotides to the incised strand, displacing the dRP as part of a flap oligonucleotide (Frosino et al., 1996). The resulting flap oligonucleotide is excised by the action of Flap endonuclease 1 (FEN-1), which is followed by sealing the nick in DNA by a DNA ligase.

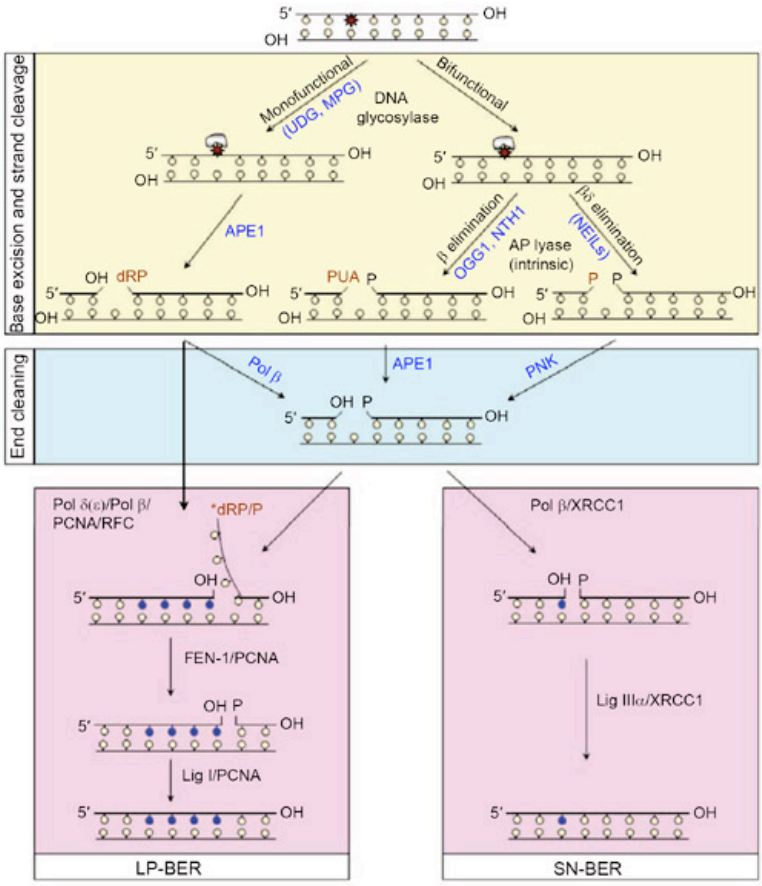

Figure 5. A schematic illustration of BER subpathways for damaged bases and DNA strand breaks. The damaged base is represented as *. Divergent base excision steps converge to common steps for end processing, followed by repair DNA synthesis (represented as blue dots) and strand sealing. Other details are discussed in the text. Adapted from Hegde *et al.*, 2008.

3.2.2.3. Nucleotide excision repair

Nucleotide excision repair (NER) is considered to be the most flexible DNA repair pathway because of its vast substrate specificity. DNA lesions that are predominantly repaired by NER are UV lesions (cyclobutane pyrimidine dimers and 6-4 photoproducts). Other NER substrates include bulky chemical adducts, DNA intrastrand crosslinks, and some forms of oxidative damage. A common feature of all lesions recognized by the NER pathway is that they cause a distortion of the DNA helix (Hess et al., 1997).

NER is a stepwise process that requires more than 30 different proteins including XPA, XPB, XPC, XPD, XPE, XPF and XPG (Gillet & Scharer, 2006). The different steps involved in this process are: i) damage recognition, ii) local opening of the DNA duplex around the lesion, iii) dual incision of the damaged DNA strand, iv) gap repair synthesis and v) strand ligation (Batty & Wood, 2000) (Figure 6). There are two distinct

subpathways of eukaryotic NER repair: i) global genome NER (GG-NER) and ii) transcription coupled NER (TC-NER). GG-NER is a slow random process that is responsible for inspecting and correcting the damage that occurs through the entire genome (Gillet & Scharer, 2006; Nouspikel, 2008), whereas TC-NER is a highly specific and efficient repair machinery that corrects damage only on the actively transcribed DNA strands (Fousteri & Mullenders, 2008).

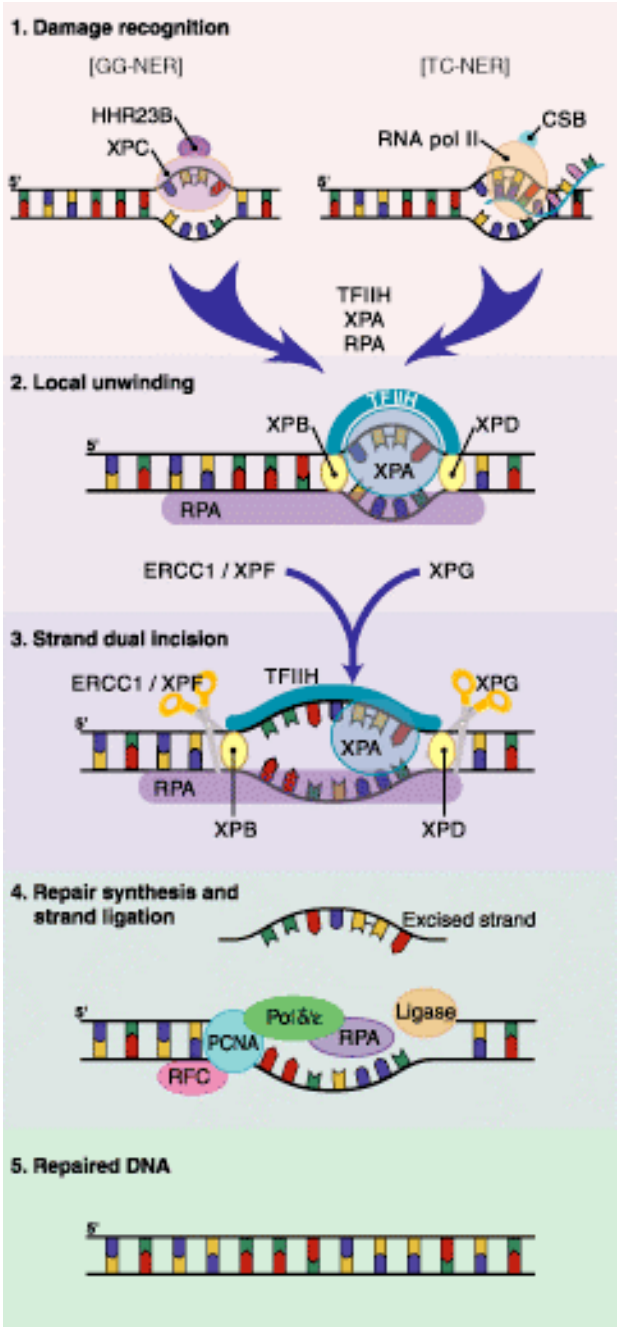

Figure 6. Nucleotide excision repair (NER). A simplified model of steps in NER is shown. See the text for details.

Except for their DNA damage recognition mechanisms, both pathways are identical. In GG-NER, the XPC/HHR23B protein complex is responsible for the initial damage detection. In contrast, damage recognition during TC-NER does not require XPC, but it is rather thought to occur when the transcription machinery is stalled at the site of DNA lesion. Hence, the first step in TC-NER is the removal of RNA polymerase complex from the stall site. This displacement reaction is followed by the recruitment of NER proteins to the damaged DNA. The factors required for the displacement of stalled RNA polymerase in eukaryotic cells are not known.

Further steps of GG-NER and TC-NER are almost the same. Following the damage recognition step, XPA and the human single-strand binding protein (hRPA) are then recruited to the sites of DNA damage. Next, the XPB and XPD helicases, components of the multi-subunit transcription factor TFIIH, unwind the DNA duplex in the immediate vicinity of the lesion. Later, the endonucleases XPG and ERCC1/XPF cleaves one strand of the DNA 3' and 5' to the damage, respectively, generating an approximately 30-mer oligonucleotide containing the lesion. The excised oligonucleotide is then displaced to initiate the gap repair synthesis. The gap repair synthesis is performed by replicative DNA polymerases pol δ and pol ε along with several replication accessory factors. Finally, the nick in the repaired strand is sealed by a DNA ligase, thus completing the NER process.

3.2.2.4. Mismatch repair

The DNA mismatch repair (MMR) pathway is generally required for the correction of replication errors such as base-base mismatches and inserion/deletion loops (IDLs), resulting from nucleotide misincorporation and template slippage, respectively. Other substrates for the MMR system are the mismatches generated by the spontaneous deamination of 5-methylcytosine and heteroduplexes formed following genetic recombination. Overall, the MMR process is similar to the other excision repair pathways described above (see LP-BER and NER). MMR includes the following steps: i) DNA lesion (mismatch or IDL) recognition, ii) excision of the DNA strand containing the lesion, iii) correction of the strand by DNA repair synthesis and iv) sealing of the nicked strand by re-ligation (Jiricny, 2006; Hsieh & Yamane, 2008) (Figure 7).

In mammals, MMR pathway is initiated by the recognition of mismatches or IDLs by the MSH2-MSH6 (MutSα) and MSH2-MSH3 (MutSβ) heterodimers. MutSα is generally involved in the recognition of base-base mismatches and single-base IDLs, whereas, larger IDLs are recognized by MutSβ (Drummond et al., 1995; Palombo et al., 1995; Palombo et al., 1996; Genschel et al., 1998). The mismatch bound MutSα or MutSβ then recruits another heterodimer MLH1-PMS2 (MutLα). This ternary complex undergoes an ATP-driven conformational switch, which converts MutSα/β into a sliding clamp that can freely move along DNA (Jiricny, 2006). Clamps that encounter Replication Factor C (RFC) bound at the 5'-terminus of a strand break, will displace it and load Exonuclease I (Exo1). The activated Exo1 then degrades the DNA strand in 5'-3' direction. The formed single-stranded gap is stabilized by binding of hRPA. In this way, the mismatch is removed from the DNA strand. The gaps in the DNA are then filled by replicative DNA polymerase pol δ along with a bound PCNA molecule. Finally, DNA ligase I seals the remaining nick to complete the repair process.

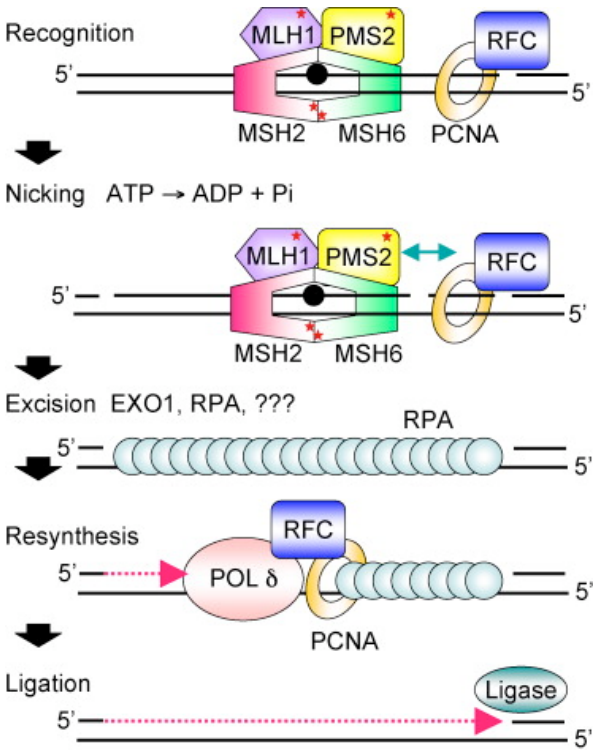

Figure 7. Overview of eukaryotic MMR. For more details see the text. Adapted from Hsieh & Yamane, 2008.

3.2.2.5. Homologous recombination

DNA double-strand breaks (DSBs) are the most serious type of DNA damage because they pose problems for numerous cellular processes including chromosome segregation, replication and transcription. DNA DSBs are caused by a variety of sources including ionizing radiation, ROS, mechanical stress on the chromosomes and certain genotoxic chemicals such as camptothecin, etoposide, anthracyclins and bleomycin (Jackson, 2002). In contrast to other types of DNA damage, DSBs affect both strands of the DNA duplex and therefore make it impossible to use the complementary strand as a template for repair. Hence, failure to repair these defects can result in chromosomal instabilities leading to carcinogenesis and cell death (Hoeijmakers, 2001). To avoid the detrimental effects of these DNA lesions, cells have evolved two different pathways of DSB repair, homologous recombination (HR) (Figure 8) and non-homologous end joining (NHEJ) (Figure 9) (Jackson, 2002).

HR is an error free DNA repair pathway that corrects DSB defects using a mechanism that copies genetic information from a homologous, undamaged DNA molecule (Figure 8) (Li & Heyer, 2008). The majority of HR-mediated repair takes place in the late S- and G2-phases of the cell cycle (Takata et al., 1998). The RAD52 epistasis group of proteins, including RAD50, RAD51, RAD52, RAD54, and MRE11 mediate this process (Sonoda et al., 2001). HR can be divided into three stages: i) presynapsis, ii) synapsis and iii) postsynapsis (San Filippo et al., 2008; Li & Heyer, 2008). During the presynapsis stage, DSBs are recognized and processed to form a 3'-OH ended single stranded tail, a process called "end resection" (Figure 10a). The MRE11/RAD50/NBS1 (MRN) complex that exhibits 3'-5' exonuclease activity is used for this purpose. The action of MRN at the damaged site exposes the 3' ends on either side of the DSB. In synapsis stage, the newly formed ssDNA ends are bound by RAD51 to form a nucleoprotein filament. Other proteins including RPA, RAD52, RAD54 and several additional RAD51-related proteins serve as accessory factors in filament assembly and subsequent RAD51 activities (San Filippo et al., 2008). The RAD51 nucleoprotein filament then searches the undamaged DNA on the sister chromatid for a homologous repair template. Once the homologous DNA has been identified, the damaged DNA strand invades the undamaged DNA duplex in a process referred to as DNA strand invasion (Figure 8a). A DNA polymerase then extends the 3' end of the invading strand,

and this intermediate structure formed during HR process is termed displacement loop (D-loop). Recent evidence suggested that a translesion polymerase (DNA polymerase η) is involved in the DNA synthesis reaction of HR process (McIlwraith et al., 2005). In the postsynapsis stage, this recombination intermediate is resolved and processed to complete the HR-directed repair.

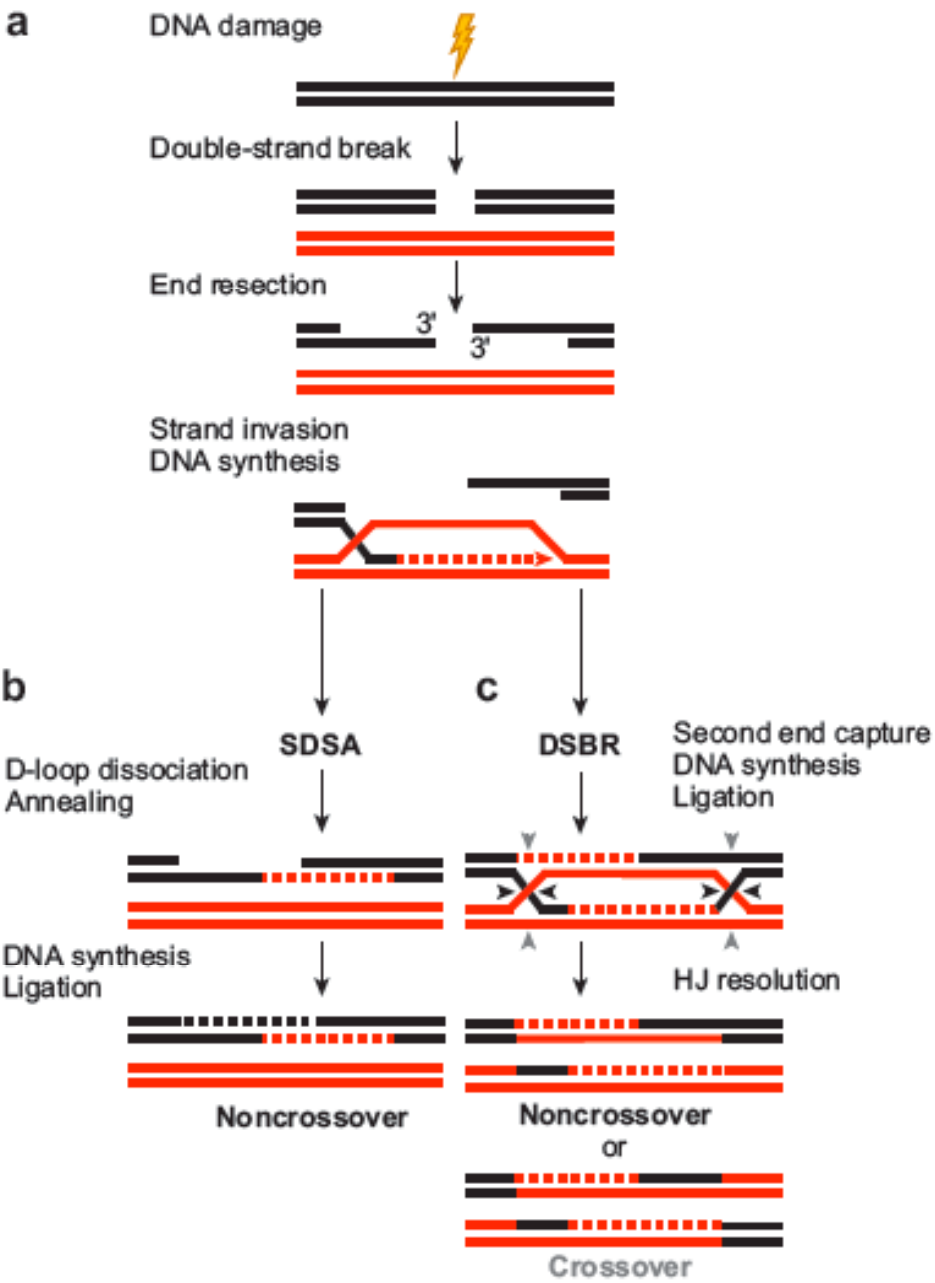

Figure 8. Pathways of DSB repairby HR. Abbreviations used are, SDSA – Synthesis Dependent Strand Annealing; DSBR – Double Strand Break Repair; HJ – Holliday Junction. Other details are described in the text. Adapted from San Filippo *et al.*, 2008.

The postsynapsis stage has at least, three different pathways. Only two of this pathway, synthesis-dependent strand annealing (SDSA) and double-strand break repair (DSBR), are shown in Figure 8. The other pathway is termed break-induced replication (BIR) (Li & Heyer, 2008). In SDSA, the invading strand is dismantled following DNA synthesis and annealed with the second end, leading to localized conversion without crossover (Figure 8b). In DSBR, both ends of the DSB are engaged, either by independent strand invasion or by second end capture, leading to double Holliday junction (DHJ) formation (Figure 8c). The resolution of such structure is carried out either by a resolvase (resulting in non-crossover or crossover products) or by a dissolution mechanism involving Bloom syndrome helicase (BLM) and TOPO IIIα (resulting in non-crossover products) (Figure 8C).

3.2.2.6. Non-homologous end joining

In contrast to HR, Non-homologous end joining (NHEJ) does not require a homologous template for DSB repair and usually is error-prone (Weterings & Chen, 2008) (Figure 9).

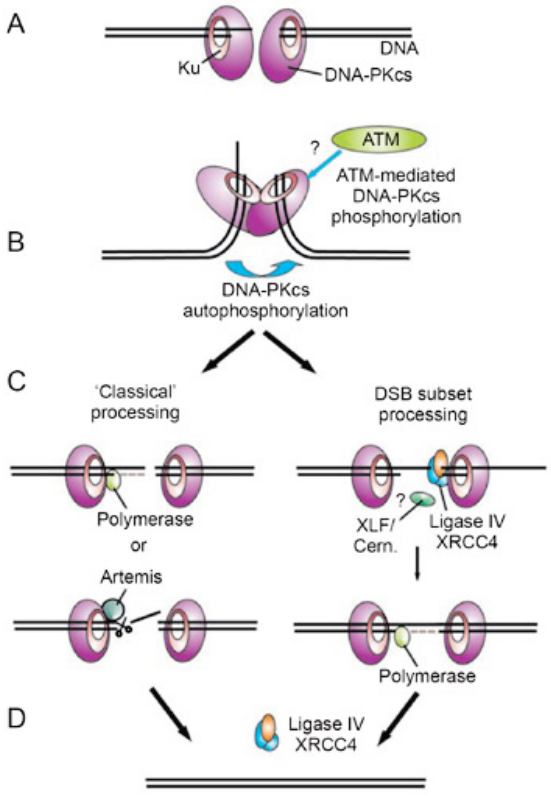

Figure 9. A model for NHEJ. See text for more details. Adapted from Weterings & Chen, 2008.

NHEJ pathway is initiated by binding of the Ku70/Ku80 heterodimeric protein to the free DNA ends (Featherstone & Jackson, 1999) (Figure 9A). The DNA-Ku heterodimer complex then recruits DNA-dependent protein kinase (DNA-PKcs) to the DNA ends that protects the DNA against degradation and premature ligation. Further, the bound DNA-PKcs tethers the DNA ends (Figure 9B). This is followed by the autophosphorylation of DNA-PKcs that facilitate the access of DNA ends by the other NHEJ enzymes (Figure 9B). Although still unclear, ATM mediated phosphorylation of DNA-PKcs is also reported to help the recruitment of other NHEJ enzymes to the damage site. This is followed by the ligation of DNA ends. Two kinds of end-joining has been reported depending on the nature of DNA ends. If the DNA ends are non-compatible, then the ligation reaction is carried out in the classical way, by either filling (DNA polymerases) or resection (Artemis) of single-strand overhangs, followed by ligation of blunted ends by XRCC4 and DNA Ligase IV (Figure 9C & D). In case of the DNA DSBs with partially complementary overhangs, ligase IV/XRCC4 and XLF/Cernunnos mediate the joining of one single-strand overhang with the opposite DNA end, followed by filling of the gap by the DNA polymerases (Figure 9C & D).

3.3. Helicases

3.3.1. Classification

Helicases are molecular motors that utilize the free energy derived from the nucleoside triphosphate (NTP) hydrolysis for unwinding DNA or RNA duplex substrates (Singleton & Wigley, 2002; Caruthers & Mckay, 2002) (Figure 10). These ubiquitous enzymes are found in all kingdoms of life and function in almost all nucleic-acid dependent metabolic processes including DNA replication and repair, transcription, translation, ribosome synthesis, RNA maturation, splicing and nuclear export processes (Tanner & Linder, 2001; Wu & Hickson, 2006; Singleton *et al*., 2007). Helicases are classified based on the sequence homology, co-factor requirements, substrate preference, subunit structure, directionality and processivity (Singleton & Wigley, 2002; Mackintosh & Raney, 2006; Singleton *et al*., 2007). Initial sequence homology studies have identified a series of conserved motifs that are believed to be a unique characteristic of helicases (Gorbalenya & Koonin, 1993). More recently, it has become evident that these motifs are characteristic of proteins termed translocases that couple NTP hydrolysis to directional motion along nucleic acid strands (Erzberger & Berger, 2006; Singleton *et al*., 2007), and helicases are a subgroup of these motor proteins.

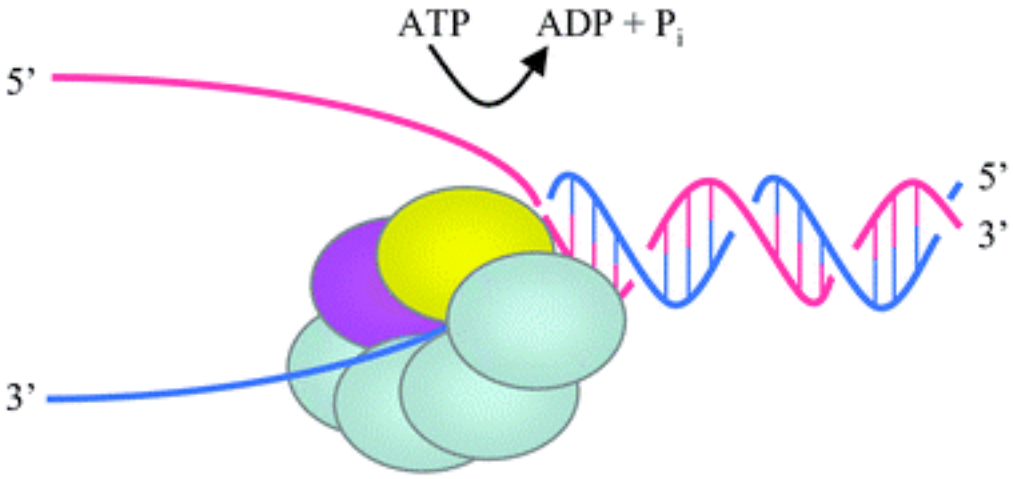

Figure 10. Schematic of nucleic-acid unwinding by a helicase. Adapted from Vindigni, 2007.

Based on amino acid sequence homology, helicases have been classified into six superfamilies (SF1 - SF6) (Singleton *et al*., 2007) (Figure 11a). Both SF1 and SF2 superfamilies are the largest and their members contain seven motifs designated I, Ia, II, III, IV, V and VI. These motifs are involved in nucleoside triphosphate (NTP) binding

and are located at the interface between two RecA-like domains as revealed by crystal structures of many SF1 and SF2 enzymes (Singleton *et al*., 2007). Members of the other superfamilies contain a lesser number of motifs (Figure 11a). For example, SF3 and SF4 members contain only three and five motifs, respectively (Caruthers & Mckay, 2002) (see Figure 11a). Additional motifs have been identified recently in SF1 and SF2 that include TxGx motif (Pause & Sonenberg, 1992), Q-motif (Tanner *et al*., 2003), motif IVa (Korolev *et al*., 1998) and TRG motif (Mahdi *et al*., 2003). SF1 and SF2 include both DNA and RNA helicases that are involved in a wide variety of cellular processes, including DNA replication, recombination and the initiation of translation (Tanner *et al*., 2003; Wu & Hickson, 2006). These helicases can unwind nucleic acids in either the 3'-5' (type A enzymes) or the 5'-3' (type B enzymes) direction (Figure 11b). The directionality of helicases is defined by polarity of strand on which the enzyme tracks along the nucleic acid substrates (Singleton & Wigley, 2002). The other four superfamilies have fewer representatives: SF3 includes helicases identified in the genomes of small DNA and RNA viruses (Gorbalenya *et al*., 1990), SF4 includes replicative helicases from bacteria and bacteriophages (Ilyina *et al*., 1992), SF5 includes the bacterial transcription termination factor Rho (Derewenda *et al*., 2004) and SF6 includes members of the AAA^+ (ATPases Associated with various cellular Activities) family of ATPase (Erzberger & Berger, 2006). While the SF3 – SF6 helicases are hexameric, the SF1 and SF2 enzymes have mainly been found to be monomeric or dimeric **(**Singleton *et al*., 2007).

3.3.2. Helicase motifs

Structural studies have revealed that the conserved helicase motifs are closely associated in the tertiary structure of the protein and that they may form a large functional domain (Hall & Matson, 1999). The organization of helicase motifs and their involvement in the catalytic function of SF1 and SF2 helicases are shown in Figure 11C. Briefly, Q motif consists of nine-amino acids including an invariant glutamine (Q). In the yeast translation-initiation factor eIF4A, this motif has been shown to be involved in ATP binding and hydrolysis (Tanner *et al*., 2003). It has also been hypothesized that the Q motif is involved in the recognition of the adenine moiety in ATP (Tanner *et al*., 2003).

a)

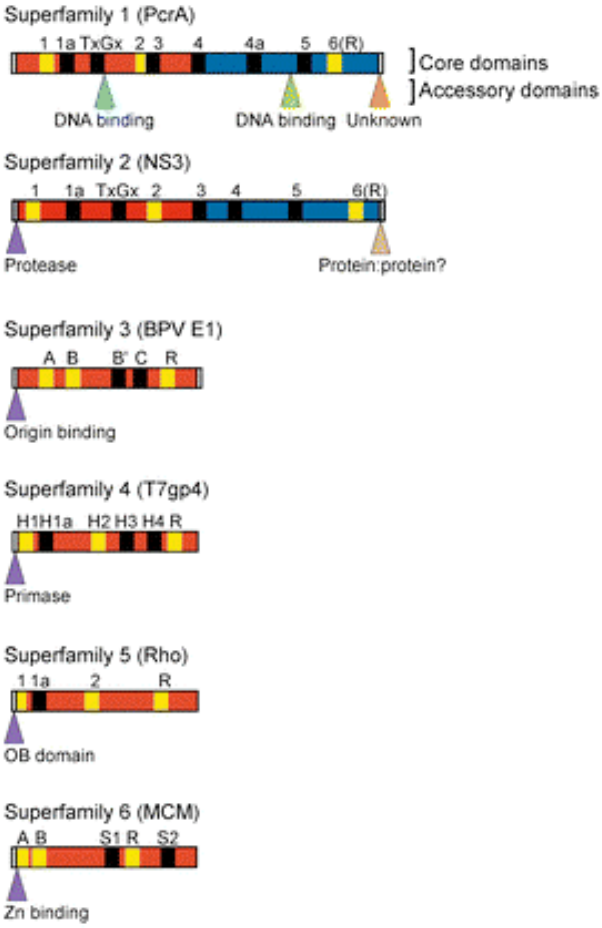

b)

Protein	Superfamily	Organism	Directionality
RecB	SF1	*E. coli*	3'–5'
RecD	SF1	*E. coli*	5'–3'
RecQ	SF2	*E. coli*	3'–5'
Sgs1	SF2	*S. cerevisiae*	3'–5'
BLM	SF2	*H. sapiens*	3'–5'
WRN	SF2	*H. sapiens*	3'–5'
RECQ1	SF2	*H. sapiens*	3'–5'
RECQ5	SF2	*H. sapiens*	3'–5'
RECQ4	SF2	*H. sapiens*	3'–5'
UvrD	SF1	*E. coli*	3'–5'
Srs2	SF1	*S. cerevisiae*	3'–5'
Fbh1	SF1	*S. pombe*	3'–5'
Mer3	SF2	*S. cerevisiae*	3'–5'
PriA	SF2	*E. coli*	3'–5'
RecG	SF2	*E. coli*	3'–5'
Pif1	SF1	*S. cerevisiae*	5'–3'
Rrm3	SF1	*S. cerevisiae*	5'–3'
FANC-J	SF2	*H. sapiens*	5'–3'
FANC-M	SF2	*H. sapiens*	ND

c)

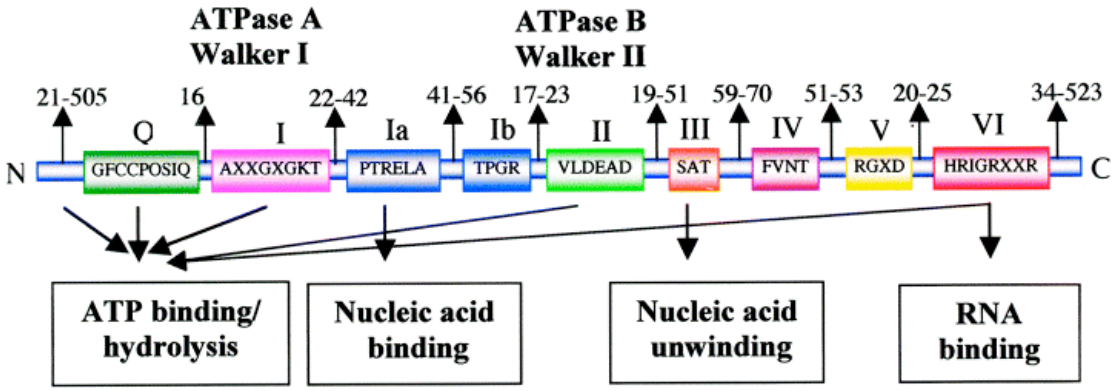

Figure 11. a) Classification of helicases and translocases. The classification is based largely on the work of Gorbalenya & Koonin (1993). One representative of each of the six helicase superfamilies is given in parentheses. The "core domains" and the positions of the signature motifs therein are shown for each class of helicases. Motifs coloured yellow represent universal structural elements in all helicases. The positions of additional motifs are shown by black boxes, but in contrast to the core domains, these are specific to each protein. Adapted from Singleton *et al.*, 2007. b) Characteristics of selected DNA helicases. Adapted from Wu & Hickson, 2006. c) Schematic representation of DEAD box helicases. Boxes represent conserved helicase motifs showing consensus sequences by single letter amino acid (aa) code (Z = D, E, H, K, R; O = S, T; X = any aa). The numbers between the motifs are the typical range of aa residues. The proposed functions of the individual motifs are also indicated. Adapted from Tuteja & Tuteja, 2004.

Motif I contains the conserved sequence GXGKS/T and is called Walker A box (Walker *et al*., 1982). This motif is essential for ATP binding, and its lysine residue has been shown to bind the β and γ phosphates of the ATP molecule and the hydroxyl group of serine/threonine residue is involved in the coordination of the magnesium (Mg^{2+}) ion, which is required for ATP binding and hydrolysis. Motif Ia has been shown to contribute to ssDNA binding (Marintcheva & Weller, 2003). Motif II contains the so-called Walker "B" motif (DEAD, DEAH, or DEXH), and the proteins containing this motif are also called DEAD-box proteins (Linder *et al*., 1989). The first two residues (D and E) of these sequences are highly conserved and the aspartate (D) residue has been shown to interact with the Mg^{2+} ion (Pause & Sonenberg, 1992). Motif III of SF2 helicase has been shown to be involved in the coupling of ATP hydrolysis to DNA unwinding (Pause & Sonenberg, 1992; Graves-Woodward *et al*., 1997). The other SF1 and SF2 motifs are proposed to mediate the following functions: motif IV along with motif I (in both SF1 and SF2 helicases) have been shown to make direct contacts with the nucleotide in the enzyme-ADP binary complexes (Hall & Matson, 1999); motif V and motif Ia of SF2 family members makes direct contacts with the bound oligonucleotide and interact primarily with the sugar-phosphate backbone (Hall & Matson, 1999); motif VI has been proposed to be required for the movement of helicase along the DNA substrate (Pause & Sonenberg, 1992). More details on the roles of the helicase motifs can be found in recent review articles (Caruthers & McKay, 2002; Tuteja & Tuteja, 2004).

3.3.3. Mechanisms of nucleic acid translocation and unwinding by SF1 and SF2 helicases

SF1 and SF2 are the largest and most closely related among the six superfamilies of helicases that have been classified to date (Singleton *et al*., 2007). However, the structural and biochemical studies have revealed that there are mechanistic differences between the SF1 and SF2 helicases in the nature of contacts between the translocating motor and the DNA substrate (Singleton & Wigley, 2002). Structural studies conducted with the SF1 helicases, PcrA and Rep, revealed that they bind to the substrate through hydrophobic interactions with the bases and thus translocate along ssDNA. In contrast, structural data available for SF2 helicases suggest that these enzymes interacts with nucleic acids via contacts with the phosphodiester backbone, which would allow the helicase motor to translocate on both ssDNA and dsDNA (Singleton & Wigley, 2002). In

accordance with the structural data, ATP hydrolysis by SF1 helicases is stimulated only by ssDNA (type α), whereas the ATPase activity of SF2 helicases is stimulated by both ssDNA (type α) and dsDNA (type β) (Singleton & Wigley, 2002; Singleton *et al.*, 2007).

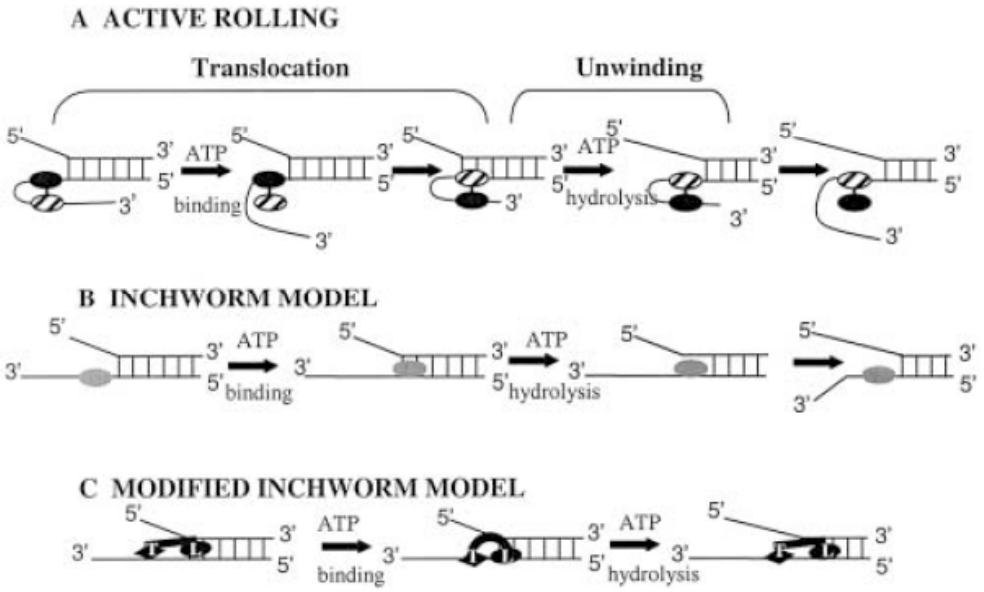

Figure 12. Models for DNA helicase unwinding and translocation. See text for details. Adapted from Tuteja & Tuteja, 2004.

Based on structural and biochemical studies, various models have been proposed for the mechanism of translocation and unwinding by SF1 and SF2 helicases. Two generally accepted models are the inchworm model and the active rolling model (Yarranton & Gefter, 1979; Lohman & Bjornson, 1996; Velankar *et al.*, 1999) (Figure 12). In the inchworm model, the enzyme is bound to ssDNA and upon binding of ATP, it starts to translocate along the DNA strand. Helix destabilization and release of one of the ssDNA strands takes place as ATP is hydrolyzed (Yarranton & Gefter, 1979) (see Figure 12B). The modified inchworm model has been proposed based on the structural studies conducted with the PcrA helicase (SF1 type). This model explains the movement of a monomeric helicase along ssDNA (Figure 12C and Figure 13). It has been shown that ssDNA is bound to domains 1A and 2A of the protein (Velanker *et al.*, 1999) (Figure 13). After ATP binding, the cleft between these domains closes. During this conformational change in the protein, domain 1A releases its grip on ssDNA and slides along it, while domain 2A maintains a tight grip on ssDNA (Figure 13b). Upon ATP hydrolysis, the inter-domain cleft opens and DNA passes through domain 2A resulting in protein translocation along ssDNA (Figure 13c).

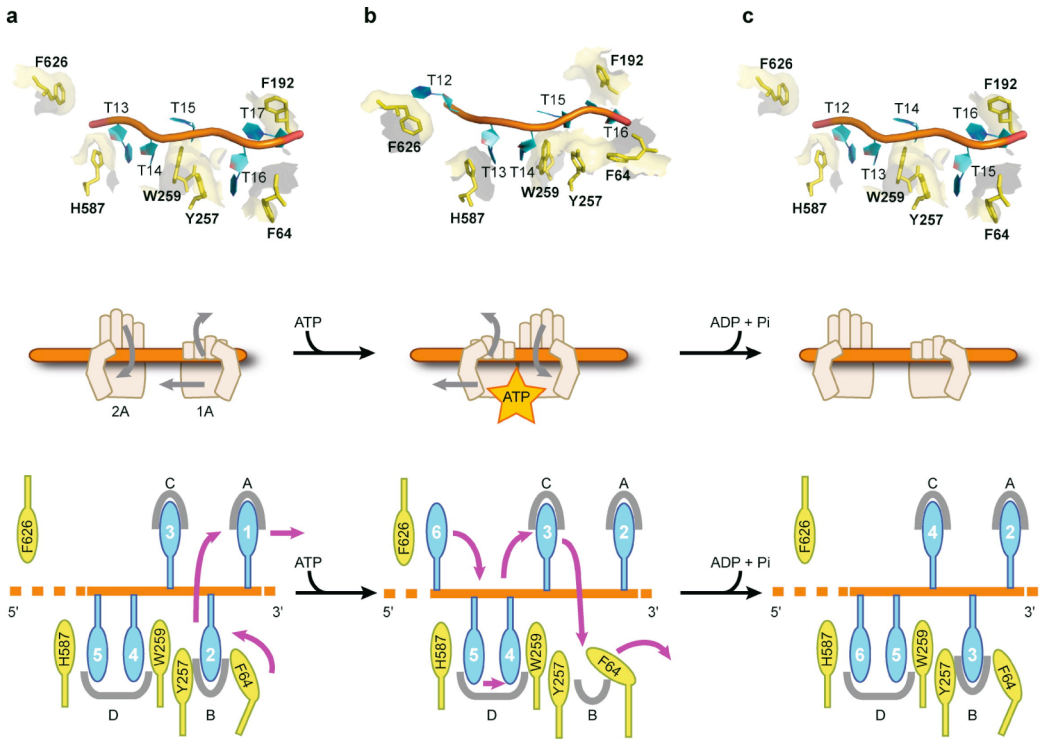

Figure 13. Translocation mechanism of SF1 enzymes. Three different steps associated with the translocation process of PcrA are shown (a-c). The top row shows molecular contacts based on crystal structures of translocation intermediates. Protein residues are in yellow, and the ssDNA is shown as an orange rod, with the bases T12-T17 in cyan. The middle row shows each stage as an analogy with hands gripping a rod to show which domains have tight or loose grips on the bound ssDNA. The bottom row depicts the structural data in the top row in cartoon form showing the locations of pockets (A-D) on the enzyme responsible for binding the nucleotide bases of the bound ssDNA. Adapted from Singleton et al. 2007.

The active rolling model requires a dimeric enzyme in which the two subunits bind alternatively to ssDNA and dsDNA at the ssDNA/dsDNA junction (Lohman & Bjornson, 1996). Initially, both subunits of the dimer are bound to ssDNA. Upon ATP binding, one of the subunit releases ssDNA and binds to the duplex region (Figure 12A). The helix destabilization and the release of one of the DNA strand take place following the hydrolysis of ATP. The best example of active rolling mechanism is DNA unwinding by the Rep helicase (SF1 type). In the absence of DNA, the Rep protein exists as a monomer. Upon DNA binding, it changes its conformation and forms a homodimer. The Rep dimer unwinds DNA by an active rolling mechanism in which the two subunits alternate in binding dsDNA and 3'ssDNA at the ssDNA/dsDNA junction. In this model, translocation along ssDNA is coupled to ATP binding, whereas ATP hydrolysis drives the unwinding of multiple DNA base pairs for each catalytic event (Hsieh *et al.*, 1999; Delagoutte & von Hippel, 2002).

Recent structural studies on the SF1A helicase, UvrD, suggested that DNA unwinding occurs by a combined "wrench-and-inchworm" mechanism (Lee & Yang, 2006). In this case, ATP binding (1st step) induces domain closing between 2A and 1A/1B/2B, which leads to the separation of the first base pair (-1) at the ds-ss junction (Figure 14). During this step, the rearrangement of the +4 nt and exit of the +5 nt prepare the ssDNA for translocation. In the second step (after ATP hydrolysis), release of ADP and Pi leads to domain opening and ssDNA translocation. These two steps complete the unwinding and translocation of 1 bp.

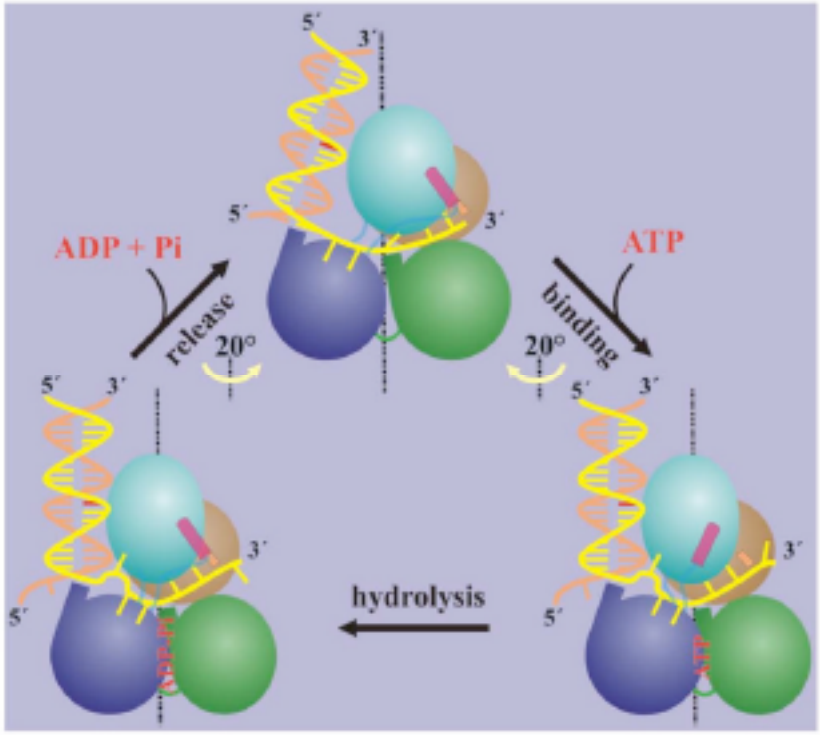

Figure 14. Cartoon presentation of the "Wrench-and-inchworm mechanism" for DNA unwinding. Each domain is color-coded: Green – domain 1A; Brown – domain 1B; Violet – domain 2A; Blue – domain 2B. The gating helix is highlighted in pink.

3.3.4. Helicase functions

Helicases are implicated in various nuclear processes ranging from DNA replication to ATP-dependent chromatin remodeling (Gorbalenya & Koonin, 1993; Singleton & Wigley, 2002; Becker & Horz, 2002; von Hippel & Delagoutte, 2003). They have been first characterized as nucleic-acid dependent ATPases (Wickner *et al.*, 1974; Richet & Kohiyama, 1976; Abdel-Monem *et al.*, 1977). Studies over the past four decades have established that helicases are motor proteins that utilize the energy derived from NTP hydrolysis to translocate along double or single stranded nucleic acids (Figure 15a).

Most of the proteins containing helicase motifs have the ability to catalyze the unwinding of duplex nucleic acids (Mackintosh & Raney, 2006; Wu & Hickson, 2006) (Figure 15b). The basic unwinding reaction catalyzed by all known DNA helicases is similar. They all share the following common biochemical properties: nucleic-acid binding; NTP binding; nucleic-acid stimulated hydrolysis of NTP; NTP/dNTP hydrolysis dependent unwinding of duplex nucleic acids with specific polarity (Tuteja & Tuteja, 2004).

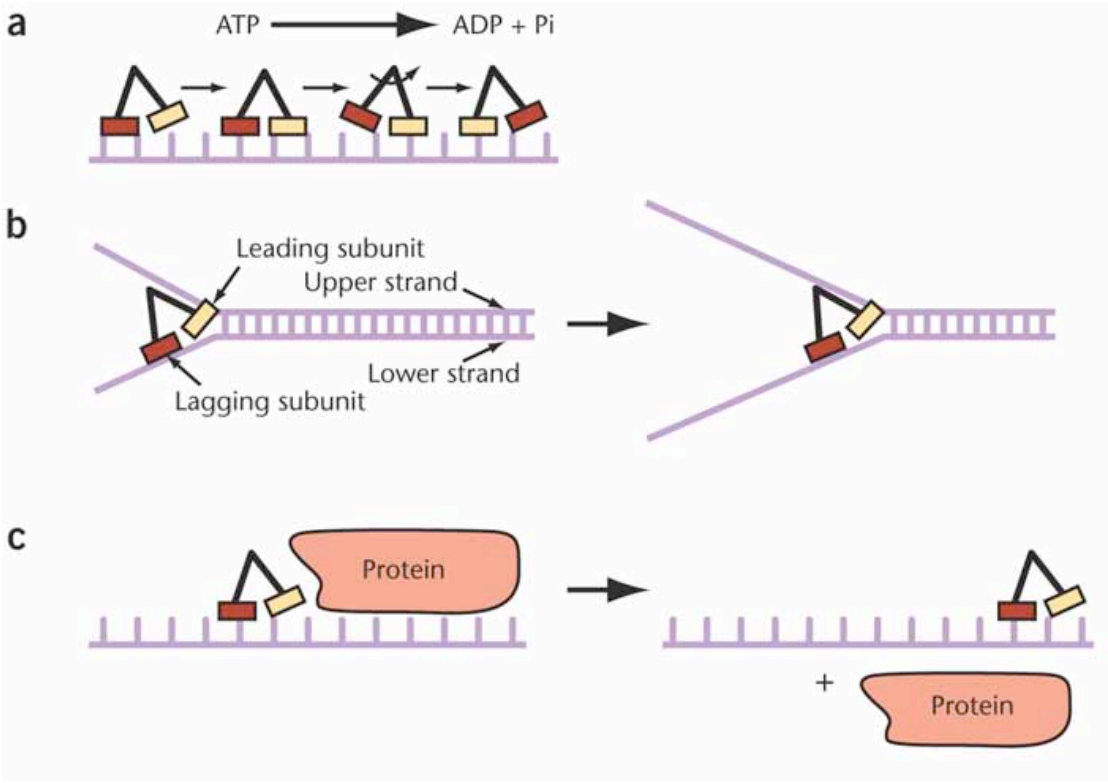

Figure 15. Overview of the helicase functions. (a) Classical motor protein mechanism for the movement of a helicase along a single-stranded nucleic acid. The helicase representation used can correspond either to a monomeric helicase with two alternatively binding foot domains or to a dimeric helicase with alternatively binding subunits (leading and lagging subunits). (b) Helicase driven unwinding of double-stranded nucleic acid. (c) Helicase driven displacement of a bound protein complex from ssDNA or ssRNA. Adapted from von Hippel, 2004.

Recent studies have also shown that some helicases can disrupt protein/DNA or protein/RNA complexes (Jankowsky *et al.*, 2001; Linder *et al.*, 2001; Krejci *et al.*, 2003; Fairman *et al.*, 2004; Flores *et al.*, 2005; Hu *et al.*, 2007; Bugreev *et al.*, 2007) (Figure 15c). These studies indicated that helicases also carry out functions that have nothing to do with opening base pairs. Rather, they are shown to translocate along DNA or RNA to remove or rearrange proteins that are bound to their nucleic-acid tracks. In some cases, the helicases do so by interacting directly with the target proteins.

More specialized function have also been reported for helicases that are governed by the presence of additional functional domains in their flanking regions. For instance, cooperation of helicase with a nuclease domain (Huang *et al*., 1998; Komori *et al*., 2004), a type IA topoisomerase domain (Déclais *et al*., 2000) and a strand-annealing domain (Bachrati & Hickson, 2008) is common in members of the SF2 superfamily. More details on novel functions of the helicases are discussed in the following sections.

3.4. RecQ Family of DNA Helicases

3.4.1. Introduction

The RecQ family of helicases, belonging to SF2, is one of the most highly conserved groups of DNA helicases (Bachrati & Hickson, 2003; Bachrati & Hickson, 2008). While bacteria and lower eukaryotes such as yeast have a single RecQ homologue, the number of *RecQ* gene present in higher eukaryotes varies from two to seven (Gangloff *et al*., 1994; Nakayama, 2002; Bachrati & Hickson, 2008) (see Figure 17). To date, at least two, four, five and seven RecQ homologues were found in *Drosophila*, *C.elegans*, mammals and plants, respectively (Kusano *et al*., 1999; Hartung & Puchta, 2006; Hanada & Hickson, 2007; Bachrati & Hickson, 2007). Five RecQ family genes that have been identified in humans are designated as RECQ1, BLM (RECQ2), WRN (RECQ3), RECQ4 and RECQ5 (Puranam & Blackshear, 1994; Ellis *et al*., 1995; Yu *et al*., 1996; Kitao *et al*., 1998; Kitao *et al*., 1999) (see Figure 17).

Clinical and experimental evidences suggested that the RecQ helicases contribute to the maintenance of genome stability across various species (Fukuchi *et al*., 1989; German, 1993; Gangloff *et al*., 1994; Hanada *et al*., 1997; Lindor *et al*., 2000; Siitonen *et al*., 2003; Van Maldergem *et al*., 2006). Currently, the intense interest in understanding the biology of RecQ helicases is driven largely by their connection with human genetic diseases.

Defects in at least three (BLM, WRN and RECQ4) of five human RecQ homologues are responsible for defined genetic syndromes (Figure 16). Mutations in BLM and WRN lead to Bloom's syndrome and Werner's syndrome, respectively (Ellis *et al*., 1995; Yu *et al*., 1996). Mutations in RECQ4 results in at least three different RECQ4 syndromes namely Rothmund-Thomson syndrome (RTS), RAPADILINO and Baller-Gerold syndrome (BGS) (Kitao *et al*., 1999; Siitonen *et al*., 2003; Van Maldergem *et al*., 2006). Indeed, each syndrome exhibits different phenotypes. However, all are characterized by an increased predisposition to cancer, which is consistent with increased chromosomal aberrations and hypermutability observed in cultured cells (Hanada & Hickson, 2007). More details on these syndromes are described in the next sections.

All the members of the RecQ helicase family contain the conserved set of seven helicase-motifs characteristic of SF2 helicases (Bachrati & Hickson, 2003). Apart from

the conserved helicase motifs, most of the RecQ family members also contain two other conserved domains: the RQC (**Rec**Q **C**-terminal) and HRDC (**H**elicase and **R**Nase**D C**-terminal) domains (Liu *et al*., 1999; Bachrati & Hickson, 2003; Bernstein and Keck, 2003) (Figure 17). Recent structural studies on the *E.coli* RecQ helicase revealed that the RQC domain is comprised of the Zinc (Zn^{2+})-binding motif and the **W**inged-**H**elix (WH) domain (Bernstein *et al*., 2003). As the name suggests, the Zn^{2+}-binding motif is responsible for the binding of Zn^{2+} metal ion and is shown to be important for the stability and the DNA binding ability of many RecQ proteins (Bernstein *et al*., 2003; Janscak *et al*., 2003; Ren *et al*., 2008). Whereas, the WH domain serves as a double-stranded DNA (dsDNA)-binding motif, and also in few RecQ's, it facilitates their interaction with other proteins (Bernstein *et al*., 2003; Lee *et al*., 2005). The RQC domain along with the conserved helicase motifs constitutes the catalytic core of the RecQ enzymes. The HRDC domain in some RecQ helicases has been proposed to serve as an auxiliary DNA-binding domain (Liu *et al*., 1999; Bernstein and Keck, 2003; Janscak *et al*., 2003). Recent evidence also suggested that this domain in BLM confers DNA structure specificity to the protein (Wu *et al*., 2005).

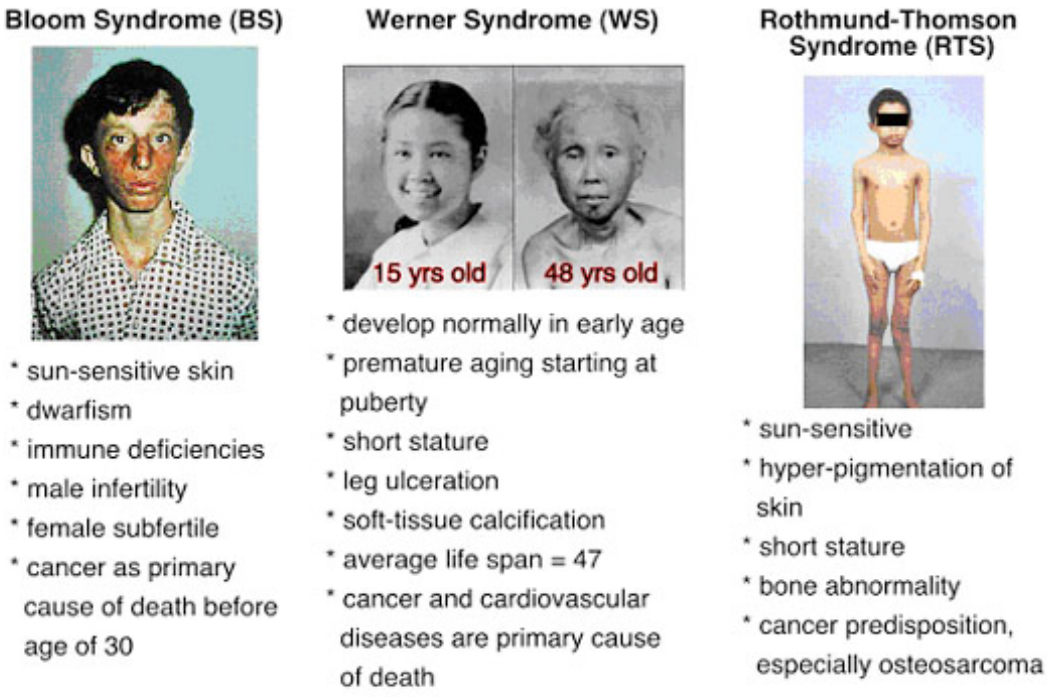

Figure 16. Human RecQ syndromes. Various disease symptoms exhibited by different RecQ deficient patients are listed below. Adpated from http://radonc.yale.edu/faculty/liu.html

Most eukaryotic RecQ family members usually have additional N- and C- terminal domains flanking the RecQ core (Figure 17). Earlier studies have revealed that the additional regions are required for mediating protein-protein interactions (Bachrati & Hickson, 2003). Recent studies revealed that, in some cases, the additional domain codes for the specialized function of the RecQ protein (Huang *et al*., 1998; Shen *et al*., 1998; Opresko *et al*., 2004; Garcia *et al*., 2004; Sangrithi *et al*., 2005). More details on novel functions of the RecQ helicases are described in the next sections.

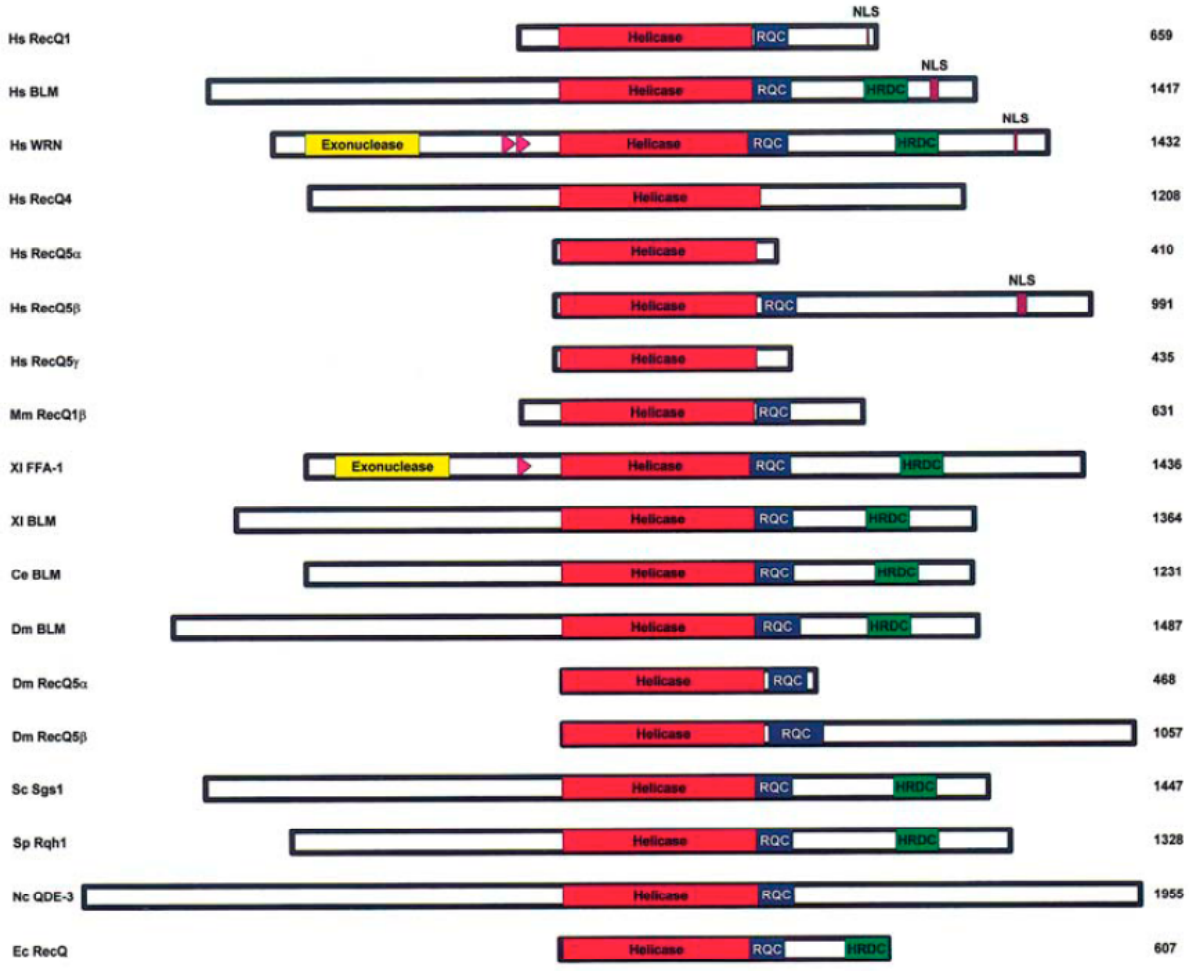

Figure 17. Scheme of RecQ helicases present in various organisms. The name of each polypeptide is indicated on the left. Hs, Mm, Xl, Ce, Dm, Sc and Sp stands for *Homo sapiens*, *Mus musculus*, *Xenopus laevis*, *Caenorhabditis elegans*, *Drosophila melanogaster*, *Saccharomyces cerevisiae* and *Schizosacharomyces pombe*, respectively. The length of each protein (in amino acids) is indicated on the right. The conserved helicase, RQC and HRDC domains are depicted in red, blue and green respectively. The conserved exonuclease domain of WRN and FFA-1 (Xenopus homologue of WRN) is shown in yellow. The 27-amino-acid direct repeat of WRN and FFA-1 is indicated by pink triangle. The regions marked "NLS" stands for Nuclear Localization Signal of the respective protein. Adapted from Bachrati & Hickson, 2003.

Numerous enzymatic activities have been reported and characterized for the RecQ proteins *in vitro* (Hanada & Hickson, 2007). They possess a DNA dependent ATPase and an ATP dependent 3' - 5' DNA helicase activity. They can also mediate the annealing of complementary single strands of DNA. RecQ enzymes are proficient in the branch migration of Holliday junctions. Also, RecQ helicases have been shown to bind and unwind variety of DNA structures that includes DNA replication, recombination and repair intermediates such as forked DNA, G4-quadruplex DNA, DNA displacement loops (D-loops), DNA containing double Holliday junctions (DHJs) and triplex DNA (Bachrati & Hickson, 2003). The preferred substrates for the RecQ helicases are presented in Figure 18.

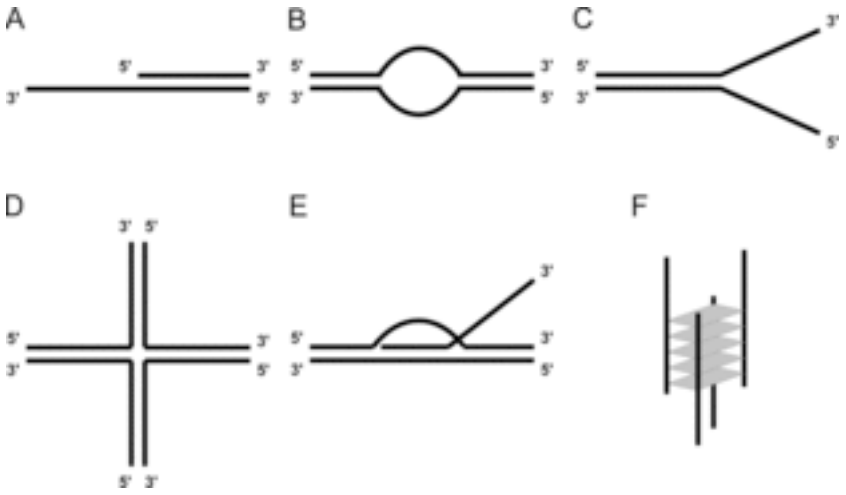

Figure 18. Preferred substrates for the RecQ helicases. A) 3'-tailed duplex, B) bubble substrate, C) Forked duplex, D) Holliday junction, E) D-loop, F) G-quadruplex structure. Adapted from Cheok *et al*., 2005.

Recent studies have demonstrated that RecQ proteins combine DNA strand-annealing and helicase activities to promote fork-regression/strand-exchange on model replication fork substrates (Machwe *et al*., 2005; Ralf *et al*., 2006; Kanagaraj *et al*., 2006; Machwe *et al*., 2006). Also, some RecQ helicases were shown capable of displacing proteins from DNA (Hu *et al*., 2007; Bugreev *et al*., 2007).

3.4.2. The *Escherichia coli* RecQ

3.4.2.1. Domain organization and structure

The *Escherichia coli* (*E. coli*) RecQ gene was identified during a screen for mutants resistant to thymine starvation (Nakayama et al., 1984). Following this finding, genetic mapping and cloning of the RecQ gene was achieved (Nakayama et al., 1984; Nakayama et al., 1985). Later, the same group determined the primary structure of RecQ from the nucleotide sequence of the cloned gene (Irino et al., 1986; Umezu et al., 1990) (Figure 19). The *E. coli* RecQ gene codes for a protein of length of 610 amino acids. The *E.coli* RecQ protein was purified and shown to possess an ATP dependent 3' – 5' DNA helicase activity (Umezu et al., 1990).

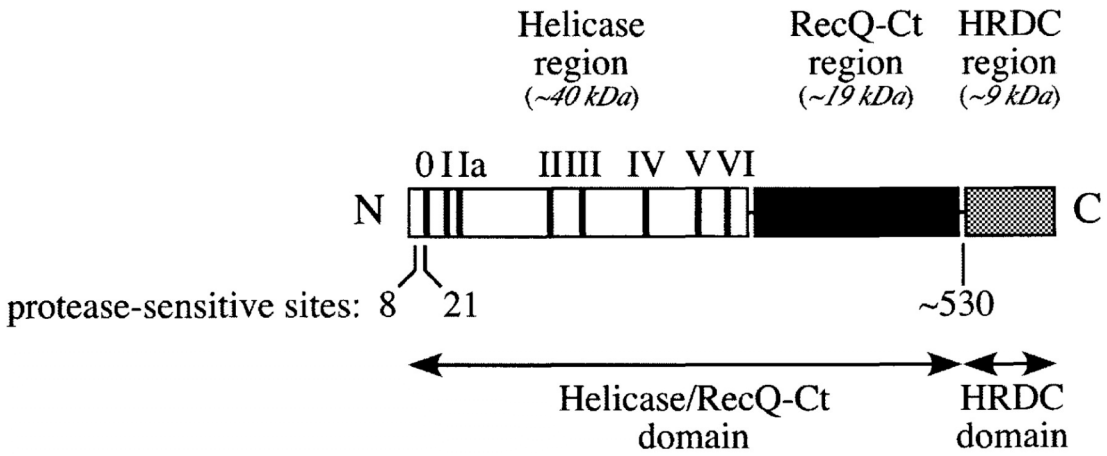

Figure 19. Schematic diagram of *E.coli* RecQ. Adapted from Bernstein & Keck, 2003.

Like most helicases, *E.coli* RecQ possesses seven conserved motifs namely I, Ia, II, III, IV, V and VI (Nakayama, 2005). These motifs are located in a region comprised of about 350 amino acids (helicase region). In addition, motif 0 was found to be present in *E.coli* RecQ (Bernstein & Keck, 2003). Besides the helicase region, two additional domains, RecQ-Ct and HRDC domain (see previous section for more details), that are characteristic of most RecQ helicases are also present in *E.coli* RecQ (Bernstein & Keck 2003) (Figure 19). Limited proteolysis of *E.coli* RecQ revealed that the enzyme has a two-domain structure consisting of a larger domain comprising the helicase and RecQ-Ct (RQC) regions and a smaller domain constituted by the HRDC region (Bernstein & Keck, 2003). Functional studies have revealed that the large domain, although unable to stably bind DNA, is sufficient to exhibit normal levels of the ATPase and helicase activities *in vitro*. Hence, this domain is considered to be the

catalytic core of the *E.coli* RecQ enzyme. Additionally, the removal of the first 20 N-terminal residues (including a part of motif 0) from *E.coli* RecQ dramatically decreased the helicase and ATPase activities but not the DNA binding ability of the enzyme.

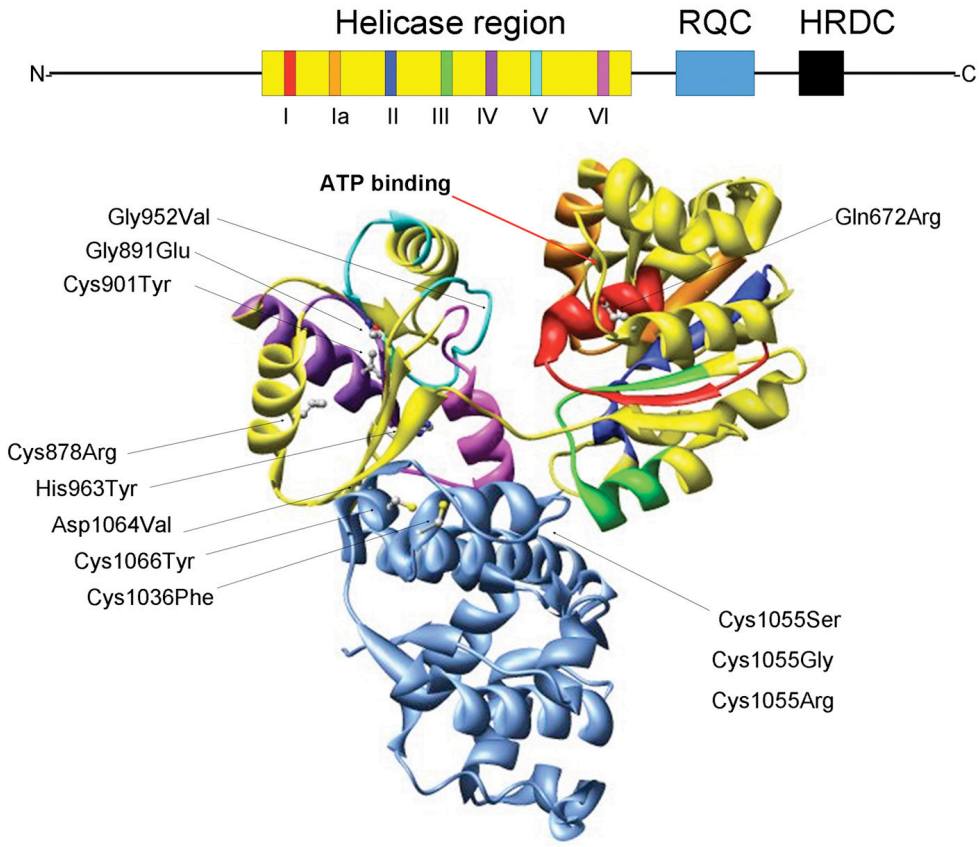

Figure 20. Structure of the catalytic core of *E.coli* RecQ. Subdomains consisting the helicase and RecQ-Ct regions are shown in yellow and blue ribbons, respectively. Adapted from Bernstein & Keck, 2003.

Structural analysis of the catalytic core of *E.coli* RecQ has revealed that it consist of four subdomains: two subdomains are constituted by the helicase region and two other subdomains are formed by the RecQ-Ct region (Bernstein et al., 2003) (Figure 20). The helicase subdomains form a deep cleft, the walls of which are lined by the helicase motifs including motif 0 (Figure 20). The proximal RecQ-Ct subdomain is involved in Zinc (Zn^{2+}) binding, whereas the distal RecQ-Ct subdomain adopts a helix-turn-helix structure called winged helix (WH), known to bind DNA. It has been proposed that the cleft between the two RecQ-Ct subdomains could serve as a binding site for double-stranded (ds) DNA (Bernstein et al., 2003). More recently, crystal structure of the *E.coli* RecQ HRDC domain was solved (Bernstein & Keck, 2005). The HRDC domain adopted a globular fold and was preferentially bound to single-stranded DNA. Further, mutational studies of the HRDC domain in the full-length *E.coli* RecQ revealed that it is

important for the structure specific DNA binding ability of the enzyme (Bernstein & Keck, 2005).

3.4.2.2. Biochemical properties

An important feature of *E.coli* RecQ is that it does not require free DNA ends to initiate unwinding of the DNA substrate (Harmon & Kowalczykowski, 2001). Also, in comparison with other RecQ helicases, the *E.coli* RecQ protein exhibits a wider substrate specificity and a higher processivity. It is able to unwind long partial and blunt ended duplexes (Bachrati & Hickson, 2003). Addition of *E.coli* single-stranded DNA binding (SSB) protein to the helicase reaction enhances the DNA unwinding activity of *E.coli* RecQ by increasing both the initial rate and the extent of unwinding (Umezu & Nakayama, 1993; Harmon & Kowalczykowski, 2001). Other substrates that are unwound by *E.coli* RecQ *in vitro* are replication fork-like structures, four-way/three-way junctions, D-loops and G-quadruplex structures (Harmon & Kowalczykowski, 2001; Wu & Maizels, 2001; Bachrati & Hickson, 2003). Unlike other RecQ helicases, *E.coli* RecQ shows a very poor DNA branch-migration activity (Bachrati & Hickson, 2003). The quaternary structure of the functional form of *E.coli* RecQ is still unclear and contradictory reports are available in this regard. Earlier report on the basis of kinetic studies suggested that the enzyme exist as an oligomer (Harmon & Kowalczykowski, 2001). But the gel filtration studies conducted later suggested that the enzyme exists as a monomer in solution (Xu et al., 2003).

E.coli RecQ together with SSB was shown to promote the joint molecule formation by *E.coli* RecA *in vitro*, using fully duplexed DNA and supercoiled plasmid (Harmon & Kowalczykowski, 1998) (Figure 21). Based on this data, it was proposed that *E.coli* RecQ is involved in the initiation of recombination. The recombination intermediates formed in this reaction are also disrupted by the helicase activity of *E.coli* RecQ (Harmon & Kowalczykowski, 1998) (Figure 21). Hence, *E.coli* RecQ is called anti-recombinase. Also, in the presence of SSB, *E.coli* RecQ can unwound covalently closed plasmids, generating a substrate for topoisomerase III (Topo III) (Harmon et al., 1999). A combination of RecQ, Topo III and SSB has been shown to give rise to several forms of fully catenated, covalently closed plasmid multimers (Harmon et al., 1999; Harmon et al., 2003). These data demonstrated that the *E.coli* RecQ helicase may act late in recombination together with Topo III. Also, *E.coli* RecQ specifically binds and unwinds

DNA substrates that mimic a stalled replication fork with a gap in the leading strand (Hishida et al., 2004) (see Figure 22).

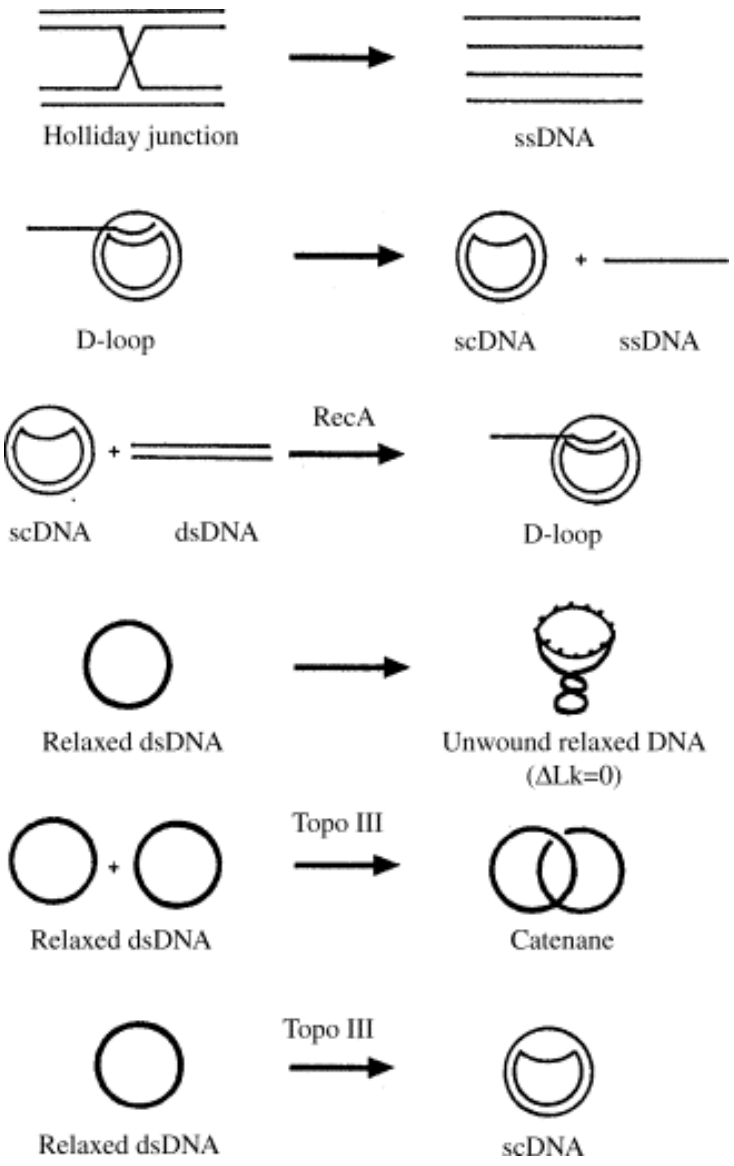

Figure 21. Examples of *E.coli* RecQ catalyzed reactions. See the text for more details. Adapted from Nakayama, 2005

3.4.2.3. Cellular functions

At the cellular level, *E.coli* RecQ has been shown to play crucial roles in both DNA recombination and DNA replication (Heyer, 2004; Nakayama, 2005; Magner et al., 2007). Earlier studies revealed that in *recBC sbcB* cells, *E.coli* RecQ mutations enhance UV sensitivity and decrease the efficiency of conjugational recombination (Nakayama et al., 1984). Further these studies showed that in the absence of RecBCD pathway, *E.coli* RecQ catalyzed recombination on DNA substrates that contain gaps and nicks. They do

so by participating in the RecF pathway that includes RecA, RecF, RecG, RecJ, RecO, RecR and RuvABC proteins. Further, it was shown that the rate of illegitimate recombination was enhanced 30 – 300 fold in *E.coli* RecQ mutants (Hanada et al., 1997). This anti-recombination function of RecQ now seems to be conserved among some eukaryotic RecQ proteins (Gangloff et al., 1994; Hu et al., 2007; Bugreev et al., 2007) (Figure 22B). A recent study has also shown that *E.coli* RecQ promotes the net accumulation of bimolecular recombination intermediates (BRIs) *in vivo*, suggesting a pro-recombination function for the RecQ proteins (Magner et al., 2007).

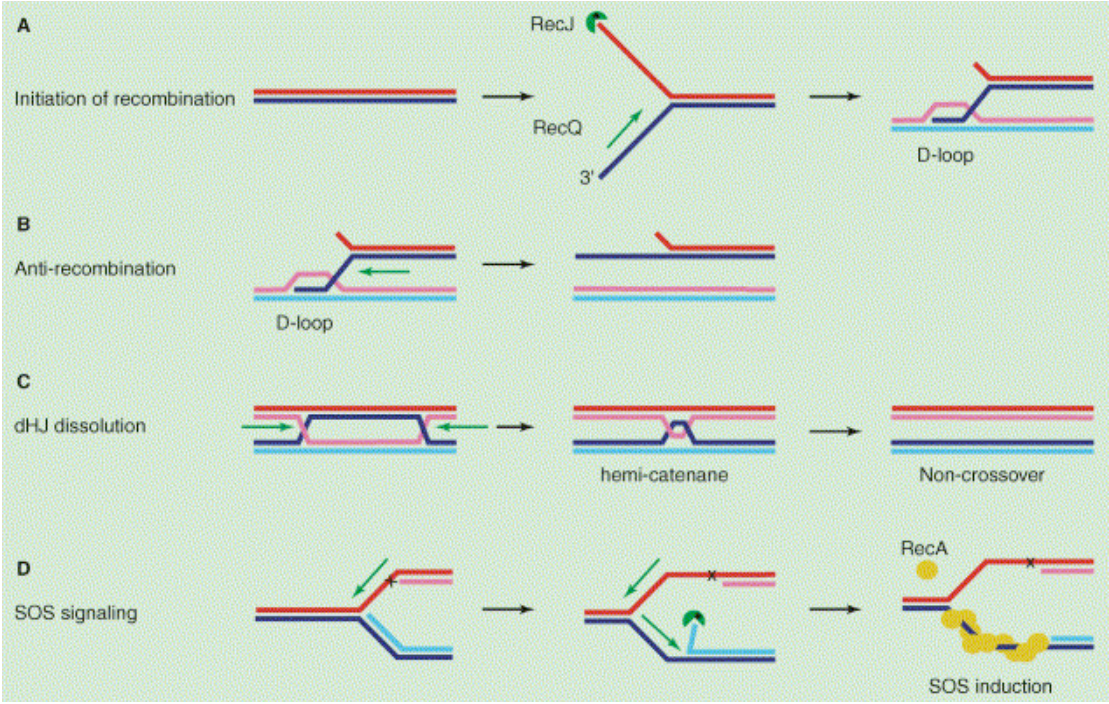

Figure 22. Proposed roles of *E.coli* RecQ DNA helicase in genome maintenance. Details are explained in the text. Adapted from Heyer, 2004.

Two different roles of *E.coli* RecQ helicase had been demonstrated in chromosomal replication (Courcelle & Hanawalt, 1999; Courcelle et al., 2003; Chow & Courcelle, 2004; Hishida et al., 2004). First, RecQ can function as a road-block remover i.e., the unwinding of secondary structures on the template strand that block replication. In agreement with this hypothesis, it has been shown that *E.coli* RecQ allows DNA replication to pass through a hairpin structure on the template strand (Cromie et al., 2000). Other replication-blocking structures such as G4 tetraplex DNA also serve as good substrates for *E.coli* RecQ *in vitro* (Wu & Maizels, 2001). The second function of RecQ is the processing of arrested/stalled replication forks. It has

been shown in *E.coli* that when the replication fork is stalled by a blockade, the nascent lagging-strand DNA is degraded by the combined action of RecQ helicase and RecJ exonuclease (Courcelle & Hanawalt, 1999; Courcelle et al., 2003; Chow & Courcelle, 2004) (Figure 22A). This process is controlled by other recombination proteins in the RecF pathway namely RecFOR proteins. As a result, extended single-stranded regions are formed on the lagging strand template that would facilitate the loading of RecA to this site in the presence of RecFOR (Chow & Courcelle, 2004). Recent evidence had shown that the RecA loading not only provides protection to stalled replication forks but also generates the SOS signal (Hishida et al., 2004) (Figure 22D).

3.4.3. Sgs1

3.4.3.1. Discovery

Sgs1, the sole RecQ helicase in the budding yeast *Saccharomyces cerevisiae*, was identified independently by three different groups. Gangloff et al., first isolated *sgs1* in a screen for suppressors of the top3 slow growth phenotype (Gangloff et al., 1994). Later, Hickson's group identified the same gene in a yeast two-hybrid screen for interaction partners of topoisomerase II (Watt et al., 1995). Also, Lu et al., isolated the *sgs1* gene based on its genetic interaction with mutations in topoisomerase I (Lu et al., 1996).

3.4.3.2. Cellular phenotypes of Sgs1 deficiency

sgs1 mutants showed more than 50% decrease in lifespan compared with wild-type cells (Sinclair et al., 1997; Mankouri & Morgan, 2001). *sgs1* mutants displayed intra- and inter-chromosome hyper-recombination, elevated frequency of sister-chromatid exchanges (SCEs), gross chromosomal rearrangements and all types of loss-of-heterozygosity events (Bachrati & Hickson, 2003; Khakhar et al., 2003; Wu & Hickson, 2006). They also showed an increased rate of illegitimate recombination (Yamagata et al., 1998). Mutations in *sgs1* suppresses the severe growth and viability defects of *top3*Δ or *rmi*1Δ mutants, suggesting that Sgs1 acts upstream of these genes (Wu & Hickson, 2006). Double mutants of the *sgs1* and the telomerase RNA component (either *tlc1* or *est2*) showed an increased rate of telomere shortening, suggesting a role for Sgs1 in telomere maintenance (Hickson, 2003). *sgs1* null strains were hypersensitive to UV light (Miyajima et al., 2000; Mullen et al., 2000), methylmethane sulfonate (MMS) (Gangloff et al., 2000; Saffi et al., 2000) and hydroxyurea (HU) (Miyajima et al., 2000).

3.4.3.3. Domain structure

The *Sgs1* gene encodes a 1447 amino acid protein with a predicted molecular mass of 164 kDa. Based on its primary structure, Sgs1 protein can be divided into two parts: i) a non-conserved N-terminal region and ii) a C-terminal region containing the conserved domains of RECQ helicases i.e., helicase motifs, RQC and HRDC domains. The primary structure of the protein is similar to the human BLM helicase (see Figure 17).

3.4.3.4. Biochemical properties

Noone has been successful in the expression and purification of full-length Sgs1 so far. Biochemical studies were performed with a deletion variant of Sgs1 spanning aminoacids 400 to 1268 ($Sgs1^{400\text{-}1268}$). Wang group showed that the purified protein

displayed an ATP- and dATP-dependent 3'-5' helicase activity (Bennett et al., 1998). In addition, Sgs1 was shown to unwind DNA/RNA heteroduplexes. Later, the same group showed that Sgs1 is proficient in binding and unwinding of forked DNA structures, three-way and four-way junctions (Bennett et al., 1999). Also, Sgs1 was shown to unwind the G4-quadruplex structures (Sun et al., 1999; Huber et al., 2002).

3.4.3.5. Interaction partners and cellular roles

Sgs1 has been shown to play multiple roles in DNA metabolism (Cobb & Bjergbaek, 2006). The major interaction partners of Sgs1 are topoisomerases. Sgs1 has been shown to physically and genetically interact with all three nuclear topoisomerases: topoisomerase I, II and III (Gangloff et al., 1994; Watt et al., 1995; Lu et al., 1996). The role of topoisomerase I - Sgs1 complex has not been identified yet. Topoisomerase II and Sgs1 have been reported to act together to avoid chromosome non-disjunction, suggesting that they are involved in the same pathway for chromosome segregation (Watt et al., 1996). Based on the primary structure and genetic studies, Sgs1 is considered as the yeast homologue of human BLM helicase, and hence it was proposed that Sgs1 in concert with topoisomerase III can dissolve double Holliday junctions (DHJs) (Ira et al., 2003). Such activity is important for the suppression of crossing-over during DSB repair by homologous recombination (HR). Consistent with this, *sgs1*Δ mutants were shown to accumulate RAD51-dependent X-shaped molecules during perturbed S-phase (Liberi et al., 2005). Two recent studies have identified a third member of the Sgs1-topoisomerase III complex termed Rmi1/NCE4 (Chang et al., 2005; Mullen et al., 2005). Functional studies revealed that Rmi1 is a structure-specific DNA binding protein with a preference for cruciform structures. Based on these evidences, the authors proposed that the DNA binding specificity of Rmi1 plays a crucial role in targeting Sgs1-topoisomerase III to appropriate DNA structures (Mullen et al., 2005). Recent studies have shown that Sgs1 play a crucial function in meiotic HR (Oh et al., 2007). In this report, it has been shown that absence of Sgs1 in cells lead to the formation of higher levels of joint molecules (JMs) that comprise three and four interconnected duplexes (Figure 23). Further, the authors provide direct *in vivo* evidence suggesting that Sgs1 suppresses DHJ formation between sister chromatids.

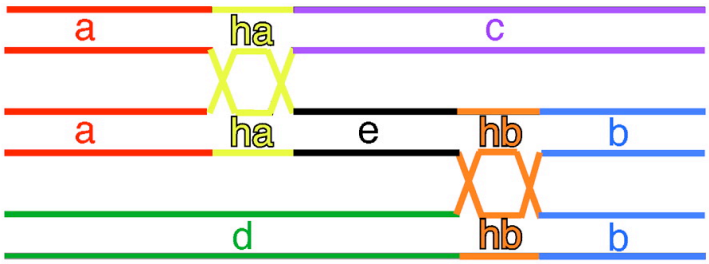

Figure 23. Cartoon representation of ternary JMs formed in *sgs1* mutants. Adapted from Oh et al., 2007.

Analysis of DNA replication using DNA combing revealed that in cells lacking Sgs1, replication forks progressed more quickly through much of the genome than in wild-type cells (Versini et al., 2003). On the basis of this study, it has been proposed that Sgs1 protein modulates replication fork progression in the absence of exogenous damage. Indeed, Sgs1 exhibited a focal distribution in S phase that coincides with some sites of *de novo* DNA synthesis during S phase (Frei & Gasser, 2000). Moreover, chromatin immunoprecipitation (ChIP) experiments revealed that Sgs1 binds to unperturbed replication forks (Cobb et al., 2003). Also, Sgs1 was shown to be required for the stabilization of arrested replication forks. In cells without Sgs1, polε and other factors failed to remain associated with the stalled fork and, as a consequence, the reestablishment of replication was impaired (Cohen & Sinclair, 2001; Cobb et al., 2003; Bjergbaek et al., 2005). Sgs1 also plays a role in S-phase checkpoint signaling after DNA damage that is redundant with Rad24 (Frei & Gasser, 2000). It has been shown that *rad24 sgs1* double mutants have a severely compromised intra-S-phase checkpoint and fail to suppress late-origin firing in the presence of DNA damage. All these data suggested that there is a link between the Sgs1 helicase and the DNA replication process.

3.4.4. RECQ1

3.4.4.1. *RECQ1* gene and phenotypic consequences of its dysfunction

RECQ1 or RECQL was the first human RecQ helicase to be identified. The cDNA encoding human RECQ1 was cloned by two groups independently (Puranam & Blackshear, 1994; Seki et al., 1994). It is the shortest human RecQ protein made of 649 amino acids with a predicted molecular mass of 73 kDa. The *RECQ1* gene is located on chromosome 12p11-12 (Puranam & Blackshear, 1994; Puranam et al., 1995). This chromosomal location has been found to coincide with cytogenetic alterations in testicular germ-cell tumors (Suijkerbuijk et al., 1993). Also, RECQ1 is differentially upregulated in transformed cells or cells that are actively proliferating (Kawabe et al., 2000). Interestingly, no genetic disorder has been reported to occur due to mutation in RECQ1. But, recent analysis has revealed an association of RECQ1 with a reduced survival of pancreatic cancer patients (Li, Frazier et al., 2006; Li, Liu et al., 2006).

Knockout studies using chicken DT40 cells have shown that RECQ1 has a role in promoting cell viability only in the absence of Bloom syndrome helicase (BLM), indicating a back up function (Wang et al., 2003). However, knockout studies in mice have shown that both BLM and RECQ1 have non-redundant roles in suppressing crossovers (Sharma et al., 2007). Cytogenetic analysis of embryonic fibroblasts from RECQ1-deficient mice revealed aneuploidy, spontaneous chromosomal breakage and frequent translocation events. These observations suggest that RECQ1 play a vital role in the maintenance of genomic stability.

3.4.4.2. Biochemical properties

A 73 kDa ATPase, called ATPase Q1 (now identified as RECQ1), was purified and shown to exhibit 3' – 5' helicase activity (Seki et al., 1994). Analytical ultracentrifugation, gel-filtration and dynamic light scattering analysis revealed that the purified human RECQ1 protein exist as dimer in the presence or absence of DNA (Cui et al., 2003; Cui et al., 2004). Recently, the same group showed that RECQ1 exist in two assembly states i.e., higher order oligomers consistent with pentamers or hexamers, and smaller oligmers consistent with monomers or dimers (Muzzolini et al., 2007). Further, they showed that the presence of ssDNA and nucleotide co-factors (ATP or ATPγS) favoured the oligomeric form of the protein.

RecQ1 alone exhibited a poor helicase activity and it was capable of unwinding only short partial duplexes. In the presence of human replication protein A (hRPA), it displayed an enhanced processivity and could unwind partial duplexes upto 501 bp long (Cui et al., 2004). RecQ1 was also shown to unwind other substrates such as Holliday junctions and D-loops (Sharma et al., 2005). Apart from helicase activity, RECQ1 protein was shown to possess strand-annealing function (Sharma et al., 2005). Also, it was shown that RECQ1 oligomeric state is associated with the switch from the DNA unwinding to the strand-annealing mode (Muzzolini et al., 2007).

3.4.4.3. Interaction partners and cellular roles

RECQ1 is the most abundant RecQ helicase in human cells (Kawabe et al., 2000). However, very little is known about its cellular function. The first two interaction partners of RECQ1 helicase, Qip1 and Rch1, were identified in a yeast two-hybrid screen for proteins that interact with a C-terminal part of RECQ1 (Seki et al., 1997). These proteins are homologous to importin-α homologues that are involved in nuclear-cytoplasmic transport. Also, RECQ1 was found to interact directly with hRPA and hRPA was shown to stimulate the helicase activity of RECQ1 (Cui et al., 2004). Physical and functional interaction of RECQ1 with the mismatch-repair proteins MutSα and EXO1 was also reported (Doherty et al., 2005).

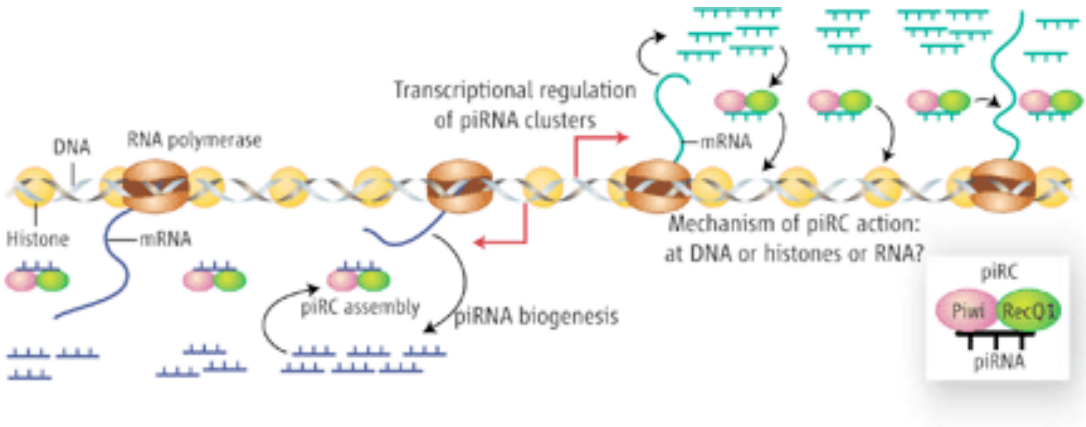

Figure 24. Schematic diagram showing the assembly of piRC complexes containing piRNAs, Piwi and RecQ1. Shown here is a genomic region that generates a cluster of piRNAs. The left side of the region generates antisense RNA transcripts (blue) and the right side generates sense transcripts (green). An RNA polymerase of unknown identity is shown in active transcription. These transcripts are processed into 25- to 31- nucleotide piRNAs by an unknown mechanism. piRNAs then associate with Piwi and RecQ1 to form piRC complexes. These complexes might regulate the genome at the level of DNA or histones, or at a posttranscriptional level. Adapted from Carthew, 2006.

RECQ1 deficient cells were shown to be hypersensitive to ionizing radiation and exhibited an increased load of DNA damage, suggesting that RECQ1 has a unique cellular role in DNA repair (Sharma et al., 2007). More recently, RECQ1 was identified as a member of a piRNA protein complex that is important for gene silencing (Lau et al., 2006) (Figure 24). Also, the mechanistic similarities between piRNA synthesis and DNA replication processes (Bateman & Wu, 2007) reveal that RECQ1 and its associated DNA replication/repair proteins may function together in piRNA biogenesis (Figure 24). Interestingly, QDE-3, the RECQ1 homologue of *Neurospora crassa* has also been implicated in gene silencing (Cogoni & Macino, 1999). More future studies are required to find out the exact role of RECQ1 in gene silencing and chromosomal stability maintenance.

3.4.5. The Bloom syndrome helicase

3.4.5.1. Bloom syndrome

Bloom syndrome (BS) is an extremely rare, autosomal, recessive genetic disorder of humans (Bloom, 1954). It is caused by the genetic defects in the gene BLM that is located on chromosome 15q26.1 (Bachrati & Hickson, 2003). The first incidence of BS was reported in 1954 (Bloom, 1954). BS is characterized by stunted growth, disproportionately small head and unusual skull/facial configuration. The skin present on the nose and cheeks shows erythema and this can become chronic upon exposure to sun. BS patients show impaired fertility, learning disabilities, moderate mental deficiency and most importantly immune deficiency. Type II diabetes mellitus has also been observed in young patients. BS patients also show a very high incidence of cancers of most types. Leukaemias predominate in childhood, and lymphomas and carcinomas appear during adulthood.

Most of the BLM mutations found in BS are either nonsense mutations or a frameshifts leading to a truncated protein. Approximately, 15% of BS cases are due to missense mutations in BLM and these mostly map to exons encoding the helicase domain of the enzyme (Sanz et al., 2003) (Figure 25).

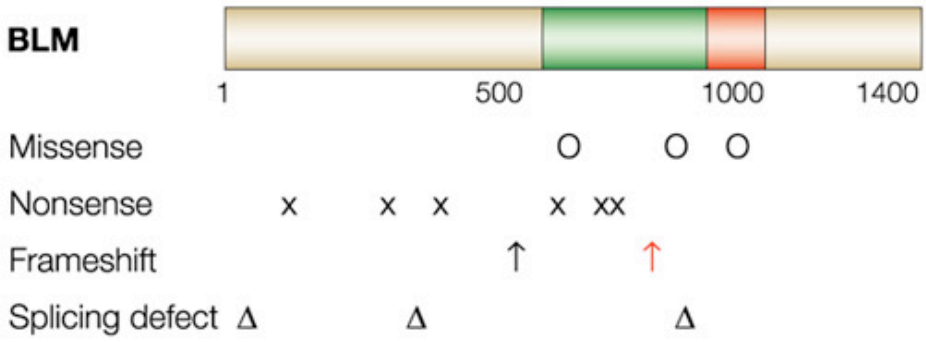

Figure 25. Cartoon diagram showing the positions of mutation identified in BS patients. Helicase and RQC domains are shown in green and orange box, respectively. Adapted from Hickson, 2003.

3.4.5.2. Cellular phenotypes of BLM deficiency

The hallmark feature of BS cells is the elevated frequency of sister chromatid exchanges (SCEs), approximately 10-fold higher as compared to normal cells (Chaganti, 1974; German, 1977). Isolated ES cells, lymphocytes, primary or immortalized fibroblasts of *BLM* knockout mice (Chester et al., 1998; Luo et al., 2000) and *BLM* deficient DT40 cells (Wang et al., 2000; Imamura et al., 2002) all show an

increase in the frequency of SCEs. In clinics, test for SCEs are even carried now to diagnose BS in humans. Moreover, BS cells and BLM deficient fibroblasts were shown to accumulate micronuclei at very high rates (Yankiwski et al., 2000). *BLM* deficient ES and DT40 cells show an elevated frequency of gene targeting (Luo et al., 2000; Wang et al., 2000; Imamura et al., 2002). Increased loss of heterozygosity was also reported in BLM deficient mice (Luo et al., 2000).

Increased sensitivity of BLM deficient cells to treatment with ethyl/methyl methanesulphonate, mitomycin C, 4-nitroquinoline-1-oxide (4NQO), γ-irradiation, radiomimetic drugs, UV radiation, camptothecin (topoisomerase I inhibitor) and hydroxy urea (HU; the ribonucleotide reductase inhibitor) has been reported (Bachrati & Hickson, 2003; Bachrati & Hickson, 2008). Also, BS cells are shown to accumulate abnormal sized DNA replication intermediates (Lonn et al., 1990).

3.4.5.3. Biochemical properties

The BLM protein contains 1417 amino acids. Size-exclusion chromatography indicated that it exists as an oligomer in solution. Electron-microscopy studies showed that BLM formed tetrameric and hexameric ring structures (Karow et al., 1999). These results were supported further by gel-filtration studies conducted using a recombinant N-terminal fragment of BLM, BLM^{1-431}, which indicated that this fragment forms oligomers (Beresten et al., 1999).

BLM can unwind a large variety of DNA structures (Bachrati & Hickson, 2003). Preferred DNA substrates for the BLM helicase are Holliday junctions, G4 DNA and D-loops. BLM is also capable of promoting branch-migration of RecA-generated Holliday junction intermediates up to a distance of 2.7 kilobases (Karow et al., 2000). BLM was also shown to mediate annealing of complementary single-stranded DNA (Cheok et al., 2005) and to promote replication fork regression *in vitro* (Machwe et al., 2005; Ralf et al., 2006). A unique biochemical characteristic of BLM is that, in conjunction with TOPO IIIα, it is able to resolve double Holliday junctions (DHJs) *via* a strand passage mechanism in a reaction termed DHJ dissolution (Wu & Hickson, 2003) It was also shown that the HRDC domain of BLM is important for this dissolution (Wu et al., 2005). This finding explained the molecular basis for the elevated rate of SCEs in BS cells. More recently, it was shown that BLM is responsible for the disruption of RAD51 filaments to prevent aberrant recombination (Bugreev eta al., 2007).

3.4.5.4. Interaction partners and cellular roles

BLM interacts physically and functionally with many proteins that play critical roles in the maintenance of genomic integrity. BLM has been identified as a component of the multienzyme complex, called BASC, that has been partially purifed from human cells. BASC contains BRCA1 and several other DNA surveillance proteins including MLH1, MSH6, MSH2, RFC (replication factor C), RAD50 and ATM (Wang et al., 2000). BLM and BRCA1 have been shown to co-localize in untreated cells to discrete nuclear foci. Treatment of cells with HU greatly increases the percentage of BLM and BRCA1 co-localizing foci (Wang et al., 2000).

Direct physical interaction between BLM and p53 has also been demonstrated *in vivo* (Yang et al., 2002). It was also shown that p53 inhibits the unwinding of Holliday junction by BLM. Physical association of BLM and human RAD51 has been shown *in vivo* and *in vitro*, and the interacting regions on BLM have been mapped to the N- and C-terminal parts of the BLM polypeptide (Wu et al., 2001). Also, MLH1and BLM have been demonstrated to interact directly *in vitro* and *in vivo*. In addition, both proteins co-localize in untreated as well as in aphidicolin treated cells (Pedrazzi et al., 2001). BLM also interacts physically with human single stranded DNA binding protein (hRPA) through a direct interaction with the 70 kDa subunit of hRPA (Brosh et al., 2000). Interaction between BLM and hRPA is required for the hRPA-mediated increase of the processivity of the BLM helicase. Also, the direct interaction between BLM and WRN (another human RecQ helicase) was identified, and it was shown that BLM inhibits the exonuclease activity of WRN (von Kobbe et al., 2002). Telomere proteins TRF1 and TRF2 have been shown to co-localize with BLM. This co-localization occurs in telomere-associated PML bodies. Further, direct interaction between TRF2 and BLM was identified *in vivo* and *in vitro* (Opresko et al., 2002; Stavropoulos et al., 2002). TRF2 has also been found to regulate the helicase activity of BLM *in vitro*. Also, recently it has been found that BLM is present in a complex with five of the known Fanconi Anemia (FA) proteins (termed FANC A, C, E, F and G) (Meetei et al., 2003). These data suggest that there may be a functional connection between BLM and the FANC proteins.

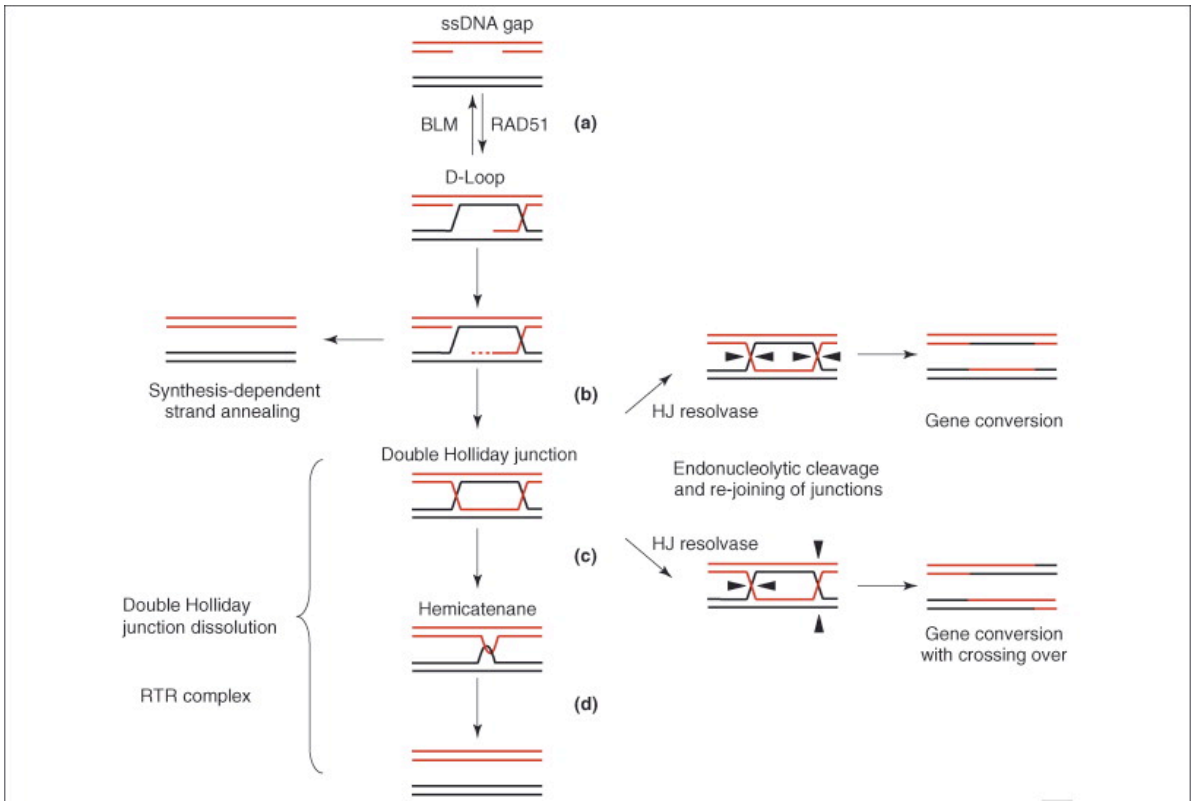

Figure 26. Diagrammatic representation of the putative roles of the BLM-TOPOIIIα-BLAP75/RMI1 (human RTR) complex in processing HR intermediates. (a) RAD51 mediated strand invasion and D-loop formation is shown. (b) If homologous recombination repair does proceed, a key HR intermediate known as the "double Holliday junction" (DHJs) forms. These DHJ intermediates are processed by either the human RTR complex or putative HJ resolvases. Cleavage by HJ resolvases gives either a noncrossover or crossover products. Alternatively, human RTR complex dissolve the DHJ intermediates without any crossing over of genetic material. (c) Branch migrationof individual HJs to create a hemicatenane intermediate. (d) Decatenation of the hemicatenane structures. Adaptd from Mankouri & Hickson, 2007.

BLM and TOPO IIIα co-localize to discrete nuclear foci in exponentially growing cells (Johnson et al., 2000; Wu et al., 2000). Moreover, it was found that TOPO IIIα is not localized correctly in BS cells. Further, the N-terminal 133 residues of BLM are necessary for the interaction with TOPO IIIα (Hu et al., 2001). Functional studies using BLM and TOPO IIIα revealed that they act together in the dissolution of DHJ recombination intermediates to generate predominantly non-crossover products (Wu & Hickson, 2003) (Figure 26). Additional functional studies revealed that BLAP75, human homologue of yeast RMI1, strongly stimulated the reaction (Wu et al., 2006; Raynard et al., 2006) (Figure 26). It is proposed that the branch migration activity of BLM converts the DHJs into a hemicatenane. Following this, the TOPO IIIα-BLAP75 complex resolves the hemicatenane structure using the ssDNA strand passage activity of TOPO IIIα. In this way, DHJ is removed without any crossing over (Figure 26).

BLM can also form nuclear foci at sites of DNA replication, indicating a role for BLM at damaged DNA replication forks (Sengupta et al., 2003). Further, BS cells show defects in DNA replication (Lonn et al., 1990). It was also shown that BLM protein is required for correct relocalization of the MRE11/RAD50/NBS1 (MRN) complex after replication fork arrest (Franchitto & Pichierri, 2002). More recent studies have shown a role for BLM in replication-fork restart and in suppression of origin firing after replicative stress (Davies et al., 2007). The authors further showed that these functions required the helicase activity of BLM and the threonine residue at the position 99 (Thr 99) of BLM that is targeted by stress-activated kinases.

3.4.6. The Werner syndrome helicase

3.4.6.1. Werner syndrome

Werner syndrome (WS) is a rare autosomal recessive disorder characterized by an early onset of many features of aging (Werner, 1904; Epstein et al., 1966; Martin, 1978; Goto, 1997). WS patients suffer from bilateral ocular cataracts, type II diabetes mellitus, osteoporosis, various forms of arteriosclerosis including atherosclerosis, and hypogonadism at a relatively young age. The aged appearance is due to the short stature, premature graying and loss of hair, scleroderma-like skin changes, and regional atrophy of subcutaneous fat. WS patients have an elevated risk of various cancers particularly sarcomas (Goto et al., 1996). The disease frequency is 1-22 cases per million of the population worldwide. The frequency is quite high in Japan with an estimated frequency of 35 WS patients per million of the Japanese population (Satoh et al., 1999).

WS is caused by mutations in the WRN gene belonging to RecQ family of DNA helicases (Yu et al., 1996). The WRN gene is located in the p11-p12 region of chromosome 8 (Matsumoto et al., 1997).

3.4.6.2. Cellular phenotypes of WRN deficiency

A hallmark feature of WS cells is that in culture, these cells undergo replicative senescence much more rapidly than normal cells. The average lifespan of WS fibroblasts in culture is about 27% of that of normal cells, and the population doubling time is approximately double compared to that of normal cells (Salk et al., 1981). Increased sensitivity to 4-nitroquinoline 1-oxide (4NQO) is another hallmark of the WS cells (Prince et al., 1999; Imamura et al., 2002; Poot et al., 2002). WS cells are also more sensitive to DNA cross-linking drugs such as mitomycin C, melphalan and cisplatin (Poot et al., 2001; Saintigny et al., 2002). Furthermore these cells are sensitive to the inhibitor of topoisomerase I, Camptothecin (Lebel & Leder, 1998; Okada et al., 1998). WS cells also show a slight hypersensitivity to γ-irradiation.

At the chromosomal level, the genomic instability caused due to defect in WRN results in a greater frequency of a variety of chromosomal rearrangements, transclocations and inversions, as well as a high frequency of extensive deletions (Fukuchi et al., 1999). The spontaneous level of DNA breaks has also been found to be higher in WS cells than in wild-type cells (Pichierri et al., 2001).

3.4.6.3. Domain structure

Based on the sequence alignment, it has been found that apart from conserved helicase domains in the central region, WRN also contain a nuclease domain that is located in the N-terminal part of the protein (Yu et al., 1996; Moser et al., 1997). Like other RecQ helicases, WRN also possess RQC (Zn-binding and WH subdomains) and HRDC domains (Morozov et al., 1997). Based on the data obtained from *E.coli* RecQ, it may be proposed that the zinc (Zn^{2+}) finger motif of WRN is involved in the regulation of its enzymatic activity by modulating DNA binding as well as protein folding of WRN helicase (Liu et al., 2004). Structural analysis of the DNA- and protein-binding domain (DPBD; which includes the WH motif) of WRN suggests that this domain may play a role in guiding the WRN protein to the site of action (Hu et al., 2005). Indeed, the DPBD region overlaps with a number of known protein-interacting regions of WRN (Lee et al., 2005). Based on the structural studies, the HRDC region of WRN was proposed as a DNA binding site (Liu et al., 1999). Further, recent data demonstrated that the WRN protein accumulates at sites of double-stranded DNA breaks in a manner dependent on its HRDC domain (Lan et al., 2005). Biochemical studies demonstrated that substrate-specific DNA binding of WRN is mediated through the following three domains: N-terminal, RQC, and HRDC (von Kobbe et al., 2003).

3.4.6.4. Biochemical properties

Like other RecQ family members, WRN exhibits ATP dependent 3' – 5' DNA helicase activity. WRN displayed a strong helicase activity on DNA bubble substrates. WRN is able to unwind G-quadruplex DNA, D-loop structures and to branch migrate Holliday junctions (Bachrati & Hickson, 2003). In addition to the helicase activity, WRN possesses a 3' – 5' exonuclease activity (Huang et al., 2000). The exonuclease domain of WRN is located at its N-terminus. WRN can coordinate its helicase and exonuclease activities to disrupt D-loop structures *in vitro*. It has been demonstrated that WRN first acts as helicase to unwind the duplex of the invading strand in the D-loop, followed by exonucleolytic digestion of unwound DNA strand (Orren et al., 2002). Recently, WRN has been shown to possess strand annealing and strand exchange activities (Machwe et al., 2005) and the ability to promote fork regression (Machwe et al., 2006).

3.4.6.5. Interacting partners and cellular roles

Numerous proteins have been shown to interact with WRN through its RQC or HRDC domains (Cheng & Bohr, 2003; Brosh & Bohr, 2007). Characterizaton of these interactions revealed that WRN participates in multiple DNA metabolic pathways (Cheng & Bohr, 2003). The WRN protein is involved in DNA double-strand break (DSB) repair by nonhomologous end joining (NHEJ) in concert with the DNA-protein kinase complex (DNA-protein kinase catalytic subunit, Ku70, and Ku80) (Cooper et al., 2000; Li et al., 2001; Yannone et al., 2001). Also, a role of WRN in genetic recombination is evident from the *in vitro* and *in vivo* studies (Prince et al., 2001; Swanson et al., 2004; Cheng et al., 2006). Physical and functional association of WRN with flap endonuclease 1 (FEN-1) (Brosh et al., 2001; Sharma et al., 2005), DNA polymerase β (Harrigan et al., 2003), poly (ADP-ribose) polymerase 1 (PARP-1) (Li et al., 2004; von Kobbe et al., 2004), and apurinic/apyrimidinic endonuclease 1 (APE1) (Ahn et al., 2004) reveal a role of WRN in base excision repair. An involvement of WRN protein in DNA replication is suggested by its interaction with DNA topoisomerase I (Laine et al., 2003) and DNA polymerase δ (Szekely et al., 2000). Furthermore, the tumor suppressor p53 binds to and inhibits WRN exonuclease activity (Brosh et al., 2001). Physical and functional association of WRN and RNAPII was also shown and that in the absence of WRN, cells exhibited reduced transcription efficiency (Balajee et al., 2001). Physical interaction of telomeric repeat binding factor 2 (TRF-2) and WRN protein, in conjunction with biochemical data demonstrating the disruption of D-loops by WRN protein, suggests that WRN may participate in the maintenance of telomeres (Orren et al., 2002; Opresko et al., 2004). WRN protein has been shown to be involved in the lagging strand synthesis at telomeres (Crabbe et al., 2004) (Figure 27). In this report, it has been shown that G-quartet (G4) formation on the lagging telomeric DNA is normally resolved by WRN, enabling efficient replication of lagging strand G-rich telomeres. In the absence of WRN, G4 formation on the lagging telomere leads to replication fork stalling and deletion of lagging-strand telomeres (Crabbe et al., 2004) (Figure 27). The resulting dysfunctional telomeres can initiate a p53-dependent DNA-damage response, leading to premature onset of replicative senescence.

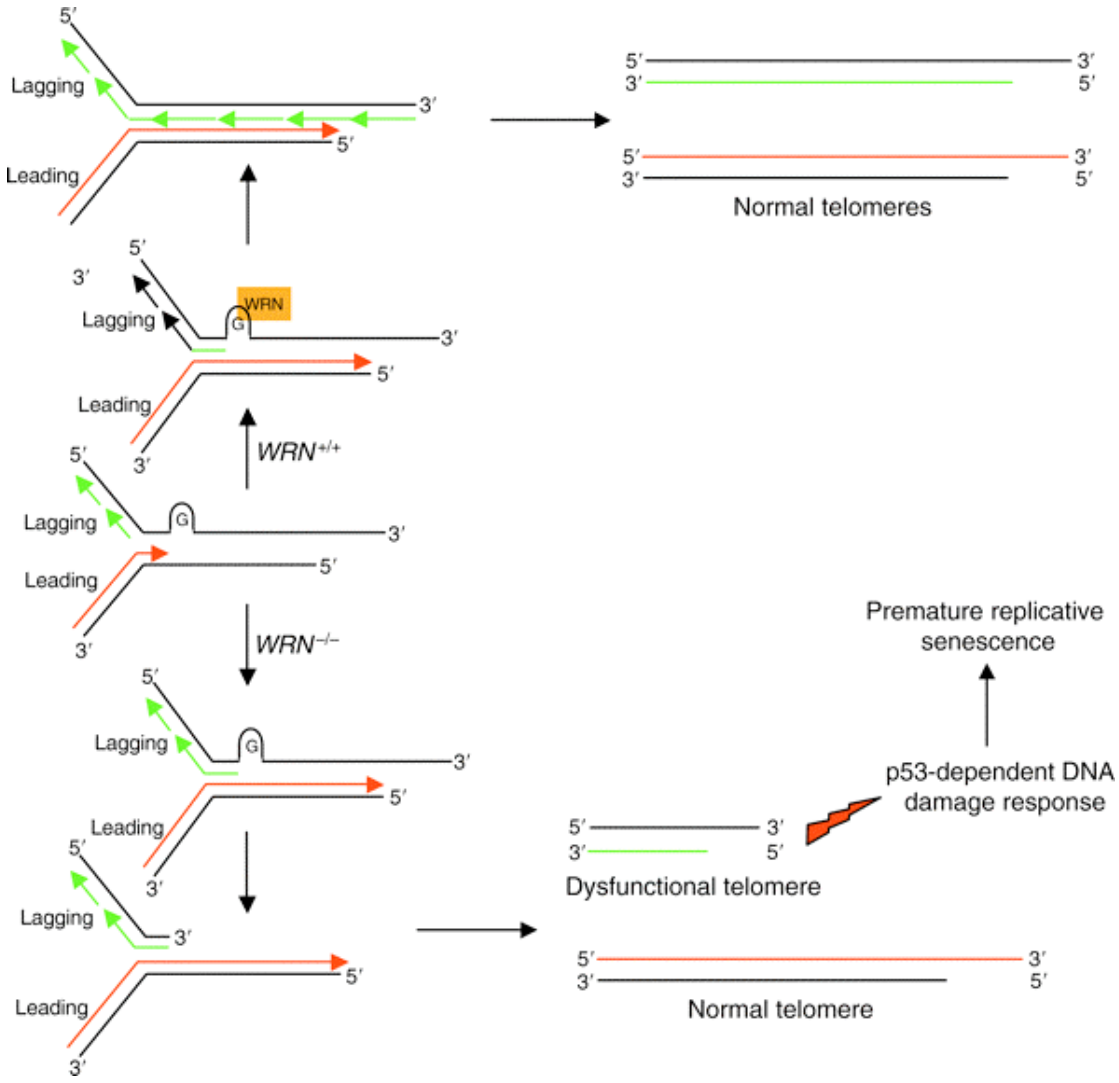

Figure 27. WRN is required for the lagging strand synthesis at telomeres. See text for more details. Adapted from Multani & Chang, 2005.

Collectively, WRN protein with two different activities (helicase and exonuclease) may be used for various DNA transactions involved in repair, replication, recombination and transcription. It is now a challenge to understand how WRN can operate in a number of DNA transactions and DNA repair processes.

3.4.7. RECQ4

3.4.7.1. RECQ4 and genetic diseases

The *RECQ4* gene was cloned in 1998 (Kitao et al., 1998). It lies on chromosome 8q24.3 and encodes a 1208 amino acid protein. Mutations in the RECQ4 gene have been found to be associated with three different human disorders namely Rothmund-Thomson (RTS), RAPADILINO and Baller-Gerold (BGS) syndromes (Kitao et al., 1999; Siitonen et al., 2003; Van Maldergem et al., 2006). RTS is an unusual autosomal recessive disorder characterized by poikiloderma, growth deficiency, juvenile cataracts, premature aging and a predisposition to cancer, particularly osteosarcomas (Rothmund, 1868; Thomson, 1936; Vennos et al., 1992). Upto 300 RTS cases have been reported so far (Vennos et al., 1992; Wang et al., 2001). Interestingly, mutations in the *RECQ4* gene cause only 60% of all RTS cases (Kitao et al., 1999). In most of the cases, the mutations result in premature termination of the protein resulting in truncated RECQ4 that lacks the helicase domain (Lindor et al., 2000).

RAPADILINO syndrome was originally described in 14 patients from Finland (Siitonen et al., 2003). This name came from the characteristic clinical features exhibited by these patients: **RA**dial hypo-/aplasia, Patellae hypo-/aplasia and cleft or highly arched **PA**late, **DI**arrhoea and Dislocated joints, **LI**ttle size and LImb malformation, **NO**se slender and NOrmal intelligence. Also, RAPADILINO patients exhibit photosensitivity and growth deficiency. Only 7% of RAPADILINO patients were reported to develop cancer (osteosarcomas) (Kellermayer et al., 2005). The most common mutations of the *RECQ4* gene in RAPADILINO patients represent in-frame deletion of exon 7 which do not affect the helicase domain of RECQ4 (Siitonen et al., 2003).

BGS was discovered in 1950 (Baller, 1950), and only recently it was found to be linked to mutations in the *RECQ4* gene (Van Maldergem et al., 2006). 24 cases of BGS have been reported to date (Van Maldergem et al., 2006). The clinical hallmarks of BGS are radial aplasia/hypoplasia and craniosynostosis. Most mutations of RECQ4 found in BGS patients represent an R1021W missense mutation and a 2886 delta T frameshift mutaion of exon 9. Surprisingly, none of the 24 BGS patients reported so far showed predisposition to cancer (Van Maldergem et al., 2006).

3.4.7.2. Cellular phenotypes of RECQ4 deficiency

Cells derived from RTS patients showed genomic instability, including aneuploidy and chromosomal rearrangements (Der Kaloustian et al., 1990; Vennos et al., 1992). Additionally, RTS cells are sensitive to ionizing radiation and oxidative damage (Vennos & James, 1995; Werner et al., 2006). Three different RECQ4 knockout mice were made. Extensive disruption of the RECQ4 gene resulted in embryonic lethality associated with severe proliferation defects (Ichikawa et al., 2002). Hoki et al.. generated another RECQ4-knockout mouse by deleting exon 13 of the *RECQ4* gene that encodes for a part of the helicase domain (Hoki et al., 2003). This mouse showed severe growth retardation and several tissue abnormalities that resemble defects observed in RTS patients. Only 5% of the mutant mice survived the first 14 days, and these mice failed to develop tumors. Further, cells derived from mutant mice showed a decreased proliferation rate.

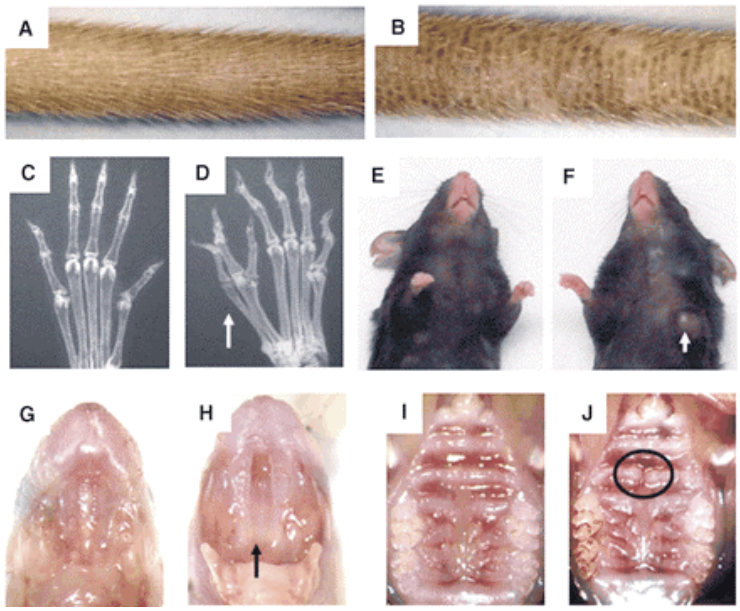

Figure 28. RECQ4 deficient mice with RTS phenotypes. Photographs of the tails of a wild-type (A) and a RECQ4 deficient (B) mouse. Pigmented areas on the tail is obvious in RECQ4 deficient mouse. Images D and F show the radial ray defects in RECQ4 deficient mice. Images C and E are from the wild-type mice that show no radial ray defects. Images G-J are the Palatal photographs of the wild-type (G & I) and RECQ4 deficient (H & J) mouse. RECQ4 deficient mouse show severe cleft palate (indicated by arrow) and patterning defect in the palate (indicated by circle). Adapted from Mann et al., 2005.

The third RECQ4 knockout mouse carried deletion of exons 9-13 removing the entire helicase domain (Mann et al., 2005). More than 80% of these mice survived to adulthood, with some exhibiting typical clinical features of RTS including pigmented

skin, skeletal limb defects and palatal patterning defects (Figure 28). Furthermore, chromosomal analysis using different cell types derived from the RECQ4-deficient mice displayed aneuploidy and a significant increase in the frequency of premature centromere separation.

3.4.7.3. Domain structure

The helicase domain of the RECQ4 is located in the central region of the protein. The additional regions present at the N- and C-termini of RECQ4 do not show any sequence similarity with other RecQ family members (Bachrati & Hickson, 2003). RECQ4 does not contain RQC and HRDC domains that are present in other RecQ helicases downstream of the helicase domain. The C-terminal region of RECQ4 contains a stretch of acidic amino acids (Bachrati & Hickson, 2003). In addition, the N-terminal region of RECQ4 bears a portion that shows sequence homology to the yeast proteins Sld2 and DRC1 (Sangrithi et al., 2005). For further details, see the text below.

3.4.7.4. Biochemical properties

Very little is known about the biochemical properties of the RECQ4 protein. The first biochemical study of RECQ4 was performed using immunoprecipitated RECQ4 protein from HeLa cell extracts (Yin et al., 2004). Later, full-length RECQ4 was expressed and purified from *E.coli* (Macris et al., 2006). Both studies showed that RECQ4 exhibits a DNA-dependent ATPase activity, but not the DNA unwinding function. In addition, Macris et al., showed that RECQ4 binds preferentially to ssDNA and promotes strand annealing (Macris et al., 2006).

3.4.7.5. Interaction partners and cellular roles

Initial attempts to identify proteins that associate with RECQ4 have revealed that RECQ4 exists in a complex with UBR1 and UBR2 that belong to the family of E3 ubiquitin ligases acting in the N-end rule pathway (Yin et al., 2004). Surprisingly, RECQ4 was not found to be ubiquitylated *in vivo*, and the function of the direct interaction between RECQ4 and UBR1/UBR2 still remains unclear. Also, RECQ4 is found in a complex with RAD51 *in vivo* (Petkovic et al., 2005). Further, it was found that a fraction of RECQ4 and RAD51 nuclear foci colocalized after the treatment of cells with the DSB inducing agent etoposide, suggesting that RECQ4 plays a role in the repair of DSBs by homologous recombination. Recently, Cut5 was shown to interact with the *Xenopus laevis* homologue of RECQ4 both *in vitro* and *in vivo* (Matsuno et al., 2006).

The yeast homologue of Cut5, named Dpb11, was shown to be required for loading DNA polymerases onto chromatin (Van Hatten et al., 2002; Hashimoto et al., 2003). Also, the N-terminus of RECQ4 has similarity to Sld2 (synthetically lethal with *dpb11*) that is found to interact with Dpb11 (Kamimura et al., 1998; Sangrithi et al., 2005). Thus, these findings provide evidence that RECQ4 participates in DNA replication. Also, physical association between RECQ4 and poly (ADP-ribose) polymerase-1 (PARP-1) has been reported (Woo et al., 2006). Additionally, PARP-1 was shown to modify i.e., poly ADP-ribosylate RECQ4 *in vitro*.

Analysis of RECQ4 homologue in *Xenopus laevis* (xRTS) has indicated a new role for RECQ4 in the initiation of DNA replication (Sangrithi et al., 2005). This report showed that depletion of RECQ4 in *Xenopus laevis* egg extracts leads to a reduction and delay of sperm chromatin replication. Also, it was showed that this effect was rescued by supplementing the extracts with purified human RECQ4 protein. Another recent publication showed that purified N-terminal fragments of xRTS were able to rescue the DNA replication activity of RECQ4-depleted *Xenopus laevis* egg extracts (Matsuno et al., 2006). Also, knocking down the murine homologue of RECQ4 in cultured cells revealed that the rate of DNA replication was highly affected. Further, these works showed that xRTS is important for the loading of RPA at the replication site (Sangrithi et al., 2005), and also for the chromatin binding of DNA polymerase in the initiation of DNA replication (Matsuno et al., 2006). Taken together, these findings suggest that RECQ4 functions after pre-replication complex (pre-RC) assembly to make origins of replication accessible for loading of subsequent replication factors, which is the early step in the initiation of eukaryotic DNA replication (Figure 29).

Collectivelly, the published data indicate that RECQ4 is involved in DNA replication and repair processes, and further functional studies are needed to characterize in more detail the exact role of RECQ4 in these processes.

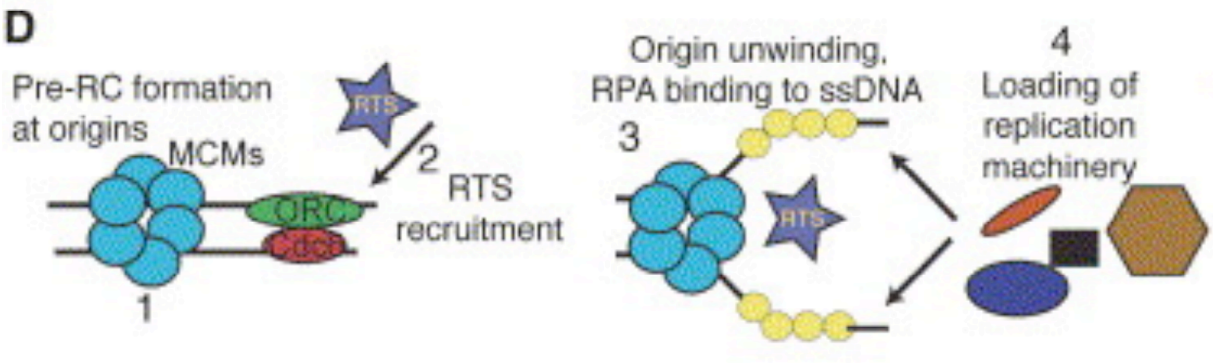

Figure 29. Proposed model for the function of RECQ4 (here xRTS) during replication initiation. Other details are described in the text. Adapted from Sangrithi et al., 2005.

3.4.8. RECQ5

3.4.8.1. Cloning

The *RECQ5* gene has been mapped to chromosome position 17q25 and cloned by Kitao and his colleagues in 1998 (Kitao et al., 1998). Loss of heterozygosity in this region has been found to be associated with ovarian cancers and familial breast carcinomas (Sekelsky et al., 1999). No human genetic disease has been found to be associated thus far with a deficiency in the *RECQ5* gene.

3.4.8.2. Cellular phenotypes of RECQ5 deficiency

Recent studies using chicken DT40 cells and knockout mice suggested that RECQ5 is important for the maintenance of chromosomal stability (Wang et al., 2003; Hu et al., 2005; Hu et al., 2007). RECQ5 deficiency in DT40 cells does not result in genomic instability (Imamura et al., 2002; Wang et al., 2003). However, DT40 cells lacking both *RECQ5* and *BLM* exhibited much higher levels of sister chromatid exchanges (SCEs) than a $BLM^{-/-}$ mutant (Wang et al., 2003). RECQ5 deficiency in *Caenorhabditis elegans* reduced lifespan and increased cellular sensitivity to ionizing radiation (Jeong et al., 2003).

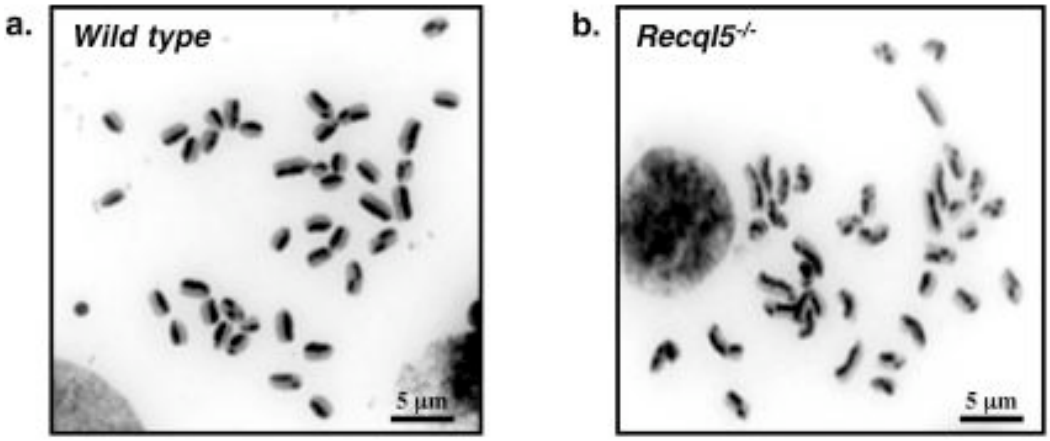

Figure 30. Image showing the elevated frequency of SCEs in RECQ5 deficient cells. Representative metaphase spreads from wild-type (a) and RECQ5 deficient (b) mouse ES cells are shown here. Adapted from Hu et al., 2005.

Complementation studies in yeast suggested that *Drosophila* RECQ5 (DmRECQ5) was able to fully complement the *sgs1* (yeast RecQ helicase) phenotypes of the synthetic growth defects with *Srs2*, the hypersensitivity to hydroxyurea/methylmethanesulfonate (MMS) and the elevated rate of SCEs, but very

poorly complemented the suppression of slow growth in topoisomerase III (Nakayama et al., 2004). They further showed that the C-terminus of DmRECQ5 was dispensable for complementing the *sgs1 srs2 phenotype*, but was required for complementation of *sgs1 top3*. Transgenic flies that overexpressed RECQ5 in their developing eye primordia showed mild roughening of the ommatidial lattice (Nakayama et al., 2006). Further, overexpression of RECQ5 perturbed the progression of the cell-cycle in response to DNA damage in the eye imaginal discs. Hu et al. showed that mouse embryonic stem cells lacking BLM or RECQ5 genes displayed a significant increase in the frequency of SCEs (Hu et al., 2005) (Figure 30). Further, deletion of both genes lead to an even higher frequency of SCE. Thus, these data suggested that BLM and RECQ5 have non-redundant roles in suppressing crossovers during homologous recombination. Later, the same group showed that the deletion of *RECQ5* in mice resulted in increased susceptibility to cancer, accumulation of spontaneous double-strand breaks and elevated frequencies of homologous recombination (HR) (Hu et al., 2007).

3.4.8.3. Domain structure

RECQ5 exists in at least three different isoforms, named RECQ5α, RECQ5β and RECQ5γ, resulting from alternative RNA splicing (Sekelsky et al., 1999; Shimamoto et al., 2000) (Figure 31). These proteins have the predicted molecular masses of 46 kDa, 108.9 kDa and 49 kDa, respectively (Shimamoto et al., 2000). The first 410 amino acids of these isoforms are identical and constitute the helicase domain of the enzyme. RECQ5α is the shortest variant including only the helicase domain (410 amino acids). RECQ5β contains the helicase domain and a putative RQC domain, which is followed by a long C-terminal region that shows no homology with the other RecQ helicases. No putative HRDC domain was found present in RECQ5β. RECQ5γ includes the helicase domain followed by a C-terminal extension of 25 amino acids that is not present in RECQ5β. Interestingly, only the largest splice variant RECQ5β localizes to the nucleus, whereas the short isoforms are only present in the cytoplasm (Shimamoto et al., 2000).

3.4.8.4. Biochemical properties

Initial biochemical characterization of RECQ5 was done in Matson's group using the *Drosophila melanogaster* (Dm) small isoform of RECQ5 (Ozsoy et al., 2001). The purified DmRECQ5 protein displayed ATP-/dATP-dependent 3'-5' helicase activity on a M13 based partial duplex substrate. Later, the same group showed that the small

isoform of DmRECQ5 is a structure-specific helicase that is capable of unwinding forked DNA, 3'-flap/5'-flap duplexes, three-way and four way junctions (Ozsoy et al., 2003). Also, the protein showed a preference for unwinding the "lagging-strand arm" in a structure resembling a stalled replication forks (Ozsoy et al., 2003). Gel filtration experiments conducted by Kawasaki et al., indicated that the largest isoforms of RECQ5 (DmRECQ5β) adopts an oligomeric structure (Kawasaki et al., 2002). Further, they showed that DmRECQ5β protein hrdrolyzed GTP, much more efficiently than ATP, in the presence of single-stranded (ss) DNA. Also, it was noticed that GTP stimulated the ATP-driven DNA unwinding activity of DmRECQ5.

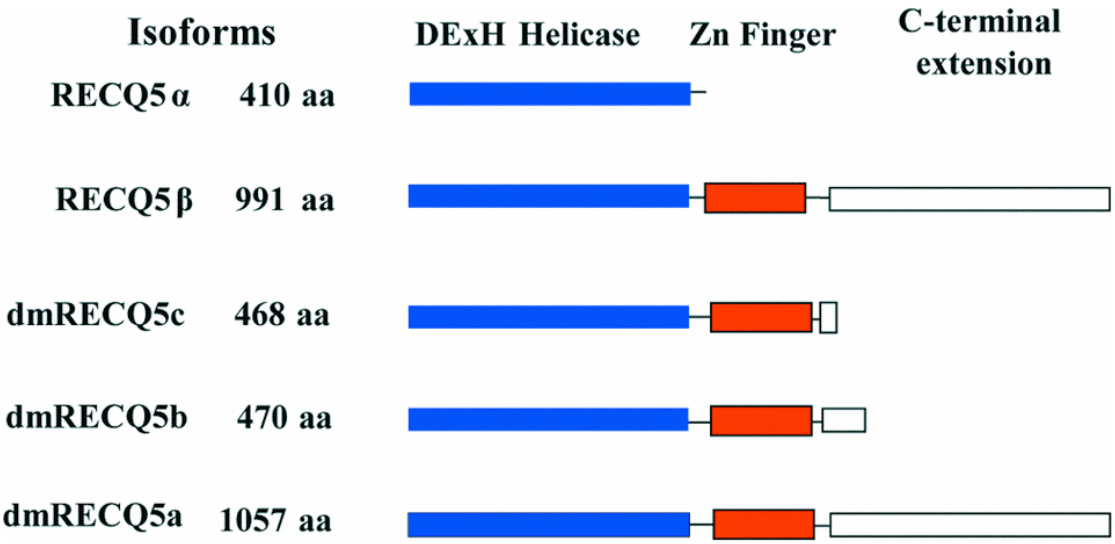

Figure 31. Schematic representation of human RECQ5α, RECQ5β and their homologues from Drosophila melanogaster (dmRECQ5c, dmRECQ5b and dmRECQ5a). Adapted from Ren et al., 2008.

The first biochemical characterization of human RECQ5 protein was conducted in our laboratory and published in 2004 (Garcia et al., 2004). It was found that human RECQ5β protein exist as monomer even in the presence DNA and nucleotide cofactors. Functional studies revealed that RECQ5β possesses two enzymatic activities: i) ATP-dependent 3'-5' helicase activity and ii) DNA strand-annealing activity. The human replication protein A (hRPA) was found to stimulate the helicase function and inhibit the strand-annealing activity of RECQ5β. It was also found that the strand-annealing function of RECQ5β resides in the unique C-terminal region of the protein. Further, it was found that the ATP-bound form of RECQ5β cannot promote strand annealing. Also, it was shown that human RECQ5β promoted the branch migration of synthetic Holliday junctions (Garcia et al., 2004). More recently, human RECQ5β protein was shown to be

capable of removing RAD51 from single-stranded DNA in a reaction that required ATP hydrolysis and RPA (Hu et al., 2007). For more biochemical properties of human RECQ5 helicase, see the chapter 4 & 5 of this thesis.

3.4.8.5. <u>Interaction partners and cellular roles</u>

The first reported interaction partners of RECQ5β were TOPO IIIα and TOPO IIIβ (Shimamoto et al., 2000). In this study, RECQ5β was found to co-immunoprecipitate with TOPO IIIα and TOPO IIIβ from HeLa cell extracts. The presence of this complex in the cell was further confirmed by immunocytochemical staining. However, the functional significance of this complex is still unknown. Based on cellular and biochemical studies, it was earlier proposed that RECQ5β may serve as a backup for BLM (Garcia et al., 2004). However, later it was found that RECQ5β-TOPO IIIα complex was unable to effect the dissolution of DHJs (Wu et al., 2005).

RECQ5 was found to directly interact with RAD51 protein, which function in the initiation of HR pathway (Hu et al., 2007). It was shown that RECQ5 deficient cells exhibited an increased frequency of RAD51 and γ-H2AX foci. Further, elevated frequency of HR-mediated repair was noticed in RECQ5 deficient cells. Taken together, these data indicated that RECQ5 deficiency is associated with increased DSB repair by HR. Also, it was shown that RECQ5 regulates HR and prevent aberrant recombination in the cells by suppressing RAD51-mediated D-loop formation (Hu et al., 2007) (Figure 32).

More recently, RECQ5β was shown to directly interact with RNA polymerase II (RNAPII) (Izumikawa et al., 2008). At least four RNAPII subunits were found associated with RECQ5β. It was found that RECQ5β is associated with hypo- and hyper-phosphorylated forms of the largest subunit of RNAPII (Rpb1). Further, RECQ5β was found associated with the coding regions of the LDL receptor and β–actin genes, and knockdown of the RECQ5β transcript increased the transcription of those genes. Collectively, these data suggested that RECQ5β plays suppressive roles in events associated with RNAPII dependent transcription. More interaction partners of RECQ5 are described in Chapter 4 & 5.

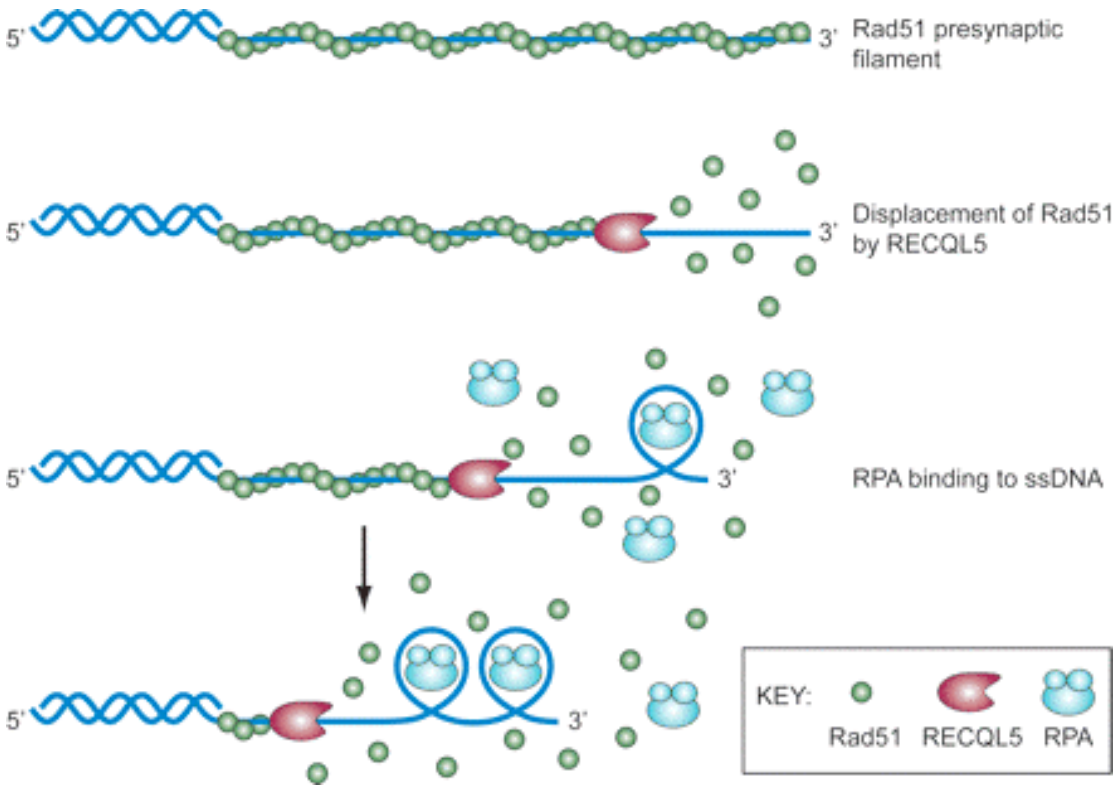

Figure 32. Proposed model for the mechanism of action of RECQ5 (here RECQL5) on Rad51 presynaptic filaments. RECQL5 utilizes the free energy from ATP hydrolysis to catalyze the dismantling of the Rad51 presynaptic filament. The ssDNA generated as a result of Rad51 removal is immediately occupied by RPA to prevent the reloading of Rad51. Adapted from Hu et al., 2007.

4. Results

The aim of this thesis is:

(i) To characterize the biochemical properties and the cellular functions of the human RECQ5 protein, and

(ii) To elucidate the function of the cellular complexes comprised of the Werner syndrome helicase and the mismatch repair (MMR) initiation proteins.

Significant findings of this thesis are described in the following sections. Publications that have arisen from this work are included in the Appendix.

4.1. Human RECQ5β helicase promotes strand exchange on synthetic DNA structures resembling a stalled replication fork

RecQ helicases are an increasingly studied class of DNA unwinding enzymes. Recent studies have shown that, in addition to the helicase function, the human RecQ helicases RECQ1, BLM, WRN, RECQ4 and RECQ5 possess a single-strand-annealing (SSA) activity. Studies on the RECQ5 helicase revealed that its SSA activity resides in the unique C-terminal portion of the protein. These biochemical characteristics suggested that RECQ5 could be involved in DNA transactions that require coordinated action of helicase and strand-annealing activities such as replication fork regression. Fork regression is believed to facilitate DNA damage bypass during replication, allowing the replicative polymerase to use undamaged sister chromatid as a template for synthesis of the sequence complementary to the blocking lesion. Fork regression includes unwinding of the newly replicated arms of the fork, annealing of the nascent DNA strands and re-pairing of the parental strands to form a Holliday-Junction structure.

Our results using the oligonucleotide based fork structures demonstrated that RECQ5β was capable of promoting strand exchange between arms of synthetic forked DNA structures that resembled a stalled replication fork in a reaction stimulated by human replication protein A (hRPA). This activity was not detected when ATP was substituted with its poorly hydrolysable analogue ATPγS, indicating that it is dependent on the helicase activity of RECQ5β. Although, similar strand exchange reactions were also seen with BLM and WRN, in the presence of hRPA, the action of these RecQ-type helicases was strongly biased towards unwinding of the parental duplex, an effect not

seen with RECQ5β. Collectively, these findings indicated that RECQ5β is capable of promoting fork regression *in vitro*.

To further understand the mechanism of RECQ5β-mediated strand exchange, we have examined the action of RECQ5β on synthetic forked structures with non-complementary arms to monitor DNA unwinding events associated with this reaction. The obtained results revealed that RECQ5β preferentially unwinds the lagging strand arm on such structures. This preference was dramatically enhanced upon addition of hRPA to the reaction. We also analysed the action of the BLM and WRN helicases using the same substrates. In contrast to RECQ5β, BLM and WRN displayed a strong preference for unwinding of the parental arm on all these structures. These results highlight mechanistic differences between RECQ5β and other human RecQ helicases in processing of forked DNA structures. Further work to identify the region of RECQ5β that is required for its ability to unwind the lagging strand arm of the fork revealed that the portion of RECQ5β spanning the amino acids 561-651 is critical for its strand-exchange activity, perhaps being involved in loading of the helicase on the three-way junction.

To explore whether RECQ5β acts at DNA replication forks *in vivo*, we investigated the sub-cellular localization of RECQ5β protein by indirect immunofluorescence imaging. These studies revealed that RECQ5β localizes exclusively to the nucleus. Using synchronized human cells, we found that RECQ5β is associated with the DNA replication machinery, particularly in early and late S phase, as revealed by the nearly complete co-localisation of RECQ5β foci with the foci formed by the replication processivity factor PCNA during those stages of cell cycle. We further found that the RECQ5β foci in late S co-localised with promyelocytic leukemia protein (PML), indicating that RECQ5β associates with PML nuclear bodies, a dynamic nuclear protein structure serving as DNA-damage sensors. We have also observed that RECQ5β forms discrete foci in response to DNA damage caused upon exposing cells to UVC irradiation and cisplatin treatment, and that these foci co-localize with the PCNA foci formed upon this damage. These data indicate that RECQ5β is present in replication-repair factories formed at the sites of stalled replication forks.

In addition, we showed that RECQ5β directly interacts with PCNA *in vivo* and *in vitro*. We also found that the region spanning the last 200 amino acids of RECQ5β is

essential for its interaction with PCNA, suggesting that this interaction is mediated through the putative PCNA-binding motif (between amino acids 964-971) located in this region. These results further suggest that the observed recruitment of RECQ5β to replication foci may occur *via* a direct interaction with PCNA.

The data presented in this work showed that RECQ5β utilizes its helicase and SSA activities to promote strand exchange between arms of forked DNA structures resembling a stalled replication fork. Collectively, our findings suggest that RECQ5β mediates regression of stalled replication forks *in vivo* to facilitate damage bypass by template switching. This conclusion is consistent with the elevated level of mitotic crossovers observed in mouse cells upon inactivation of the RECQ5β homologue, as these can result from recombinational repair of broken replication forks (Figure 33).

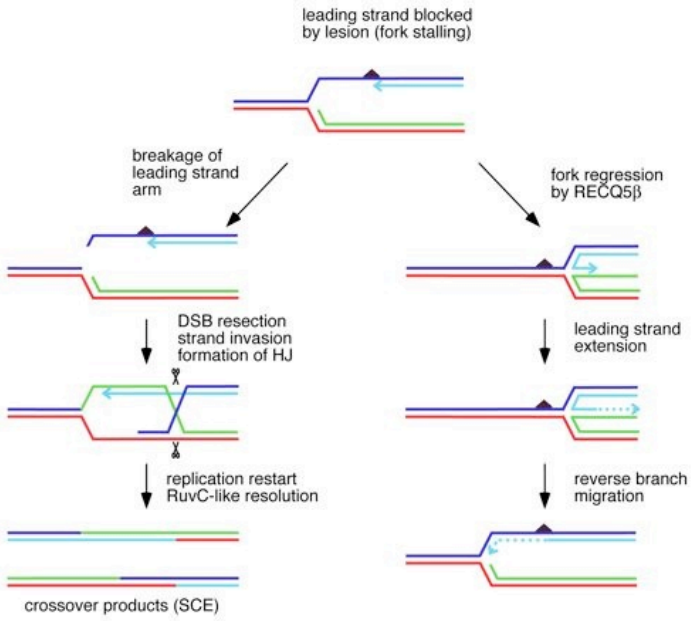

Figure 33. A model for the role of RECQ5β in suppression of mitotic recombination. A DNA lesion on the leading strand template causes replication fork stalling. RECQ5β promotes regression of stalled replication forks, which allow template switching to the undamaged chromatid. This prevents fork breakage and subsequent recombinational repair of DSBs that can result in sister chromatid exchanges (SCEs).

4.2. The zinc-binding motif of human RECQ5β suppresses the intrinsic strand annealing activity of its DExH helicase domain and is essential for the helicase activity of the enzyme

Human RECQ5 protein exists in three different isoforms, namely RECQ5α (1 - 410 aa), RECQ5β (1 - 991 aa) and RECQ5γ (1 - 435 aa), resulting from alternative splicing of the RECQ5 transcript. The N-terminal 410 amino acids of these proteins are identical and include the set of seven conserved helicase motifs (helicase domain). RECQ5β additionally contains a putative zinc (Zn^{2+})-binding domain followed by a long non-conserved C-terminal region, whereas RECQ5γ possesses 25 amino acid C-terminal extension that is not present in RECQ5β. The biochemical characteristics of the two short isoforms of RECQ5 are not known yet.

We found that RECQ5α, which contain the conserved helicase motifs, did not exhibit ATPase and helicase activity although it was proficient in ATP binding. Our experiments further showed that the inability of RECQ5β to unwind DNA was caused by its failure to hydrolyze ATP. Surprisingly, like RECQ5β, the RECQ5α isoform was also able to promote annealing of complementary single-stranded oligonucleotides. In contrast to RECQ5β, ATP dramatically inhibited the annealing activity of RECQ5α. As shown for RECQ5β, we found that the strand annealing activity of RECQ5α was inhibited by human replication protein A (hRPA).

Next, we investigated the minimal region of RECQ5 protein that is essential for its helicase function. Our results revealed that the region encompassing 410 – 475 amino acids of RECQ5β, which includes the putative Zn^{2+}-binding motif, is crucial for the ATPase and helicase activities of the enzyme. Further, replacement of the cysteine residue at the position 431 with a serine (C431S) significantly reduced not only the Zn^{2+} binding capacity of RECQ5β, but also its ATPase and helicase activities. Additional band-shift experiments demonstrated that the Zn^{2+}-binding motif confers the DNA binding ability to the RECQ5β helicase and it preferentially binds double-stranded (ds) DNA.

Taken together, these data suggest that the Zn^{2+}-binding motif regulates the enzymatic activity of RECQ5β, i.e. it suppresses the strand-annealing function of the helicase domain and promotes strand separation.

4.3. The MRE11/RAD50/NBS1 complex links RECQ5 helicase to sites of DNA damage

The molecular mechanisms that exist in mammalian cells to regulate homologous recombination events during mitosis are poorly understood. RECQ5 helicase is proposed to prevent inappropriate homologous-recombination events, but its exact role in DNA metabolism remains elusive. To shed more light on the cellular role of RECQ5, we initiated studies to determine the proteins interacting with RECQ5. Two different approaches were used: (i) Genetic approach that involves screening a human cDNA library by the yeast two-hybrid system using RECQ5 as bait, and (ii) Proteomic approach that involves analysis of RECQ5 immunoprecipitates from human cells by mass spectrometry. The most prominent interaction partner of RECQ5 identified by the mass spectrometry approach was the MRE11/RAD50/NBS1 (MRN) complex, an important factor in the cellular response to DNA double-strand breaks (DSBs). The cellular level of the RECQ5/MRN complex was not altered upon induction of different types of DNA damage or during different stages of the cell cycle, suggesting a constitutive association. Further, the direct interaction between RECQ5 and MRN was confirmed by performing affinity pull-down assays using purified recombinant proteins. The obtained results suggested that RECQ5 binds directly to the MRE11 and NBS1 subunit of the MRN complex. The experiments with the NBS1 deficient cells revealed that the absence of NBS1 protein did not affect the complex formation between RECQ5 and MRE11. Similarly, the complex formation between RECQ5 and NBS1 proteins was seen in MRE11-deficient cells, although the cellular level of NBS1 was dramatically reduced in MRE11-deficient cells.

We next investigated the effect of MRN on the biochemical activities of RECQ5 protein. Our results showed that the MRN complex did not significantly alter the helicase and strand-exchange activities of RECQ5. We then investigated the effect of RECQ5 on the nuclease activity of the MRN complex. Our results revealed that the 3'-5' exonuclease activity of the MRN and MR complexes was inhibited by RECQ5, but not by the *E. coli* RecQ. Collectively, these data suggest that RECQ5 negatively regulate the MRN complex by attenuating its exonuclease function through direct interaction with the MRE11 protein.

To explore the function of the RECQ5/MRN complex in the maintenance of genomic stability, we used indirect immunofluorescence microscopy to examine whether these proteins co-localize at sites of DNA damage. We found that, in cells that have been exposed to DNA damaging agents, RECQ5 extensively co-localized with RAD50 in nuclear foci. Further, shRNA mediated MRE11 knockdown studies in U2OS cells revealed that MRE11 protein is essential for the recruitment of RECQ5 to sites of DNA damage. This result was further confirmed using MRE11-deficient ATLD1 cells.

Collectively, these data suggest that RECQ5 helicase is recruited to sites of DNA damage through interaction with the MRN complex and inhibits MRE11-associated exonuclease activity.

4.4. Physical and functional interactions between Werner syndrome helicase and mismatch-repair initiation factors

The DNA mismatch-repair (MMR) system maintains genomic integrity by correcting DNA replication errors. It is also known that proteins involved in the initiation of post-replicative MMR, such as MSH2, MSH6, MLH1 and PMS2, act during double strand break (DSB) repair to suppress recombination between homeologous (divergent) DNA sequences. Moreover, there is evidence in yeast suggesting the involvement of Sgs1 helicase in the suppression of recombination between divergent DNA sequences. These findings led to the proposal that MMR proteins act in conjunction with Sgs1 to unwind DNA recombination intermediates containing mismatches. We initiated a project to check whether the same holds true in mammalian cells. In other words, we wanted to check whether Werner syndrome protein (WRN), the human orthologue of Sgs1 helicase, and the MMR system cooperate in rejection of homeologous recombination (heteroduplex rejection).

To this end, we initially checked whether WRN and MMR proteins bind directly to each other. Using ELISA-based protein-binding assay, we found that WRN interacted directly with MutSα (a heterodimer of MSH2/MSH6), MutSβ (a heterodimer of MSH2/MSH3) and MutLα (a heterodimer of MLH1/PMS2) proteins. Our co-immunoprecipitation studies revealed that WRN formed a stable complex with MutLα, but not with MutSα *in vivo*. GST pull-down experiments using different fragments of WRN revealed the regions of WRN required for its interaction with MMR proteins. While all the three MMR proteins interacted with the helicase core region of WRN (500 - 946

amino acids), both MutSβ and MutLα also made additional contacts on WRN. MutSβ was found to interact with the winged-helix (WH) motif of WRN (947 – 1149 amino acids), and MutLα was found to interact with the N-terminal region of WRN that includes the exonuclease domain (51 – 449 amino acids). To identify the subunits of MutSα, MutSβ and MutLα that mediate the interaction with WRN, we carried out a yeast two-hybrid (YTH) assay using the full-length WRN as prey. We found WRN to interact with MLH1 and MSH2, but not with MSH3 and MSH6, indicating that the MutSα – WRN and MutSβ- WRN interactions are mediated by MSH2, and the MutLα – WRN interaction is mediated by MLH1.

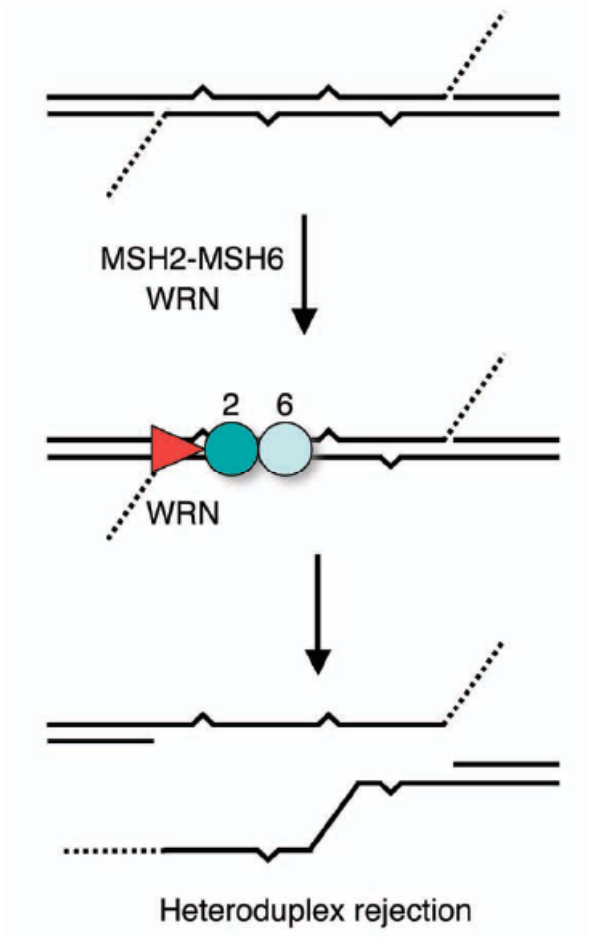

Figure 34. A model showing heteroduplex rejection mediated by the MMR initiation factors and WRN helicase on SSA intermediates. First, a DNA mismatch present in the SSA intermediate is recognized by MutSα. Later, MutSα recruits the WRN helicase to unwind the annealed region and thereby prevent homeologous recombination.

Functional studies indicated that both MutSα and MutSβ, but not MutLα, strongly stimulated the helicase activity of WRN specifically on forked DNA structures with a 3'-single-stranded arm resembling strand-pairing intermediates of the single-strand-

annealing (SSA) pathway of homologous recombination (HR). The stimulatory effect of MutSα on WRN-mediated unwinding was enhanced by the presence of a G/T mismatch in the DNA duplex ahead of the fork. Since MutLα is known to bind to MutSα-heteroduplex complexes, we investigated whether it can affect the WRN-mediated unwinding of G/T and G/C substrates induced by MutSα. We found that MutLα did not significantly alter the MutSα-dependent helicase activity of WRN on these DNA structures.

Collectively, our results support the model in which MMR proteins work in conjunction with a RecQ DNA helicase to disrupt HR intermediate containing mismatches (Figure 34).

5. Conclusion and future perspectives

Defects in many DNA repair genes have been linked to tumorigenesis and tumor progression (Bartkova *et al*., 2005; Gorgoulis *et al*., 2005; Bartkova *et al*., 2006; Bartek *et al*., 2007), and hence these genes are classified as tumor suppressor genes. More than 150 human DNA repair genes have been identified thus far (Wood *et al*., 2005). Proteins belonging to the RecQ family of DNA helicases are conserved in evolution and play critical roles in the genome maintenance (Bachrati & Hickson, 2003). Studies over the last decade have identified human RecQ helicases (RECQ1, WRN, BLM, RECQ4 and RECQ5) as an important tumour suppressor proteins and the loss of which cause genomic instability (Hanada & Hickson, 2007; Brosh & Bohr, 2007). Also, the published data suggested that each of these helicases play unique roles in the maintenance of genome stability. However the exact DNA transactions mediated by these proteins and the DNA repair pathways in which they act are currently unclear.

In the first work (**Kanagaraj *et al*., 2006**), we showed that the human RECQ5 helicase possesses the ability to promote strand exchange on synthetic forked DNA structures that mimic a stalled replication fork. Moreover, RECQ5 protein was found to be present at the DNA replication factories in S phase cells and persisted at the sites of stalled replication forks. Also, RECQ5 was found to associate with PCNA *in vitro* and *in vivo*. Based on these findings, we proposed that the RECQ5 helicase could mediate regression of stalled replication forks *in vivo* to facilitate DNA damage bypass by template-switching mechanism (Higgins *et al*., 1976; Cox, 2001; Sogo *et al*., 2002). This could explain the finding that inactivation of the mouse RECQ5 homologue is associated with a significant increase in the frequency of sister chromatid exchanges (SCEs) (Hu *et al*., 2005).

Recent studies from Dr. David Orren's and Dr. Leonard Wu's laboratories have shown that the other human RecQ helicases namely BLM and WRN also could mediate strand exchange and fork regression (Machwe *et al*., 2005; Ralf *et al*., 2006; Machwe *et al*., 2006; Machwe *et al*., 2007), suggesting a role for these proteins in template switching. It should be noted that strand exchange activity of BLM and WRN was also shown in our work (Kanagaraj *et al*., 2006), and in addition we have shown that the human replication protein A (hRPA) blocked strand exchange mediated by BLM and WRN, but not by RECQ5. Hence, to assess which human RecQ helicase is more likely

to promote fork regression *in vivo*, the effect of hRPA on fork regression by BLM, WRN and RECQ5 should be examined.

On the other hand, a very recent finding from Dr. Lajos Haracska's laboratory on the yeast Rad5 protein has made the role of human RecQ helicases in template switching rather questionable. In the budding yeast, fork regression associated with template switching is thought to be the underlying mechanism of the RAD5-subpathway of RAD6-dependent postreplicative repair, which is highly conserved from yeast to humans (Torres-Ramos *et al*., 2002). As this DNA damage tolerance process, which involves non-destructive polyubiquitination of PCNA, is largely independent of the HR machinery, other means such as helicase-promoted DNA unwinding, would be required for fork regression (Torres-Ramos *et al*., 2002; Hoege *et al*., 2002). Biochemical evidence published by Blastyák *et al*., have shown that the Rad5 protein concertedly unwinds and anneals the nascent and the parental strands in the stalled forks without exposing extended single-stranded regions, and hence it seems to be a good candidate for the enzyme responsible for promoting fork regression *in vivo* (Blastyák *et al*., 2007).

Two recent publications have questioned the template-switching model (Lopes *et al*., 2006 and Heller & Marians, 2006). These studies established that DNA lesions in the leading strand did not block replication, but temporarily stalled the fork, and DNA synthesis was resumed following a repriming event downstream of the DNA lesion, thus leaving a gap opposite the lesion. Also, these results argued for a discontinuous mode of leading-strand synthesis and provided additional support for similar findings previously reported (reviewed in Ogawa & Okazaki, 1980). Further, these data suggested that lesion need not be repaired, and neither fork regression nor fork breakage is required in order to resume DNA synthesis.

Taken together, it is more likely that the increased level of mitotic recombination observed in RECQ5 deficient cells (Hu *et al*., 2005) is due to a defect in another DNA repair mechanisms (see below). In support of this, Luo's and Sung's laboratories have recently obtained evidence suggesting that RECQ5 suppresses unscheduled recombination during DNA replication by disruption of inappropriately formed RAD51 presynaptic filaments (Hu *et al*., 2007) in the same manner as the Srs2 (Krejci *et al*., 2003) and UvrD helicases (Veaute *et al*., 2005). Moreover, RECQ5 was found to be present at the ongoing DNA replication factories and at the sites of stalled DNA

replication forks (Kanagaraj *et al*., 2006). Therefore, it is more likely that RECQ5 functions primarily during S-phase and hence one may address the following questions in the future: 1) Do RECQ5 deficient cells exhibit defect in DNA replication? 2) Do cells require RECQ5 for efficient replication-fork restart after replication blockade?

In the second work (**Ren *et al*., 2008)**, we have identified an essential function for the zinc (Zn^{2+})-binding domain (379-454 aa) of human RECQ5 protein. Our work had showed that the Zn^{2+}-binding motif of RECQ5 suppresses strand-annealing activity residing in the N-terminal helicase domain (1-410 aa) of the protein. Further, our results illustrated that the Zn^{2+}-binding motif of RECQ5 is important for DNA binding and therefore is essential for the strand-separation activity of the enzyme. The involvement of the Zn^{2+}-binding motif in the DNA binding was also shown previously for the *E.coli* RecQ and human BLM helicases (Liu *et al*., 2004; Guo *et al*., 2005). Interestingly, human RECQ4, which does not contain the conserved Zn^{2+}-binding domain failed to unwind DNA (Macris *et al*., 2005). Taken together, all these data establish a clear link between the presence of the Zn^{2+}-binding motif and the helicase activity of RecQ helicases.

Our future goal is to understand the complete domain organization of the human RECQ5 helicase. In addition to the conserved helicase domain, RecQ helicases contain additional domains flanking the helicase motif (Bachrati and Hickson, 2003). In some RecQ helicases, additional enzymatic activities have been found to reside in those flanking regions. The WRN protein was found to exhibit a 3'-5' exonuclease activity residing in its unique N-terminal region (Huang *et al*., 1998; Kamath-Loeb *et al*., 1998). The unique C-terminal region of RECQ5 helicase was found to retain a strand-annealing activity (Garcia *et al*., 2004). The Helicase and RNaseD C-terminal (HRDC) domain of the BLM helicase was shown to be essential for the dissolution of double-Holliday junctions by BLM/TOPO IIIα complex (Wu *et al*., 2005). The N-terminal domain of RECQ4 helicase that bears sequence homology to the yeast replication factors Sld2/DRC1 was shown to be important for the initiation of DNA replication (Sangrithi *et al*., 2005).

Our bioinformatics analysis of the human RECQ5 protein revealed the presence of two conserved motifs in the C-terminal part of the RECQ5 polypeptide. The first is **T**ranslocation **R**ec**G** (TRG) motif that has been earlier discovered in the *E.coli* Mfd

protein (Mahdi *et al*., 2003; Chambers *et al*., 2003), a transcription-repair coupling factor capable of disrupting stalled transcription complexes (Park *et al*., 2002; Chambers *et al*., 2003; Saxowsky & Doetsch, 2006). The second is **S**et2-**R**pb1 **I**nteracting (SRI) domain that has been shown to bind specifically and with a high affinity to the doubly phosphorylated CTD repeats of RNA polymerase II (Kizer *et al*., 2005). The identification of these two motifs has led to the proposal that RECQ5 helicase might be involved in the disruption of stalled transcription complexes. This question will be addressed in our future studies.

To gain insights into the biological functions of RECQ5, we initiated studies to identify the interaction partners of RECQ5. We have discovered a strong interaction between the human RECQ5 protein and the MRE11/RAD50/NBS1 (MRN) complex *in vitro* and *in vivo* (**Zheng *et al*., manuscript to be submitted**). Upon genotoxic stress, RECQ5 and MRN proteins were found to simultaneously accumulate at sites of stalled DNA replication forks and DNA double strand breaks (DSBs). Moreover, we showed that MRE11 is required for the foci formation of RECQ5 following DNA damage. The observed defect in RECQ5 foci formation was unlikely caused by reduced level of the RECQ5 protein, since comparable amounts of RECQ5 were found in MRE11 proficient and deficient cells. In addition, our biochemical studies revealed that RECQ5 negatively regulates the MRN complex by attenuating its 3'-5' exonuclease activity. Collectively, these data suggest a functional interplay between the RECQ5 helicase and the MRN complex. Certainly, more work is required to elucidate the exact DNA transactions mediated by this helicase – nuclease complex. The questions that should be addressed in future are highlighted below.

The MRN complex was shown to play critical roles in DNA DSB repair, G2/M checkpoint activation, telomere length maintenance, meiotic recombination and the maintenance of genome stability during DNA replication (D'Amours & Jackson, 2002; van den Bosch *et al*., 2003). Accumulating evidence suggest that the MRN complex acts as a DSB sensor through its DNA-end processing activities and activates the ATM-dependent signaling pathways that co-ordinate cell cycle arrest with DNA repair (Williams *et al*., 2007; Lavin, 2007). However, the factors involved in the control of this resection process remain uncertain. Evidence from Tanya Paull's laboratory suggested that the activities of MRN complex could be controlled by the adenylate kinase activity of

RAD50 (Bhaskara *et al*., 2007). In addition, two works published recently have shown that CtIP promotes DNA DSB resection in a manner dependent on the MRN complex (Limbo *et al*., 2007; Sartori *et al*., 2007). Our finding that RECQ5 inhibits the 3'-5' exonuclease activity of the MRN complex adds one more controlling mechanism that prevents malfunctioning of the MRN complex and thereby allows the proper repair of DNA DSBs *via* homologous recombination (HR). Another attractive possibility could be a cooperative role of RECQ5 helicase and MRN nuclease in the regulation of HR. It is well known that the MRN complex is involved in the initial resection step of DNA DSB repair (D'Amours & Jackson, 2002). Recent studies suggested that RECQ5 negatively regulates the early step of HR by dismantling the hRAD51 filament (Hu *et al*., 2007). Hence, it will be of primary interest now to test the effect of MRN complex on this activity of RECQ5. Since our results (Zheng *et al*., manuscript to be submitted) clearly demonstrated that the MRN complex function as a recruitment factor for RECQ5 upon DNA damage, one can speculate that RECQ5-MRN complex acts as an anti-recombinase by preventing malfunctioning of hRAD51.

Apart from the 3'-5' exonuclease activity, the MRN complex was shown to possess an endonuclease activity specific for hairpin structures and the 3'-single-stranded DNA tail (Trujillo *et al*., 1998; Paull & Gellert, 1999; Trujillo & Sung, 2001). Hence, it will be interesting to check the effect of RECQ5 protein on this activity of MRN using similar substrates. Based on speculation that the MRN complex might mediate the endonucleolytic cleavage of the 5'-strand at secondary structures formed upon DNA unwinding, one can check whether the lagging strand liberated by the action of RECQ5 on substrate mimicking a stalled fork (with a gap on leading strand) is processed by the MRN endonuclease. In this case, one may assume that the unwound lagging strand could form a hairpin structure and thereby it serves as substrate for MRN cleavage. Similar model had been proposed earlier for *E.coli* RecQ and RecJ exonuclease (Courcelle & Hanawalt 1999; Morimatsu & Kowalczykowski 2003; Hishida *et al*., 2004). It was demonstrated that RecQ helicase in conjunction with RecJ, both belonging to the RecF pathway of recombinational repair, promoted degradation of nascent DNA on the lagging strand at blocked replication forks and subsequent events promoted recovery from DNA damage via homologous recombination (HR). Also, we believe that such an

action in mammalian cells may help stabilize the replication fork allowing resumption of DNA synthesis following the removal of DNA damage.

Previous studies conducted with BLM and WRN demonstrated that these proteins interacted physically and functionally with the MRN complex (Franchitto & Pichierri, 2002; Cheng *et al*., 2004; Franchitto & Pichierri, 2004). Similar to RECQ5, WRN was found recruited to the sites of DNA damage via the MRN complex (Franchitto and Pichierri, 2004). BLM was shown to be required for correct relocalization of the MRN complex after replication fork arrest (Franchitto and Pichierri, 2002). Further studies will be needed to fully understand the molecular mechanisms by which the RecQ helicases and MRN proteins work together to maintain genomic stability.

Finally, we demonstrated that WRN interacts physically with proteins that are involved in the initiation of mismatch repair (MMR) and the rejection of recombination between divergent sequences (**Saydam *et al*., 2007**). Most importantly, our experiments revealed that MutSα and MutSβ can stimulate the helicase activity of WRN on forked DNA structures with a 3'-single-strand (ss) arm that resemble intermediates of single-strand annealing (SSA) pathway of homologous recombination (HR). In addition, we found that a single G/T mismatch located ahead of the fork junction increased the efficiency of the MutSα-dependent unwinding by WRN. Our data provide a biochemical evidence for a model that had been proposed earlier in yeast in which the MMR initiation factors prevent homeologous recombination by activating a DNA helicase for unwinding of recombination intermediates containing mismatches (Sugawara *et al*., 2004; Goldfarb & Alani, 2005).

Obviously, the detailed functional aspects of the observed interactions have to be addressed in the course of future studies. Both the MMR system and the WRN helicase are multifunctional enzymes that are known to play a vital role in several different pathways of DNA metabolism (Jiricny, 2006; Hanada & Hickson, 2007). We have recently found that like WRN, MMR proteins accumulate at the sites of laser-induced DNA DSBs (Lan *et al*., 2005; unpublished observation). In future, we will learn how the interaction between the MMR factors and WRN affect the outcome of mitotic recombination events.

G-quadruplex structures, which can readily form in G-rich genomic loci such as immunoglobulin class switch regions or telomeric repeats, form a barrier for progression

of DNA replication forks. Recently, human MutSα has been shown to bind efficiently to G-quadruplex DNA, which is a preferred substrate for both BLM and WRN (Mohaghegh *et al*., 2001; Larson *et al*., 2005). Moreover, Msh2 deficiency in mice is associated with loss of telomeres and an elevated level of telomere end-to-end fusion, a phenotype similar to that manifested by WRN-deficient cells (Crabbe et al. 2004; Campbell et al. 2006). Taken together, it is now tempting to speculate that the MMR proteins might mediate recruitment of the WRN helicase to G-quadruplex structures formed at telomeres and hence facilitate their removal.

In our work (Saydam *et al*., 2007), we found that MutLα did not alter the WRN-mediated unwinding of substrates mimicking the SSA intermediates, even in presence of MutSα or MutSβ. Our data are consistent with the yeast finding that the Mlh1 and Pms1 proteins have only minor roles in the rejection of homeologous recombination *in vivo* (Sugawara *et al*., 2004). Therefore, the direct interaction identified between WRN and MutLα might have another functional implication. Interestingly, we found that the MLH1 protein is located in the PML nuclear bodies (NBs), irrespective of the presence or absence of DNA damage (unpublished observation). These dynamic nuclear protein structures serve as DNA-damage sensors and are implicated in several DNA-repair pathways as well as in alternative lengthening of telomeres (ALT) *via* homologous recombination (Dellaire and Bazett-Jones, 2004). WRN has been shown to localize to a subset of PML NBs after DNA damage or in S phase of ALT cells (Blander *et al*., 2002; Opresko *et al*., 2004). Therefore, it is possible that the recruitment of WRN to these structures could be facilitated through a direct interaction with MLH1. Moreover, it remains to be seen whether inactivation of the MMR system in Werner syndrome cells will further increase genomic instability in these cells. Such studies will shed more light on the molecular mechanisms underlying the process of tumorigenesis.

In conclusion, the findings described in this thesis significantly advance our understanding of the biological role of the human RecQ helicases and provide good basis for future work on these important guardians of genome integrity.

6. References

Abdel-Monem, M., M. C. Chanal, et al. (1977). "DNA unwinding enzyme II of Escherichia coli. 1. Purification and characterization of the ATPase activity." Eur J Biochem **79**(1): 33-8.

Ahn, B., J. A. Harrigan, et al. (2004). "Regulation of WRN helicase activity in human base excision repair." J Biol Chem **279**(51): 53465-74.

Bachrati, C. Z. and I. D. Hickson (2003). "RecQ helicases: suppressors of tumorigenesis and premature aging." Biochem J **374**(Pt 3): 577-606.

Bachrati, C. Z. and I. D. Hickson (2008). "RecQ helicases: guardian angels of the DNA replication fork." Chromosoma **117**(3): 219-33.

Balajee, A. S., A. Machwe, et al. (1999). "The Werner syndrome protein is involved in RNA polymerase II transcription." Mol Biol Cell **10**(8): 2655-68.

Baller, F. (1950). "Radiosaplasic und Inzucht." Z. Menschl. Vererb.Konstitutionsl. **29**: 782-790.

Bartek, J., J. Lukas, et al. (2007). "DNA damage response as an anti-cancer barrier: damage threshold and the concept of 'conditional haploinsufficiency'." Cell Cycle **6**(19): 2344-7.

Bartkova, J., Z. Horejsi, et al. (2005). "DNA damage response as a candidate anti-cancer barrier in early human tumorigenesis." Nature **434**(7035): 864-70.

Bartkova, J., N. Rezaei, et al. (2006). "Oncogene-induced senescence is part of the tumorigenesis barrier imposed by DNA damage checkpoints." Nature **444**(7119): 633-7.

Bateman, J. R. and C. T. Wu (2007). "DNA replication and models for the origin of piRNAs." Bioessays **29**(4): 382-5.

Batty, D. P. and R. D. Wood (2000). "Damage recognition in nucleotide excision repair of DNA." Gene **241**(2): 193-204.

Becker, P. B. and W. Horz (2002). "ATP-dependent nucleosome remodeling." Annu Rev Biochem **71**: 247-73.

Bennett, R. J., J. L. Keck, et al. (1999). "Binding specificity determines polarity of DNA unwinding by the Sgs1 protein of S. cerevisiae." J Mol Biol **289**(2): 235-48.

Bennett, R. J., J. A. Sharp, et al. (1998). "Purification and characterization of the Sgs1 DNA helicase activity of Saccharomyces cerevisiae." J Biol Chem **273**(16): 9644-50.

Beresten, S. F., R. Stan, et al. (1999). "Purification of overexpressed hexahistidine-

tagged BLM N431 as oligomeric complexes." Protein Expr Purif **17**(2): 239-48.

Bernstein, D. A. and J. L. Keck (2003). "Domain mapping of Escherichia coli RecQ defines the roles of conserved N- and C-terminal regions in the RecQ family." Nucleic Acids Res **31**(11): 2778-85.

Bernstein, D. A. and J. L. Keck (2005). "Conferring substrate specificity to DNA helicases: role of the RecQ HRDC domain." Structure **13**(8): 1173-82.

Bernstein, D. A., M. C. Zittel, et al. (2003). "High-resolution structure of the E.coli RecQ helicase catalytic core." Embo J **22**(19): 4910-21.

Bhaskara, V., A. Dupre, et al. (2007). "Rad50 adenylate kinase activity regulates DNA tethering by Mre11/Rad50 complexes." Mol Cell **25**(5): 647-61.

Bjergbaek, L., J. A. Cobb, et al. (2005). "Mechanistically distinct roles for Sgs1p in checkpoint activation and replication fork maintenance." Embo J **24**(2): 405-17.

Blander, G., N. Zalle, et al. (2002). "DNA damage-induced translocation of the Werner helicase is regulated by acetylation." J Biol Chem **277**(52): 50934-40.

Blastyak, A., L. Pinter, et al. (2007). "Yeast Rad5 protein required for postreplication repair has a DNA helicase activity specific for replication fork regression." Mol Cell **28**(1): 167-75.

Bloom, D. (1954). "Congenital telangiectatic erythema resembling lupus erythematosus in dwarfs; probably a syndrome entity." AMA Am J Dis Child **88**(6): 754-8.

Brosh, R. M., Jr. and V. A. Bohr (2007). "Human premature aging, DNA repair and RecQ helicases." Nucleic Acids Res **35**(22): 7527-44.

Brosh, R. M., Jr., P. Karmakar, et al. (2001). "p53 Modulates the exonuclease activity of Werner syndrome protein." J Biol Chem **276**(37): 35093-102.

Brosh, R. M., Jr., J. L. Li, et al. (2000). "Replication protein A physically interacts with the Bloom's syndrome protein and stimulates its helicase activity." J Biol Chem **275**(31): 23500-8.

Brosh, R. M., Jr., C. von Kobbe, et al. (2001). "Werner syndrome protein interacts with human flap endonuclease 1 and stimulates its cleavage activity." Embo J **20**(20): 5791-801.

Bugreev, D. V., X. Yu, et al. (2007). "Novel pro- and anti-recombination activities of the Bloom's syndrome helicase." Genes Dev **21**(23): 3085-94.

Campbell, M. R., Y. Wang, et al. (2006). "Msh2 deficiency leads to chromosomal abnormalities, centrosome amplification, and telomere capping defect." Oncogene **25**(17): 2531-6.

Carthew, R. W. (2006). "Molecular biology. A new RNA dimension to genome control." Science **313**(5785): 305-6.

Caruthers, J. M. and D. B. McKay (2002). "Helicase structure and mechanism." Curr Opin Struct Biol **12**(1): 123-33.

Chaganti, R. S., S. Schonberg, et al. (1974). "A manyfold increase in sister chromatid exchanges in Bloom's syndrome lymphocytes." Proc Natl Acad Sci U S A **71**(11): 4508-12.

Chambers, A. L., A. J. Smith, et al. (2003). "A DNA translocation motif in the bacterial transcription--repair coupling factor, Mfd." Nucleic Acids Res **31**(22): 6409-18.

Chang, M., M. Bellaoui, et al. (2005). "RMI1/NCE4, a suppressor of genome instability, encodes a member of the RecQ helicase/Topo III complex." Embo J **24**(11): 2024-33.

Cheng, W. H. and V. A. Bohr (2003). "Diverse dealings of the Werner helicase/nuclease." Sci Aging Knowledge Environ **2003**(31): PE22.

Cheng, W. H., R. Kusumoto, et al. (2006). "Collaboration of Werner syndrome protein and BRCA1 in cellular responses to DNA interstrand cross-links." Nucleic Acids Res **34**(9): 2751-60.

Cheng, W. H., C. von Kobbe, et al. (2004). "Linkage between Werner syndrome protein and the Mre11 complex via Nbs1." J Biol Chem **279**(20): 21169-76.

Cheok, C. F., C. Z. Bachrati, et al. (2005). "Roles of the Bloom's syndrome helicase in the maintenance of genome stability." Biochem Soc Trans **33**(Pt 6): 1456-9.

Cheok, C. F., L. Wu, et al. (2005). "The Bloom's syndrome helicase promotes the annealing of complementary single-stranded DNA." Nucleic Acids Res **33**(12): 3932-41.

Chester, N., F. Kuo, et al. (1998). "Stage-specific apoptosis, developmental delay, and embryonic lethality in mice homozygous for a targeted disruption in the murine Bloom's syndrome gene." Genes Dev **12**(21): 3382-93.

Chow, K. H. and J. Courcelle (2004). "RecO acts with RecF and RecR to protect and maintain replication forks blocked by UV-induced DNA damage in Escherichia coli." J Biol Chem **279**(5): 3492-6.

Cleaver, J. E. and E. Crowley (2002). "UV damage, DNA repair and skin carcinogenesis." Front Biosci **7**: d1024-43.

Cobb, J. A. and L. Bjergbaek (2006). "RecQ helicases: lessons from model organisms." Nucleic Acids Res **34**(15): 4106-14.

Cobb, J. A., L. Bjergbaek, et al. (2003). "DNA polymerase stabilization at stalled

replication forks requires Mec1 and the RecQ helicase Sgs1." Embo J **22**(16): 4325-36.

Cogoni, C. and G. Macino (1999). "Posttranscriptional gene silencing in Neurospora by a RecQ DNA helicase." Science **286**(5448): 2342-4.

Cohen, H. and D. A. Sinclair (2001). "Recombination-mediated lengthening of terminal telomeric repeats requires the Sgs1 DNA helicase." Proc Natl Acad Sci U S A **98**(6): 3174-9.

Cooper, M. P., A. Machwe, et al. (2000). "Ku complex interacts with and stimulates the Werner protein." Genes Dev **14**(8): 907-12.

Costa, R. M., V. Chigancas, et al. (2003). "The eukaryotic nucleotide excision repair pathway." Biochimie **85**(11): 1083-99.

Courcelle, J., J. R. Donaldson, et al. (2003). "DNA damage-induced replication fork regression and processing in Escherichia coli." Science **299**(5609): 1064-7.

Courcelle, J. and P. C. Hanawalt (1999). "RecQ and RecJ process blocked replication forks prior to the resumption of replication in UV-irradiated Escherichia coli." Mol Gen Genet **262**(3): 543-51.

Cox, M. M. (2001). "Recombinational DNA repair of damaged replication forks in Escherichia coli: questions." Annu Rev Genet **35**: 53-82.

Crabbe, L., R. E. Verdun, et al. (2004). "Defective telomere lagging strand synthesis in cells lacking WRN helicase activity." Science **306**(5703): 1951-3.

Cromie, G. A., C. B. Millar, et al. (2000). "Palindromes as substrates for multiple pathways of recombination in Escherichia coli." Genetics **154**(2): 513-22.

Cui, S., D. Arosio, et al. (2004). "Analysis of the unwinding activity of the dimeric RECQ1 helicase in the presence of human replication protein A." Nucleic Acids Res **32**(7): 2158-70.

Cui, S., R. Klima, et al. (2003). "Characterization of the DNA-unwinding activity of human RECQ1, a helicase specifically stimulated by human replication protein A." J Biol Chem **278**(3): 1424-32.

Cumin, I., J. Y. Cohen, et al. (1996). "Rothmund-Thomson syndrome and osteosarcoma." Med Pediatr Oncol **26**(6): 414-6.

D'Amours, D. and S. P. Jackson (2002). "The Mre11 complex: at the crossroads of dna repair and checkpoint signalling." Nat Rev Mol Cell Biol **3**(5): 317-27.

Daniels, D. S., T. T. Woo, et al. (2004). "DNA binding and nucleotide flipping by the human DNA repair protein AGT." Nat Struct Mol Biol **11**(8): 714-20.

Davies, S. L., P. S. North, et al. (2007). "Role for BLM in replication-fork restart and suppression of origin firing after replicative stress." Nat Struct Mol Biol **14**(7): 677-9.

Daya-Grosjean, L. and A. Sarasin (2005). "The role of UV induced lesions in skin carcinogenesis: an overview of oncogene and tumor suppressor gene modifications in xeroderma pigmentosum skin tumors." Mutat Res **571**(1-2): 43-56.

De la Torre, C., J. Pincheira, et al. (2003). "Human syndromes with genomic instability and multiprotein machines that repair DNA double-strand breaks." Histol Histopathol **18**(1): 225-43.

Declais, A. C., J. Marsault, et al. (2000). "Reverse gyrase, the two domains intimately cooperate to promote positive supercoiling." J Biol Chem **275**(26): 19498-504.

Delagoutte, E. and P. H. von Hippel (2002). "Helicase mechanisms and the coupling of helicases within macromolecular machines. Part I: Structures and properties of isolated helicases." Q Rev Biophys **35**(4): 431-78.

Dellaire, G. and D. P. Bazett-Jones (2004). "PML nuclear bodies: dynamic sensors of DNA damage and cellular stress." Bioessays **26**(9): 963-77.

Der Kaloustian, V. M., J. J. McGill, et al. (1990). "Clonal lines of aneuploid cells in Rothmund-Thomson syndrome." Am J Med Genet **37**(3): 336-9.

Derewenda, U., A. Oleksy, et al. (2004). "The crystal structure of RhoA in complex with the DH/PH fragment of PDZRhoGEF, an activator of the Ca(2+) sensitization pathway in smooth muscle." Structure **12**(11): 1955-65.

Doherty, K. M., S. Sharma, et al. (2005). "RECQ1 helicase interacts with human mismatch repair factors that regulate genetic recombination." J Biol Chem **280**(30): 28085-94.

Drummond, J. T., G. M. Li, et al. (1995). "Isolation of an hMSH2-p160 heterodimer that restores DNA mismatch repair to tumor cells." Science **268**(5219): 1909-12.

Dulbecco, R. (1949). "Reactivation of ultra-violet-inactivated bacteriophage by visible light." Nature **163**(4155): 949.

Ellis, N. A., J. Groden, et al. (1995). "The Bloom's syndrome gene product is homologous to RecQ helicases." Cell **83**(4): 655-66.

Epstein, C. J., G. M. Martin, et al. (1966). "Werner's syndrome a review of its symptomatology, natural history, pathologic features, genetics and relationship to the natural aging process." Medicine (Baltimore) **45**(3): 177-221.

Erzberger, J. P. and J. M. Berger (2006). "Evolutionary relationships and structural mechanisms of AAA+ proteins." Annu Rev Biophys Biomol Struct **35**: 93-114.

Fairman, M. E., P. A. Maroney, et al. (2004). "Protein displacement by DExH/D "RNA helicases" without duplex unwinding." Science **304**(5671): 730-4.

Fang, Q., S. Kanugula, et al. (2005). "Function of domains of human O6-alkylguanine-DNA alkyltransferase." Biochemistry **44**(46): 15396-405.

Featherstone, C. and S. P. Jackson (1999). "Ku, a DNA repair protein with multiple cellular functions?" Mutat Res **434**(1): 3-15.

Flores, M. J., N. Sanchez, et al. (2005). "A fork-clearing role for UvrD." Mol Microbiol **57**(6): 1664-75.

Fortini, P., B. Pascucci, et al. (2003). "The base excision repair: mechanisms and its relevance for cancer susceptibility." Biochimie **85**(11): 1053-71.

Fousteri, M. and L. H. Mullenders (2008). "Transcription-coupled nucleotide excision repair in mammalian cells: molecular mechanisms and biological effects." Cell Res **18**(1): 73-84.

Franchitto, A. and P. Pichierri (2002). "Bloom's syndrome protein is required for correct relocalization of RAD50/MRE11/NBS1 complex after replication fork arrest." J Cell Biol **157**(1): 19-30.

Franchitto, A. and P. Pichierri (2004). "Werner syndrome protein and the MRE11 complex are involved in a common pathway of replication fork recovery." Cell Cycle **3**(10): 1331-9.

Frei, C. and S. M. Gasser (2000). "RecQ-like helicases: the DNA replication checkpoint connection." J Cell Sci **113 (Pt 15)**: 2641-6.

Friedberg, E. C. (1995). "Out of the shadows and into the light: the emergence of DNA repair." Trends Biochem Sci **20**(10): 381.

Friedberg, E. C. (2003). "DNA damage and repair." Nature **421**(6921): 436-40.

Frosina, G., P. Fortini, et al. (1996). "Two pathways for base excision repair in mammalian cells." J Biol Chem **271**(16): 9573-8.

Fukuchi, K., G. M. Martin, et al. (1989). "Mutator phenotype of Werner syndrome is characterized by extensive deletions." Proc Natl Acad Sci U S A **86**(15): 5893-7.

Gangloff, S., J. P. McDonald, et al. (1994). "The yeast type I topoisomerase Top3 interacts with Sgs1, a DNA helicase homolog: a potential eukaryotic reverse gyrase." Mol Cell Biol **14**(12): 8391-8.

Gangloff, S., C. Soustelle, et al. (2000). "Homologous recombination is responsible for cell death in the absence of the Sgs1 and Srs2 helicases." Nat Genet **25**(2): 192-4.

Garcia, P. L., Y. Liu, et al. (2004). "Human RECQ5beta, a protein with DNA helicase and strand-annealing activities in a single polypeptide." Embo J **23**(14): 2882-91.

Genschel, J., S. J. Littman, et al. (1998). "Isolation of MutSbeta from human cells and comparison of the mismatch repair specificities of MutSbeta and MutSalpha." J Biol Chem **273**(31): 19895-901.

German, J. (1993). "Bloom syndrome: a mendelian prototype of somatic mutational disease." Medicine (Baltimore) **72**(6): 393-406.

German, J., S. Schonberg, et al. (1977). "Bloom's syndrome. IV. Sister-chromatid exchanges in lymphocytes." Am J Hum Genet **29**(3): 248-55.

Gillet, L. C. and O. D. Scharer (2006). "Molecular mechanisms of mammalian global genome nucleotide excision repair." Chem Rev **106**(2): 253-76.

Goldfarb, T. and E. Alani (2005). "Distinct roles for the Saccharomyces cerevisiae mismatch repair proteins in heteroduplex rejection, mismatch repair and nonhomologous tail removal." Genetics **169**(2): 563-74.

Goosen, N. and G. F. Moolenaar (2008). "Repair of UV damage in bacteria." DNA Repair (Amst) **7**(3): 353-79.

Gorbalenya, A. E., E. V. Koonin, et al. (1990). "A new superfamily of putative NTP-binding domains encoded by genomes of small DNA and RNA viruses." FEBS Lett **262**(1): 145-8.

Gorbalenya, A. E. a. K., E.V. (1993). "Helicases: amino acid sequence comparisons and structure-function relationships." Curr. Opin. Struct. Biol. **3**: 419-429.

Gorgoulis, V. G., L. V. Vassiliou, et al. (2005). "Activation of the DNA damage checkpoint and genomic instability in human precancerous lesions." Nature **434**(7035): 907-13.

Goto, M. (1997). "Hierarchical deterioration of body systems in Werner's syndrome: implications for normal ageing." Mech Ageing Dev **98**(3): 239-54.

Goto, M., R. W. Miller, et al. (1996). "Excess of rare cancers in Werner syndrome (adult progeria)." Cancer Epidemiol Biomarkers Prev **5**(4): 239-46.

Graves-Woodward, K. L., J. Gottlieb, et al. (1997). "Biochemical analyses of mutations in the HSV-1 helicase-primase that alter ATP hydrolysis, DNA unwinding, and coupling between hydrolysis and unwinding." J Biol Chem **272**(7): 4623-30.

Guo, R. B., P. Rigolet, et al. (2005). "Structural and functional characterizations reveal the importance of a zinc binding domain in Bloom's syndrome helicase." Nucleic Acids Res **33**(10): 3109-24.

Hakem, R. (2008). "DNA-damage repair; the good, the bad, and the ugly." Embo J **27**(4): 589-605.

Hall, M. C. and S. W. Matson (1999). "Helicase motifs: the engine that powers DNA unwinding." Mol Microbiol **34**(5): 867-77.

Hanada, K. and I. D. Hickson (2007). "Molecular genetics of RecQ helicase disorders." Cell Mol Life Sci **64**(17): 2306-22.

Hanada, K., T. Ukita, et al. (1997). "RecQ DNA helicase is a suppressor of illegitimate recombination in Escherichia coli." Proc Natl Acad Sci U S A **94**(8): 3860-5.

Harmon, F. G., J. P. Brockman, et al. (2003). "RecQ helicase stimulates both DNA catenation and changes in DNA topology by topoisomerase III." J Biol Chem **278**(43): 42668-78.

Harmon, F. G., R. J. DiGate, et al. (1999). "RecQ helicase and topoisomerase III comprise a novel DNA strand passage function: a conserved mechanism for control of DNA recombination." Mol Cell **3**(5): 611-20.

Harmon, F. G. and S. C. Kowalczykowski (1998). "RecQ helicase, in concert with RecA and SSB proteins, initiates and disrupts DNA recombination." Genes Dev **12**(8): 1134-44.

Harmon, F. G. and S. C. Kowalczykowski (2001). "Biochemical characterization of the DNA helicase activity of the escherichia coli RecQ helicase." J Biol Chem **276**(1): 232-43.

Harrigan, J. A., P. L. Opresko, et al. (2003). "The Werner syndrome protein stimulates DNA polymerase beta strand displacement synthesis via its helicase activity." J Biol Chem **278**(25): 22686-95.

Hartung, F. and H. Puchta (2006). "The RecQ gene family in plants." J Plant Physiol **163**(3): 287-96.

Hashimoto, Y. and H. Takisawa (2003). "Xenopus Cut5 is essential for a CDK-dependent process in the initiation of DNA replication." Embo J **22**(10): 2526-35.

Hegde, M. L., T. K. Hazra, et al. (2008). "Early steps in the DNA base excision/single-strand interruption repair pathway in mammalian cells." Cell Res **18**(1): 27-47.

Heinen, C. D., C. Schmutte, et al. (2002). "DNA repair and tumorigenesis: lessons from hereditary cancer syndromes." Cancer Biol Ther **1**(5): 477-85.

Helleday, T., J. Lo, et al. (2007). "DNA double-strand break repair: from mechanistic understanding to cancer treatment." DNA Repair (Amst) **6**(7): 923-35.

Heller, R. C. and K. J. Marians (2006). "Replication fork reactivation downstream of a

blocked nascent leading strand." Nature **439**(7076): 557-62.

Hess, M. T., U. Schwitter, et al. (1997). "Bipartite substrate discrimination by human nucleotide excision repair." Proc Natl Acad Sci U S A **94**(13): 6664-9.

Heyer, W. D. (2004). "Damage signaling: RecQ sends an SOS to you." Curr Biol **14**(20): R895-7.

Hickson, I. D. (2003). "RecQ helicases: caretakers of the genome." Nat Rev Cancer **3**(3): 169-78.

Higgins, N. P., K. Kato, et al. (1976). "A model for replication repair in mammalian cells." J Mol Biol **101**(3): 417-25.

Hishida, T., Y. W. Han, et al. (2004). "Role of the Escherichia coli RecQ DNA helicase in SOS signaling and genome stabilization at stalled replication forks." Genes Dev **18**(15): 1886-97.

Hoege, C., B. Pfander, et al. (2002). "RAD6-dependent DNA repair is linked to modification of PCNA by ubiquitin and SUMO." Nature **419**(6903): 135-41.

Hoeijmakers, J. H. (2001). "Genome maintenance mechanisms for preventing cancer." Nature **411**(6835): 366-74.

Hoki, Y., R. Araki, et al. (2003). "Growth retardation and skin abnormalities of the Recql4-deficient mouse." Hum Mol Genet **12**(18): 2293-9.

Hsieh, J., K. J. Moore, et al. (1999). "A two-site kinetic mechanism for ATP binding and hydrolysis by E. coli Rep helicase dimer bound to a single-stranded oligodeoxynucleotide." J Mol Biol **288**(2): 255-74.

Hsieh, P. and K. Yamane (2008). "DNA mismatch repair: Molecular mechanism, cancer, and ageing." Mech Ageing Dev.

Hu, J. S., H. Feng, et al. (2005). "Solution structure of a multifunctional DNA- and protein-binding motif of human Werner syndrome protein." Proc Natl Acad Sci U S A **102**(51): 18379-84.

Hu, P., S. F. Beresten, et al. (2001). "Evidence for BLM and Topoisomerase IIIalpha interaction in genomic stability." Hum Mol Genet **10**(12): 1287-98.

Hu, Y., X. Lu, et al. (2005). "Recql5 and Blm RecQ DNA helicases have nonredundant roles in suppressing crossovers." Mol Cell Biol **25**(9): 3431-42.

Hu, Y., S. Raynard, et al. (2007). "RECQL5/Recql5 helicase regulates homologous recombination and suppresses tumor formation via disruption of Rad51 presynaptic filaments." Genes Dev **21**(23): 3073-84.

Huang, S., S. Beresten, et al. (2000). "Characterization of the human and mouse WRN 3'-->5' exonuclease." Nucleic Acids Res **28**(12): 2396-405.

Huang, S., B. Li, et al. (1998). "The premature ageing syndrome protein, WRN, is a 3'-->5' exonuclease." Nat Genet **20**(2): 114-6.

Huber, M. D., D. C. Lee, et al. (2002). "G4 DNA unwinding by BLM and Sgs1p: substrate specificity and substrate-specific inhibition." Nucleic Acids Res **30**(18): 3954-61.

Hussein, M. R. (2005). "Ultraviolet radiation and skin cancer: molecular mechanisms." J Cutan Pathol **32**(3): 191-205.

Ichikawa, K., T. Noda, et al. (2002). "[Preparation of the gene targeted knockout mice for human premature aging diseases, Werner syndrome, and Rothmund-Thomson syndrome caused by the mutation of DNA helicases]." Nippon Yakurigaku Zasshi **119**(4): 219-26.

Ilyina, T. V. and E. V. Koonin (1992). "Conserved sequence motifs in the initiator proteins for rolling circle DNA replication encoded by diverse replicons from eubacteria, eucaryotes and archaebacteria." Nucleic Acids Res **20**(13): 3279-85.

Imamura, O., K. Fujita, et al. (2002). "Werner and Bloom helicases are involved in DNA repair in a complementary fashion." Oncogene **21**(6): 954-63.

Ira, G., A. Malkova, et al. (2003). "Srs2 and Sgs1-Top3 suppress crossovers during double-strand break repair in yeast." Cell **115**(4): 401-11.

Irino, N., K. Nakayama, et al. (1986). "The recQ gene of Escherichia coli K12: primary structure and evidence for SOS regulation." Mol Gen Genet **205**(2): 298-304.

Iyer, R. R., A. Pluciennik, et al. (2006). "DNA mismatch repair: functions and mechanisms." Chem Rev **106**(2): 302-23.

Izumikawa, K., M. Yanagida, et al. (2008). "Association of human DNA helicase RecQ5beta with RNA polymerase II and its possible role in transcription." Biochem J.

Jackson, A. L. and L. A. Loeb (1998). "The mutation rate and cancer." Genetics **148**(4): 1483-90.

Jackson, S. P. (2002). "Sensing and repairing DNA double-strand breaks." Carcinogenesis **23**(5): 687-96.

Jankowsky, E., C. H. Gross, et al. (2001). "Active disruption of an RNA-protein interaction by a DExH/D RNA helicase." Science **291**(5501): 121-5.

Janscak, P., P. L. Garcia, et al. (2003). "Characterization and mutational analysis of the RecQ core of the bloom syndrome protein." J Mol Biol **330**(1): 29-42.

Jeong, Y. S., Y. Kang, et al. (2003). "Deficiency of Caenorhabditis elegans RecQ5 homologue reduces life span and increases sensitivity to ionizing radiation." DNA Repair (Amst) **2**(12): 1309-19.

Jiricny, J. (2006). "The multifaceted mismatch-repair system." Nat Rev Mol Cell Biol **7**(5): 335-46.

Johnson, F. B., D. B. Lombard, et al. (2000). "Association of the Bloom syndrome protein with topoisomerase IIIalpha in somatic and meiotic cells." Cancer Res **60**(5): 1162-7.

Kamimura, Y., H. Masumoto, et al. (1998). "Sld2, which interacts with Dpb11 in Saccharomyces cerevisiae, is required for chromosomal DNA replication." Mol Cell Biol **18**(10): 6102-9.

Kanagaraj, R., N. Saydam, et al. (2006). "Human RECQ5beta helicase promotes strand exchange on synthetic DNA structures resembling a stalled replication fork." Nucleic Acids Res **34**(18): 5217-31.

Karow, J. K., A. Constantinou, et al. (2000). "The Bloom's syndrome gene product promotes branch migration of holliday junctions." Proc Natl Acad Sci U S A **97**(12): 6504-8.

Karow, J. K., R. H. Newman, et al. (1999). "Oligomeric ring structure of the Bloom's syndrome helicase." Curr Biol **9**(11): 597-600.

Kawabe, T., N. Tsuyama, et al. (2000). "Differential regulation of human RecQ family helicases in cell transformation and cell cycle." Oncogene **19**(41): 4764-72.

Kawasaki, K., S. Maruyama, et al. (2002). "Drosophila melanogaster RECQ5/QE DNA helicase: stimulation by GTP binding." Nucleic Acids Res **30**(17): 3682-91.

Kellermayer, R., H. A. Siitonen, et al. (2005). "A patient with Rothmund-Thomson syndrome and all features of RAPADILINO." Arch Dermatol **141**(5): 617-20.

Kennedy, R. D. and A. D. D'Andrea (2006). "DNA repair pathways in clinical practice: lessons from pediatric cancer susceptibility syndromes." J Clin Oncol **24**(23): 3799-808.

Khakhar, R. R., J. A. Cobb, et al. (2003). "RecQ helicases: multiple roles in genome maintenance." Trends Cell Biol **13**(9): 493-501.

Kitao, S., N. M. Lindor, et al. (1999). "Rothmund-thomson syndrome responsible gene, RECQL4: genomic structure and products." Genomics **61**(3): 268-76.

Kitao, S., I. Ohsugi, et al. (1998). "Cloning of two new human helicase genes of the RecQ family: biological significance of multiple species in higher eukaryotes." Genomics **54**(3): 443-52.

Kizer, K. O., H. P. Phatnani, et al. (2005). "A novel domain in Set2 mediates RNA polymerase II interaction and couples histone H3 K36 methylation with transcript elongation." Mol Cell Biol **25**(8): 3305-16.

Komori, K., M. Hidaka, et al. (2004). "Cooperation of the N-terminal Helicase and C-terminal endonuclease activities of Archaeal Hef protein in processing stalled replication forks." J Biol Chem **279**(51): 53175-85.

Korolev, S., N. Yao, et al. (1998). "Comparisons between the structures of HCV and Rep helicases reveal structural similarities between SF1 and SF2 super-families of helicases." Protein Sci **7**(3): 605-10.

Krejci, L., S. Van Komen, et al. (2003). "DNA helicase Srs2 disrupts the Rad51 presynaptic filament." Nature **423**(6937): 305-9.

Kunkel, T. A. and D. A. Erie (2005). "DNA mismatch repair." Annu Rev Biochem **74**: 681-710.

Kusano, K., M. E. Berres, et al. (1999). "Evolution of the RECQ family of helicases: A drosophila homolog, Dmblm, is similar to the human bloom syndrome gene." Genetics **151**(3): 1027-39.

Laine, J. P., P. L. Opresko, et al. (2003). "Werner protein stimulates topoisomerase I DNA relaxation activity." Cancer Res **63**(21): 7136-46.

Lan, L., S. Nakajima, et al. (2005). "Accumulation of Werner protein at DNA double-strand breaks in human cells." J Cell Sci **118**(Pt 18): 4153-62.

Larson, E. D., M. L. Duquette, et al. (2005). "MutSalpha binds to and promotes synapsis of transcriptionally activated immunoglobulin switch regions." Curr Biol **15**(5): 470-4.

Lau, N. C., A. G. Seto, et al. (2006). "Characterization of the piRNA complex from rat testes." Science **313**(5785): 363-7.

Lavin, M. F. (2007). "ATM and the Mre11 complex combine to recognize and signal DNA double-strand breaks." Oncogene **26**(56): 7749-58.

Lebel, M. and P. Leder (1998). "A deletion within the murine Werner syndrome helicase induces sensitivity to inhibitors of topoisomerase and loss of cellular proliferative capacity." Proc Natl Acad Sci U S A **95**(22): 13097-102.

Lee, J. W., J. Harrigan, et al. (2005). "Pathways and functions of the Werner syndrome protein." Mech Ageing Dev **126**(1): 79-86.

Lee, J. W., R. Kusumoto, et al. (2005). "Modulation of Werner syndrome protein function by a single mutation in the conserved RecQ domain." J Biol Chem **280**(47): 39627-36.

Lee, J. Y. and W. Yang (2006). "UvrD helicase unwinds DNA one base pair at a time by a two-part power stroke." Cell **127**(7): 1349-60.

Lehmann, A. R., A. Niimi, et al. (2007). "Translesion synthesis: Y-family polymerases and the polymerase switch." DNA Repair (Amst) **6**(7): 891-9.

Li, B. and L. Comai (2001). "Requirements for the nucleolytic processing of DNA ends by the Werner syndrome protein-Ku70/80 complex." J Biol Chem **276**(13): 9896-902.

Li, B., S. Navarro, et al. (2004). "Identification and biochemical characterization of a Werner's syndrome protein complex with Ku70/80 and poly(ADP-ribose) polymerase-1." J Biol Chem **279**(14): 13659-67.

Li, D., M. Frazier, et al. (2006). "Single nucleotide polymorphisms of RecQ1, RAD54L, and ATM genes are associated with reduced survival of pancreatic cancer." J Clin Oncol **24**(11): 1720-8.

Li, D., H. Liu, et al. (2006). "Significant effect of homologous recombination DNA repair gene polymorphisms on pancreatic cancer survival." Cancer Res **66**(6): 3323-30.

Li, X. and W. D. Heyer (2008). "Homologous recombination in DNA repair and DNA damage tolerance." Cell Res **18**(1): 99-113.

Liberi, G., G. Maffioletti, et al. (2005). "Rad51-dependent DNA structures accumulate at damaged replication forks in sgs1 mutants defective in the yeast ortholog of BLM RecQ helicase." Genes Dev **19**(3): 339-50.

Limbo, O., C. Chahwan, et al. (2007). "Ctp1 is a cell-cycle-regulated protein that functions with Mre11 complex to control double-strand break repair by homologous recombination." Mol Cell **28**(1): 134-46.

Lindahl, T. (1996). "The Croonian Lecture, 1996: endogenous damage to DNA." Philos Trans R Soc Lond B Biol Sci **351**(1347): 1529-38.

Lindahl, T., B. Sedgwick, et al. (1988). "Regulation and expression of the adaptive response to alkylating agents." Annu Rev Biochem **57**: 133-57.

Linder, P., P. F. Lasko, et al. (1989). "Birth of the D-E-A-D box." Nature **337**(6203): 121-2.

Linder, P., N. K. Tanner, et al. (2001). "From RNA helicases to RNPases." Trends Biochem Sci **26**(6): 339-41.

Lindor, N. M., Y. Furuichi, et al. (2000). "Rothmund-Thomson syndrome due to RECQ4 helicase mutations: report and clinical and molecular comparisons with Bloom syndrome and Werner syndrome." Am J Med Genet **90**(3): 223-8.

Liu, J. L., P. Rigolet, et al. (2004). "The zinc finger motif of Escherichia coli RecQ is

implicated in both DNA binding and protein folding." J Biol Chem **279**(41): 42794-802.

Liu, Z., M. J. Macias, et al. (1999). "The three-dimensional structure of the HRDC domain and implications for the Werner and Bloom syndrome proteins." Structure **7**(12): 1557-66.

Lohman, T. M. and K. P. Bjornson (1996). "Mechanisms of helicase-catalyzed DNA unwinding." Annu Rev Biochem **65**: 169-214.

Lonn, U., S. Lonn, et al. (1990). "An abnormal profile of DNA replication intermediates in Bloom's syndrome." Cancer Res **50**(11): 3141-5.

Lopes, M., M. Foiani, et al. (2006). "Multiple mechanisms control chromosome integrity after replication fork uncoupling and restart at irreparable UV lesions." Mol Cell **21**(1): 15-27.

Lu, J., J. R. Mullen, et al. (1996). "Human homologues of yeast helicase." Nature **383**(6602): 678-9.

Luo, G., I. M. Santoro, et al. (2000). "Cancer predisposition caused by elevated mitotic recombination in Bloom mice." Nat Genet **26**(4): 424-9.

Machwe, A., L. Xiao, et al. (2005). "RecQ family members combine strand pairing and unwinding activities to catalyze strand exchange." J Biol Chem **280**(24): 23397-407.

Machwe, A., L. Xiao, et al. (2006). "The Werner and Bloom syndrome proteins catalyze regression of a model replication fork." Biochemistry **45**(47): 13939-46.

Machwe, A., L. Xiao, et al. (2007). "Replication fork regression in vitro by the Werner syndrome protein (WRN): holliday junction formation, the effect of leading arm structure and a potential role for WRN exonuclease activity." Nucleic Acids Res **35**(17): 5729-47.

Mackintosh, S. G. and K. D. Raney (2006). "DNA unwinding and protein displacement by superfamily 1 and superfamily 2 helicases." Nucleic Acids Res **34**(15): 4154-9.

Macris, M. A., L. Krejci, et al. (2006). "Biochemical characterization of the RECQ4 protein, mutated in Rothmund-Thomson syndrome." DNA Repair (Amst) **5**(2): 172-80.

Magner, D. B., M. D. Blankschien, et al. (2007). "RecQ promotes toxic recombination in cells lacking recombination intermediate-removal proteins." Mol Cell **26**(2): 273-86.

Mahdi, A. A., G. S. Briggs, et al. (2003). "A model for dsDNA translocation revealed by a structural motif common to RecG and Mfd proteins." Embo J **22**(3): 724-34.

Mankouri, H. W. and I. D. Hickson (2007). "The RecQ helicase-topoisomerase III-Rmi1 complex: a DNA structure-specific 'dissolvasome'?" Trends Biochem Sci **32**(12): 538-46.

Mankouri, H. W. and A. Morgan (2001). "The DNA helicase activity of yeast Sgs1p is

essential for normal lifespan but not for resistance to topoisomerase inhibitors." Mech Ageing Dev **122**(11): 1107-20.

Mann, M. B., C. A. Hodges, et al. (2005). "Defective sister-chromatid cohesion, aneuploidy and cancer predisposition in a mouse model of type II Rothmund-Thomson syndrome." Hum Mol Genet **14**(6): 813-25.

Margison, G. P. and M. F. Santibanez-Koref (2002). "O6-alkylguanine-DNA alkyltransferase: role in carcinogenesis and chemotherapy." Bioessays **24**(3): 255-66.

Marintcheva, B. and S. K. Weller (2003). "Helicase motif Ia is involved in single-strand DNA-binding and helicase activities of the herpes simplex virus type 1 origin-binding protein, UL9." J Virol **77**(4): 2477-88.

Martin, C. A. (1978). "Lavender Rose or Gray Panther?" Aging(285-286): 28-30.

Matsumoto, T., O. Imamura, et al. (1997). "Mutation and haplotype analyses of the Werner's syndrome gene based on its genomic structure: genetic epidemiology in the Japanese population." Hum Genet **100**(1): 123-30.

Matsumoto, Y. and K. Kim (1995). "Excision of deoxyribose phosphate residues by DNA polymerase beta during DNA repair." Science **269**(5224): 699-702.

Matsumoto, Y., K. Kim, et al. (1994). "Proliferating cell nuclear antigen-dependent abasic site repair in Xenopus laevis oocytes: an alternative pathway of base excision DNA repair." Mol Cell Biol **14**(9): 6187-97.

Matsuno, K., M. Kumano, et al. (2006). "The N-terminal noncatalytic region of Xenopus RecQ4 is required for chromatin binding of DNA polymerase alpha in the initiation of DNA replication." Mol Cell Biol **26**(13): 4843-52.

McIlwraith, M. J., A. Vaisman, et al. (2005). "Human DNA polymerase eta promotes DNA synthesis from strand invasion intermediates of homologous recombination." Mol Cell **20**(5): 783-92.

Meetei, A. R., S. Sechi, et al. (2003). "A multiprotein nuclear complex connects Fanconi anemia and Bloom syndrome." Mol Cell Biol **23**(10): 3417-26.

Memisoglu, A. and L. Samson (2000). "Base excision repair in yeast and mammals." Mutat Res **451**(1-2): 39-51.

Miyajima, A., M. Seki, et al. (2000). "Sgs1 helicase activity is required for mitotic but apparently not for meiotic functions." Mol Cell Biol **20**(17): 6399-409.

Mohaghegh, P., J. K. Karow, et al. (2001). "The Bloom's and Werner's syndrome proteins are DNA structure-specific helicases." Nucleic Acids Res **29**(13): 2843-9.

Morimatsu, K. and S. C. Kowalczykowski (2003). "RecFOR proteins load RecA protein

onto gapped DNA to accelerate DNA strand exchange: a universal step of recombinational repair." Mol Cell **11**(5): 1337-47.

Morozov, V., A. R. Mushegian, et al. (1997). "A putative nucleic acid-binding domain in Bloom's and Werner's syndrome helicases." Trends Biochem Sci **22**(11): 417-8.

Moser, M. J., W. R. Holley, et al. (1997). "The proofreading domain of Escherichia coli DNA polymerase I and other DNA and/or RNA exonuclease domains." Nucleic Acids Res **25**(24): 5110-8.

Mullen, J. R., V. Kaliraman, et al. (2000). "Bipartite structure of the SGS1 DNA helicase in Saccharomyces cerevisiae." Genetics **154**(3): 1101-14.

Mullen, J. R., F. S. Nallaseth, et al. (2005). "Yeast Rmi1/Nce4 controls genome stability as a subunit of the Sgs1-Top3 complex." Mol Cell Biol **25**(11): 4476-87.

Multani, A. S. and S. Chang (2007). "WRN at telomeres: implications for aging and cancer." J Cell Sci **120**(Pt 5): 713-21.

Nakayama, H. (2002). "RecQ family helicases: roles as tumor suppressor proteins." Oncogene **21**(58): 9008-21.

Nakayama, H. (2005). "Escherichia coli RecQ helicase: a player in thymineless death." Mutat Res **577**(1-2): 228-36.

Nakayama, H., K. Nakayama, et al. (1984). "Isolation and genetic characterization of a thymineless death-resistant mutant of Escherichia coli K12: identification of a new mutation (recQ1) that blocks the RecF recombination pathway." Mol Gen Genet **195**(3): 474-80.

Nakayama, K., N. Irino, et al. (1985). "The recQ gene of Escherichia coli K12: molecular cloning and isolation of insertion mutants." Mol Gen Genet **200**(2): 266-71.

Nakayama, M., K. Kawasaki, et al. (2004). "The possible roles of the DNA helicase and C-terminal domains in RECQ5/QE: complementation study in yeast." DNA Repair (Amst) **3**(4): 369-78.

Nakayama, M., S. Maruyama, et al. (2006). "Relationships of Drosophila melanogaster RECQ5/QE to cell-cycle progression and DNA damage." FEBS Lett **580**(30): 6938-42.

Neveling, K., A. Bechtold, et al. (2007). "Genetic instability syndromes with progeroid features." Z Gerontol Geriatr **40**(5): 339-48.

Niida, H. and M. Nakanishi (2006). "DNA damage checkpoints in mammals." Mutagenesis **21**(1): 3-9.

Nouspikel, T. (2008). "Nucleotide excision repair and neurological diseases." DNA Repair (Amst).

Ogawa, T. and T. Okazaki (1980). "Discontinuous DNA replication." Annu Rev Biochem **49**: 421-57.

Oh, S. D., J. P. Lao, et al. (2007). "BLM ortholog, Sgs1, prevents aberrant crossing-over by suppressing formation of multichromatid joint molecules." Cell **130**(2): 259-72.

Okada, M., M. Goto, et al. (1998). "Differential effects of cytotoxic drugs on mortal and immortalized B-lymphoblastoid cell lines from normal and Werner's syndrome patients." Biol Pharm Bull **21**(3): 235-9.

Opresko, P. L., M. Otterlei, et al. (2004). "The Werner syndrome helicase and exonuclease cooperate to resolve telomeric D loops in a manner regulated by TRF1 and TRF2." Mol Cell **14**(6): 763-74.

Opresko, P. L., C. von Kobbe, et al. (2002). "Telomere-binding protein TRF2 binds to and stimulates the Werner and Bloom syndrome helicases." J Biol Chem **277**(43): 41110-9.

Orren, D. K., S. Theodore, et al. (2002). "The Werner syndrome helicase/exonuclease (WRN) disrupts and degrades D-loops in vitro." Biochemistry **41**(46): 13483-8.

Ozsoy, A. Z., H. M. Ragonese, et al. (2003). "Analysis of helicase activity and substrate specificity of Drosophila RECQ5." Nucleic Acids Res **31**(5): 1554-64.

Ozsoy, A. Z., J. J. Sekelsky, et al. (2001). "Biochemical characterization of the small isoform of Drosophila melanogaster RECQ5 helicase." Nucleic Acids Res **29**(14): 2986-93.

Palombo, F., P. Gallinari, et al. (1995). "GTBP, a 160-kilodalton protein essential for mismatch-binding activity in human cells." Science **268**(5219): 1912-4.

Palombo, F., I. Iaccarino, et al. (1996). "hMutSbeta, a heterodimer of hMSH2 and hMSH3, binds to insertion/deletion loops in DNA." Curr Biol **6**(9): 1181-4.

Park, J. S., M. T. Marr, et al. (2002). "E. coli Transcription repair coupling factor (Mfd protein) rescues arrested complexes by promoting forward translocation." Cell **109**(6): 757-67.

Paull, T. T. and M. Gellert (1999). "Nbs1 potentiates ATP-driven DNA unwinding and endonuclease cleavage by the Mre11/Rad50 complex." Genes Dev **13**(10): 1276-88.

Pause, A. and N. Sonenberg (1992). "Mutational analysis of a DEAD box RNA helicase: the mammalian translation initiation factor eIF-4A." Embo J **11**(7): 2643-54.

Pedrazzi, G., C. Perrera, et al. (2001). "Direct association of Bloom's syndrome gene product with the human mismatch repair protein MLH1." Nucleic Acids Res **29**(21): 4378-86.

Petkovic, M., T. Dietschy, et al. (2005). "The human Rothmund-Thomson syndrome gene product, RECQL4, localizes to distinct nuclear foci that coincide with proteins involved in the maintenance of genome stability." J Cell Sci **118**(Pt 18): 4261-9.

Pichierri, P., A. Franchitto, et al. (2001). "Werner's syndrome protein is required for correct recovery after replication arrest and DNA damage induced in S-phase of cell cycle." Mol Biol Cell **12**(8): 2412-21.

Poot, M., K. A. Gollahon, et al. (2002). "Werner syndrome diploid fibroblasts are sensitive to 4-nitroquinoline-N-oxide and 8-methoxypsoralen: implications for the disease phenotype." Faseb J **16**(7): 757-8.

Poot, M., J. S. Yom, et al. (2001). "Werner syndrome cells are sensitive to DNA cross-linking drugs." Faseb J **15**(7): 1224-6.

Prince, P. R., M. J. Emond, et al. (2001). "Loss of Werner syndrome protein function promotes aberrant mitotic recombination." Genes Dev **15**(8): 933-8.

Prince, P. R., C. E. Ogburn, et al. (1999). "Cell fusion corrects the 4-nitroquinoline 1-oxide sensitivity of Werner syndrome fibroblast cell lines." Hum Genet **105**(1-2): 132-8.

Puranam, K. L. and P. J. Blackshear (1994). "Cloning and characterization of RECQL, a potential human homologue of the Escherichia coli DNA helicase RecQ." J Biol Chem **269**(47): 29838-45.

Puranam, K. L., E. Kennington, et al. (1995). "Chromosomal localization of the gene encoding the human DNA helicase RECQL and its mouse homologue." Genomics **26**(3): 595-8.

Ralf, C., I. D. Hickson, et al. (2006). "The Bloom's syndrome helicase can promote the regression of a model replication fork." J Biol Chem **281**(32): 22839-46.

Raynard, S., W. Bussen, et al. (2006). "A double Holliday junction dissolvasome comprising BLM, topoisomerase IIIalpha, and BLAP75." J Biol Chem **281**(20): 13861-4.

Ren, H., S. X. Dou, et al. (2008). "The zinc-binding motif of human RECQ5beta suppresses the intrinsic strand-annealing activity of its DExH helicase domain and is essential for the helicase activity of the enzyme." Biochem J **412**(3): 425-33.

Richet, E. and M. Kohiyama (1976). "Purification and characterization of a DNA-dependent ATPase from Escherichia coli." J Biol Chem **251**(3): 808-12.

Rothmund, A. (1868). "Ueber cataracten in verbindung mit einer eigenthumlichen Hautdegeneration." Arch. Klin. Exp.Opthal. **4**: 159-182.

Saffi, J., V. R. Pereira, et al. (2000). "Importance of the Sgs1 helicase activity in DNA repair of Saccharomyces cerevisiae." Curr Genet **37**(2): 75-8.

Saintigny, Y., K. Makienko, et al. (2002). "Homologous recombination resolution defect in werner syndrome." Mol Cell Biol **22**(20): 6971-8.

Salk, D., E. Bryant, et al. (1981). "Systematic growth studies, cocultivation, and cell hybridization studies of Werner syndrome cultured skin fibroblasts." Hum Genet **58**(3): 310-6.

San Filippo, J., P. Sung, et al. (2008). "Mechanism of Eukaryotic Homologous Recombination." Annu Rev Biochem **77**: 229-257.

Sancar, A. and J. T. Reardon (2004). "Nucleotide excision repair in E. coli and man." Adv Protein Chem **69**: 43-71.

Sangrithi, M. N., J. A. Bernal, et al. (2005). "Initiation of DNA replication requires the RECQL4 protein mutated in Rothmund-Thomson syndrome." Cell **121**(6): 887-98.

Sanz, M. M., Ellis, N. A., and German, J. (2003). "Cellular localization of nonfunctional BLM protein in cells from persons with Bloom's syndrome (BS) who have inherited missense mutations." Am. J. Hum. Genet. **67**: 89.

Sartori, A. A., C. Lukas, et al. (2007). "Human CtIP promotes DNA end resection." Nature **450**(7169): 509-14.

Satoh, M., M. Imai, et al. (1999). "Prevalence of Werner's syndrome heterozygotes in Japan." Lancet **353**(9166): 1766.

Saxowsky, T. T. and P. W. Doetsch (2006). "RNA polymerase encounters with DNA damage: transcription-coupled repair or transcriptional mutagenesis?" Chem Rev **106**(2): 474-88.

Saydam, N., R. Kanagaraj, et al. (2007). "Physical and functional interactions between Werner syndrome helicase and mismatch-repair initiation factors." Nucleic Acids Res **35**(17): 5706-16.

Scharer, O. D. and J. Jiricny (2001). "Recent progress in the biology, chemistry and structural biology of DNA glycosylases." Bioessays **23**(3): 270-81.

Sedgwick, B. (1997). "Nitrosated peptides and polyamines as endogenous mutagens in O6-alkylguanine-DNA alkyltransferase deficient cells." Carcinogenesis **18**(8): 1561-7.

Sedgwick, B., P. A. Bates, et al. (2007). "Repair of alkylated DNA: recent advances." DNA Repair (Amst) **6**(4): 429-42.

Sekelsky, J. J., M. H. Brodsky, et al. (1999). "Drosophila and human RecQ5 exist in different isoforms generated by alternative splicing." Nucleic Acids Res **27**(18): 3762-9.

Seki, M., H. Miyazawa, et al. (1994). "Molecular cloning of cDNA encoding human DNA

helicase Q1 which has homology to Escherichia coli Rec Q helicase and localization of the gene at chromosome 12p12." Nucleic Acids Res **22**(22): 4566-73.

Seki, M., J. Yanagisawa, et al. (1994). "Purification of two DNA-dependent adenosinetriphosphatases having DNA helicase activity from HeLa cells and comparison of the properties of the two enzymes." J Biochem **115**(3): 523-31.

Seki, T., S. Tada, et al. (1997). "Cloning of a cDNA encoding a novel importin-alpha homologue, Qip1: discrimination of Qip1 and Rch1 from hSrp1 by their ability to interact with DNA helicase Q1/RecQL." Biochem Biophys Res Commun **234**(1): 48-53.

Sengupta, S., S. P. Linke, et al. (2003). "BLM helicase-dependent transport of p53 to sites of stalled DNA replication forks modulates homologous recombination." Embo J **22**(5): 1210-22.

Sharma, S. and R. M. Brosh, Jr. (2007). "Human RECQ1 is a DNA damage responsive protein required for genotoxic stress resistance and suppression of sister chromatid exchanges." PLoS ONE **2**(12): e1297.

Sharma, S., J. A. Sommers, et al. (2005). "Biochemical analysis of the DNA unwinding and strand annealing activities catalyzed by human RECQ1." J Biol Chem **280**(30): 28072-84.

Sharma, S., J. A. Sommers, et al. (2005). "The interaction site of Flap Endonuclease-1 with WRN helicase suggests a coordination of WRN and PCNA." Nucleic Acids Res **33**(21): 6769-81.

Shen, J. C., M. D. Gray, et al. (1998). "Werner syndrome protein. I. DNA helicase and dna exonuclease reside on the same polypeptide." J Biol Chem **273**(51): 34139-44.

Shimamoto, A., K. Nishikawa, et al. (2000). "Human RecQ5beta, a large isomer of RecQ5 DNA helicase, localizes in the nucleoplasm and interacts with topoisomerases 3alpha and 3beta." Nucleic Acids Res **28**(7): 1647-55.

Siitonen, H. A., O. Kopra, et al. (2003). "Molecular defect of RAPADILINO syndrome expands the phenotype spectrum of RECQL diseases." Hum Mol Genet **12**(21): 2837-44.

Sinclair, D. A., K. Mills, et al. (1997). "Accelerated aging and nucleolar fragmentation in yeast sgs1 mutants." Science **277**(5330): 1313-6.

Singleton, M. R., M. S. Dillingham, et al. (2007). "Structure and mechanism of helicases and nucleic acid translocases." Annu Rev Biochem **76**: 23-50.

Singleton, M. R. and D. B. Wigley (2002). "Modularity and specialization in superfamily 1 and 2 helicases." J Bacteriol **184**(7): 1819-26.

Sogo, J. M., M. Lopes, et al. (2002). "Fork reversal and ssDNA accumulation at stalled

replication forks owing to checkpoint defects." Science **297**(5581): 599-602.

Sonoda, E., M. Takata, et al. (2001). "Homologous DNA recombination in vertebrate cells." Proc Natl Acad Sci U S A **98**(15): 8388-94.

Spry, M., T. Scott, et al. (2007). "DNA repair pathways and hereditary cancer susceptibility syndromes." Front Biosci **12**: 4191-207.

Srivenugopal, K. S., X. H. Yuan, et al. (1996). "Ubiquitination-dependent proteolysis of O6-methylguanine-DNA methyltransferase in human and murine tumor cells following inactivation with O6-benzylguanine or 1,3-bis(2-chloroethyl)-1-nitrosourea." Biochemistry **35**(4): 1328-34.

Stavropoulos, D. J., P. S. Bradshaw, et al. (2002). "The Bloom syndrome helicase BLM interacts with TRF2 in ALT cells and promotes telomeric DNA synthesis." Hum Mol Genet **11**(25): 3135-44.

Sugawara, N., T. Goldfarb, et al. (2004). "Heteroduplex rejection during single-strand annealing requires Sgs1 helicase and mismatch repair proteins Msh2 and Msh6 but not Pms1." Proc Natl Acad Sci U S A **101**(25): 9315-20.

Suijkerbuijk, R. F., R. J. Sinke, et al. (1993). "Overrepresentation of chromosome 12p sequences and karyotypic evolution in i(12p)-negative testicular germ-cell tumors revealed by fluorescence in situ hybridization." Cancer Genet Cytogenet **70**(2): 85-93.

Sun, H., R. J. Bennett, et al. (1999). "The Saccharomyces cerevisiae Sgs1 helicase efficiently unwinds G-G paired DNAs." Nucleic Acids Res **27**(9): 1978-84.

Swanson, C., Y. Saintigny, et al. (2004). "The Werner syndrome protein has separable recombination and survival functions." DNA Repair (Amst) **3**(5): 475-82.

Szekely, A. M., Y. H. Chen, et al. (2000). "Werner protein recruits DNA polymerase delta to the nucleolus." Proc Natl Acad Sci U S A **97**(21): 11365-70.

Takata, M., M. S. Sasaki, et al. (1998). "Homologous recombination and non-homologous end-joining pathways of DNA double-strand break repair have overlapping roles in the maintenance of chromosomal integrity in vertebrate cells." Embo J **17**(18): 5497-508.

Tanner, N. K., O. Cordin, et al. (2003). "The Q motif: a newly identified motif in DEAD box helicases may regulate ATP binding and hydrolysis." Mol Cell **11**(1): 127-38.

Tanner, N. K. and P. Linder (2001). "DExD/H box RNA helicases: from generic motors to specific dissociation functions." Mol Cell **8**(2): 251-62.

Thompson, L. H. and D. Schild (2002). "Recombinational DNA repair and human disease." Mutat Res **509**(1-2): 49-78.

Thoms, K. M., C. Kuschal, et al. (2007). "Lessons learned from DNA repair defective syndromes." Exp Dermatol **16**(6): 532-44.

Thomson, M. S. (1936). "Pokiloderma congenitale." Br. J. Dermatol. **48**: 221-234.

Torres-Ramos, C. A., S. Prakash, et al. (2002). "Requirement of RAD5 and MMS2 for postreplication repair of UV-damaged DNA in Saccharomyces cerevisiae." Mol Cell Biol **22**(7): 2419-26.

Trujillo, K. M. and P. Sung (2001). "DNA structure-specific nuclease activities in the Saccharomyces cerevisiae Rad50*Mre11 complex." J Biol Chem **276**(38): 35458-64.

Trujillo, K. M., S. S. Yuan, et al. (1998). "Nuclease activities in a complex of human recombination and DNA repair factors Rad50, Mre11, and p95." J Biol Chem **273**(34): 21447-50.

Tuteja, N. and R. Tuteja (2004). "Unraveling DNA helicases. Motif, structure, mechanism and function." Eur J Biochem **271**(10): 1849-63.

Umezu, K. and H. Nakayama (1993). "RecQ DNA helicase of Escherichia coli. Characterization of the helix-unwinding activity with emphasis on the effect of single-stranded DNA-binding protein." J Mol Biol **230**(4): 1145-50.

Umezu, K., K. Nakayama, et al. (1990). "Escherichia coli RecQ protein is a DNA helicase." Proc Natl Acad Sci U S A **87**(14): 5363-7.

van den Bosch, M., R. T. Bree, et al. (2003). "The MRN complex: coordinating and mediating the response to broken chromosomes." EMBO Rep **4**(9): 844-9.

van Gent, D. C., J. H. Hoeijmakers, et al. (2001). "Chromosomal stability and the DNA double-stranded break connection." Nat Rev Genet **2**(3): 196-206.

Van Hatten, R. A., A. V. Tutter, et al. (2002). "The Xenopus Xmus101 protein is required for the recruitment of Cdc45 to origins of DNA replication." J Cell Biol **159**(4): 541-7.

Van Maldergem, L., H. A. Siitonen, et al. (2006). "Revisiting the craniosynostosis-radial ray hypoplasia association: Baller-Gerold syndrome caused by mutations in the RECQL4 gene." J Med Genet **43**(2): 148-52.

Veaute, X., S. Delmas, et al. (2005). "UvrD helicase, unlike Rep helicase, dismantles RecA nucleoprotein filaments in Escherichia coli." Embo J **24**(1): 180-9.

Velankar, S. S., P. Soultanas, et al. (1999). "Crystal structures of complexes of PcrA DNA helicase with a DNA substrate indicate an inchworm mechanism." Cell **97**(1): 75-84.

Vennos, E. M., M. Collins, et al. (1992). "Rothmund-Thomson syndrome: review of the world literature." J Am Acad Dermatol **27**(5 Pt 1): 750-62.

Vennos, E. M. and W. D. James (1995). "Rothmund-Thomson syndrome." Dermatol Clin **13**(1): 143-50.

Versini, G., I. Comet, et al. (2003). "The yeast Sgs1 helicase is differentially required for genomic and ribosomal DNA replication." Embo J **22**(8): 1939-49.

Vindigni, A. (2007). "Biochemical, biophysical, and proteomic approaches to study DNA helicases." Mol Biosyst **3**(4): 266-74.

von Hippel, P. H. (2004). "Helicases become mechanistically simpler and functionally more complex." Nat Struct Mol Biol **11**(6): 494-6.

von Hippel, P. H. and E. Delagoutte (2003). "Macromolecular complexes that unwind nucleic acids." Bioessays **25**(12): 1168-77.

von Kobbe, C., J. A. Harrigan, et al. (2004). "Poly(ADP-ribose) polymerase 1 regulates both the exonuclease and helicase activities of the Werner syndrome protein." Nucleic Acids Res **32**(13): 4003-14.

von Kobbe, C., P. Karmakar, et al. (2002). "Colocalization, physical, and functional interaction between Werner and Bloom syndrome proteins." J Biol Chem **277**(24): 22035-44.

von Kobbe, C., N. H. Thoma, et al. (2003). "Werner syndrome protein contains three structure-specific DNA binding domains." J Biol Chem **278**(52): 52997-3006.

Walker, J. E., M. Saraste, et al. (1982). "Distantly related sequences in the alpha- and beta-subunits of ATP synthase, myosin, kinases and other ATP-requiring enzymes and a common nucleotide binding fold." Embo J **1**(8): 945-51.

Wang, L. L., M. L. Levy, et al. (2001). "Clinical manifestations in a cohort of 41 Rothmund-Thomson syndrome patients." Am J Med Genet **102**(1): 11-7.

Wang, W., M. Seki, et al. (2003). "Functional relation among RecQ family helicases RecQL1, RecQL5, and BLM in cell growth and sister chromatid exchange formation." Mol Cell Biol **23**(10): 3527-35.

Wang, W., M. Seki, et al. (2000). "Possible association of BLM in decreasing DNA double strand breaks during DNA replication." Embo J **19**(13): 3428-35.

Wang, Y., D. Cortez, et al. (2000). "BASC, a super complex of BRCA1-associated proteins involved in the recognition and repair of aberrant DNA structures." Genes Dev **14**(8): 927-39.

Watt, P. M., I. D. Hickson, et al. (1996). "SGS1, a homologue of the Bloom's and Werner's syndrome genes, is required for maintenance of genome stability in Saccharomyces cerevisiae." Genetics **144**(3): 935-45.

Watt, P. M., E. J. Louis, et al. (1995). "Sgs1: a eukaryotic homolog of E. coli RecQ that interacts with topoisomerase II in vivo and is required for faithful chromosome segregation." Cell **81**(2): 253-60.

Werner, O. (1904). Ueber Katarakt in Verbindung mit Sklerodemie., Kiel University.

Werner, S. R., A. K. Prahalad, et al. (2006). "RECQL4-deficient cells are hypersensitive to oxidative stress/damage: Insights for osteosarcoma prevalence and heterogeneity in Rothmund-Thomson syndrome." Biochem Biophys Res Commun **345**(1): 403-9.

Weterings, E. and D. J. Chen (2008). "The endless tale of non-homologous end-joining." Cell Res **18**(1): 114-24.

Wickner, S., M. Wright, et al. (1974). "Association of DNA-dependent and -independent ribonucleoside triphosphatase activities with dnaB gene product of Escherichia coli." Proc Natl Acad Sci U S A **71**(3): 783-7.

Williams, R. S., J. S. Williams, et al. (2007). "Mre11-Rad50-Nbs1 is a keystone complex connecting DNA repair machinery, double-strand break signaling, and the chromatin template." Biochem Cell Biol **85**(4): 509-20.

Wiseman, H. and B. Halliwell (1996). "Damage to DNA by reactive oxygen and nitrogen species: role in inflammatory disease and progression to cancer." Biochem J **313 (Pt 1)**: 17-29.

Wogan, G. N., S. S. Hecht, et al. (2004). "Environmental and chemical carcinogenesis." Semin Cancer Biol **14**(6): 473-86.

Woo, L. L., K. Futami, et al. (2006). "The Rothmund-Thomson gene product RECQL4 localizes to the nucleolus in response to oxidative stress." Exp Cell Res **312**(17): 3443-57.

Wood, R. D., M. Mitchell, et al. (2005). "Human DNA repair genes, 2005." Mutat Res **577**(1-2): 275-83.

Wu, L., C. Z. Bachrati, et al. (2006). "BLAP75/RMI1 promotes the BLM-dependent dissolution of homologous recombination intermediates." Proc Natl Acad Sci U S A **103**(11): 4068-73.

Wu, L., K. L. Chan, et al. (2005). "The HRDC domain of BLM is required for the dissolution of double Holliday junctions." Embo J **24**(14): 2679-87.

Wu, L., S. L. Davies, et al. (2001). "Potential role for the BLM helicase in recombinational repair via a conserved interaction with RAD51." J Biol Chem **276**(22): 19375-81.

Wu, L., S. L. Davies, et al. (2000). "The Bloom's syndrome gene product interacts with topoisomerase III." J Biol Chem **275**(13): 9636-44.

Wu, L. and I. D. Hickson (2003). "The Bloom's syndrome helicase suppresses crossing over during homologous recombination." Nature **426**(6968): 870-4.

Wu, L. and I. D. Hickson (2006). "DNA helicases required for homologous recombination and repair of damaged replication forks." Annu Rev Genet **40**: 279-306.

Wu, X. and N. Maizels (2001). "Substrate-specific inhibition of RecQ helicase." Nucleic Acids Res **29**(8): 1765-71.

Xu, H. Q., E. Deprez, et al. (2003). "The Escherichia coli RecQ helicase functions as a monomer." J Biol Chem **278**(37): 34925-33.

Yamagata, K., J. Kato, et al. (1998). "Bloom's and Werner's syndrome genes suppress hyperrecombination in yeast sgs1 mutant: implication for genomic instability in human diseases." Proc Natl Acad Sci U S A **95**(15): 8733-8.

Yang, Q., R. Zhang, et al. (2002). "The processing of Holliday junctions by BLM and WRN helicases is regulated by p53." J Biol Chem **277**(35): 31980-7.

Yankiwski, V., R. A. Marciniak, et al. (2000). "Nuclear structure in normal and Bloom syndrome cells." Proc Natl Acad Sci U S A **97**(10): 5214-9.

Yannone, S. M., S. Roy, et al. (2001). "Werner syndrome protein is regulated and phosphorylated by DNA-dependent protein kinase." J Biol Chem **276**(41): 38242-8.

Yarranton, G. T. and M. L. Gefter (1979). "Enzyme-catalyzed DNA unwinding: studies on Escherichia coli rep protein." Proc Natl Acad Sci U S A **76**(4): 1658-62.

Yin, J., Y. T. Kwon, et al. (2004). "RECQL4, mutated in the Rothmund-Thomson and RAPADILINO syndromes, interacts with ubiquitin ligases UBR1 and UBR2 of the N-end rule pathway." Hum Mol Genet **13**(20): 2421-30.

Yu, C. E., J. Oshima, et al. (1996). "Positional cloning of the Werner's syndrome gene." Science **272**(5259): 258-62.

Zheng L, K. R., Mihaljevic B, Schwendener S, Janscak P (2008). The MRE11/RAD50/NBS1 complex links RECQ5 helicase to sites of DNA damage.

Zhou, B. B. and S. J. Elledge (2000). "The DNA damage response: putting checkpoints in perspective." Nature **408**(6811): 433-9.

Published online 26 September 2006 *Nucleic Acids Research, 2006, Vol. 34, No. 18* ***5217–5231***
doi:10.1093/nar/gkl677

Human RECQ5β helicase promotes strand exchange on synthetic DNA structures resembling a stalled replication fork

Radhakrishnan Kanagaraj, Nurten Saydam, Patrick L. Garcia, Lu Zheng and Pavel Janscak*

Institute of Molecular Cancer Research, University of Zurich, Winterthurerstrasse 190, CH-8057 Zurich, Switzerland

Received July 25, 2006; Revised August 30, 2006; Accepted September 4, 2006

ABSTRACT

The role of the human RECQ5β helicase in the maintenance of genomic stability remains elusive. Here we show that RECQ5β promotes strand exchange between arms of synthetic forked DNA structures resembling a stalled replication fork in a reaction dependent on ATP hydrolysis. BLM and WRN can also promote strand exchange on these structures. However, in the presence of human replication protein A (hRPA), the action of these RecQ-type helicases is strongly biased towards unwinding of the parental duplex, an effect not seen with RECQ5β. A domain within the non-conserved portion of RECQ5β is identified as being important for its ability to unwind the lagging-strand arm and to promote strand exchange on hRPA-coated forked structures. We also show that RECQ5β associates with DNA replication factories in S phase nuclei and persists at the sites of stalled replication forks after exposure of cells to UV irradiation. Moreover, RECQ5β is found to physically interact with the polymerase processivity factor proliferating cell nuclear antigen *in vitro* and *in vivo*. Collectively, these findings suggest that RECQ5β may promote regression of stalled replication forks to facilitate the bypass of replication-blocking lesions by template-switching. Loss of such activity could explain the elevated level of mitotic crossovers observed in RECQ5β-deficient cells.

INTRODUCTION

The progression of DNA replication forks is frequently impaired by DNA damage, particularly if the blocking lesion is located on the leading-strand template (1). In this case, synthesis of the leading strand is halted at the lesion, while the lagging-strand synthesis continues beyond the lesion site, resulting in a fork structure with an extensive gap in the leading strand (2,3). Replication fork stalling poses a serious threat to genomic stability because it can trigger unscheduled DNA recombination events and hence lead to gross chromosomal re-arrangements that can induce tumorigenesis (4,5). To avoid these detrimental consequences of DNA replication arrest, cells can switch to different DNA damage bypass modes that permit replication across the lesion (1,3,6,7). One of these mechanisms is proposed to involve a transient template switch to the undamaged sister chromatid, allowing the replicative polymerase to synthesize the sequence complementary to the blocking lesion in an error-free manner (8). It is believed that such template-switching is achieved by a movement of the fork backward so as to re-anneal the original template strands and displace the newly synthesized strands which themselves anneal to generate a Holliday junction structure with a short arm (1). Indeed, such structures have been observed to accumulate upon replication arrest both in prokaryotic and in eukaryotic cells (8–11). However, it is not clear whether the formation of these structures is promoted enzymatically or occurs spontaneously.

Proteins belonging to the RecQ family of 3′–5′ DNA helicases are implicated in the processing of aberrant DNA structures arising during DNA replication and repair (12). Defects in three of the five known human RecQ homologues have been found to be associated with different autosomal recessive disorders characterized by genomic instability and cancer predisposition—mutations in BLM, WRN and RECQ4 give rise to Bloom syndrome, Werner syndrome and Rothmund–Thomson syndrome, respectively (12). BLM is known to suppress crossovers during homologous recombination (HR) presumably through its unique ability to act in conjunction with DNA topoisomerase IIIα to decatenate recombination intermediates containing double Holliday junctions (13). WRN promotes lagging-strand replication of G-rich telomeric regions and resolves telomeric D-loops in a manner regulated by the TRF1 and TRF2 proteins (14,15). RECQ4 is proposed to be important for the initiation of DNA replication by promoting the loading of replication protein A on unwound origins (16).

The role of the human RECQ5 protein in the maintenance of genomic stability remains to be elucidated. The inactivation

*To whom correspondence should be addressed. Tel: +41 44 635 3470; Fax: +41 44 635 3484; Email: pjanscak@imcr.unizh.ch

of the *Recq5* gene in mouse embryonic stem cells results in a significant increase in the frequency of sister chromatid exchanges (SCEs) comparable to that caused by *Blm* gene inactivation (17). Deletion of both *Recq5* and *Blm* genes leads to an even higher frequency of SCEs compared to the single mutants, suggesting that BLM and RECQ5 operate in different pathways that suppress mitotic recombination (17). In contrast to the other human RecQ homologues, RECQ5 exists in at least three different isoforms resulting from alternative mRNA splicing (18). The largest splice variant, RECQ5β functions not only as a 3′–5′ DNA helicase, but also possesses an intrinsic DNA strand-annealing activity residing in the unique C-terminal half of the protein (19). This strand-annealing activity is suppressed if the helicase is in its ATP-bound state, suggesting that RECQ5β may mediate DNA transactions that require a coordinated action of helicase and strand-annealing activities, such as replication fork regression.

Here we show that the RECQ5β helicase has the ability to promote strand exchange between arms of synthetic forked DNA structures that resemble a stalled replication fork in a reaction stimulated by the human replication protein A (hRPA). In contrast, hRPA is found to block strand exchange by BLM and WRN by driving these helicases to mediate unwinding of the parental duplex. On forked DNA structures with heterologous arms, RECQ5β preferentially unwinds the lagging-strand duplex, whereas BLM and WRN show a strong preference for unwinding of the parental duplex even in the absence of hRPA. The ability of RECQ5β to catalyze the lagging-strand unwinding and strand exchange on hRPA-coated forked structures is dependent on a short region located within the non-conserved portion of RECQ5β. In addition, we show by immunofluorescence microscopy that RECQ5β localizes to DNA replication factories in S phase nuclei and persists at the sites of stalled replication forks. Moreover, we have found that RECQ5β physically interacts with the polymerase processivity factor proliferating cell nuclear antigen (PCNA) *in vivo* and *in vitro*. Based on these findings, we propose that RECQ5β could mediate regression of stalled replication forks to facilitate DNA damage bypass by template-switching.

MATERIALS AND METHODS

Plasmid constructions and protein purifications

The bacterial expression vectors for the RECQ5β fragments encompassing the amino acid residues 1–774 (pPG13) and 542–991 (pPG14), fused to the C-terminus of glutathione-*S*-transferase (GST), were constructed by PCR amplification of the corresponding regions of the RECQ5β cDNA and their insertion in pGEX-2TK between the EcoRI and BamHI sites. The bacterial vectors expressing $RECQ5^{1–725}$ (pPG18), $RECQ5^{1–651}$ (pPG20), $RECQ5^{1–561}$ (pPG21) and $RECQ5^{1–475}$ (pPG19) as C-terminal fusions with a self-cleaving tag including chitin-binding domain (CBD) were constructed in the same way as the vector for the full-size RECQ5β (19). The BamHI–NcoI fragment of BLM cDNA in pcDNA3 (20), and the NcoI–XhoI fragment of pJK1 (21), including the remaining part of the BLM coding sequence fused C-terminally to a His_6 tag, were cloned in pFastBac1 via BamHI and XhoI sites to yield the plasmid pZL4, which was used to generate a bacmid for the expression of BLM in Sf9 cells by the means of baculovirus system.

The RECQ5β protein and its variants were produced in bacteria and purified as described previously (19). His-tagged BLM was produced in Sf9 by the means of baculovirus system and purified on a 5 ml HighTrap Chelating (Ni^{2+}) column under previously described conditions (21). To increase the purity, the BLM protein was further loaded on to a 1 ml MonoQ column equilibrated with buffer containing 50 mM Tris (pH 7.5), 10% (v/v) glycerol, 200 mM NaCl and 0.1 mM EDTA, and eluted with a linear concentration gradient of NaCl (200–650 mM). WRN, hRPA and PCNA were prepared essentially as described (22–24). *Escherichia coli* single-strand DNA-binding protein was purchased from Promega.

Antibodies

An antibody against the C-terminal fragment of RECQ5β encompassing amino acids 675–991 was raised in rabbit (Clonestar Ltd, Czech Republic) and purified on a RECQ5β-Sepharose 4A column.

DNA substrates

All oligonucleotides used for the preparation of DNA substrates were purchased PAGE-purified from Microsynth (Switzerland). The sequences of the oligonucleotides (RK1-7) and the schemes of DNA substrates are shown in Supplementary Table 1. Where required, oligonucleotides were labeled at the 5′ end with T4 polynucleotide kinase (NEB) and [γ-^{32}P]ATP using standard procedure. The oligonucleotides were annealed under conditions described previously (25).

Strand exchange and helicase assays

Reactions were carried out at 37°C in buffer HA containing 20 mM Tris–acetate (pH 7.9), 50 mM KOAc, 10 mM $Mg(OAc)_2$, 1 mM DTT and 50 μg/ml BSA. Where required, $Mg(OAc)_2$ concentration was varied in the range from 0 to 10 mM. For the strand exchange assays, 1 nM RK1/RK2 partial duplex was incubated with 40 nM RECQ5β and either 1 nM RK3 oligonucleotide or 1 nM RK3/RK4 partial duplex in a volume of 100 μl of buffer HA to generate forked DNA structures depicted in Figures 1A and 2A, respectively. After 10 min, ATP was added to a final concentration of 2 mM. Aliquots (5 μl) were removed at different reaction time points (both before and after the addition of ATP) and analyzed. In the control experiment, ATP was substituted with ATPγS (2 mM). The 3′-flap duplex for strand-exchange assays with BLM (10 nM) and WRN (5 nM) was pre-formed by the spontaneous annealing of the constituent oligonucleotides RK1, RK2 and RK3, with the RK2 oligonucleotide being present in a 5-fold molar excess over the others. Helicase reactions were carried out as described previously (19). Where required, hRPA (20 nM) was added to DNA 1 min before the addition of RecQ proteins and ATP. All reactions were terminated by adding 0.5 reaction volumes of solution S (150 mM EDTA, 2% SDS, 30% glycerol and 0.1% bromophenol blue) and

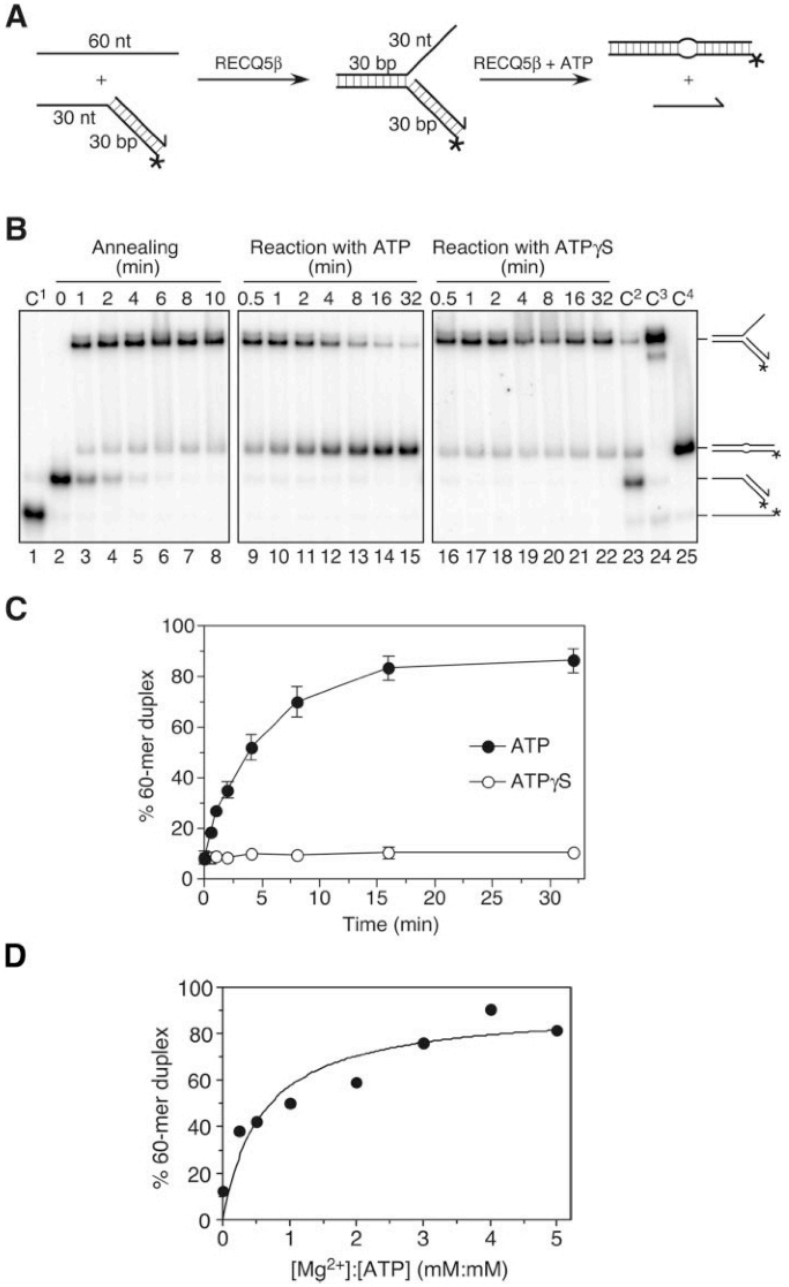

Figure 1. Strand-exchange by RECQ5β on synthetic forked DNA structure with homologous arms lacking the leading strand. (**A**) Scheme of the assay. The lengths of individual arms are indicated in nucleotides (nt) or base pairs (bp). The 3′ end of the lagging oligonucleotide is indicated by an arrow and the position of the 5′-^{32}P label is marked by an asterisk. The homologous leading and lagging arms have a 5 nt heterology at the fork junction to prevent spontaneous strand exchange. (**B**) 1 nM ^{32}P-labeled 30mer/60mer duplex (RK1/RK2) was incubated with 1 nM 60mer complementary oligonucleotide (RK3) in the presence of 40 nM RECQ5β to form the forked DNA structure. After 10 min, either ATP or ATPγS were added to a final concentration of 2 mM. Aliquots from different reaction time points, before and after addition of the nucleotide, were analyzed by non-denaturing PAGE followed by phosphorimaging. C^1–C^4, markers for the DNA substrate and the reaction products. (**C**) Quantification of the ATP and ATPγS containing reactions. Relative concentration of the 60mer duplex product is plotted versus reaction time. The data points represent the average values from three independent experiments. (**D**) Dependence of the strand-exchange activity of RECQ5β on Mg^{2+} ion concentration. Reaction mixtures contained 1 nM 3′-flap DNA substrate, 40 nM RECQ5β and 2 mM ATP with increasing concentrations of $Mg(OAc)_2$. Relative concentration of the 60mer duplex product after 32 min was measured as in (B) and (C). The lines drawn are only to guide the eye.

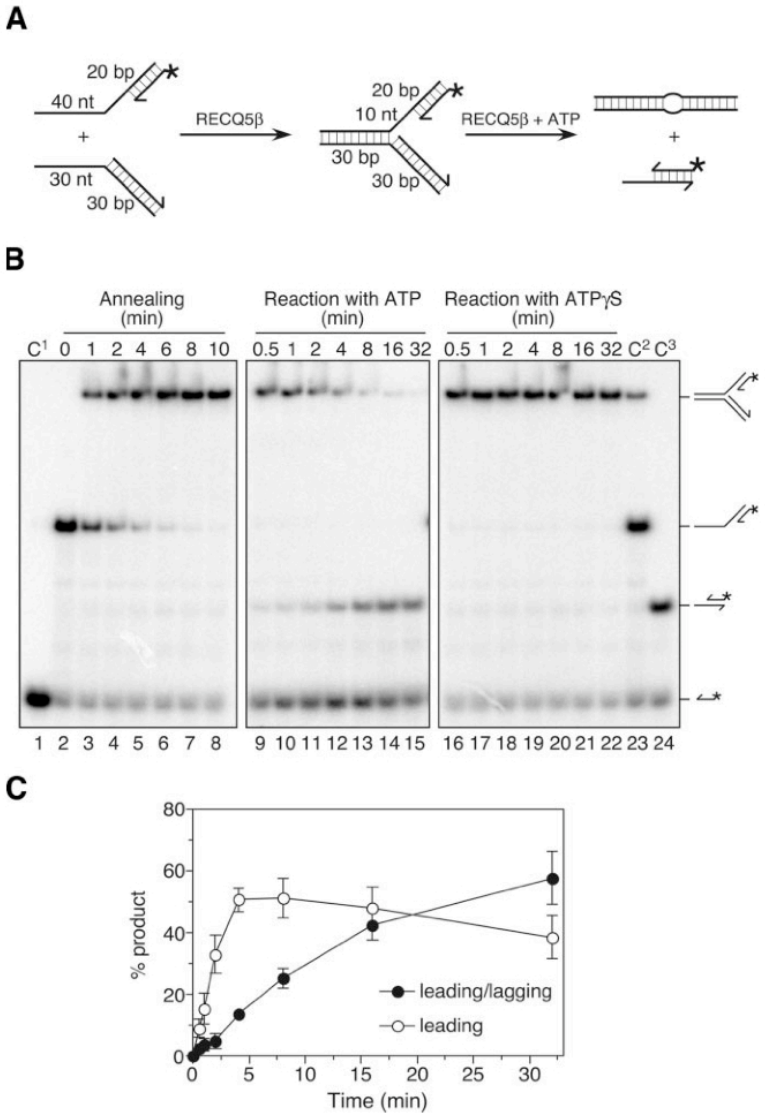

Figure 2. Strand-exchange by RECQ5β on synthetic forked DNA duplex with a leading-strand gap. (**A**) Scheme of the assay. The oligonucleotides used are the same as in Figure 1, except for an additional 20mer representing the leading strand. (**B**) 1 nM ^{32}P-labeled 20mer/60mer duplex (RK1/RK2) was incubated with 1 nM 30mer/60mer duplex (RK3/RK4) in the presence of 40 nM RECQ5β to form the forked DNA structure. After 10 min, either ATP or ATPγS were added to a final concentration of 2 mM. Aliquots of the annealing and the nucleotide-driven reactions were analyzed by non-denaturing PAGE. C^1–C^3, markers for the DNA substrate and the reaction products. (**C**) Quantification of the ATP- driven reaction. The relative concentrations of the unwound 20mer oligonucleotide (leading strand; open circles) and subsequently formed 20mer/30mer partial duplex (leading/lagging duplex; closed circles) are plotted versus reaction time. The data points represent the average values from three independent experiments.

subsequently treated with proteinase K (0.1 mg/ml) at 37°C for 10 min. The reaction mixtures were resolved by electrophoresis in a 10% (w/v) non-denaturing polyacrylamide gel (PAGE; acrylamide/bis-acrylamide 19:1). Radiolabeled DNA species were visualized by autoradiography and quantified using a Molecular Dynamics Typhoon 9400 scanner with associated IMAGEQUANT software. The relative concentration of radiolabeled products was expressed as percentage of total DNA.

Strand annealing assays

Strand annealing activity of RECQ5β and its deletion variants was measured using complementary 50mer oligonucleotides as described previously (19).

Cell culture

All the cell lines used in this study were maintained in DMEM (OmniLab) supplemented with 10% fetal calf

serum (Life Technologies) and streptomycin/penicillin (100 U/ml). To prepare synchronized population of cells, cultures at ~60% confluency were treated with 2 mM hydroxyurea (HU) for 16 h. UV treatments (at a dose of 20 J/m^2) were carried out in a UV-Stratalinker 1800 equipped with a 254 nm UV lamp (Stratagene). Where required, *cis*-diamminedichloro-platinum (CDDP) was added to a final concentration of 20 μM. For cell cycle analyses, ethanol-fixed cells were stained with propidium iodide (20 μg/ml; Molecular Probes) and subjected to flow cytometry in a Becton Dickinson cell sorter.

Immunofluorescence assays

Cells grown on cover slips were fixed in methanol for 30 min at −20°C, which was followed by incubation in acetone for 30 s. After blocking in PBS supplemented with 3% low-fat milk (blocking solution), cover slips were incubated overnight at 4°C with primary antibodies [rabbit polyclonal anti-RECQ5β (this study; 1:800) and mouse monoclonal anti-PCNA (PC-10, Santa Cruz; 1:200); all antibodies were diluted in blocking solution]. After washing with PBS, the cells were incubated with FITC-conjugated sheep anti-rabbit (Sigma; 1:700) and Texas Red-conjugated donkey anti-mouse (Abcam; 1:200) secondary antibodies for 1 h at 37°C. The nuclei were then counterstained with DAPI (0.1 μg/ml; Sigma) for 10 min, washed with water and mounted in SlowFade Antifade reagent (Molecular Probes). Images were captured by Olympus IX81 fluorescence microscope. At least 150 nuclei were analyzed in each experiment.

Immunoprecipitation assays

Cells were subjected to trypsinization, harvested by centrifugation and resuspended in lysis buffer [50 mM Tris–HCl, pH 8.0, 120 mM NaCl and 0.5% (v/v) NP-40] supplemented with protease inhibitor cocktail (Complete, Mini; Roche). After a 30 min incubation on ice, the lysate was treated with 10 U of RNase-free DNase I (Roche) at 25°C for 30 min, and clarified by centrifugation. The protein extracts (1 mg) were incubated overnight at 4°C with purified rabbit anti-RECQ5β IgGs (1 μg) or with IgGs purified from pre-immune serum (1 μg). Immune complexes were subsequently incubated with protein A/G–agarose beads (20 μl, Amersham Biosciences) for 1 h at 4°C. Immunoprecipitates were analyzed by western blotting.

GST/CBD pull-down assays

GST- and CBD-tagged fragments of RECQ5β were produced in *E.coli* BL21-CodonPlus(DE3)-RIL cells (Stratagene) and bound to Glutathione–Sepharose beads (20 μl; Amersham Biosciences) and chitin beads (20 μl; NEB), respectively, in NET-T150 buffer [10 mM Tris (pH 8.0), 1 mM EDTA, 150 mM NaCl and 0.1% (v/v) Triton X-100]. The beads were incubated with recombinant PCNA (0.5–2 μg) in 400 μl of NET-T150 buffer supplemented with ethidium bromide (50 μg/ml) for 2 h at 4°C. Bound proteins were analyzed by western blotting.

RESULTS

RECQ5β promotes strand exchange on synthetic DNA structures mimicking a stalled replication fork

To investigate whether the RECQ5β helicase is capable of promoting replication fork regression, we examined its activity on oligonucleotide-based forked structures with homologous arms, which had a 5 nt region of heterology adjacent to the three-way junction to prevent spontaneous branch migration. First, we prepared a partial forked duplex lacking the leading strand (3′-flap duplex) by RECQ5β-mediated annealing of a 60mer oligonucleotide representing the leading-strand template to a 3′-tailed duplex composed of a 30mer oligonucleotide and a ^{32}P-labeled 60mer oligonucleotide representing the lagging strand and the corresponding template strand, respectively (Figure 1A). This resulted in a rapid formation of the forked structure as detected by electrophoresis in non-denaturing polyacrylamide gel followed by phosphorimaging (Figure 1B, lanes 2–8). A small amount of the 60mer duplex was also detected, which had presumably arisen from spontaneous branch migration. Remarkably, upon the addition of ATP to this mixture, a robust strand-exchange activity was observed, resulting in the formation of the ^{32}P-labeled 60mer duplex (Figure 1B and C, lanes 9–15). Note that this duplex contains a small bubble due to the short region of heterology at the junction (Figure 1A). When ATP was substituted with its poorly hydrolysable analogue ATPγS, no strand exchange was observed over the period of 32 min, confirming that the RECQ5β-mediated strand exchange is dependent on the helicase activity of the enzyme (Figure 1B and C, lanes 16–22).

Certain RecQ DNA helicases such as human RECQ1 (26) have been shown to be sensitive to free magnesium cations. Hence, we sought to determine the optimal Mg^{2+}:ATP ratio for RECQ5β-mediated strand exchange reaction. To do so, we varied Mg^{2+} concentration in the range from 0 to 10 mM keeping ATP at a fixed concentration of 2 mM. We found that the extent of RECQ5β-mediated strand exchange on the 3′-flap substrate increased with increasing Mg^{2+} concentration in a hyperbolic fashion, reaching maximal values at Mg^{2+}:ATP ratios between 3 and 5 (Figure 1D). These data indicated that RECQ5β requires a molar excess of Mg^{2+} over ATP for efficient strand exchange activity. Therefore, all further experiments were performed using 2 mM ATP and 10 mM $Mg(OAc)_2$.

Next we investigated whether RECQ5β can promote strand exchange if the forked structure contains both the lagging and the leading strands. To mimic the structure of a replication fork blocked by a lesion on the leading-strand template, the length of the leading strand was chosen to be 10 nt shorter than the length of the lagging strand. The DNA substrate was again assembled using the strand-annealing function of RECQ5β (Figure 2A). Upon the addition of ATP, a rapid accumulation of free ^{32}P-labeled leading oligonucleotide was observed in the initial stages of the reaction which was followed by its annealing to the lagging oligonucleotide as evidenced by an accumulation of the 20mer/30mer duplex in the later stage of the reaction (Figure 2B and 2C, lanes 9–15). This indicates that RECQ5β has the ability to promote the displacement of both arms of the fork and subsequent annealing of the displaced leading and lagging strands

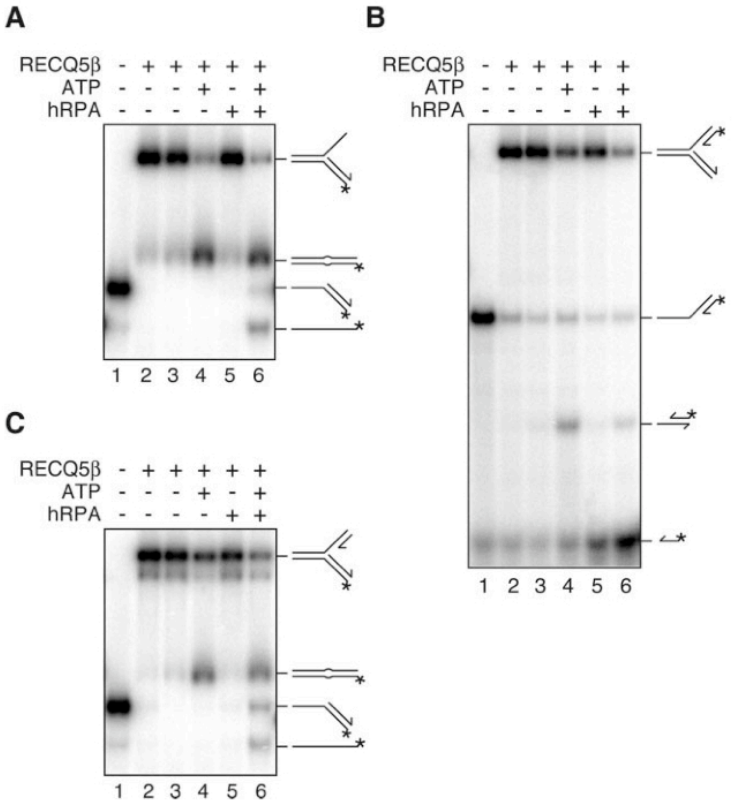

Figure 3. Effect of hRPA on RECQ5β-mediated strand exchange on forked DNA duplex lacking the leading strand (**A**) and forked DNA duplex with 10 nt leading-strand gap, radioactively labeled either on the leading-strand oligonucleotide (**B**) or on the lagging-strand template (**C**). The DNA substrates were prepared by RECQ5β mediated annealing as described in Materials and Methods and schematically indicated in Figures 1A and 2A. Reactions were carried out for 32 min as indicated. DNA, RECQ5β and hRPA were present at concentrations of 1, 40 and 20 nM, respectively. hRPA was added 2 min before the addition of ATP (2 mM).

(Figure 2B and C). No strand exchange was seen in the presence of ATPγS, indicating a requirement for the helicase activity of the enzyme (Figure 2B, lanes 16–22).

It is known that RPA covers single-stranded regions at stalled replication forks (27). Therefore, we investigated the effect of hRPA on the strand-exchange activity of RECQ5β using the synthetic forked structures described above. To monitor the annealing of the parental strands on the gapped fork structure, ^{32}P-label was also placed on the lagging-strand template. These experiments indicated that hRPA did not impair the RECQ5β-mediated annealing of the parental strands (Figure 3A and C). However, it was found to partially inhibit the annealing of the displaced leading and lagging oligonucleotides (Figure 3B). This is consistent with our earlier studies, which indicated that hRPA inhibits RECQ5β-mediated strand annealing (19). A partial shift of the reaction towards unwinding of the parental duplex was also observed, particularly with the gapped substrate (Figure 3C, compare lanes 4 and 6). However, this is not likely to be the consequence of binding of hRPA to the leading arm, since the single-strand gap on the gapped fork structure is too short (10 nt) to accommodate hRPA, assuming that the size of the DNA-binding site for RPA is ~30 nt (28).

Collectively, the findings described above suggested that RECQ5β is capable of promoting fork regression *in vitro*.

RPA blocks strand exchange by BLM and WRN

We also examined other human RecQ homologues, namely BLM and WRN, for the ability to promote strand exchange on the 3′-flap structure described above (Figure 1A). As WRN showed only negligible strand-annealing activity under the condition of our assay, the DNA substrate was prepared by spontaneous annealing of the constituent oligonucleotides, with the lagging oligonucleotide being present in a 5-fold molar excess over the parental strands. We found that both BLM and WRN could efficiently catalyze the conversion of the 3′-flap structure into the 60mer duplex (Figure 4A and B). However, if hRPA was present in the reaction, the action of both helicases was strongly biased toward unwinding of the parental duplex, as evidenced by the accumulation of the ^{32}P-labeled 30mer/60mer duplex in the course of the reaction (Figure 4C and D). In contrast, these time course experiments revealed that hRPA significantly stimulated the rate and the extent of RECQ5β-mediated strand exchange on 3′-flap structure (Figure 4).

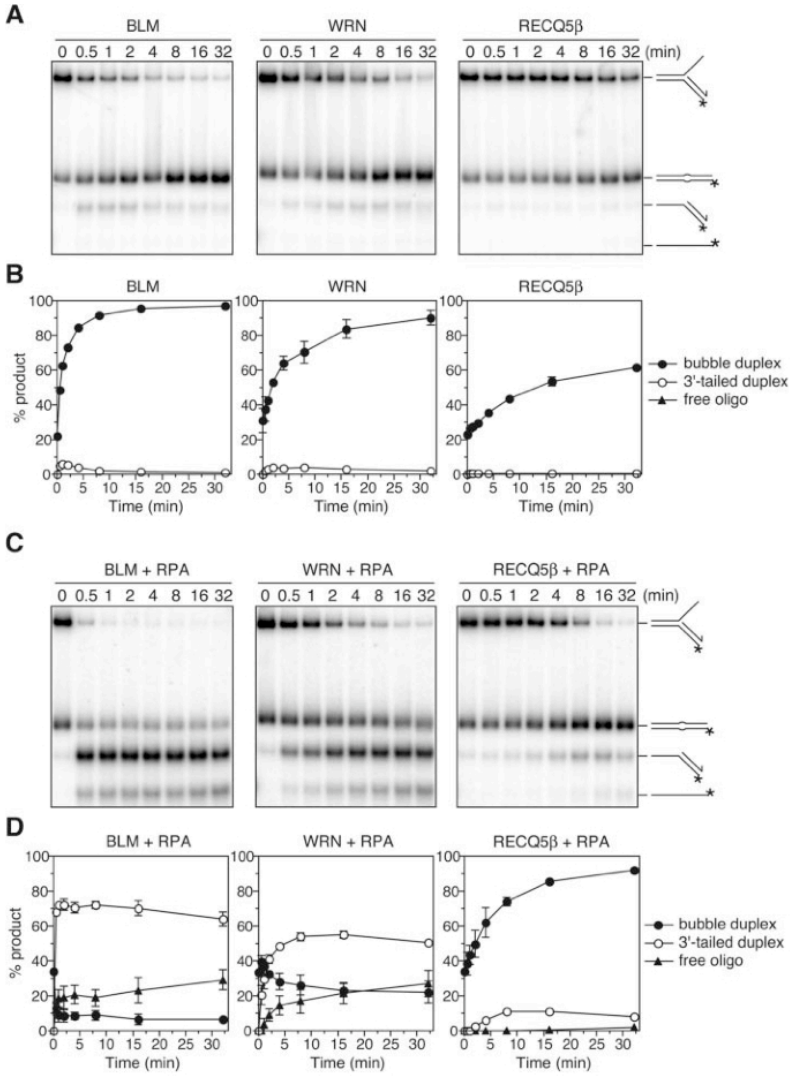

Figure 4. Strand exchange by BLM, WRN and RECQ5β in the absence and presence of hRPA. (**A**) Time course of reactions of 10 nM BLM, 5 nM WRN and 40 nM RECQ5β, respectively, with 1 nM forked DNA structure with homologous arms lacking the leading strand. (**B**) Quantification of reactions in (A). (**C**) Time course of reactions of 10 nM BLM, 5 nM WRN and 40 nM RECQ5β, respectively, with 1 nM DNA structure as in (A) in the presence of 20 nM hRPA. The DNA substrate was preincubated for 2 min with hRPA before addition of helicase. (**D**) Quantification of reactions in (C). The DNA substrate was the same as in Figure 1, except that it was prepared by spontaneous annealing of the component oligonucleotides as described in Materials and Methods. Reactions were analyzed as in Figure 1. In the graphs, relative concentrations of the products are plotted versus reaction time. The 60mer bubble duplex, filled circles; 3′-tailed 30mer/60mer duplex, open circles; free 60mer oligonucleotide, filled triangles. In all graphs, the data points represent the average values from three independent experiments.

These data indicate that there are mechanistic differences between RECQ5β and other human RecQ helicases in the mode of processing of forked DNA structures coated with hRPA.

RECQ5β actively unwinds only the lagging-strand arm of the fork

To gain insights into the mechanism of RECQ5β-mediated strand exchange, we investigated the action of RECQ5β on synthetic forked structures with heterologous arms to monitor only DNA unwinding events. In agreement with data reported for the *Drosophila* RECQ5 homologue (29), we found that on partial forked duplex lacking the leading strand (3′-flap duplex), RECQ5β showed preference for unwinding of the lagging-strand arm (Figure 5A and B). Interestingly, this reaction was significantly enhanced if the DNA substrate was pre-incubated with hRPA (compare Figure 5A and B). This could be the consequence of binding of hRPA to the single-stranded leading arm that would prevent loading of

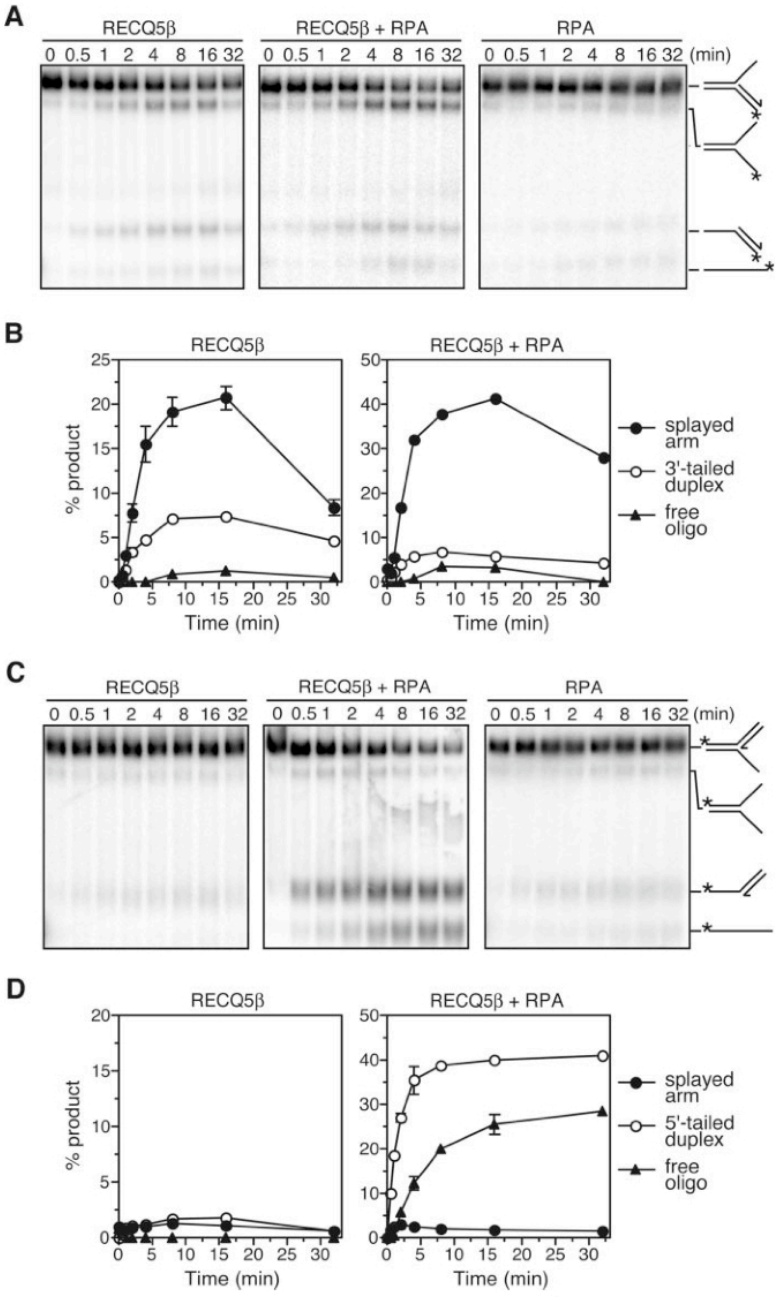

Figure 5. Unwinding of forked DNA structures with heterologous arms by RECQ5β. (**A**) Time course of RECQ5β-mediated unwinding of partial forked duplex lacking the leading strand (3′-flap duplex) in the absence and presence of 20 nM hRPA as indicated. Reaction containing RPA only is also shown as a control (**B**) Quantification of the RECQ5β-containing reactions in (A). The graph shows the relative concentrations of unwound products including the splayed arm (closed circles), the 3′-tailed duplex (open circles) and the free lagging-strand template (closed triangles). (**C**) Time course of RECQ5β-mediated unwinding of partial forked duplex lacking the lagging strand (5′-flap duplex) in the absence and presence of 20 nM hRPA. Reaction containing RPA only is also shown as a control (**D**) Quantification of the RECQ5β-containing reactions in (C). The graph shows the relative concentrations of unwound products including the splayed arm (closed circles) and the 3′-tailed duplex (open circles) and the free leading-strand template (closed triangles). All DNA substrates are derived from the same set of four oligonucleotides (RK1, RK2, RK5 and RK6) as described in Materials and Methods. The 3′ end of the leading and lagging strands are indicated by arrows. The position of the 5′-^{32}P label in each substrate is indicated by an asterisk. For all reactions, DNA substrates were present at a concentration of 1 nM. RECQ5β was 100 nM in the reactions without hRPA and 80 nM in the reactions with hRPA. Reactions were carried out and analyzed as described in Materials and Methods. In all graphs, the data points represent the average values from three independent experiments.

RECQ5β on this arm to initiate unwinding of the parental duplex. In agreement with this assumption, we found that hRPA inhibited RECQ5β-mediated unwinding of a 3′-tailed duplex if added to the DNA substrate prior to the helicase (data not shown). However, no significant stimulation of RECQ5β-mediated unwinding of the lagging-strand arm was observed with the *E.coli* single-stranded binding protein, indicating that this effect is specific for hRPA (Supplementary Figure S1).

To assess whether the RECQ5β helicase can actively unwind the leading arm of the fork, we examined its activity on partial forked duplex lacking the lagging strand (5′-flap duplex). We found that RECQ5β could catalyze only the unwinding of the parental arm on this structure, as evidenced by the accumulation of 5′-tailed duplex during the course of the reaction (Figure 5C and D). This was, however, seen only in the presence of hRPA, which is consistent with our previous finding that hRPA counteracts the intrinsic strand-annealing activity of RECQ5β (19). In the later stages of the hRPA-containing reaction, accumulation of the free leading oligonucleotide was also observed, which presumably resulted from a secondary unwinding event on the primary 5′-tail product. This observation is intriguing since the RECQ5β helicase was shown to exhibit a 3′–5′ polarity (19). It is possible that hRPA, if bound to the 5′-single stranded tail, can partially destabilize the duplex, which would allow loading of RECQ5β to mediate unwinding.

To further confirm that the RECQ5β helicase cannot actively remove the leading strand from the fork, we examined its action on a 5′-flap structure with homologous arms prepared from the same set of oligonucleotides as used in the previous strand exchange assays. If RECQ5β was capable of unwinding of the leading arm, it would promote strand exchange on this structure to form the 60mer duplex as it did on the homologous 3′-flap structure (Figure 1). However, RECQ5β did not show any strand-exchange activity on the 5′-flap structure, indicating that it cannot actively unwind the leading arm (Supplementary Figure S2).

We also examined the action of the BLM and WRN helicases on the forked DNA structures with heterologous arms described above. In contrast to RECQ5β, BLM and WRN displayed a strong preference for unwinding of the parental arm on all these structures, which was further enhanced by hRPA (Supplementary Figure S3). These findings are in agreement with previously published data (30) and further highlight mechanistic differences between RECQ5β and other human RecQ helicases in processing of forked DNA structures.

A domain within the non-conserved portion of RECQ5β is important for RECQ5β-mediated processing of forked DNA structures

To identify the functional domains in RECQ5β that are required for its ability to unwind the lagging arm of the fork and to promote strand exchange on forked structures in the presence of hRPA, we purified a series of truncated variants of RECQ5β lacking different parts of the region distal to the conserved helicase domain (Figure 6A). The RECQ5β variants lacking the C-terminal 266 or 340 amino acids ($RECQ5^{1–725}$ and $RECQ5^{1–651}$) were found to be proficient in promoting strand exchange on hRPA-coated forked structure lacking the leading strand albeit with a reduced efficiency compared to the wild-type enzyme (Figure 6B). Moreover, these variants retained the capacity to preferentially unwind the lagging-strand duplex on the forked structure with heterologous arms, being even more efficient than the wild-type enzyme (Figure 6D). This correlates with the fact that these mutants were severely impaired in promoting strand annealing (Figure 6C). In contrast, the $RECQ5^{1–475}$ and $RECQ5^{1–561}$ mutants were defective in promoting strand exchange and unwinding of the lagging arm (Figure 6B and D). However, these mutants could catalyze unwinding of the parental arm on the partial forked duplex lacking the leading strand, indicating that they retained the capacity to initiate duplex unwinding from a single-stranded tail (Figure 6D).

Collectively, these data indicate that the region of RECQ5β spanning the amino acids 561–651 is important for the processing of forked structures by this helicase.

RECQ5β is localized in DNA replication factories and persists at sites of stalled replication forks

To explore whether RECQ5β acts at DNA replications forks *in vivo*, we investigated its subcellular localization by immunofluorescence microscopy relative to PCNA that is widely used as a marker for DNA replication foci. It is known that PCNA foci undergo reproducible changes throughout S phase, with a fine punctuate pattern in early S, perinuclear and perinucleolar patterns in mid S and a characteristic late-S pattern with a few, but large foci (31). To monitor the RECQ5β localization pattern during S phase, we synchronized HeLa cells at the G_1/S transition by HU treatment and fixed them with methanol at different time points after release from the arrest. In addition to immunostaining, the cells were subjected to flow cytometry to determine the cell cycle distribution at individual time points. We observed that in HU-arrested cells, both PCNA and RECQ5β displayed exclusively nuclear staining, forming a large number of foci that partially co-localized (Figure 7). Three hours after the removal of HU (early S phase), >80% of PCNA foci in a single nucleus co-localized with RECQ5β foci in the majority of cells (Figure 7). Six hours after release (mid-S phase), the PCNA foci exhibited the characteristic peripheral pattern, while the RECQ5β foci were dispersed throughout the nucleus (Figure 7). Nine hours after release (late S phase), both PCNA and RECQ5β formed a few large foci that almost completely co-localized (Figure 7). We also examined the spatial distribution of RECQ5β and PCNA during S phase of U2OS osteosarcoma cells and obtained essentially the same results as in HeLa cells (Supplementary Figure S4). Moreover, in synchronized U2OS cells, the RECQ5β foci co-localized with sites of BrdU incorporation, a marker of ongoing DNA synthesis (Supplementary Figure S4). Using U2OS cells, we also found that the RECQ5β foci in late S phase co-localized with promyelocytic leukemia protein (PML), indicating that RECQ5β associates with PML nuclear bodies in this stage of the cell cycle (Supplementary Figure S5).

Next we investigated the effect of exogenously induced replication-blocking lesions on the cellular localization pattern of RECQ5β in non-synchronized HeLa cells. To induce

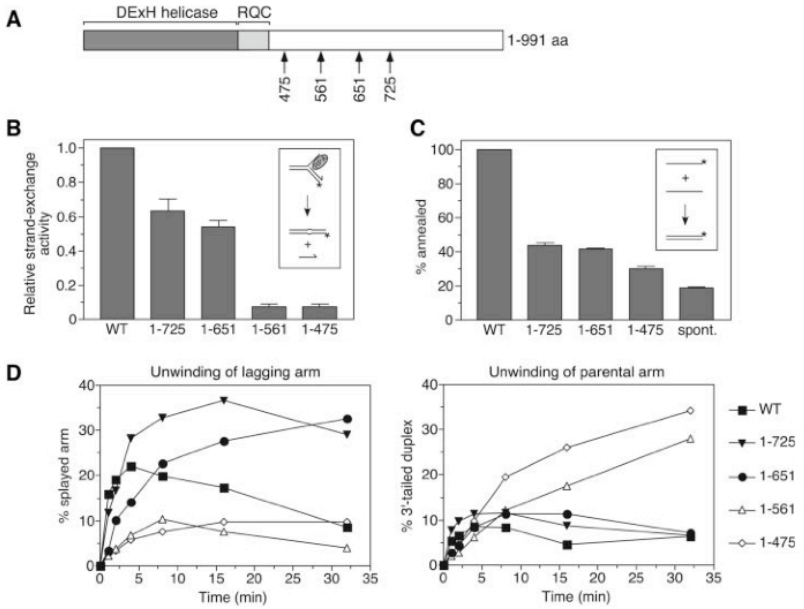

Figure 6. Characterization of RECQ5β mutants. (**A**) A schematic representation of the human RECQ5β protein demonstrating the location of the DExH helicase (dark gray) and RecQ C-terminal (RQC) (light gray) regions conserved among RecQ helicases. The arrowheads indicate the positions of the C-terminal ends of the truncated RECQ5β polypeptides used in this study. The numbers refer to the amino acid sequence of RECQ5β. (**B**) Comparison of strand-exchange activities of RECQ5β and its deletion variants (40 nM each) on forked DNA structure lacking the leading strand (1 nM) pre-coated with hRPA (20 nM). The reactions were incubated for 32 min and analyzed as described in Materials and Methods. Relative concentration of the 60mer duplex product was calculated for each reaction, and the values obtained were corrected by subtracting the background value (reaction without protein). Strand exchange activity of the mutants is expressed as a fraction of the wild-type activity. The inset shows the scheme of the reaction. (**C**) Annealing of 50mer complementary oligonucleotides, each at a concentration of 1 nM, in the presence of 20 nM wild-type and mutant RECQ5β proteins as indicated. Reactions were incubated for 32 min and the relative concentration of the strand-annealing product was determined as described in Materials and Methods. Values determined for spontaneous (spont.) reaction are also plotted. The inset shows the scheme of the reaction. (**D**) Kinetics of unwinding of 1 nM forked structure lacking the leading strand by 100 nM RECQ5β and its deletion variants as indicated. Reactions were carried out and analyzed as described in Materials and Methods. The graph on the left shows relative concentrations of splayed arm product resulting from unwinding of the lagging arm. The graph on the right shows relative concentration of the 3′-tailed duplex generated by unwinding of the parental arm. All data points represent the average values from three independent experiments.

the formation of bulky DNA adducts, cells were exposed to UVC irradiation or treated with CDDP. In asynchronous populations of cycling HeLa cells (~70% of cells in G_1 as judged from the FACS profile), PCNA showed mostly a diffuse nuclear staining, whereas RECQ5β displayed rather a punctuate distribution in the nucleus as well as a weak cytoplasmic staining (Figure 8). In a small percentage of cells (~15%), PCNA was concentrated in small nuclear foci, indicating that these cells were in S phase (data not shown). Most importantly, these PCNA foci largely co-localized with RECQ5β foci, which excludes the possibility that the pattern observed 3 h after HU removal was a consequence of DNA damage caused by HU treatment (data not shown; Figure 7).

After exposure of cells to UV irradiation at a dosage of 20 J/m^2, there was a dramatic increase in the percentage of cells in which PCNA foci co-localized with RECQ5β foci (Figure 8). Four hours after UV irradiation, ~80% of PCNA foci in a single nucleus co-localized with RECQ5β foci in 55% of cells. These foci appeared somewhat brighter than those observed in early S phase cells (compare Figure 7 and Figure 8) and persisted up to 6 h after irradiation (data not shown).

In HeLa cells treated with CDDP (20 μM), which predominantly causes intra-strand DNA cross-links mimicking pyrimidine–dimer adducts induced by UV light, RECQ5β and PCNA displayed essentially the same spatial distribution as in UV-irradiated cells, with the maximal co-localization being apparent 6 h after addition of the drug (Figure 8). Moreover, we examined spatial distribution of RECQ5β in SV40-immortalized human fibroblasts GM00637 and XP20SSV (XPA-deficient) before and after UV irradiation. We observed essentially the same patterns as in HeLa cells, excluding a cell-line specific effect (Supplementary Figure S6). In addition, the experiment with XPA-deficient cells ruled out the possibility that RECQ5β is present in the complexes that mediate repair synthesis following excision of DNA adducts by the nucleotide-excision repair pathway.

Taken together, these data suggest that RECQ5β is associated with the DNA replication machinery, particularly in early and late S phase and it is present in replication-repair factories at the sites of stalled replication forks.

RECQ5β directly interacts with PCNA

In addition to serving as a sliding clamp required for processive DNA synthesis, PCNA provides attachment sites for various other proteins that function in DNA replication, DNA repair, cell cycle progression and chromatin assembly

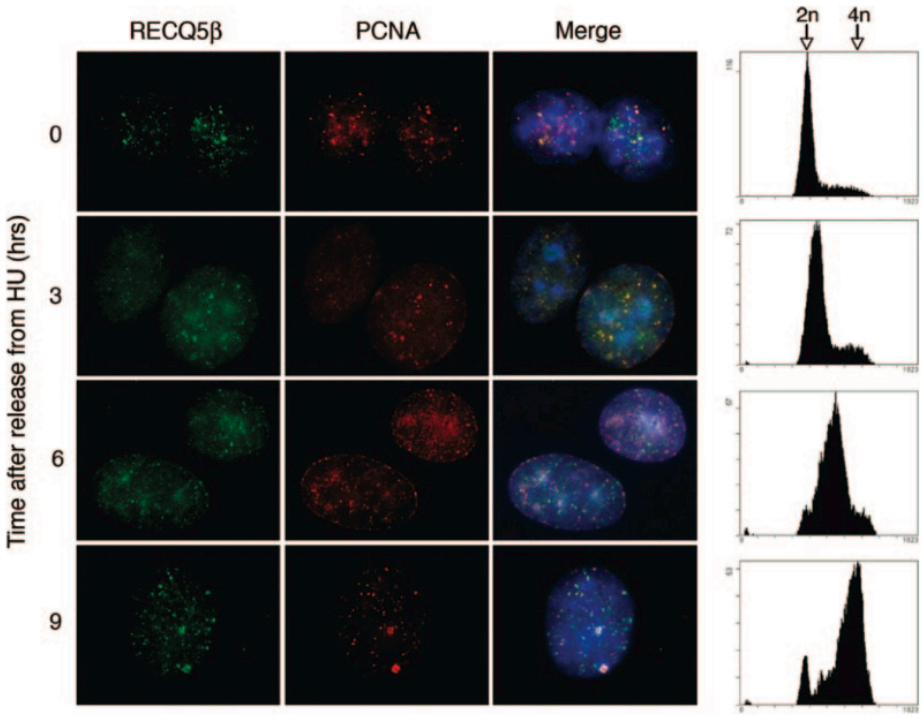

Figure 7. Co-localization of RECQ5β and PCNA in S phase nuclei of HeLa cells. Cells were synchronized at G_1/S transition by treatment with hydroxyurea (HU) for 16 h and then released to S phase by adding fresh medium without HU. At indicated time points, cells were fixed with methanol, triply stained for RECQ5β (green), PCNA (red) and DNA (blue) as described in Materials and Methods, and analyzed by fluorescence microscopy. Representative images are shown. Yellow colour in the superimposed images (Merge) indicates co-localization of RECQ5β and PCNA staining. In parallel, cells were subjected to FACS analysis. The resultant cell cycle profiles for each time point are shown on the right. Arrowheads indicate cell population in G_1 phase with a 2n DNA content and G_2/M with 4n DNA content; S phase cells have DNA content between 2n and 4n.

(32). To further explore the association of RECQ5β with the DNA replication machinery, we examined whether it interacts with PCNA, as suggested by the presence of a putative PCNA-binding motif at the C-terminus of RECQ5β (Figure 9A). First, we performed affinity pull-down assays with recombinant proteins produced in *E.coli*. We found that PCNA was bound to chitin beads coated with RECQ5β-CBD protein, but not to beads coated with McrA-CBD protein, indicating that the interaction was specific (Figure 9B). Moreover, using GST-tagged RECQ5β deletion variants, we found that the region spanning the last 200 amino acids of RECQ5β is essential for its interaction with PCNA, suggesting that this interaction is mediated through the putative PCNA-binding motif located in this region (Figure 9C).

We also examined the effect of PCNA on the strand exchange activity of RECQ5β using the synthetic forked DNA structure containing a 10 nt gap on the leading arm (Figure 2A). We found that PCNA did not affect the rate or the extent of RECQ5β-mediated strand exchange (Supplementary Figure S7).

To see whether RECQ5β interacts with PCNA *in vivo*, we conducted immunoprecipitation experiments with total extracts of human 293T embryonic kidney cells. Extracts were prepared not only from non-treated cells, but also from cells synchronized in early S phase and cells subjected to UV irradiation or CDDP treatment, since under these conditions, RECQ5β was found to localize to PCNA foci. We found that PCNA was precipitated with the anti-RECQ5β antibody, but not with control IgGs purified from pre-immune serum, indicating that RECQ5β and PCNA indeed form a complex *in vivo* (Figure 9D). Moreover, a significant larger amount of PCNA (~2 times) was detected in the immunoprecipitates of treated cells compared with non-treated cells, suggesting that the observed recruitment of RECQ5β to replication foci may occur via a direct interaction with PCNA (Figure 9D, compare lane 3 to lanes 4–6).

DISCUSSION

There is growing evidence suggesting that RecQ DNA helicases operate in various DNA repair processes induced by DNA replication defects. However, the DNA transactions mediated by these proteins at damaged replication forks still remain elusive. Here we show that the human RECQ5β helicase possesses the ability to promote strand exchange on synthetic forked DNA structures that mimic a stalled replication fork. Moreover, we provide evidence suggesting that the RECQ5β protein is localized in the DNA replication factories

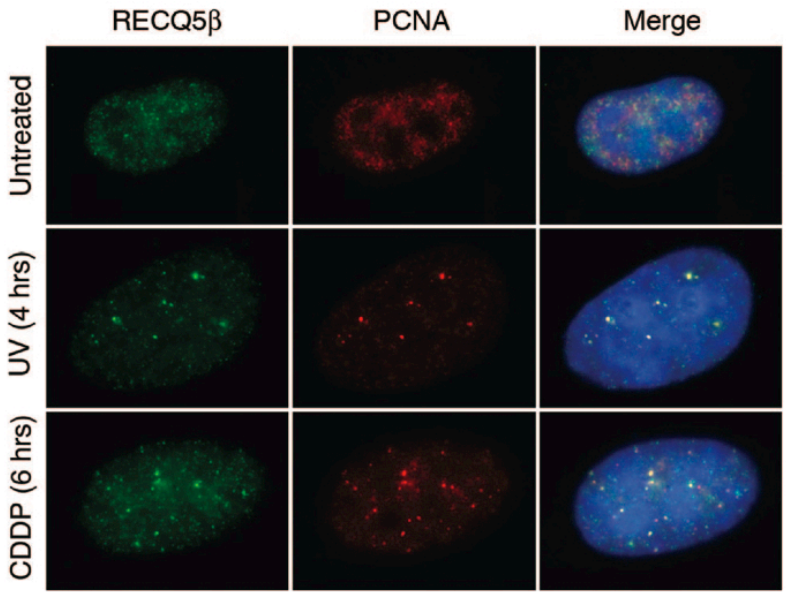

Figure 8. Co-localization of RECQ5β and PCNA in HeLa cells following UV irradiation and CDDP treatment. Non-synchronized cells were UV-irradiated at 20 J/m^2 and cultured for additional 4 h or treated with 20 μM CDDP for 6 h. After methanol fixation, cells were triply stained for RECQ5β (green), PCNA (red) and DNA (blue), and analyzed by fluorescence microscopy. Representative images are shown.

in S phase nuclei and persists at the sites of stalled replication forks. Based on these findings, we speculate that the RECQ5β helicase could mediate regression of stalled replication forks *in vivo* to facilitate DNA damage bypass by template-switching (Supplementary Figure S8). As mentioned above, such a DNA damage tolerance mechanism has been postulated to exist in both prokaryotic and eukaryotic organisms, but remains to be substantiated experimentally. In the budding yeast *Saccharomyces cerevisiae*, fork regression associated with template-switching is thought to be the underlying mechanism of the *RAD5*-subpathway of *RAD6*-dependent postreplicative repair, which is highly conserved from yeast to humans (33). As this DNA damage tolerance process, which involves non-destructive polyubiquitination of PCNA, is largely independent of the HR machinery, other means, such as helicase-promoted DNA unwinding, would be required to accomplish the strand-exchange events required for fork regression (33,34). At present, however, it is not clear whether Sgs1 helicase, the sole RecQ homologue in *S.cerevisiae*, is involved in the RAD6-dependent DNA damage tolerance, since the assessment of this possibility by epistatic analysis is complicated due to the involvement of Sgs1 in the HR pathway of postreplicative repair (6). Nevertheless, some evidence for such a function has been provided in the fission yeast *Saccharomyces pombe* by the observation that the formation of Rqh1 (Sgs1 homologue) foci upon UV irradiation is dependent on the presence of Rdh18/Rad18, a component of the Rad6 pathway (35).

Our hypothesis that RECQ5β operates in the repair of damaged replication forks is consistent with the finding that inactivation of the mouse RECQ5β homologue is associated with a significant increase in the frequency of SCEs (17), as these may represent cross-over outcomes of the HR-mediated repair of broken replication forks that arise as a consequence of the blockage of leading-strand extension by bulky lesions (Supplementary Figure S8). Similarly, elevated SCE levels have been observed in DT40 chicken cells lacking the trans-lesion polymerases Polζ and Polκ, or the Rad18 ubiquitin ligase (36). However, one cannot exclude the possibility that the increased level of mitotic recombination associated with RECQ5β deficiency results from a defect in another DNA repair mechanisms. For example, RECQ5β could operate in the synthesis-dependent strand-annealing pathway of DNA double-strand break repair by disrupting D-loops and promoting annealing of extended arms of the broken chromosome. Alternatively, RECQ5β could suppress unscheduled recombination during DNA replication by directly displacing inappropriately formed RAD51 filaments in the same manner as the Srs2 and UvrD helicases (37,38).

The biochemical and structural studies have revealed that the *E.coli* RecG helicase mediates fork regression by active unwinding of both the leading and lagging arms of the fork using a wedge domain that is simultaneously pushed into the lagging and the leading duplexes promoting strand displacement (39,40). In contrast to RecG, the RECQ5β helicase was found to unwind only the lagging-strand duplex, which raises the question of how it can promote fork regression beyond the leading-strand gap. We propose a mechanism in which RECQ5β binds to the fork junction and subsequently translocates along the lagging-strand template in the 3′–5′ direction to unwind the lagging-strand duplex. As a result, the parental strands will be free to re-anneal. Interestingly, we identified a region of 90 amino acids, located within the non-conserved portion of RECQ5β, as being required for its ability to unwind the lagging arm of the fork, but not for RECQ5β-mediated unwinding of 3′-tailed DNA duplexes.

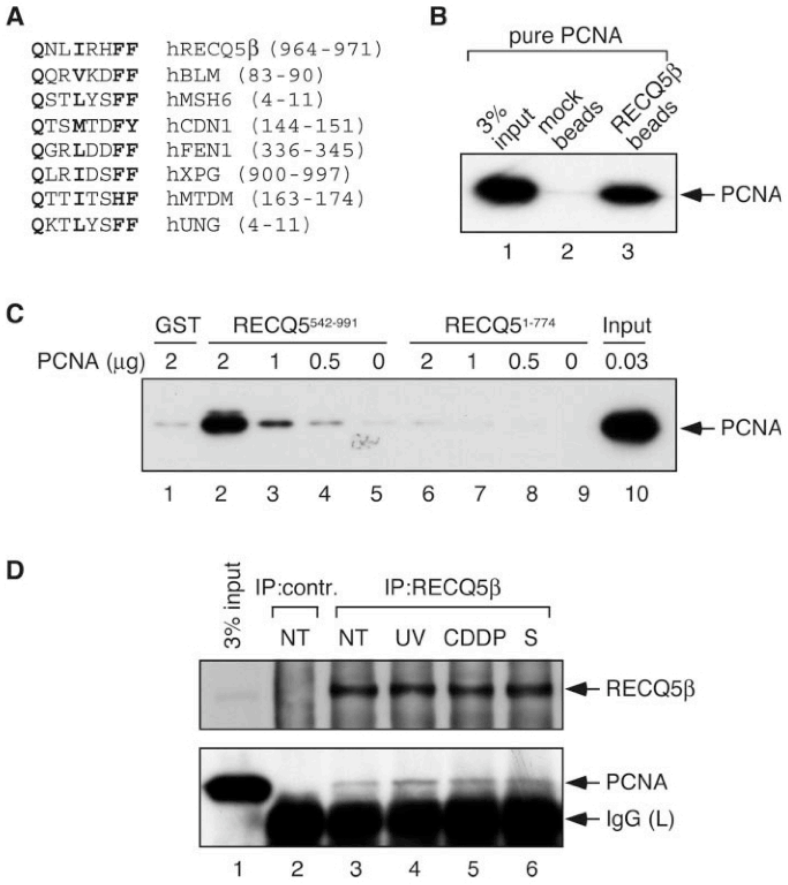

Figure 9. Interaction between RECQ5β and PCNA. (**A**) The putative PCNA-binding motif of human RECQ5β. The C-terminal amino acids 964–971 of RECQ5β are aligned with the PCNA-binding motifs identified in various PCNA-interacting proteins. The highly conserved residues are shown in boldface. (**B**) Direct interaction between RECQ5β and PCNA. Chitin beads coated with recombinant RECQ5β protein containing an intein-CBD tag were incubated with recombinant PCNA (1 μg) as described in Materials and Methods. In the control experiment, beads coated with the *E.coli* McrA endonuclease (mock beads) were used. Bound proteins were analyzed by SDS–PAGE and western blotting. Blots were probed with monoclonal anti-PCNA antibody (PC-10, Santa Cruz). (**C**) Mapping PCNA-interaction domain in RECQ5β. Glutathione beads coated with the GST-tagged RECQ5β deletion variants $RECQ5^{542–991}$ and $RECQ5^{1–774}$, respectively, were incubated with increasing amounts of purified PCNA as indicated. Bound proteins were analyzed as in (B). (**D**) Co-immunoprecipitation of PCNA with RECQ5β from extracts of 293T cells: non-treated (NT) cells (lane 3), UV-irradiated (40 J/m^2) cells incubated for 6 h (lane 4), cells treated with CDDP (20 μM) for 8 h (lane 5), cells arrested at G_1/S by HU (2 mM, 16 h) and subsequently released to S phase for 3 h (lane 6). Extracts were immunoprecipitated using affinity-purified rabbit polyclonal anti-RECQ5β antibody as described in Materials and Methods. IgGs purified from corresponding pre-immune serum served as a control (lane 2). The immunoprecipitates were analyzed as in (A). The blots were probed with anti-PCNA and anti-RECQ5β antibodies.

It is therefore plausible to propose that this domain may govern the loading of the RECQ5β helicase on the fork junction, placing the helicase motor on the parental duplex in such an orientation as to allow translocation towards the lagging arm. Furthermore, we propose that when the moving junction encounters the leading strand, spontaneous strand exchange will take place, resulting in the displacement of the leading strand and its annealing to the displaced lagging strand to form a four-way junction. This reaction will be favoured due to the concomitant unwinding of the lagging arm by RECQ5β. It is also possible that the annealing events occurring during the fork regression process are promoted by the C-terminal strand-annealing domain of RECQ5β, since we found that the deletion variants $RECQ5^{1–725}$ and $RECQ5^{1–651}$ were dramatically compromised for the strand-annealing activity and showed reduced strand-exchange activity relative to the wild-type protein.

A previous study demonstrated that BLM and WRN have the capacity to promote strand exchange on oligonucleotide-based substrates through combining their strand-pairing and helicase activities (41). More recently, the BLM helicase has been found to promote fork regression on plasmid-sized substrates, generating a four-way structure (42). Interestingly, we found that hRPA, which covers single-stranded regions at stalled forks (27), strongly modulated the action of the BLM and WRN helicases at the fork to favour unwinding of the parental duplex, which is consistent with the previous reports demonstrating that hRPA increases the processivity of the

BLM and WRN helicases through direct protein–protein interactions (43,44). However, these experiments using short DNA substrates cannot account for the possibility that fork regression is mediated by another helicase molecule loaded on the liberated lagging-strand template, an model proposed for the *E.coli* RecQ helicase (45). To assess which human RecQ helicase is more likely to promote fork regression *in vivo*, the effect of hRPA on fork regression by BLM, WRN and RECQ5β is currently being investigated using a plasmid-sized forked DNA structure containing an extensive leading-strand gap.

SUPPLEMENTARY DATA

Supplementary Data are available at NAR Online.

ACKNOWLEDGEMENTS

We thank Nina Mojas for help in fluorescence microscopy, Christiane Koenig for technical assistance and Josef Jiricny, Massimo Lopes and Ludovic Gillet for comments on the manuscript. This work was funded by the Swiss National Science Foundation and the Sassella Stiftung. Funding to pay the Open Access publication charges for this article was provided by the Swiss National Science Foundation.

Conflict of interest statement. None declared.

REFERENCES

1. Cox,M.M. (2001) Recombinational DNA repair of damaged replication forks in *Escherichia coli*: questions. *Annu. Rev. Genet.*, **35**, 53–82.
2. Cordeiro-Stone,M., Makhov,A.M., Zaritskaya,L.S. and Griffith,J.D. (1999) Analysis of DNA replication forks encountering a pyrimidine dimer in the template to the leading strand. *J. Mol. Biol.*, **289**, 1207–1218.
3. Lopes,M., Foiani,M. and Sogo,J.M. (2006) Multiple mechanisms control chromosome integrity after replication fork uncoupling and restart at irreparable UV lesions. *Mol. Cell*, **21**, 15–27.
4. Hickson,I.D. (2003) RecQ helicases: caretakers of the genome. *Nat. Rev. Cancer*, **3**, 169–178.
5. Lambert,S., Watson,A., Sheedy,D.M., Martin,B. and Carr,A.M. (2005) Gross chromosomal rearrangements and elevated recombination at an inducible site-specific replication fork barrier. *Cell*, **121**, 689–702.
6. Barbour,L. and Xiao,W. (2003) Regulation of alternative replication bypass pathways at stalled replication forks and its effects on genome stability: a yeast model. *Mutat. Res.*, **532**, 137–155.
7. Heller,R.C. and Marians,K.J. (2006) Replication fork reactivation downstream of a blocked nascent leading strand. *Nature*, **439**, 557–562.
8. Higgins,N.P., Kato,K. and Strauss,B. (1976) A model for replication repair in mammalian cells. *J. Mol. Biol.*, **101**, 417–425.
9. Seigneur,M., Bidnenko,V., Ehrlich,S.D. and Michel,B. (1998) RuvAB acts at arrested replication forks. *Cell*, **95**, 419–430.
10. Zou,H. and Rothstein,R. (1997) Holliday junctions accumulate in replication mutants via a RecA homolog-independent mechanism. *Cell*, **90**, 87–96.
11. Sogo,J.M., Lopes,M. and Foiani,M. (2002) Fork reversal and ssDNA accumulation at stalled replication forks owing to checkpoint defects. *Science*, **297**, 599–602.
12. Bachrati,C.Z. and Hickson,I.D. (2003) RecQ helicases: suppressors of tumorigenesis and premature aging. *Biochem. J.*, **374**, 577–606.
13. Wu,L. and Hickson,I.D. (2003) The Bloom's syndrome helicase suppresses crossing over during homologous recombination. *Nature*, **426**, 870–874.
14. Crabbe,L., Verdun,R.E., Haggblom,C.I. and Karlseder,J. (2004) Defective telomere lagging strand synthesis in cells lacking WRN helicase activity. *Science*, **306**, 1951–1953.
15. Opresko,P.L., Otterlei,M., Graakjaer,J., Bruheim,P., Dawut,L., Kolvraa,S., May,A., Seidman,M.M. and Bohr,V.A. (2004) The Werner syndrome helicase and exonuclease cooperate to resolve telomeric D loops in a manner regulated by TRF1 and TRF2. *Mol. Cell*, **14**, 763–774.
16. Sangrithi,M.N., Bernal,J.A., Madine,M., Philpott,A., Lee,J., Dunphy,W.G. and Venkitaraman,A.R. (2005) Initiation of DNA replication requires the RECQL4 protein mutated in Rothmund-Thomson syndrome. *Cell*, **121**, 887–898.
17. Hu,Y., Lu,X., Barnes,E., Yan,M., Lou,H. and Luo,G. (2005) Recql5 and Blm RecQ DNA helicases have nonredundant roles in suppressing crossovers. *Mol. Cell. Biol.*, **25**, 3431–3442.
18. Shimamoto,A., Nishikawa,K., Kitao,S. and Furuichi,Y. (2000) Human RecQ5β, a large isomer of RecQ5 DNA helicase, localizes in the nucleoplasm and interacts with topoisomerases 3α and 3β. *Nucleic Acids Res.*, **28**, 1647–1655.
19. Garcia,P.L., Liu,Y., Jiricny,J., West,S.C. and Janscak,P. (2004) Human RECQ5β, a protein with DNA helicase and strand-annealing activities in a single polypeptide. *EMBO J.*, **23**, 2882–2891.
20. Gaymes,T.J., North,P.S., Brady,N., Hickson,I.D., Mufti,G.J. and Rassool,F.V. (2002) Increased error-prone non homologous DNA end-joining—a proposed mechanism of chromosomal instability in Bloom's syndrome. *Oncogene*, **21**, 2525–2533.
21. Karow,J.K., Chakraverty,R.K. and Hickson,I.D. (1997) The Bloom's syndrome gene product is a 3′–5′ DNA helicase. *J. Biol. Chem.*, **272**, 30611–30614.
22. Orren,D.K., Brosh,R.M., Jr., Nehlin,J.O., Machwe,A., Gray,M.D. and Bohr,V.A. (1999) Enzymatic and DNA binding properties of purified WRN protein: high affinity binding to single-stranded DNA but not to DNA damage induced by 4NQO. *Nucleic Acids Res.*, **27**, 3557–3566.
23. Henricksen,L.A., Umbricht,C.B. and Wold,M.S. (1994) Recombinant replication protein A: expression, complex formation, and functional characterization. *J. Biol. Chem.*, **269**, 11121–11132.
24. Podust,L.M., Podust,V.N., Sogo,J.M. and Hubscher,U. (1995) Mammalian DNA polymerase auxiliary proteins: analysis of replication factor C-catalyzed proliferating cell nuclear antigen loading onto circular double-stranded DNA. *Mol. Cell. Biol.*, **15**, 3072–3081.
25. Janscak,P., Garcia,P.L., Hamburger,F., Makuta,Y., Shiraishi,K., Imai,Y., Ikeda,H. and Bickle,T.A. (2003) Characterization and mutational analysis of the RecQ core of the Bloom syndrome protein. *J. Mol. Biol.*, **330**, 29–42.
26. Sharma,S., Sommers,J.A., Choudhary,S., Faulkner,J.K., Cui,S., Andreoli,L., Muzzolini,L., Vindigni,A. and Brosh,R.M., Jr. (2005) Biochemical analysis of the DNA unwinding and strand annealing activities catalyzed by human RECQ1. *J. Biol. Chem.*, **280**, 28072–28084.
27. Zou,L. and Elledge,S.J. (2003) Sensing DNA damage through ATRIP recognition of RPA-ssDNA complexes. *Science*, **300**, 1542–1548.
28. Kim,C., Snyder,R.O. and Wold,M.S. (1992) Binding properties of replication protein A from human and yeast cells. *Mol. Cell. Biol.*, **12**, 3050–3059.
29. Ozsoy,A.Z., Ragonese,H.M. and Matson,S.W. (2003) Analysis of helicase activity and substrate specificity of Drosophila RECQ5. *Nucleic Acids Res.*, **31**, 1554–1564.
30. Brosh,R.M., Jr., Waheed,J. and Sommers,J.A. (2002) Biochemical characterization of the DNA substrate specificity of Werner syndrome helicase. *J. Biol. Chem.*, **275**, 23500–23508.
31. Leonhardt,H., Rahn,H.P., Weinzierl,P., Sporbert,A., Cremer,T., Zink,D. and Cardoso,M.C. (2000) Dynamics of DNA replication factories in living cells. *J. Cell. Biol.*, **149**, 271–280.
32. Warbrick,E. (2000) The puzzle of PCNA's many partners. *Bioessays*, **22**, 997–1006.
33. Torres-Ramos,C.A., Prakash,S. and Prakash,L. (2002) Requirement of *RAD5* and *MMS2* for postreplication repair of UV-damaged DNA in *Saccharomyces cerevisiae*. *Mol. Cell. Biol.*, **22**, 2419–2426.
34. Hoege,C., Pfander,B., Moldovan,G.L., Pyrowolakis,G. and Jentsch,S. (2002) RAD6-dependent DNA repair is linked to modification of PCNA by ubiquitin and SUMO. *Nature*, **419**, 135–141.
35. Laursen,L.V., Ampatzidou,E., Andersen,A.H. and Murray,J.M. (2003) Role for the fission yeast RecQ helicase in DNA repair in G2. *Mol. Cell. Biol.*, **23**, 3692–3705.

36. Hochegger,H., Sonoda,E. and Takeda,S. (2004) Post-replication repair in DT40 cells: translesion polymerases versus recombinases. *Bioessays*, **26**, 151–158.
37. Krejci,L., Van Komen,S., Li,Y., Villemain,J., Reddy,M.S., Klein,H., Ellenberger,T. and Sung,P. (2003) DNA helicase Srs2 disrupts the Rad51 presynaptic filament. *Nature*, **423**, 305–309.
38. Veaute,X., Delmas,S., Selva,M., Jeusset,J., Le Cam,E., Matic,I., Fabre,F. and Petit,M.A. (2005) UvrD helicase, unlike Rep helicase, dismantles RecA nucleoprotein filaments in *Escherichia coli*. *EMBO J.*, **24**, 180–189.
39. McGlynn,P. and Lloyd,R.G. (2001) Rescue of stalled replication forks by RecG: simultaneous translocation on the leading and lagging strand templates supports an active DNA unwinding model of fork reversal and Holliday junction formation. *Proc. Natl Acad. Sci. USA*, **98**, 8227–8234.
40. Singleton,M.R., Scaife,S. and Wigley,D.B. (2001) Structural analysis of DNA replication fork reversal by RecG. *Cell*, **107**, 79–89.
41. Machwe,A., Xiao,L., Groden,J., Matson,S.W. and Orren,D.K. (2005) RecQ family members combine strand pairing and unwinding activities to catalyze strand exchange. *J. Biol. Chem.*, **280**, 23397–23407.
42. Ralf,C., Hickson,I.D. and Wu,L. (2006) The Bloom's syndrome helicase can promote the regression of a model replication fork. *J. Biol. Chem.*, **281**, 22839–22846.
43. Brosh,R.M., Jr., Li,J.L., Kenny,M.K., Karow,J.K., Cooper,M.P., Kureekattil,R.P., Hickson,I.D. and Bohr,V.A. (2000) Replication protein A physically interacts with the Bloom's syndrome protein and stimulates its helicase activity. *J. Biol. Chem.*, **275**, 23500–23508.
44. Brosh,R.M., Jr., Orren,D.K., Nehlin,J.O., Ravn,P.H., Kenny,M.K., Machwe,A. and Bohr,V.A. (1999) Functional and physical interaction between WRN helicase and human replication protein A. *J. Biol. Chem.*, **274**, 18341–18350.
45. Hishida,T., Han,Y.W., Shibata,T., Kubota,Y., Ishino,Y., Iwasaki,H. and Shinagawa,H. (2004) Role of the *Escherichia coli* RecQ DNA helicase in SOS signaling and genome stabilization at stalled replication forks. *Genes Dev.*, **18**, 1886–1897.

Supplementary Figure S1

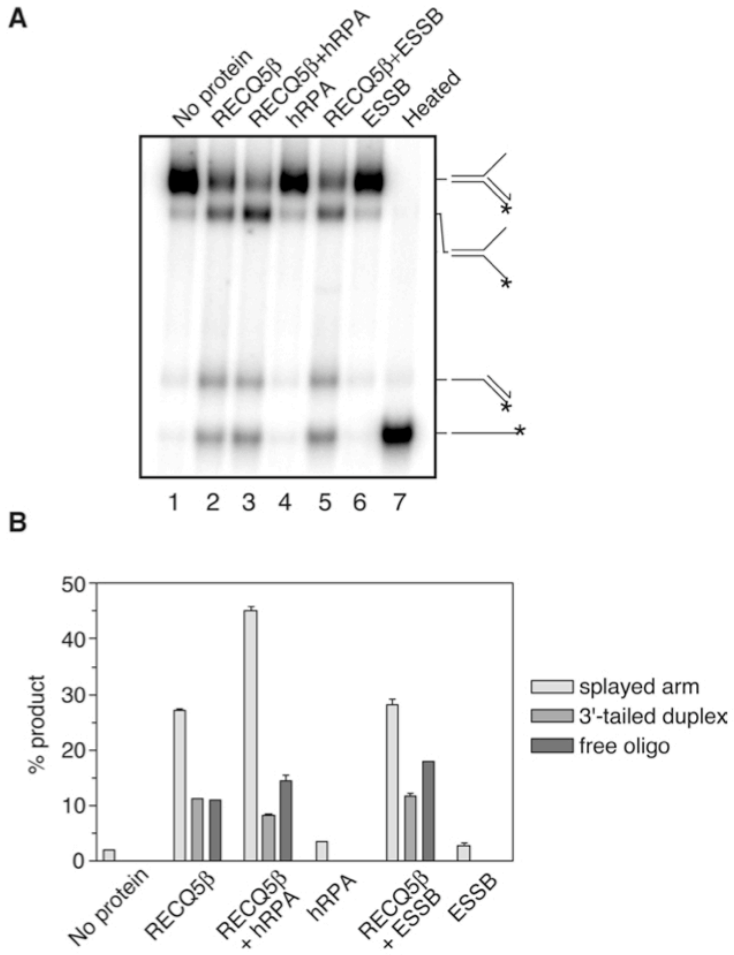

Figure S1. Effect of hRPA and ESSB on unwinding of 3'-flap duplex by RECQ5β. (A) Analysis of reaction products by non-denaturing PAGE. Reactions were carried out for 16 minutes as indicated. DNA, RECQ5β, hRPA and ESSB (monomer) were present at concentrations of 1 nM, 40 nM, 20 nM and 80 nM, respectively. hRPA and ESSB were added 2 minutes prior to addition of ATP (2 mM). Radiolabelled DNA species were visualized by phosphorimaging. (B) Quantification of the reactions in (A). The graph shows the relative concentrations of unwound products including the splayed arm, the 3'-tailed duplex and the free labelled oligonucleotide.

Supplementary Figure S2

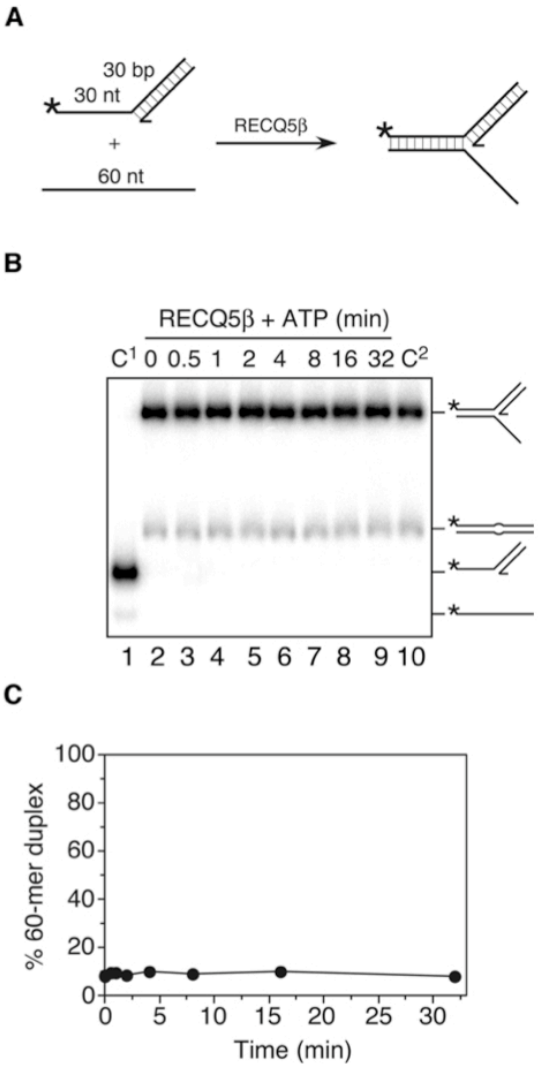

Figure S2. RECQ5β helicase does not actively unwind the leading arm of the fork. **(A)** Scheme of the preparation of DNA substrate (5'-flap duplex) by RECQ5β-mediated strand annealing. The lengths of individual arms are indicated in nucleotides (nt) or base pairs (bp). The 3'-end of the leading oligonucleotide is indicated by an arrow and the position of the 5'-^{32}P label is marked by an asterisk. The homologous leading and lagging arms have a 5-nt heterology at the fork junction to prevent spontaneous strand exchange. **(B)** 1 nM ^{32}P-labeled 60-mer/30-mer duplex (RK3/RK7) was incubated with 1 nM 60-mer complementary oligonucleotide (RK1) in the presence of 40 nM RECQ5β for 10 minutes to form the forked DNA structure. After 10 minutes, ATP was added to a final concentration of 2 mM. Aliquots from different reaction time points were analyzed by non-denaturing PAGE followed by phosphorimaging (lanes 2-9). C^1, 5'-tailed duplex; C^2, annealing mixture incubated for 32 minutes in the presence of 2 mM ATPγS. **(C)** Quantification of the reaction in (B). Relative concentration of the 60-mer duplex is plotted *versus* reaction time. The data points represent the average values from two independent experiments.

Supplementary Figure S3

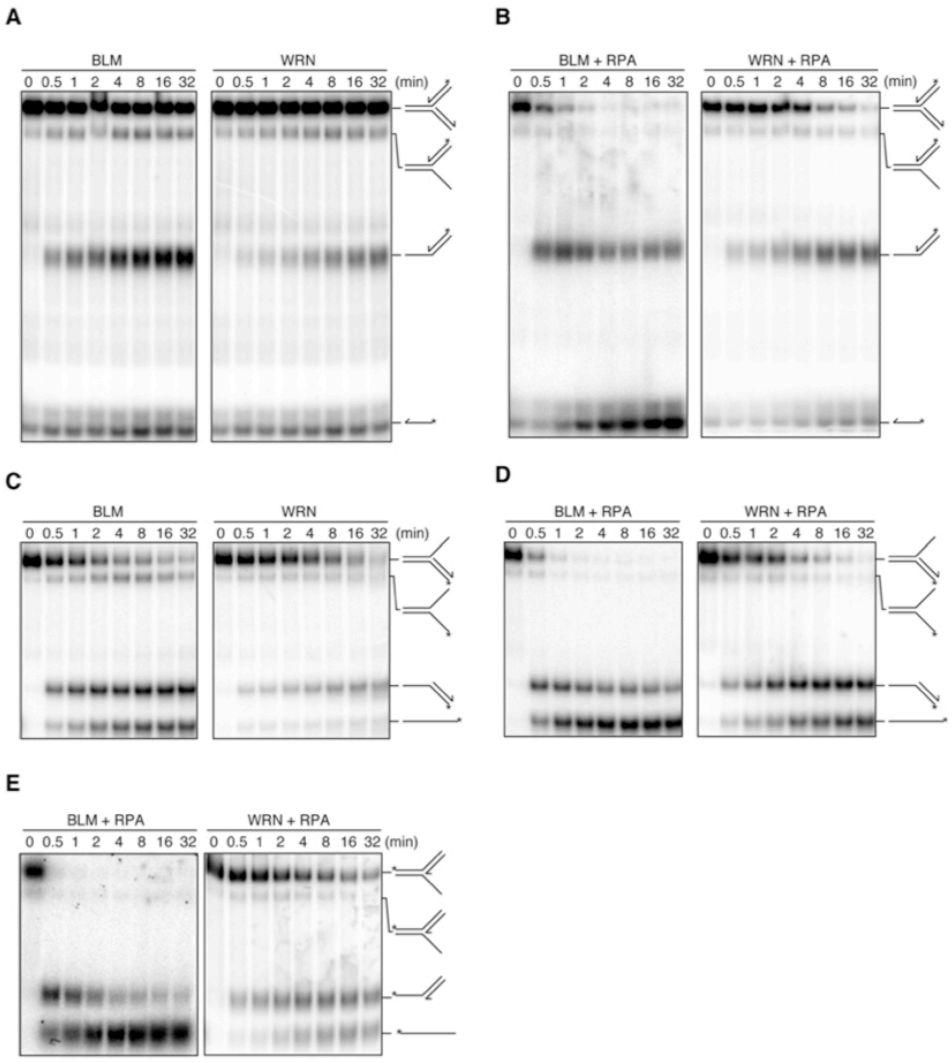

Figure S3. Unwinding of synthetic forked DNA structures with heterologous arms by BLM and WRN. **(A)** Time course of unwinding of 1 nM fully double-stranded forked structure by 10 nM BLM or 5 nM WRN. **(B)** Time course of unwinding of 1 nM fully double-stranded forked structure by 10 nM BLM or 5 nM WRN in the presence of 20 nM hRPA. **(C)** Time course of unwinding of 1 nM partial forked duplex lacking the leading strand by 10 nM BLM or 5 nM WRN. **(D)** Time course of unwinding of 1 nM partial forked duplex lacking the leading strand by 10 nM BLM or 5 nM WRN in the presence of 20 nM hRPA. **(E)** Time course of unwinding of 1 nM partial forked duplex lacking the lagging strand by 10 nM BLM or 5 nM WRN in the presence of 20 nM hRPA. Reactions were carried out and analyzed as described in Materials and Methods. All DNA substrates are derived from the same set of four oligonucleotides (Supplementary Table 1). The 3'-ends of the leading and lagging strands are indicated by arrows. The position of the 5'-^{32}P-label in each substrate is indicated by an asterisk.

Supplementary Figure S4

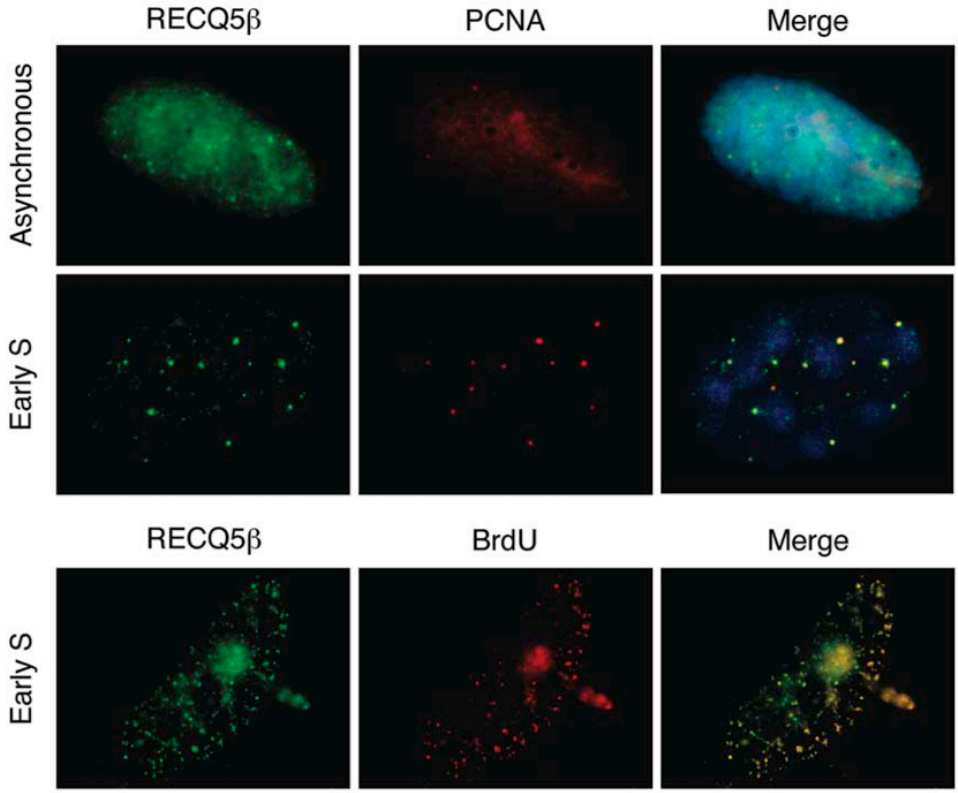

Figure S4. Localization of RECQ5β to replication foci in synchronized U2OS cells. **(A)** Co-localization of RECQ5β with PCNA in early S phase. Cells were synchronized at the G1/S transition by HU treatment and then released to S phase by adding fresh medium without HU. After three hours, cells were fixed with methanol, triply stained with anti-RECQ5β antibody (green), anti-PCNA antibody (red) and DAPI (blue), and analyzed by fluorescence microscopy as described in Materials and methods. **(B)** RECQ5β co-localizes with sites of DNA synthesis. Cells were synchronized by HU treatment and then released to S phase. After two hours, the medium was supplemented with 10 μM 5-bromo-2'-deoxyuridine (BrdU; Boehringer Mannheim) and incubation was continued for one hour. Cells were fixed with methanol and sequentially incubated with anti-RECQ5β antibody and anti-rabbit FITC-conjugated secondary antibody. Antigen-antibody complexes were fixed by immersion in ice-cold methanol for 10 min at 20°C. Subsequently, the fixed cells were treated with 2M HCl at 37°C for 60 min to denature the DNA and then neutralized with 0.1 M borate buffer (pH 8.5) and washed with PBS containing 3% low-fat milk. Sites of BrdU incorporation were stained with mouse monoclonal anti-BrdU antibody (Amersham Pharmacia; 1:100) followed by Texas Red-conjugated donkey anti-mouse secondary antibody. Stained cells were analyzed by fluorescence microscopy.

Supplementary Figure S5

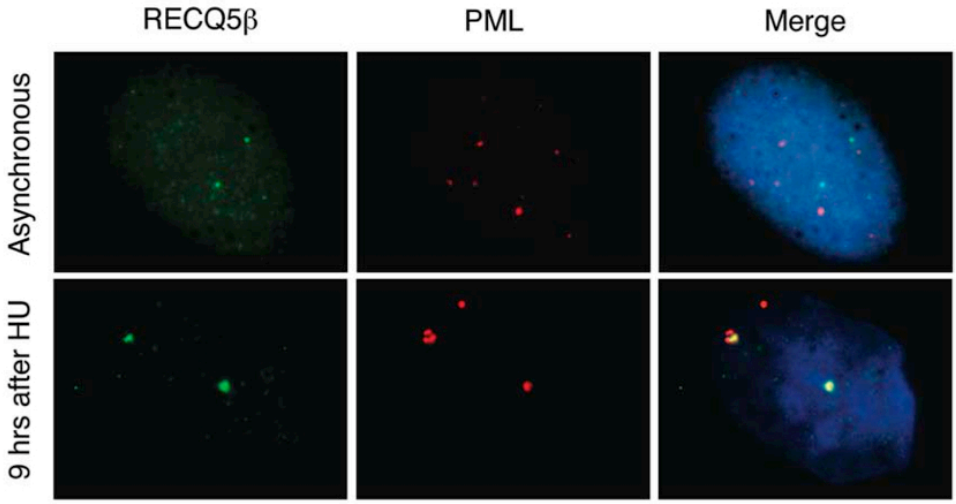

Figure S5. Co-localization of RECQ5β with PML in late S phase. Cells were synchronized by HU treatment and then released from HU block for 9 hours. FACS analysis indicated a 4n DNA content in the majority of cells (not shown). After methanol fixation, cells were triply stained for RECQ5β (green), PML (red) and DNA (blue), and analyzed by fluorescence microscopy. Representative images for asynchronous population of cells are also shown. Mouse monoclonal anti-PML antibody (PG-M3, Santa Cruz; 1:200) was used for immunostaining.

Supplementary Figure S6

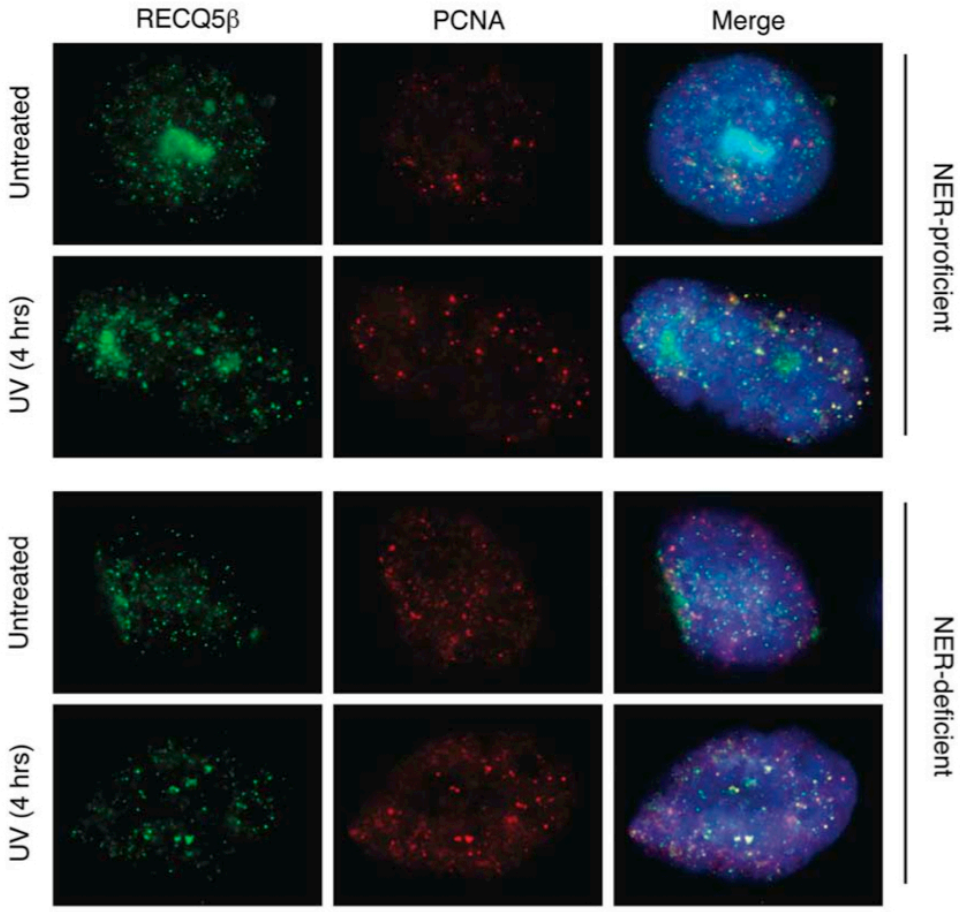

Figure S6. Co-localization of RECQ5β with PCNA in human fibroblasts after UV-irradiation. Asynchronous populations of SV40-immortalized GM00637 (NER-proficient) and XP20SSV (NER-deficient) human fibroblasts were UV-irradiated at 20 J/m^2 and cultured for additional 4 hours and 8 hours, respectively. After methanol fixation, cells were triply stained for RECQ5β (green), PCNA (red) and DNA (blue), and analyzed by fluorescence microscopy. Representative images are shown for both non-irradiated and irradiated cell populations.

Supplementary Figure S7

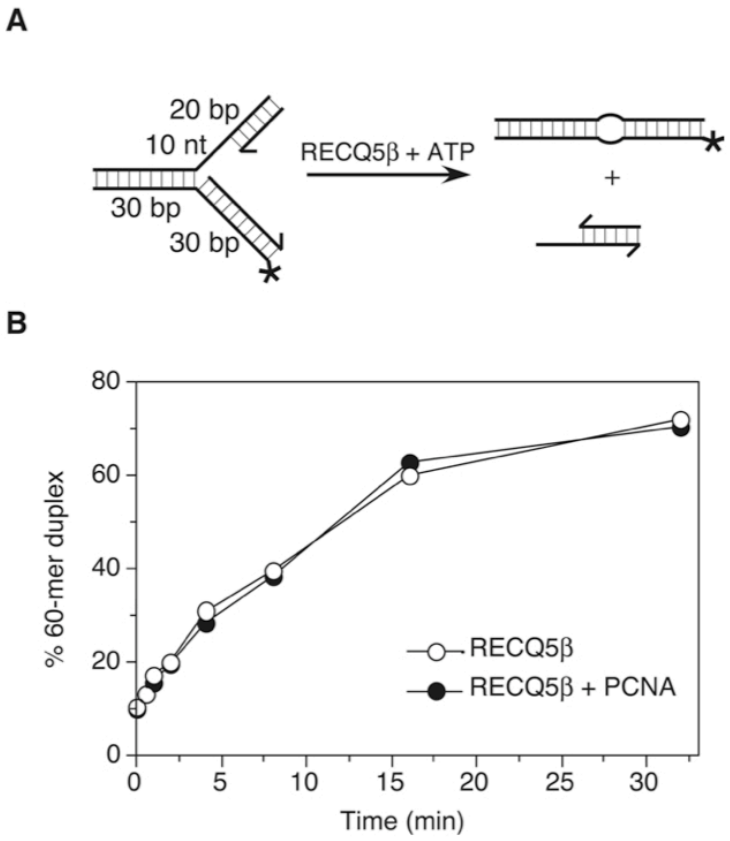

Figure S7. Effect of PCNA on strand-exchange activity of RECQ5β on forked DNA structure with a 10-nt leading strand gap. (A) Scheme of the strand-exchange assay. The DNA substrate was assembled using the strand-annealing function of RECQ5β as depicted in Figure 2A. (B) 1 nM DNA substrate was incubated with 20 nM RECQ5β and 2 mM ATP in the absence (open circles) or the presence (filled circles) of 2 μM PCNA. PCNA was added 5 minutes prior to the addition of ATP. Reaction aliquots from different time points were analysed by non-denaturing PAGE followed by phosphorimaging. The relative concentration of the 60-mer duplex product is plotted *versus* reaction time.

Supplementary Figure S8

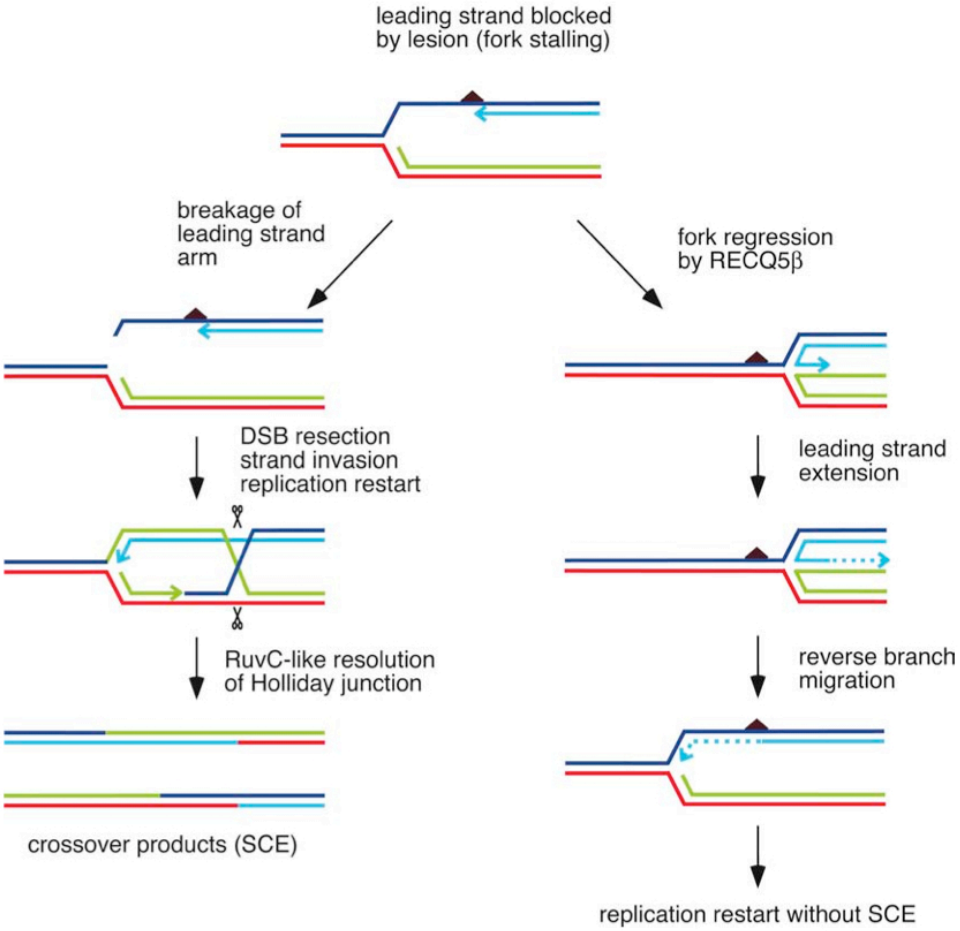

Figure S8 A model for the role of RECQ5β in suppression of mitotic recombination. A DNA lesion on the leading-strand template causes replication fork stalling. RECQ5β promotes regression of stalled replication forks, which allows template switching to the undamaged chromatid. This prevents fork breakage and subsequent recombinational repair of DSBs that can result in SCEs. For simplicity, other DNA damage tolerance pathways such as translesion synthesis or leading-strand re-priming are not shown here.

Supplementary Table 1. Oligonucleotides and schemes of DNA substrates

RK1 (60mer)	ACTATCATTCAGTCATGTAACCTAGTCAATCTGCGAGCTCGAATTCACTGGA GTGACCTC
RK2 (30mer)	ATTGACTAGGTTACATGACTGAATGATAGT
RK3 (60mer)	GAGGTCACTCCAGTGAATTCGAGCTCGCAGCCCCTCTAGGTTACATGACTGA ATGATAGT
RK4 (20mer)	ACTATCATTCAGTCATGTAA
RK5 (60mer)	GAGGTCACTCCAGTGAATTCGAGCTCGCAGTCAATGTCGACATACCTAGTAC TTTACTCC
RK6 (30mer)	GGAGTAAAGTACTAGGTATGTCGACATTGA
RK7 (30mer)	ACTATCATTCAGTCATGTAACCTAGAGGGG
Fork with heterolo-gous arms	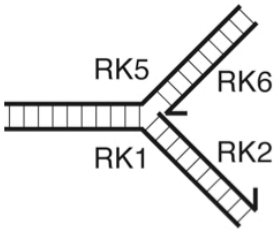
Fork with homolo-gous arms	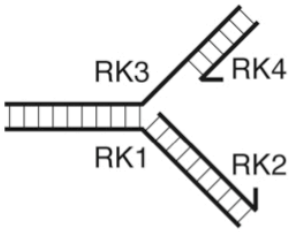

RK2 is complementary to the 5'-half of RK1. RK3 is complementary to RK1 except for the five underlined bases. RK4 is complementary to the 3'-end of RK3. The 5'-half of RK5 is complementary to the 3'-half of RK1. RK6 is complementary to the 3'-half of RK5. RK7 is complementary to the 3'-half of RK3.The polarity of the leading and lagging oligonucleotides is indicated by arrows (5'-3').

7.2. Appendix II: The zinc-binding motif of human RECQ5β suppresses the intrinsic strand-annealing activity of its DExH helicase domain and is essential for the helicase activity of the enzyme

Biochem. J. (2008) **412**, 425–433 (Printed in Great Britain) doi:10.1042/BJ20071150

The zinc-binding motif of human RECQ5β suppresses the intrinsic strand-annealing activity of its DExH helicase domain and is essential for the helicase activity of the enzyme

Hua REN*†, Shuo-Xing DOU‡, Xing-Dong ZHANG‡, Peng-Ye WANG‡, Radhakrishnan KANAGARAJ§, Jie-lin LIU*, Pavel JANSCAK§, Jin-Shan HU‖[1] and Xu Guang XI*[1]

*CNRS, UMR 2027, Institut Curie-Section de Recherche, Centre Universitaire, Bâtiment 110, F-91405 Orsay, France, †College of Life Science, East China Normal University, Science Building, 3663 North Zhongshan Road, Shanghai 200062, China, ‡Laboratory of Soft Matter Physics, Beijing National Laboratory for Condensed Matter Physics, Institute of Physics, Chinese Academy of Sciences, Beijing 100080, China, §Institute of Molecular Cancer Research, University of Zurich, Winterthurerstrasse 190, CH-8057 Zurich, Switzerland, and ‖Department of Basic Medical Sciences, College of Osteopathic Medicine of the Pacific, Western University of Health Sciences, 309 E. Second Street, Pomona, CA 91766, U.S.A.

RecQ family helicases, functioning as caretakers of genomic integrity, contain a zinc-binding motif which is highly conserved among these helicases, but does not have a substantial structural similarity with any other known zinc-finger folds. In the present study, we show that a truncated variant of the human RECQ5β helicase comprised of the conserved helicase domain only, a splice variant named RECQ5α, possesses neither ATPase nor DNA-unwinding activities, but surprisingly displays a strong strand-annealing activity. In contrast, fragments of RECQ5β including the intact zinc-binding motif, which is located immediately downstream of the helicase domain, exhibit much reduced strand-annealing activity but are proficient in DNA unwinding. Quantitative measurements indicate that the regulatory role of the zinc-binding motif is achieved by enhancing the DNA-binding affinity of the enzyme. The novel intramolecular modulation of RECQ5β catalytic activity mediated by the zinc-binding motif may represent a universal regulation mode for all RecQ family helicases.

Key words: DNA annealing, DNA unwinding, intramolecular regulation, RecQ helicase, zinc-finger motif.

INTRODUCTION

DNA helicases are molecular motors that transduce the chemical energy derived from NTP hydrolysis into a mechanical force to unwind dsDNA (double-stranded DNA) [1,2]. Therefore helicases display both DNA-stimulated ATPase and ATP-dependent helicase activities. Structural studies revealed that helicases from SF1 and SF2 (superfamily 1 and 2) contain a structural module that consists of two RecA-related domains [3,4]. Residues involved in ATP binding/hydrolysis and DNA binding are located in the cleft separating the two RecA-like domains. It is postulated that these domains serve as a DNA translocation motor [4].

The RecQ family DNA helicase are highly conserved from bacteria to man and play essential roles in the maintenance of genomic stability [5–8]. In humans, five RecQ family members, namely RECQ1 [9,10], BLM [11], WRN [12], RECQ4 [13] and RECQ5 [14], have been identified. Defects in BLM, WRN and RECQ4 lead to human hereditary disorders: BS (Bloom syndrome), WRN (Werner syndrome) and RTS (Rothmund–Thompson syndrome) respectively, that are characterized by genome instability and cancer predisposition [15]. In addition to the highly conserved DExH helicase domain containing seven helicase motifs, most RecQ family helicases contain a unique RQC (RecQ conserved) domain which is composed of a zinc-binding motif and a WH (winged helix-turn-helix) motif [16,17]. RecQ helicase activity is highly regulated not only through intermolecular protein–protein interactions [18], but also through intramolecular interactions between different domains [19]. In the present study, we have chosen the human RECQ5 protein as a model to study the functional modulation of the DExH-helicase core by the zinc-binding domain. The striking feature of human RECQ5 is that it exists in three different isoforms, namely RECQ5α, RECQ5β and RECQ5γ, which result from alternative splicing of the RECQ5 transcript [14,20]. The three proteins are identical within the N-terminal region of 410 residues which constitutes the helicase domain with the conserved set of seven helicase motifs (see Supplementary Figure S1 at http://www.BiochemJ.org/bj/412/bj4120425add.htm). RECQ5α is the shortest variant including only the helicase domain (410 amino acids). RECQ5β contains the helicase domain and a putative RQC domain, which is followed by a long C-terminal region that shows no homology with the other RecQ helicases. RECQ5γ includes the helicase domain followed by a C-terminal extension of 25 amino acids that is not present in RECQ5β. At present, only RECQ5β has been biochemically characterized [21]. It possesses both DNA-unwinding and DNA strand-annealing activities [21]. In addition, RECQ5β has been shown to promote strand exchange on forked DNA structures [22]. However, the molecular mechanism that underlies the co-ordination of DNA-unwinding and strand-annealing activities of RECQ5β remains largely elusive.

The RECQ5α and RECQ5β proteins offer an attractive model system to characterize the enzymatic activities of a RecQ helicase domain in isolation and in association with other sub-domains on the same polypeptide. This unique property allows us to address some interesting and important questions that have not yet been resolved with any DNA helicase. These questions include: (i) is the helicase domain sufficient to catalyse dsDNA separation; (ii) does the helicase domain have an intrinsic strand-annealing activity as suggested by its structural similarity to the strand-exchange protein RecA; (iii) what is the role of the accessory

Abbreviations used: p[NH]ppa, adenosine 5′-[β,γ-imido]triphosphate; ATP[S], adenosine 5′-[γ-thio]triphosphate; dsDNA, double-stranded DNA; DTT, dithiothreitol; FRET, fluorescence resonance energy transfer; mantATP, 2′(3′)-*O*-(*N*-methylanthraniloyl) adenosine-5′-triphosphate; PAR, 4-(2-pyridylazo)resorcinol; RPA, replication protein A; RQC, RecQ conserved; SF, superfamily; ssDNA, single-stranded DNA.

[1] Correspondence may be addressed to either of these authors (email jshu@westernu.edu or xu-guang.xi@curie.u-psud.fr).

domains, namely the zinc-binding domain, in the helicase activity of the enzyme. In the present study, we found that the helicase domain of RECQ5 does not possess DNA-unwinding capability, but exhibits an intrinsic strand-annealing activity. More importantly, the zinc-binding motif is found to act as a molecular switch that suppresses the strand-annealing activity of the helicase domain and triggers DNA-unwinding activity through modulating DNA binding.

MATERIALS AND METHODS

Proteins and DNA substrates

The human RECQ5α and RECQ5β proteins were produced as C-terminal fusions with a self-cleaving chitin-binding domain and purified as described previously [21]. The truncation mutants of RECQ5β were amplified by PCR and cloned into pET15b as N-terminal fusions with a hexahistidine tag. The resulting plasmids were transformed into the *Escherichia coli* strain BL21-codonPlus (Stratagene). The cells were grown to the mid-exponential phase (A_{600} of 0.5–0.6) at 37 °C and the protein expression was induced by 0.25 mM IPTG (isopropyl β-D-thiogalactoside) at 15 °C for 18 h. The cells were lysed in buffer containing 50 mM Tris/HCl (pH 7.5), 500 mM NaCl, 0.1 % Triton X-100, 0.1 μM PMSF and 10 % ethylene glycol. The cell lysate was clarified by centrifugation (23 000 ***g*** for 45 min at 4 °C) and the supernatant was applied to a 20 ml Ni^{2+}-column connected to an ÄKTA FPLC system. The bound proteins were eluted with a linear gradient of imidazole (0.02–0.4 M; 300 ml). Fractions containing the proteins of interest were identified by SDS/PAGE (see Supplementary Figure S2 at http://www.BiochemJ.org/bj/412/bj4120425add.htm). Proteins were further purified using size-exclusion chromatography (Superdex 200, Amersham). Human RPA (replication protein A) was produced and purified according to a procedure described previously [23].

PAGE-purified DNA oligonucleotides (see Supplementary Table S1 at http://www.BiochemJ.org/bj/412/bj4120425add.htm) were purchased from Proligo. The DNA duplex substrates were prepared as described previously [24]. Briefly, 250 μM component oligonucleotides were denatured in the 1 × TE buffer [10 mM Tris/HCl (pH 7.5) and 1 mM EDTA] containing 1 M NaCl or KCl by heating at 95 °C for 10 min. The denatured DNA was then annealed at 37 °C for 48 h. The annealed products were separated on native-PAGE (8 % gel) containing 10 mM KCl run at 4 °C for 12 h with a constant current of 20 mA.

Quantification of protein-bound Zn^{2+} ions

Protein-bound Zn^{2+} ion was measured using PAR [4-(2-pyridylazo)resorcinol], a reporter dye that absorbs light at 490 nm when bound to Zn^{2+}. To precisely quantify the Zn^{2+} content, all buffers were treated with Chelex®-100 resin (Bio-Rad). The proteins were dialysed against the EDTA-free Chelex®-treated buffer, passed over a 10-cm column of Chelex®-100 and re-concentrated. To facilitate the Zn^{2+} release, the protein (approx. 1 nmol in 40 μl) was first denatured with Chelex®-treated 7 M guanidine/HCl, and then transferred to a 1 ml cuvette. PAR was added to the cuvette to a final concentration of 100 μM and the volume was adjusted to 1 ml with PAR buffer containing 20 mM Tris/HCl (pH 8.0) and 150 mM NaCl. The absorbance was recorded from 300 to 600 nm on an UVIKON spectrophotometer 941 (Kontron) at 25 °C. The quantity of Zn^{2+} was determined using the absorbance coefficient for the Zn $(PAR)_2$ complex ($\varepsilon_{500} = 6.6 \times 10^4\ M^{-1} \cdot cm^{-1}$). As a control, 20 nmol of the pure $ZnCl_2$ was quantified under identical conditions.

ATP-binding assay

mantATP [2′(3′)-*O*-(*N*-methylanthraniloyl) adenosine-5′-triphosphate], a fluorescent nucleotide analogue of ATP, was used to determine the apparent dissociation constant for ATP binding by RECQ5 proteins. For that purpose, the fluorescence spectra of the proteins at a concentration of 0.5 μM were first measured using a FluoroMax-2 spectrofluorimeter (Jobin Yvon, Spex Instruments S.A.) at 25 °C in a 10 mm × 10 mm × 40 mm quartz cuvette. The proteins were excited at 280 nm and their intrinsic fluorescence emission near 350 nm was monitored. This measurement was useful for confirming the overlap of the fluorescence emission spectra of the proteins and the excitation spectrum of mantATP near 350 nm. When excited at 280 nm, this overlap would result in, due to FRET (fluorescence resonance energy transfer), an enhancement of the emission of mantATP at 440 nm after its binding to the proteins.

The mantATP-binding assay was performed using a Bio-Logic auto-titrator (TCU-250) and a Bio-Logic optical system (MOS450/AF-CD) in fluorescence mode. Various amounts of mantATP were added to 1 ml of binding buffer [20 mM Tris/HCl, 50 mM NaCl, 1 mM $MgCl_2$ and 0.1 mM DTT (dithiothreitol)] containing 0.5 μM protein. After 1 min incubation, fluorescence at 440 nm was measured. Titrations were performed in a temperature-controlled cuvette at 25 °C. The solution was stirred continuously using a magnetic stir bar during the whole titration process. The apparent dissociation constant K_d was determined by fitting the fluorescence intensity at 440 nm (corrected for the inner filter effect) with eqn (1):

$$F = F_s c_d + f_d x + f_c \times \frac{(x + 0.5c_d + K_d) - \sqrt{(x + 0.5c_d + K_d)^2 - 4 \times 0.5c_d \times x}}{2} \quad (1)$$

where F_s is the starting fluorescence of the reaction mixture, f_d is the fluorescence coefficient of free mantATP, f_c is the fluorescence coefficient of the complex formed and x is the total concentration of mantATP. $c_d = V_0/(V_0 + V_i) \equiv 1 - x/[\text{mantATP}]$ is included to correct accurately for the sample dilution effect, where V_0 is the initial sample volume, V_i is the volume of titrant added and [mantATP] is the mantATP concentration of the titrant.

ATPase assay

The ATPase activity of the RECQ5 proteins was determined by measuring the concentration of P_i produced by ATP hydrolysis [25]. The reaction was carried out in ATPase reaction buffer [50 mM Tris/HCl (pH 8.0), 3 mM $MgCl_2$ and 0.5 mM DTT] at 37 °C in a volume of 100 μl. The reactions were initiated by the addition of enzyme into a reaction mixture containing 1.5 μM heat-denatured Hind III-cut pGEM-7Zf linear DNA and the mixture of ATP and [γ-^{32}P]ATP. The reaction was stopped by adding 0.2 ml of stopping buffer consisting of 8.1 mM ammonium molybdate and 0.8 M HCl. The liberated $^{32}P_i$ was extracted with a solution of 2-butanol/benzene/acetone/ammonium molybdate (750:750:15:1) saturated with water. An aliquot of 60 μl was removed from the organic phase and the radioactivity was quantified using a liquid-scintillation counter.

DNA-binding assays

DNA binding of RECQ5 proteins was analysed using a fluorescence polarization anisotropy assay as described previously

[24]. The DNA-binding assay was performed using the Bio-Logic auto-titrator (TCU-250) and the Bio-Logic optical system (MOS450/AF-CD) in fluorescence anisotropy mode. Various amounts of proteins were added to 1 ml of binding buffer (as above) containing 1 nM DNA substrate. After 1 min incubation, the fluorescence polarization anisotropy was measured. The temperature was controlled at 25 °C and the solution was stirred continuously during the whole titration process. The equilibrium dissociation constant was determined by fitting the data to the Michaelis–Menten or Hill equation using the program KaleidaGraph (Synergy Software).

DNA helicase assays

DNA-unwinding reactions were carried out at 37 °C in 20 μl of the mixture containing 25 mM Hepes/NaOH (pH 7.5), 25 mM NaOAc, 7.5 mM $Mg(OAc)_2$, 2 mM ATP, 1 mM DTT and 0.1 mg/ml BSA, and indicated ^{32}P-labelled partial DNA duplex substrate (10 fmol, 3000 c.p.m/fmol). Where required, RPA was added at the indicated concentration. The reaction was initiated by addition of the indicated concentration of the RECQ5 protein and incubated at 37 °C for 30 min. Reactions were terminated by the addition of 5 μl of 5 × loading buffer (50 mM EDTA, 0.5 % SDS, 0.1 % xylene cyanol, 0.1 % Bromophenol Blue and 50 % glycerol). The reaction products were resolved on PAGE [12 % (w/v) gel] run in TBE buffer [90 mM Tris, 90 mM boric acid (pH 8.3) and 1 mM EDTA] at 100 V for 2 h at 4 °C. Radiolabelled species were visualized using a Storm 860 Phosphoimager (Amersham Biosciences).

A stopped-flow DNA-unwinding assay was performed according to Zhang et al. [26]. Briefly, the experiment was carried out using a Bio-logic SFM-400 mixer with a 1.5 mm × 1.5 mm cell (Bio-Logic, FC-15) and a Bio-Logic MOS450/AF-CD optical system equipped with a 150 W mercury–xenon lamp. Fluorescein was excited at 492 nm, and its emission was monitored at 525 nm. The unwinding assay was performed in a two-syringe-mixing mode, where the protein and dsDNA substrates were pre-incubated in syringe #1 for 5 min, while ATP was present in syringe #4. Both syringes contained the unwinding reaction buffer [25 mM Tris/HCl (pH 7.5), 50 mM NaCl, 1 mM $MgCl_2$ and 0.1 mM DTT]. The unwinding reaction was initiated by a rapid mixing of the contents of the two syringes. The dsDNA substrates had both strands labelled with fluorescein and hexachlorofluorescein respectively, and their sequences are listed in Supplementary Table S1. During the unwinding process, the fluorescein emission signal at 525 nm was enhanced due to the loss of FRET, i.e. the separation of the two dye molecules on the two ssDNA (single-stranded DNA). For converting the output signal change from volts into percentage of unwinding, a calibration experiment was performed in a four-syringe-mixing mode, where there was the helicase in syringe #1, hexachlorofluorescein-labelled ssDNA in syringe #2, fluorescein-labelled ssDNA in syringe #3 and ATP in syringe #4, all incubated in unwinding reaction buffer. The fluorescent signal of the mixed solution from the four syringes corresponded to 100 % unwinding. The standard reaction was carried out at 25 °C.

DNA strand-annealing assay

The DNA-annealing activity of the RECQ5 isoforms was assayed using complementary synthetic oligonucleotides (0.5 nM) with one strand 5′-end labelled using [γ-^{32}P]ATP and T4 polynucleotide kinase. In this assay, the labelled oligonuclotide was added to reaction buffer (20 μl) containing 20 mM Tris/acetate (pH 7.9), 50 mM KOAc, 10 mM $Mg(OAc)_2$, 1 mM DTT and 50 μg/ml BSA and the indicated protein concentration. Where required, ATP, ATP[S] (adenosine 5′-[γ-thio]triphosphate), p[NH]ppA (adenosine 5′-[β,γ-imido]triphosphate) or ADP were also added to a final concentration of 2 mM. The reaction was initiated by adding the unlabelled oligonuclotide and incubated at 37 °C for 30 min. The resulting DNA products were analysed as described for the helicase reactions.

The stopped-flow DNA strand-annealing assay was carried out under similar conditions as the helicase assay. The reaction was performed in a three-syringe-mixing mode, where the helicase was in syringe #1 while fluorescein- and hexachlorofluorescein-labelled complementary ssDNA were in syringe #2 and syringe #3 respectively, in buffer containing 25 mM Tris/HCl (pH 7.5), 50 mM NaCl, 1 mM $MgCl_2$ and 0.1 mM DTT. The sequences of the two 45-mer ssDNA substrates are indicated in Supplementary Table S1. The reaction was initiated by rapidly mixing the contents of the three syringes. During the annealing process, the fluorescein emission signal at 525 nm was reduced due to FRET from fluorescein to hexachlorofluorescein on the two ssDNA. For converting the output signal change from volts into percentage of annealing, we performed another experiment in a two-syringe-mixing mode, where the helicase was in syringe #1 and the annealed dsDNA was in syringe #4, both in the same buffer as indicated above. The fluorescent signal of the mixed solution from the two syringes corresponded to 100 % annealing. The reaction was carried out 25 °C.

RESULTS AND DISCUSSION

RECQ5 helicase domain alone catalyses strand annealing, but not strand separation

To analyse the function of an isolated helicase domain of RecQ DNA helicases, we investigated the biochemical properties of the human RECQ5α protein. We first compared the unwinding activities of RECQ5α and RECQ5β using a gel-shift-based helicase assay. The results showed that RECQ5β efficiently unwound a partial DNA duplex in a dose-dependent manner, whereas RECQ5α displayed hardly any detectable helicase activity (Figure 1A), even in the presence of human RPA (results not shown), which was reported to stimulate RECQ5β-mediated DNA unwinding [21]. To confirm this result, we employed a FRET-based helicase assay, which allowed the helicase-mediated DNA unwinding to be monitored in real-time in a stop-flow experiment [26]. Consistent with earlier studies, RECQ5α displayed non-detectable helicase activity, whereas RECQ5β unwound the DNA substrate efficiently (Figure 1B). Under multiple-turnover conditions, the unwinding kinetics of RECQ5β was biphasic. The fitting using a sum of two exponential terms gave two rate constants of 4.54 and 0.84 min^{-1} for the fast and slow phases respectively (Figure 1B and Table 1).

Next, we tested RECQ5α and RECQ5β for the ability to promote strand-annealing using two complementary 50-mer oligonucleotides. Remarkably, RECQ5α was found to promote strand annealing as efficiently as RECQ5β (Figure 2A). This result was rather surprising, since the strand-annealing activity of RECQ5β was previously shown to reside in the C-terminal portion of the RECQ5β polypeptide [21]. We then examined the effect of ATP on the annealing activities of the RECQ5 proteins. Consistent with previously published results [21], we found that ATP had no effect on the annealing activity of RECQ5β, whereas ATP[S], a poorly hydrolysable analogue of ATP, dramatically suppressed this reaction (Figure 2B, lanes 2 and 3). In contrast, ATP dramatically inhibited the annealing activity of RECQ5α as it did ATP[S] (Figure 2B, lanes 8 and 9). We also examined the effect of ADP on the strand-annealing activities of RECQ5α and RECQ5β.

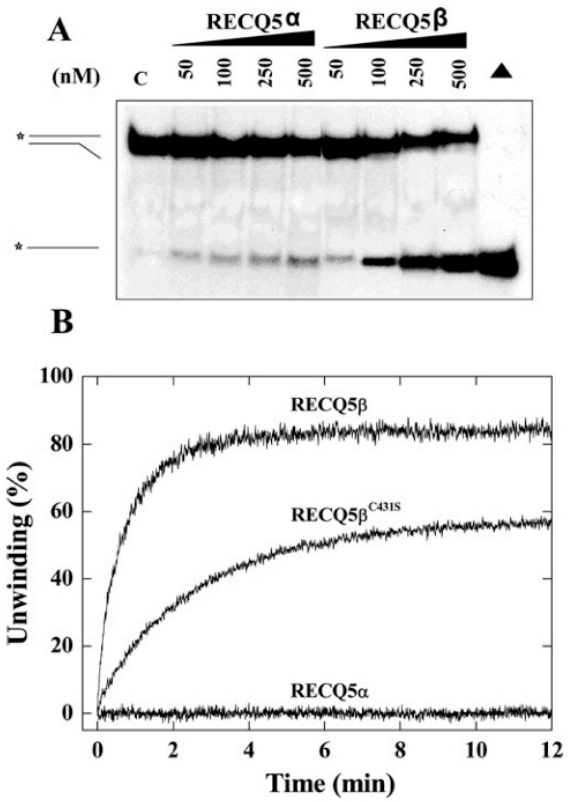

Figure 1 Helicase assays of RECQ5α and RECQ5β

(**A**) Gel-based assay of DNA unwinding using 0.5 nM 5′-^{32}P-labelled 23-base DNA duplex (UA/UB). Reactions were carried out at 37 °C for 30 min under conditions as described in the Materials and methods section. The reaction products were analysed by non-denaturing PAGE (12 % gels). (**B**) Stopped-flow DNA-unwinding assay. As described in the Materials and methods section, 1 nM 56:16-mer DNA substrate (UFA/UFB) was pre-incubated with 20 nM helicase for 5 min at 25 °C. The unwinding reaction was initiated by mixing with 1 mM ATP. The increase of the fluorescence signal of fluorescein at 525 nm (excited at 492 nm) during unwinding was monitored. The fraction of DNA unwound was obtained by normalization of the fluorescence signal F using the value F_{max} as obtained from the calibration measurement that corresponded to 100 % unwinding (see the Materials and methods section), i.e. fraction unwound $= (F - F_s)/(F_{max} - F_s)$, where F_s is the fluorescence signal at the start of unwinding.

We found that ADP partially inhibited the annealing activity of RECQ5β, but had no effect on the annealing activity of RECQ5α (Figure 2B, lanes 4 and 10). Since previous studies showed that RPA efficiently inhibited the strand-annealing activities of RECQ5β and RECQ1 [21,27], we also tested the effect of this single-strand binding protein on the strand-annealing activity of RECQ5α. We found that, similar to RECQ5β, RECQ5α-mediated strand-annealing activity was inhibited by RPA in a dose-dependent manner (Figure 2C). To quantitatively compare the DNA-annealing kinetics of the RECQ5 isoforms, a FRET-based assay was used, which was essentially identical with the stop-flow helicase assay described above. The only difference was that the annealing assay monitored the decrease, instead of the increase, in the fluorescence emission due to FRET (Figure 2D). The measured annealing reaction rates were 0.95 min^{-1} and 0.14 min^{-1} for RECQ5β and RECQ5α respectively. Thus RECQ5β promoted strand annealing approx. 7-fold faster than RECQ5α (Figure 2E). However, when evaluated by the extent of annealing, RECQ5α was more active than RECQ5β (Figure 2E and Table 1).

In order to understand the molecular basis of the RECQ5α-mediated strand annealing, we studied the quaternary structure of RECQ5α in the absence and in the presence of ATP and/or ssDNA by means of size-exclusion chromatography on a Superdex™ 75 column. These experiments (see Supplementary Table S2 at http://www.BiochemJ.org/bj/412/bj4120425add.htm) revealed an apparent molecular mass of 40 ~ 70 kDa at all conditions tested, indicating that RECQ5α promotes strand annealing as a monomer (the predicted molecular mass of monomeric RECQ5α is 46.3 kDa).

The RECQ5 helicase domain binds ATP efficiently, but displays a poor ATPase activity

To understand why RECQ5α does not catalyse DNA unwinding, we analysed its ATP-binding and ATPase activities relative to RECQ5β. To quantify ATP-binding of RECQ5α and RECQ5β, mantATP, a fluorescent analogue of ATP, was used. The apparent dissociation constants (K_d) measured were 48.4 ± 2.5 and 51.0 ± 4.9 μM for RECQ5α and RECQ5β respectively (Figure 3A and Table 1), indicating that the two isoforms bind ATP with a similar affinity.

The ATPase activities of the RECQ5 proteins were determined by measuring the release of inorganic $^{32}P_i$ from ATP in the presence of denatured dsDNA (2.9 kb) (Figure 3B). In agreement with previously published results [21], RECQ5β was found to

Table 1 Summary of the measured parameters for RECQ5 isoforms and mutants

					Helicase activity		DNA binding	
Protein	[Zn^{2+}]/[P]	ATP binding K_d (μM)	Annealing (%)	ATPase k_{cat} (s^{-1})	%	k_{obs} (min^{-1})	K_d for ssDNA (nM)	K_d for dsDNA (nM)
RECQ5α	0.03 ± 0.02	48.4 ± 2.5	95.2 ± 8.6	ND	ND	ND	1.0 × 10^6 ± 219[2]	1.8 × 10^6 ± 267[2]
RECQ5β	0.98 ± 0.18	51.0 ± 4.9	57.3 ± 5.6	15.6 ± 1.4	84.1 ± 3.5	4.54 and 0.84[1]	46.6 ± 2.5	59.3 ± 2.0
RECQ5β^{C431S}	0.35 ± 0.12		78.6 ± 3.5	4.8 ± 0.6	58.3 ± 2.8	0.50 and 0.03[1]	67.5 ± 12.1	201 ± 23.4
RECQ5β^{1-475}	0.96 ± 0.11		25.5 ± 6.5	14.8 ± 1.1	90.3 ± 4.9	5.03 and 0.87[1]	64.2 ± 5.4	79.8 ± 2.4
RECQ5β^{1-662}	1.02 ± 0.15		55.3 ± 10.5	16.3 ± 1.3	92.5 ± 5.6	5.65 and 0.92[1]	55.8 ± 2.5	70.3 ± 3.2
RECQ5$\beta^{379-662}$	1.01 ± 0.14						680 ± 63	149 ± 6.7
RECQ5$\beta^{454-662}$							1308 ± 116	1539 ± 32

[1] Values corresponding to the fast-rate constant and the slow-rate constant respectively.

[2] DNA-binding affinity is determined with K_d (app) = 218.2 ± 7.8 nM and Hn = 2.68 ± 0.18 for dsDNA and K_d (app) = 149.8 nM and Hn = 2.76 for ssDNA using the equation $K_d = [K_d(app)]^{(Hn)}$.

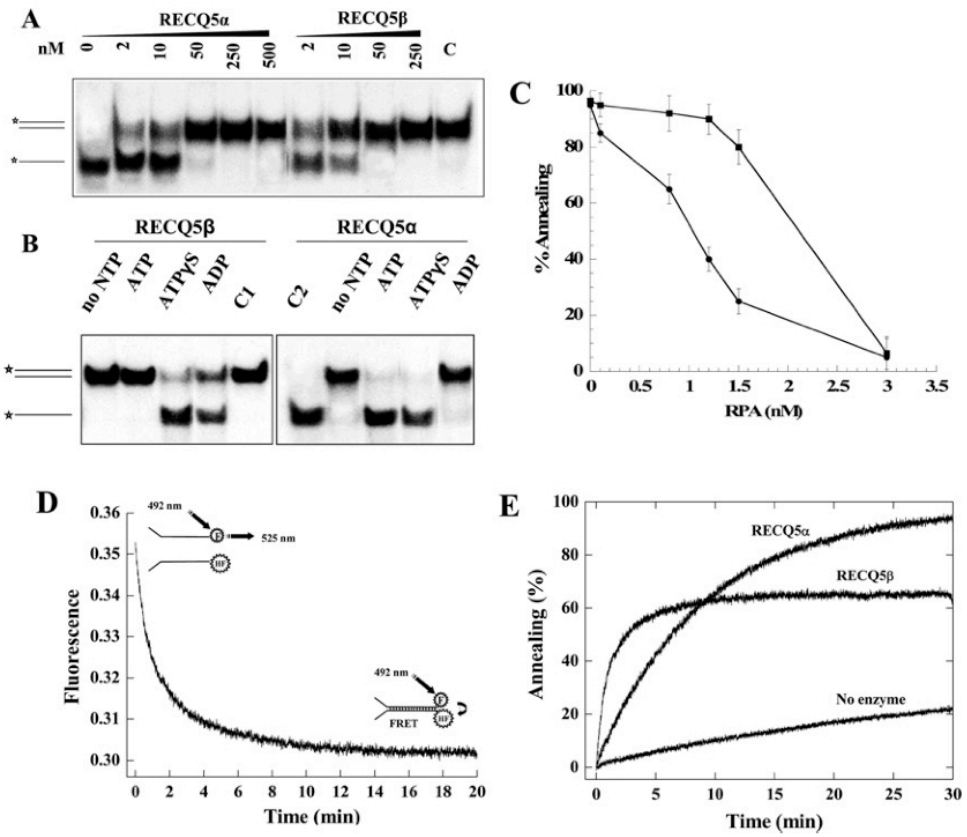

Figure 2 RECQ5-mediated ssDNA annealing

(**A**) Annealing of the 5′-^{32}P-labelled SPA (0.5 nM) and SPB ssDNA substrates by RECQ5α and RECQ5β. Reactions were incubated with the indicated protein concentrations for 30 min at 37 °C. The reaction products were separated by non-denaturing PAGE (12 % gels) and visualized by a PhosphoImager. (**B**) Effect of nucleotides on the RECQ5-mediated ssDNA annealing. The reactions contained 50 nM RECQ5α or RECQ5β and were carried out under the same conditions as in (**A**). Preformed 50 bp duplex and 50-mer ss-oligonucleotide were loaded as markers (C1 and C2 respectively). The indicated nucleotides were present at a concentration of 2 mM. (**C**) Strand-annealing activity of RECQ5α (●) and RECQ5β (■) in the presence of the increasing concentration of RPA. The complementary 50-mer oligonucleotides (0.5 nM) were incubated with or without RPA for 5 min at room temperature (25 °C). The RECQ5 proteins were added to a final concentration of 40 nM and incubation was continued at 37 °C for 20 min. Reaction products were analysed as in (**A**) and quantified using ImageQuant software. The results are the average of three independent experiments. (**D**) FRET-based ssDNA-annealing assay. The annealing was measured by monitoring the decrease in fluorescence at 525 nm caused by FRET between fluorescein and hexachlorofluorescein labels on the oligonuclotide substrates as indicated. The reaction mixture contained 0.5 nM fluorescein-labelled SPFA DNA, 0.5 nM hexachlorofluorescein-labelled complementary SPFB DNA and 30 nM RECQ5β. (**E**) Time course of ssDNA annealing by RECQ5α and RECQ5β proteins measured by the assay in (**C**). Proteins were present at a concentration of 30 nM. The fraction of annealed DNA (Table 1) was obtained by normalization of fluorescence signal F using the value F_{min} as obtained from the calibration measurement that corresponded to 100 % annealing (see the Materials and methods section), i.e. fraction annealed $= (F_s - F)/(F_s - F_{min})$, where F_s is the fluorescence signal at the start of annealing.

exhibit a robust ATPase activity, with a k_{cat} of 15.6 ± 1.4 s^{-1}. However, under identical conditions, RECQ5α had no measurable ATPase activity (Figure 3B and Table 1). These data indicate that the inability of RECQ5α to unwind DNA is caused by its failure to hydrolyse ATP. Moreover, these results provide an explanation for the differential effect of ATP on the strand-annealing activities of RECQ5α and RECQ5β (Figure 2B). As RECQ5α cannot hydrolyse ATP, it would persist in ATP-bound form, which is not proficient in strand annealing [21]. In the case of RECQ5β, this inhibitory effect can be seen only with poorly hydrolysable ATP[S].

A zinc-binding motif is essential for the helicase activity of RECQ5β

The observation that the isolated helicase domain of RECQ5β failed to unwind dsDNA suggested a role for a C-terminal part of RECQ5β in performing its helicase function. Therefore C-terminal truncation mutants of RECQ5β, including RECQ5β^{1-475} and RECQ5β^{1-662}, were assayed to identify the C-terminal region responsible for the intramolecular stimulation of the helicase activity of RECQ5β. We found that these two mutants had essentially identical ATPase and DNA-unwinding activities with respect to the full-length RECQ5β protein (Figure 3B and Table 1). Together, these observations suggest that the region of RECQ5β spanning amino acid residues 410–475 that constitute the putative zinc-binding domain (Figure 4A) play an essential role in the ATPase and helicase activities of the enzyme. Molecular modelling of the zinc-binding motif of RECQ5β revealed the distances between the cysteine side-chain sulfur groups and the zinc atom for Cys^{411} [2.46 Å (1 Å = 0.1 nm)], Cys^{427} (2.36 Å), Cys^{431} (2.42 Å) and Cys^{434} (2.39 Å)] are close to the ideal distance (2.35 ± 0.09 Å) for structural metal zinc-co-ordination sites [28]

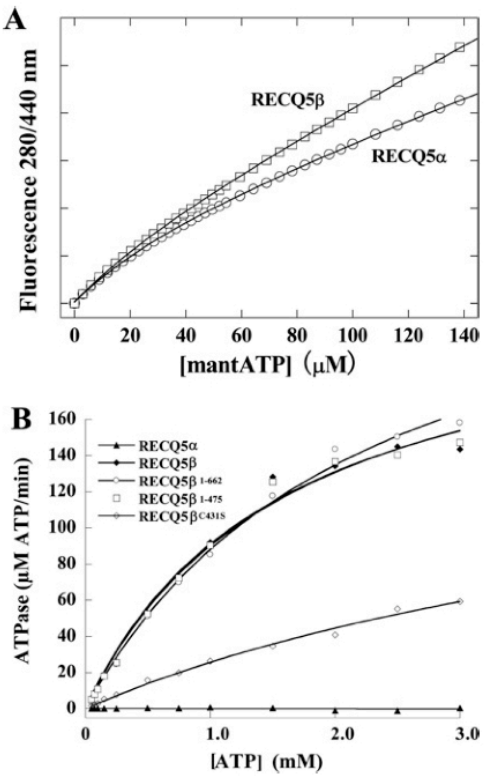

Figure 3 ATP-binding affinity and ATPase activity of RECQ5 proteins

(**A**) Changes in fluorescence intensity at 440 nm as 0.5 μM RECQ5α and RECQ5β, were titrated with an increasing concentration of mantATP. Solid lines represent the best fit of the data to eqn (1). Apparent K_d values are summarized in Table 1. (**B**) ATPase activities of wild-type and mutant RECQ5 proteins. The initial rate of ATP hydrolysis by RECQ5 proteins is plotted as a function of the ATP concentration. Reactions contained 250 nM RECQ5 protein and 1.5 μM heated dsDNA and were carried out as described in the Materials and methods section. The lines in the graph correspond to the best fits by Michaelis–Menten equation: $V = V_{max}[ATP]/(K_m + [ATP])$, where V is the initial reaction rate, [ATP] is the concentration of ATP and k_m is the Michaelis–Menten constant. Each value represents the mean of at least three independent measurements.

(Figure 4B). In agreement with this prediction, using a PAR assay, we found that RECQ5β contains 0.98 ± 0.18 mol of Zn^{2+} ion (Figure 4C and Table 1). Similar results were obtained for RECQ5β^{1-475} and RECQ5β^{1-662} deletion mutants (Table 1). In contrast, the PAR assay indicated that RECQ5α did not contain any Zn^{2+} ion, with a measured Zn^{2+} value of 0.03 ± 0.02 (Table 1).

To evaluate further the role of the zinc-binding motif in the helicase function of RECQ5β, we generated a panel of mutants in which one or more of the four conserved cysteine residues were replaced by serine residues. However, these mutant proteins either formed aggregates or were degraded except for the C431S mutant, which was subjected to biochemical analysis. We found that the replacement of Cys^{431} with serine reduced the protein-bound Zn^{2+} to 0.35 ± 0.12 mol (Table 1). Accordingly, this mutant had significantly reduced ATPase and helicase activities relative to wild-type RECQ5β (Figures 1B and 3B, and Table 1). Taken together, these results suggest that the zinc-binding motif modulates the enzymatic activity of RECQ5β: it suppresses the strand-annealing function of the helicase domain and promotes strand separation.

Molecular mechanism of intramolecular stimulation of the helicase activity of RECQ5 by the zinc-binding motif

In order to understand the molecular mechanism underlying the essential role of the zinc-binding motif in the helicase activity of RECQ5β, we compared the DNA-binding properties of RECQ5α and RECQ5β using a fluorescence polarization assay with fluorescently labelled oligonucleotide substrates [24]. This method allows direct measurment of DNA binding in solution under equilibrium conditions. K_d values for RECQ5α and RECQ5β determined from protein titration curves indicated that RECQ5α displayed much lower binding affinities for ssDNA and dsDNA than RECQ5β (Figure 5 and Table 1).

It has been shown that ATP binding stimulates DNA binding of some helicases, which in turn triggers ATP hydrolysis [29–32]. Therefore we measured the DNA-binding activities of RECQ5 proteins in the presence of a non-hydrolysable ATP analogue, p[NH]ppA and/or ATP[S]. We found that the ssDNA-binding affinity of RECQ5β was enhanced approx. 2–3-fold in the presence of 2 mM p[NH]ppA, whereas no noticeable effect could be observed with RECQ5α, even in the presence of ATP (ATP cannot be hydrolysed by RECQ5α; results not shown). These results imply that in RECQ5α there is no co-operativity between the ATP and DNA-binding sites.

To further explore the role of the zinc-binding motif in DNA binding by RECQ5β, the RECQ5β^{1-475} and RECQ5β^{1-662} truncation mutants were assayed for their DNA-binding activities. We found that these two mutants had similar DNA-binding affinities to the wild-type RECQ5β protein, suggesting that the non-conserved C-terminal region of RECQ5β does not play a role in DNA binding by the enzyme and that the zinc-binding motif confers the DNA-binding proficiency to the RECQ5β helicase core (Figures 5A and 5B, and Table 1).

To determine whether the zinc-binding motif of RECQ5β is directly involved in DNA binding, we sought to examine the DNA-binding properties of the isolated zinc-binding domain. Our first attempts to generate a fragment including only the zinc-binding fold (RECQ5$\beta^{379-454}$) failed because this protein was found to be rapidly degraded. We then performed DNA-binding experiments with RECQ5$\beta^{379-662}$ and RECQ5$\beta^{454-662}$ that could be purified to homogeneity. We found that RECQ5$\beta^{379-662}$, which contains the intact zinc-binding motif, was bound to DNA showing a preference for dsDNA (K_d values of 149 ± 6.7 nM and 680 ± 63 nM for dsDNA and ssDNA respectively). In contrast, RECQ5$\beta^{454-662}$ with a truncated zinc-binding motif displayed hardly any detectable DNA-binding activity (Figures 5C and 5D). Together, these experiments revealed that the zinc-binding domain enhances the DNA-binding affinity of the RECQ5β helicase core through direct DNA binding.

Model for the role of the zinc-binding motif in the function of RecQ helicases

Based on the results presented above, in combination with structural information for SF2 helicases, we proposed a model for the function of the zinc-binding motif of RecQ DNA helicases in DNA unwinding (Figure 6). Crystal structures of several DNA helicases including the *E. coli* RecQ helicase core suggested that ATP is bound at the top of domain 1A, while the ssDNA substrate is bound at the bottom of domains 1A and 2A (Figure 6). Since more residues in domain 1A are implicated in DNA binding than in domain 2A, as revealed by the crystal structures of NS3 helicase [33] and DEAD-Box helicase Vasa [34], it is likely that DNA may be bound more tightly to domain 1A than to domain 2A. Consequently, the portion of DNA that is bound to domain 2A may

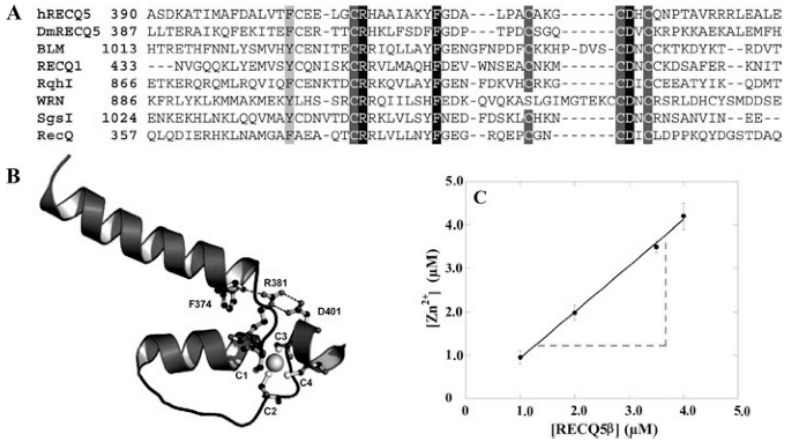

Figure 4 Identification of the zinc-binding motif of RECQ5β helicase

(**A**) Amino-acid-sequence alignment of the zinc-binding domains of RecQ family helicases. The multiple sequence alignment was performed using ClustalW software and refined manually. The conserved cysteine residue and other residues are highlighted. (**B**) Ribbon diagram showing the zinc-binding domain of the RECQ5β helicase as revealed by molecular modelling based on the crystal structure of *E. coli* RecQ. The zinc ion is shown as a sphere. The positions of the four conserved cysteine residues are labelled as C1–C4. The conserved arginine, aspartic acid and aromatic residues, involved in three very important hydrogen bonds (broken lines) that stabilize the conformation of the zinc-binding domain, are shown in ball and stick representation. (**C**) Plot of the concentration of protein-bound Zn^{2+} against RECQ5β protein concentration as determined using the PAR assay. The absorption spectra were scanned from 300 to 600 nm at 25 °C. As a control, 20 nmol of $ZnCl_2$ complexed with PAR was scanned under identical conditions.

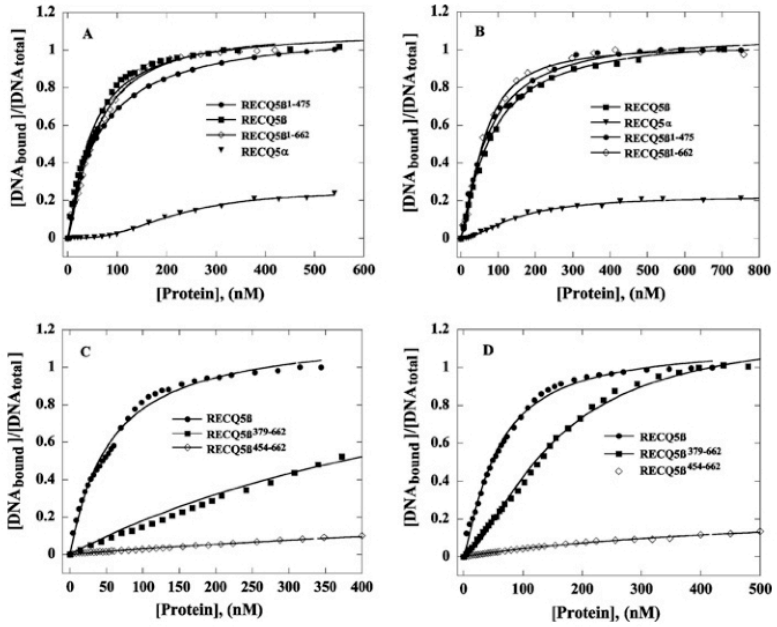

Figure 5 DNA-binding activities of wild-type and mutant RECQ5 proteins

The anisotropy-based binding isotherms were obtained by varying the protein concentration in the presence of 5 nM 3′-fluorescently labelled (**A** and **C**) ssDNA (BA) and (**B** and **D**) dsDNA (BA/BB). The data were fitted by Michaelis–Menten or Hill equations. The apparent K_d values are summarized in Table 1.

undergo large conformational fluctuation. In this case, the distance between the two helicase domains is too far to interact with each other to form the functional ATPase site that is essential for DNA unwinding. However, it is conceivable that while domain 1A binds ssDNA tightly, domain 2A can capture another ssDNA molecule. Thus RECQ5α would function as a 'molecular crowding agent' [35] that increases the effective concentrations of ssDNA substrates, thereby promoting the hybridization between complementary ssDNA molecules (Figure 6). However, in the presence of the zinc-binding motif, the double-stranded part of the DNA substrate would be tightly bound to the enzyme, enhancing the ssDNA binding to domain 2A (Figure 6). The tight binding of

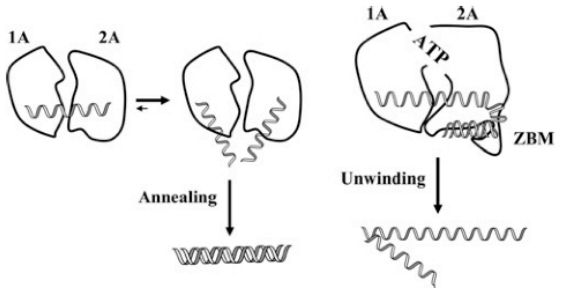

Figure 6 Model for the role of the zinc-binding motif in the function of a RecQ helicase

In the absence of the zinc-binding motif (left-hand side), the helicase domains bind ssDNA with low affinity. Although one part of the ssDNA binds relatively tightly to domain 1A, the other part of the ssDNA may dissociate from domain 2A due to thermal fluctuation, providing an opportunity for domain 2A to capture a complementary ssDNA. In this situation, RECQ5α brings the two complementary strands into close proximity, promoting the hybridization of the complementary ssDNA. In this state, although ATP is bound tightly to domain 1A, the distance between domains 1A and 2A is too long to form a functional ATPase site. In the presence of the zinc-binding motif (ZBM; right-hand side), the DNA substrate is tightly bound to the enzyme through an additional interaction between the zinc-binding motif and the duplex region of the substrate, which stabilizes ssDNA binding to the domains 1A and 2A. This tight DNA binding induces conformational changes in the protein that bring the two helicase sub-domains into a closed form, allowing ATP hydrolysis, a prerequisite for helicase function.

DNA to domains 1A and 2A, in collaboration with ATP binding, brings the domains into the closed form. In this structure, ATP is efficiently hydrolysed and the energy is coupled to DNA unwinding.

Concluding remarks

The zinc-binding motif conserved among the RecQ family helicases does not have substantial structural similarity with any other known zinc-finger folds. It is therefore important to determine its specific function in the RecQ helicase family. We have previously shown that the zinc-binding motifs of *E. coli* RecQ and human BLM are important for DNA binding and protein folding of these helicases [25,36]. Thus there is a clear correlation between the presence of the zinc-binding motif and the helicase activity of RecQ helicases. Interestingly, the human RECQ4 protein, the only RecQ family member without a zinc-binding motif, fails to unwind DNA, but catalyses DNA annealing, which is in agreement with our results obtained with RECQ5α [37]. Thus all of these studies establish the RecQ-specific zinc-binding motif as an essential DNA-binding module required for RecQ family helicase activity.

We thank Dr Pascal Rigolet (Department of Biochemistry, ENS de Cachan, France) for help with molecular modelling, Dr Robert Pansu and Dr Loussiné Zargarian (Department of Biocehmistry, ENS de Cachan, France) for assistance in the fluorescence measurements. We are grateful to Yan He (Department of Pharmacy, Guiyang Medical College, China) and Nicolas Bazeille (Section de Recerche, Institut Curie, France) for carrying out some preliminary studies. This research was supported by grants from Institut National du Cancer and La Ligue Contre Le Cancer to X.G.X.; the National Natural Science Foundation of China and the Innovation Project of the Chinese Academy of Sciences, the Swiss National Science Foundation to P.J., and the grants from the American Cancer Society (RSG-03-238-01) and the American Heart Association (0335253N) to J.-S.H.

REFERENCES

1 Lohman, T. M. and Bjornson, K. P. (1996) Mechanisms of helicase-catalyzed DNA unwinding. Annu. Rev. Biochem. **65**, 169–214
2 Soultanas, P. and Wigley, D. B. (2000) DNA helicases: 'inching forward'. Curr. Opin. Struct. Biol. **10**, 124–128
3 Caruthers, J. M. and McKay, D. B. (2002) Helicase structure and mechanism. Curr. Opin. Struct. Biol. **12**, 123–133
4 Singleton, M. R. and Wigley, D. B. (2002) Modularity and specialization in superfamily 1 and 2 helicases. J. Bacteriol. **184**, 1819–1826
5 Yamagata, K., Kato, J., Shimamoto, A., Goto, M., Furuichi, Y. and Ikeda, H. (1998) Bloom's and Werner's syndrome genes suppress hyperrecombination in yeast sgs1 mutant: implication for genomic instability in human diseases. Proc. Natl. Acad. Sci. U.S.A **95**, 8733–8738
6 Hanada, K., Ukita, T., Kohno, Y., Saito, K., Kato, J. and Ikeda, H. (1997) RecQ DNA helicase is a suppressor of illegitimate recombination in *Escherichia coli*. Proc. Natl. Acad. Sci. U.S.A. **94**, 3860–3865
7 Hickson, I. D. (2003) RecQ helicases: caretakers of the genome. Nat. Rev. Cancer **3**, 169–178
8 Mankouri, H. W. and Hickson, I. D. (2004) Understanding the roles of RecQ helicases in the maintenance of genome integrity and suppression of tumorigenesis. Biochem. Soc. Trans. **32**, 957–958
9 Puranam, K. L. and Blackshear, P. J. (1994) Cloning and characterization of RECQL, a potential human homologue of the *Escherichia coli* DNA helicase RecQ. J. Biol. Chem. **269**, 29838–29845
10 Seki, M., Miyazawa, H., Tada, S., Yanagisawa, J., Yamaoka, T., Hoshino, S., Ozawa, K., Eki, T., Nogami, M., Okumura, K. et al. (1994) Molecular cloning of cDNA encoding human DNA helicase Q1 which has homology to *Escherichia coli* Rec Q helicase and localization of the gene at chromosome 12p12. Nucleic Acids Res. **22**, 4566–4573
11 Ellis, N. A., Groden, J., Ye, T. Z., Straughen, J., Lennon, D. J., Ciocci, S., Proytcheva, M. and German, J. (1995) The Bloom's syndrome gene product is homologous to RecQ helicases. Cell **83**, 655–666.
12 Yu, C. E., Oshima, J., Fu, Y. H., Wijsman, E. M., Hisama, F., Alisch, R., Matthews, S., Nakura, J., Miki, T., Ouais, S. et al. (1996) Positional cloning of the Werner's syndrome gene. Science **272**, 258–262
13 Kitao, S., Ohsugi, I., Ichikawa, K., Goto, M., Furuichi, Y. and Shimamoto, A. (1998) Cloning of two new human helicase genes of the RecQ family: biological significance of multiple species in higher eukaryotes. Genomics **54**, 443–452
14 Shimamoto, A., Nishikawa, K., Kitao, S. and Furuichi, Y. (2000) Human RecQ5β, a large isomer of RecQ5 DNA helicase, localizes in the nucleoplasm and interacts with topoisomerases 3α and 3β. Nucleic Acids Res. **28**, 1647–1655
15 Karow, J. K., Wu, L. and Hickson, I. D. (2000) RecQ family helicases: roles in cancer and aging. Curr. Opin. Genet. Dev. **10**, 32–38
16 Morozov, V., Mushegian, A. R., Koonin, E. V. and Bork, P. (1997) A putative nucleic acid-binding domain in Bloom's and Werner's syndrome helicases. Trends Biochem. Sci. **22**, 417–418
17 Bernstein, D. A., Zittel, M. C. and Keck, J. L. (2003) High-resolution structure of the *E. coli* RecQ helicase catalytic core. EMBO J. **22**, 4910–4921
18 Bachrati, C. Z. and Hickson, I. D. (2003) RecQ helicases: suppressors of tumorigenesis and premature aging. Biochem. J. **374**, 577–606
19 Hu, J. S., Feng, H., Zeng, W., Lin, G. X. and Xi, X. G. (2005) Solution structure of a multifunctional DNA- and protein-binding motif of human Werner syndrome protein. Proc. Natl. Acad. Sci. U.S.A. **102**, 18379–18384
20 Sekelsky, J. J., Brodsky, M. H., Rubin, G. M. and Hawley, R. S. (1999) *Drosophila* and human RecQ5 exist in different isoforms generated by alternative splicing. Nucleic Acids Res. **27**, 3762–3769
21 Garcia, P. L., Liu, Y., Jiricny, J., West, S. C. and Janscak, P. (2004) Human RECQ5β, a protein with DNA helicase and strand-annealing activities in a single polypeptide. EMBO J. **23**, 2882–2891
22 Kanagaraj, R., Saydam, N., Garcia, P. L., Zheng, L. and Janscak, P. (2006) Human RECQ5β helicase promotes strand exchange on synthetic DNA structures resembling a stalled replication fork. Nucleic Acids Res. **34**, 5217–5231
23 Henricksen, L. A., Umbricht, C. B. and Wold, M. S. (1994) Recombinant replication protein A: expression, complex formation, and functional characterization. J. Biol. Chem. **269**, 11121–11132
24 Dou, S. X., Wang, P. Y., Xu, H. Q. and Xi, X. G. (2004) The DNA binding properties of the *Escherichia coli* RecQ helicase. J. Biol. Chem. **279**, 6354–6363
25 Guo, R. B., Rigolet, P., Zargarian, L., Fermandjian, S. and Xi, X. G. (2005) Structural and functional characterizations reveal the importance of a zinc binding domain in Bloom's syndrome helicase. Nucleic Acids Res. **33**, 3109–3124
26 Zhang, X. D., Dou, S. X., Xie, P., Wang, P. Y. and Xi, X. G. (2005) RecQ helicase-catalyzed DNA unwinding detected by fluorescence resonance energy transfer. Acta Biochim. Biophys. Sin. (Shanghai) **37**, 593–600
27 Sharma, S., Sommers, J. A., Choudhary, S., Faulkner, J. K., Cui, S., Andreoli, L., Muzzolini, L., Vindigni, A. and Brosh, Jr, R. M. (2005) Biochemical analysis of the DNA unwinding and strand annealing activities catalyzed by human RECQ1. J. Biol. Chem. **280**, 28072–28084

28 Alberts, I. L., Nadassy, K. and Wodak, S. J. (1998) Analysis of zinc binding sites in protein crystal structures. Protein Sci. **7**, 1700–1716
29 Wong, I. and Lohman, T. M. (1992) Allosteric effects of nucleotide cofactors on *Escherichia coli* Rep helicase-DNA binding. Science **256**, 350–355
30 Jezewska, M. J. and Bujalowski, W. (1996) Global conformational transitions in *Escherichia coli* primary replicative helicase DnaB protein induced by ATP, ADP, and single-stranded DNA binding. Multiple conformational states of the helicase hexamer. J. Biol. Chem. **271**, 4261–4265
31 Jezewska, M. J. and Bujalowski, W. (2000) Interactions of *Escherichia coli* replicative helicase PriA protein with single-stranded DNA. Biochemistry **39**, 10454–10467
32 Bujalowski, W. and Jezewska, M. J. (2000) Kinetic mechanism of nucleotide cofactor binding to *Escherichia coli* replicative helicase DnaB protein. Stopped-flow kinetic studies using fluorescent, ribose-, and base-modified nucleotide analogues. Biochemistry **39**, 2106–2122
33 Kim, J. L., Morgenstern, K. A., Griffith, J. P., Dwyer, M. D., Thomson, J. A., Murcko, M. A., Lin, C. and Caron, P. R. (1998) Hepatitis C virus NS3 RNA helicase domain with a bound oligonucleotide: the crystal structure provides insights into the mode of unwinding. Structure **6**, 89–100
34 Sengoku, T., Nureki, O., Nakamura, A., Kobayashi, S. and Yokoyama, S. (2006) Structural basis for RNA unwinding by the DEAD-box protein *Drosophila* Vasa. Cell **125**, 287–300
35 Minton, A. P. (1997) Influence of excluded volume upon macromolecular structure and associations in 'crowded' media. Curr. Opin. Biotechnol. **8**, 65–69
36 Liu, J. L., Rigolet, P., Dou, S. X., Wang, P. Y. and Xi, X. G. (2004) The zinc finger motif of *Escherichia coli* RecQ is implicated in both DNA binding and protein folding. J. Biol. Chem. **279**, 42794–42802
37 Macris, M. A., Krejci, L., Bussen, W., Shimamoto, A. and Sung, P. (2006) Biochemical characterization of the RECQ4 protein, mutated in Rothmund–Thomson syndrome. DNA Repair (Amst) **5**, 172–180

Received 21 August 2007/18 February 2008; accepted 22 February 2008
Published as BJ Immediate Publication 22 February 2008, doi:10.1042/BJ20071150

BJ www.biochemj.org

Biochem. J. (2008) **412**, 425–433 (Printed in Great Britain) doi:10.1042/BJ20071150

SUPPLEMENTARY ONLINE DATA

The zinc-binding motif of human RECQ5β suppresses the intrinsic strand-annealing activity of its DExH helicase domain and is essential for the helicase activity of the enzyme

Hua REN*†, Shuo-Xing DOU‡, Xing-Dong ZHANG‡, Peng-Ye WANG‡, Radhakrishnan KANAGARAJ§, Jie-lin LIU*, Pavel JANSCAK§, Jin-Shan HU‖[1] and Xu Guang XI*[1]

*CNRS, UMR 2027, Institut Curie-Section de Recherche, Centre Universitaire, Bâtiment 110, F-91405 Orsay, France, †College of Life Science, East China Normal University, Science Building, 3663 North Zhongshan Road, Shanghai 200062, China, ‡Laboratory of Soft Matter Physics, Beijing National Laboratory for Condensed Matter Physics, Institute of Physics, Chinese Academy of Sciences, Beijing 100080, China, §Institute of Molecular Cancer Research, University of Zurich, Winterthurerstrasse 190, CH-8057 Zurich, Switzerland, and ‖Department of Basic Medical Sciences, College of Osteopathic Medicine of the Pacific, Western University of Health Sciences, 309 E. Second Street, Pomona, CA 91766, U.S.A.

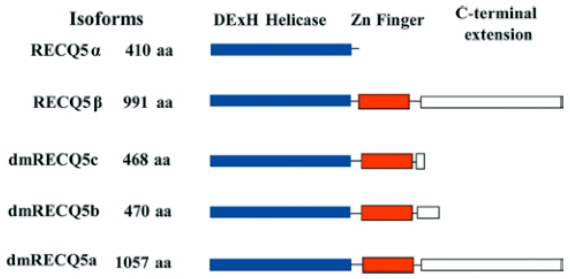

Figure S1 Schematic representation of human RECQ5α, RECQ5β and their ortholoques from *Drosophila melanogaster* (dmRECQ5a, dmRECQ5b and dmRECQ5c)

The helicase domain, zinc-binding domain and the C-terminal domain are shown as blue, red and open boxes respectively.

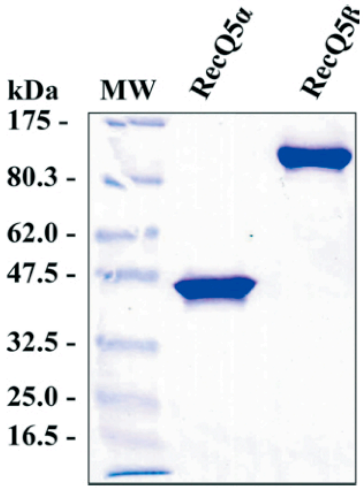

Figure S2 Coomassie-Blue-stained SDS/PAGE (10% gel) of purified RECQ5α and RECQ5β

The molecular-mass (MW) standards (in kDa) are shown on the left-hand side.

Table S1 DNA oligonucleotides used in the present study

F and H represent fluorescein and hexachlorofluoresein groups respectively.

Oligonucleotide name	Length (nucleotides)	Sequence (5′–3′)
BA	36	AATCCGTCGAGCAGAGTTAGGGTTAGGGTTAGGGTT
BB	36	AACCCTAACCCTAACCCGAAGTCTGCTCGACGGATT
UA	44	GCACTGGCCGTCGTTTTACTTGG TGACTGGGAAAACCCTGGCG
UB	44	TTTTTTTTTTTTTTTTTTTTTCCAAGTAAAACGACGGCCAGTGC
UFA	56	H-AATCCGTCGAGCAGAG (dT_{40})
UFB	16	CTCTGCTCGACGGATT-F
SPA	50	TCAAAGTCACGACCTAGACACTGCGAGCTCGAATTCACTGGAGTGACCTC
SPB	50	GAGGTCACTCCAGTGAATTCGAGCTCGCAGTGTCTAGGTCGTGACTTTGA
SPFA	45	AGATCCCTCAGACCCTTTTAGTCAGTGTGGAAAATCTCTAGCAGT-F
SPFB	45	H-ACTGCTAGAGATTTTCCACACTGACTAAAAGGGTCTGAGGGATCT
SPC	23	GCACTGGCCGTCGTTTTACTTGG

[1] Correspondence may be addressed to either of these authors (email jshu@westernu.edu or xu-guang.xi@curie.u-psud.fr).

Table S2 Summary of gel-filtration experiments

The experiments were performed using a Superdex75™ gel-filtration column run on a AKTA Purifier system (GE Healthcare). The column was equilibrated at a flow rate of 0.5 ml/min with 20 mM Tris (pH 7.5), 150 mM KCl and 1 mM DTT. When required, 2 mM $MgCl_2$, 1 mM ATP or ATP[S] were added to the elution buffer. Approx. 30 μg of recombinant RECQ5α was loaded. Proteins were detected at $A_{260/280}$. The experiments in the presence of ssDNA were performed by pre-incubating RECQ5α (2 μM) with 2-fold molar excess of oligo SPC (see Supplementary Table 1) with or without 1 mM nucleotide and 2 mM $MgCl_2$ for 20 min at 25°C. Calibration of the column was performed with the pre-mixed standard proteins of known molecular masses (Sigma).

Sample	Apparent molecular mass (kDa)
23-mer	29.8 ± 3.5
RECQ5α	42.6 ± 6.4
RECQ5α + 23-mer	93.9 ± 16.9
RECQ5α + Mg^{2+} + ATP[S]	45.9 ± 9.2
RECQ5α + Mg^{2+} + ATP[S] + 23-mer	102.5 ± 19.5

Received 21 August 2007/18 February 2008; accepted 22 February 2008
Published as BJ Immediate Publication 22 February 2008, doi:10.1042/BJ20071150

The MRE11/RAD50/NBS1 complex links RECQ5 helicase to sites of DNA damage

Lu Zheng, Radhakrishnan Kanagaraj, Boris Mihaljevic, Sybille Schwendener and

Pavel Janscak[1]

Institute of Molecular Cancer Research, University of Zurich, Winterthurerstrasse

190

CH-8057 Zurich, Switzerland

[1]corresponding author

E-mail: pjanscak@imcr.uzh.ch

Tel: +41-(0)44-635 3470

Fax: +41-(0)44-635 3484

ABSTRACT

RECQ5 DNA helicase acts as a suppressor of homologous recombination, but its exact role in DNA metabolism remains elusive. Here, we show that RECQ5 interacts physically and functionally with the MRE11/RAD50/NBS1 (MRN) complex, a nuclease that is involved in the recognition and repair of DNA double-strand breaks (DSBs). The cellular concentration of the RECQ5/MRN complex was not enhanced by DNA damage or by synchronizing cells in a particular stage of the cell cycle, suggesting a constitutive association. Experiments with purified proteins suggested that the RECQ5/MRN complex was mediated by direct binding of RECQ5 to MRE11 and NBS1. Functional assays revealed that RECQ5 strongly inhibited the 3'-5' exonuclease activity residing in the MRE11 protein. At the cellular level, the MRE11 protein was required for the recruitment of RECQ5 to sites of arrested replication forks and sites of laser-induced DSBs. Collectively, these data suggest a functional relationship between RECQ5 and the MRN complex in the cellular response to DNA damage.

INTRODUCTION

Proteins belonging to the RecQ DNA helicase family are highly conserved from bacteria to man. In humans, five RecQ homologues have been identified and named RECQ1, BLM, WRN, RECQ4 and RECQ5. Inherited defects in the genes encoding for BLM, WRN and RECQ4 have been found to cause distinct recessive disorders associated with various forms of genomic instability, premature aging and predisposition to cancer (14). Numerous biochemical and cellular studies have shown that the multiple RecQ homologues in human cells have non-redundant roles in the maintenance of genomic stability (32). Several lines of evidence suggest that BLM suppresses crossovers during homologous recombination (HR) through its unique ability to act in conjunction with DNA topoisomerase IIIα to decatenate recombination intermediates containing double Holliday junctions (39, 40). WRN acts specifically at telomeres to promote lagging-strand replication of G-rich telomeric regions, preventing telomere erosion and subsequent recombination (7, 8). RECQ4 is proposed to be important for the initiation of DNA replication by promoting the loading of replication protein A (RPA) on unwound origins (29).

The role of the human RECQ5 protein in the maintenance of genomic stability is not well understood. RECQ5 exists in at least three different isoforms resulting from alternative RNA splicing (31, 33). However, only the largest splice variant of RECQ5, named RECQ5β, localizes to the nucleus and functions as DNA helicase *in vitro* (13, 33). Like other RecQ helicases, RECQ5β can promote branch migration of Holliday junctions and exhibits strand-annealing and strand-exchange activities (13, 17). It also possesses the ability to disrupt RAD51 presynaptic filament in a reaction dependent on its ATPase activity and the presence of RPA (16). In proliferating cells, RECQ5β associates with the replication machinery and accumulates at the site of stalled replication forks (17). Hereafter RECQ5β will be referred to as RECQ5.

Mice lacking the *Recql5* gene are viable, but they are highly prone to various types of cancer (16). Recql5-deficient cells accumulate Rad51 and γ-H2AX foci and are prone to gross chromosomal rearrangements in response to replication stress (16). Moreover, Recql5-deficiency is associated with a significant increase in the frequencies of spontaneous sister-chromatid exchanges and DSB-induced HR (15, 16). These finding establish Recql5/RECQ5 as a tumor suppressor that plays a role in the control of HR, possibly through disruption of inappropriately formed Rad51 filaments (16).

The MRE11/NBS1/RAD50 (MRN) complex is an ATP-stimulated nuclease that exhibits a robust double-stranded (ds) DNA-dependent 3'-5' exonuclease activity and it can also act endonucleotically on single-stranded DNA and harpins (27, 28, 37). The nuclease domain of this

complex is located in the MRE11 subunit, while the ATP hydrolysis is mediated by the RAD50 subunit that contains a bipartite ATP binding domain split by a long repeat region that fold into an anti-parallel coiled-coil domain (1). The coiled-coil domain of RAD50 can dimerize *via* a hook structure located on the tip of this domain, which gives the MRN complex the capacity to tether DNA ends (1, 10).

The MRN complex is required for the maintenance of the integrity of DNA replication forks, DSB repair, G2/M checkpoint activation, telomere length maintenance and meiotic recombination (9). Accumulating evidence suggest that it acts as a DNA DSB sensor through its DNA-end processing activities and activates the ATM-dependent signaling pathways that co-ordinate cell cycle arrest with DNA repair (18, 19). In higher eukaryotes, null mutations in all components of the MRN complex are lethal (22, 41, 42), while hypomorphic mutations in the human *MRE11* and *NBS1* genes can give rise to Ataxia telangiectasia-like disease (ATLD) and Nijmegen breakage syndrome (NBS), respectively, that are characterized by neurological abnormalities, radiosensitivity, genomic instability and cancer predisposition (3, 24, 34).

Here we show that the RECQ5 helicase and the MRN complex constitutively interact *in vivo*. The interaction is direct and is mediated through MRE11 and possibly through NBS1. RECQ5 and the MRN complex colocalize in the nucleus in response to replication arrest and chromosomal breakage. We further show that the recruitment of RECQ5 to site of DNA damage is dependent on the presence of the MRE11 protein. Moreover, our biochemical experiments reveal that RECQ5 strongly inhibits the 3'-5' exonuclease activity associated with the MRE11 protein. Together, these data suggest that a functional relationship between RECQ5 and the MRN complex in the cellular response to DNA damage.

MATERIALS AND METHODS

Protein purification

The RECQ5 protein was produced in bacteria as fusions with self-cleaving chitin-binding domain (CBD) and purified as described previously (13). Baculoviruses expressing $(His)_6$-MRE11, $(His)_6$-NBS1 and RAD50, respectively, were a kind gift from Dr. Vilhelm Bohr. The MRN and MR complexes as well as the individual MRN subunits were produced in Sf9 cells infected with appropriate baculoviruses. Cells harvested at 72 hours after infection were suspended in buffer A [50 mM sodium phosphate (pH 7.0), 0.3 M NaCl, 0.5% Tween 20, 10% glycerol, 2 mM β-mercaptoethanol] supplemented with 20 mM imidazole and 2 mM phenylmethylsulfonylfluoride (PMSF), and disrupted by sonication. Cell extract was clarified by centrifugation at 100,000 × g

for 1 hour and loaded on a 5-ml HiTrap Chelating (Ni^{2+}) column (GE Healthcare) equilibrated with buffer A/20 mM imidazole. Bound proteins were eluted with a linear concentration gradient of imidazole (50 ml; 50 mM to 350 mM) in buffer A. Fractions containing MRN proteins were pooled, dialyzed against buffer B [20 mM Tris–HCl (pH 8.0), 100 mM NaCl, 10% glycerol and 1 mM DTT] and loaded onto a 1-ml HiTrap Q Sepharose FF column (GE Healthcare). Bound proteins were eluted with a linear concentration gradient of NaCl (12 ml; 50 mM to 500 mM) in buffer B. Rad50 was purified only on a 1-ml HiTrap Q Sepharose FF column as it was expressed without a histidine tag. Purified proteins we stored at -80°C. Protein concentration was determined using Bradford assay.

Antibodies

Rabbit polyclonal antibody against the C-terminal portion of RECQ5 (amino acids 675–991) was affinity purified as described previously (17). Additionally, the following commercially available antibodies were used in this study: mouse monoclonal anti-MRE11 antibody, clone 12D7 (Novus Biologicals), mouse monoclonal anti-RAD50 antibody, clone 13B3 (GeneTex), rabbit polyclonal anti-NBS1 antibody, ab-398 (Abcam), mouse monoclonal anti-γ–H2AX antibody, clone JBW301 (Upstate Biotechnology), rabbit polyclonal anti-TFIIH p89 antibody, sc-269 (Santacruz Biotechnology), mouse monoclonal anti-RAD51 antibody, ab1837 (Abcam) and rabbit polyclonal anti-ATM antibody (Abcam).

Cell culture and generation of DNA damage

U2OS, HeLa and 293T cells were maintained in Dulbecco modified Eagle's medium (DMEM; OmniLab) supplemented with 10% fetal calf serum (FCS; Life Technologies) and streptomycin/penicillin (100 U/ml). Immortalized ATLD1 cells transduced with retrovirus expressing the wild-type MRE11 cDNA (ATLD1-MRE11) or retrovirus harboring the empty vector were obtained from Dr. Weitzman (4) and grown in DMEM supplemented with 20% FCS, streptomycin/penicillin (100 U/ml) and 1μg/ml puromycin (Sigma-Aldrich). NBS cells stably transfected with vector containing the wild-type NBS1 cDNA (NBS-NBS1) as well as the parental NBS cells (GM7166 VA7) were obtained from Dr. Y. Shiloh (35). Cultures of NBS-NBS1 cells were supplemented with hygromycin B (100 μg/ml). If required, cells were treated with 2 mM hydroxyurea (HU) for 16 hours, 1 μM camptothecin (CPT) for 16 hours or 20 μM cis-diamminedichloroplatinum (CDDP) for 8 hours. Laser microirradiation to generate DNA DSBs in defined nuclear volumes was performed using a MMI CELCUT system containing a UVA laser of 355 nm (Molecular Machines & Industries). Prior to irradiation, cells were grown for 24 hours in the presence of 10 μM bromodeoxyuridine (BrdU). Ionizing radiation was generated using a

Faxitron X-ray system. UV irradiation (at a dose of 40 J/m^2) was performed in a UV-Stratalinker 1800 equipped with a 254 nm UV lamp (Stratagene). Immediately after exposure to radiation, cells were placed back to incubator and incubated for various periods of time as indicated. For cell cycle analyses, ethanol-fixed cells were stained with propidium iodide (20 μg/ml; Molecular Probes) and subjected to flow cytometry in a Becton Dickinson cell sorter.

RNA interference

To knock down MRE11 expression in human cells by RNA interference (RNAi), we employed short-hairpin (sh) RNA technology. The following pairs of oligonucleotides were annealed and ligated into the pSUPER vector (Oligoengine) digested with HindIII and BglII: shRNA#1-top (5'-gatcccc<u>acaggagaagagatcaact</u>ttcaagaga<u>agttgatctcttctcctgt</u>tttttggaaa-3')/shRNA#1-bottom (5'-agcttttccaaaaaacaggagaagagatcaacttctcttgaaagttgatctcttctcctgtggg-3') and shRNA#2-top (5'-gatccccgagcataactccataagtattcaagagatacttatggagttatgctcttttggaaa-3')/shRNA#2-bottom (agcttttccaaaaa<u>gagcataactccataagta</u>tctcttgaa<u>tacttatggagttatgctcggg</u>). The regions homologous to the MRE11 sequence are underlined in each oligonucleotide. For control RNAi experiments, the oligonucleotides shRNA-C-top (5'-gatccccagacgtgtacacaactagtttcaagagaactagttgtgtacacgtctttttggaaa-3') and shRNA-C-bottom (5'-agcttttccaaaaaagacgtgtacacaactagttctcttgaaactagttgtgtacacgtctggg-3') were annealed and processed as above. These oligonucleotides were designed by scrambling of the shRNA#1 sequence within the MRE11 homology region. The resulting plasmid constructs were further modified by introducing a puromycin resistance marker. To do so, the 1.4 kb BamHI/PvuI fragment of pPUR (Clontech) was ligated into the BamHI and SmaI sites of the pSUPER derivatives. The shRNA plasmids were introduced into U2OS cells by liposomal trasfection with Metafectene (Biontex) according to the manufacturer instructions. At 24 hours post transfection, cell cultures were supplemented with puromycin (2 μg/ml) to enhance the fraction of shRNA-expressing clones. Cells were usually harvested 3 days after addition of puromycin and further analyzed.

Immunofluorescence staining and analyses

Cells grown on cover slips were fixed in methanol for 30 min at -20°C, which was followed by incubation in acetone for 30 s. After blocking in PBS supplemented with 2% FCS (blocking solution), cover slips were incubated overnight at 4°C with appropriate primary antibodies [rabbit polyclonal anti-RECQ5 (1:1000), mouse monoclonal anti-RAD50 (1:200), mouse monoclonal anti-γ-H2AX (1:200); all antibodies were diluted in blocking solution]. After washing with PBS, the cells were incubated with FITC-conjugated sheep anti-rabbit (Sigma; dilution of 1:700) and Texas Red-conjugated donkey anti-mouse (Abcam; dilution of 1:200) secondary antibodies for 1

hour at room temperature. The cover slips were then mounted with Vectashield (Vector Labs) and sealed. Images were captured by an Olympus IX81 fluorescence microscope. At least 150 nuclei were analyzed in each experiment.

Immunoprecipitation assay

Cells grown in a 10 cm dish were subjected to trypsinization, harvested by centrifugation and suspended in 0.5 ml of lysis buffer [50 mM Tris–HCl (pH 8.0), 120 mM NaCl and 0.5% (v/v) NP-40] supplemented with a protease inhibitor cocktail (Complete, Mini; Roche). After a 30-minute incubation on ice, the lysate was treated with 50 U of RNase-free DNase I (Roche) at 25°C for 30 minutes, and clarified by centrifugation. In some cases, DNAse I was omitted or the lysates were supplemented with ethidium bromide (EtBr) to a final concentration of 50 μg/ml. The protein extract (1 mg of total protein) was incubated overnight at 4°C with purified rabbit anti-RECQ5 IgGs (1 μg) or with IgGs purified from pre-immune serum (1 μg). Immune complexes were subsequently incubated with protein A/G–agarose beads (20 μl, GE Healthcare) for 1 hour at 4°C. Immunoprecipitates were analyzed by Western blotting.

CBD pull-down assays

CBD-tagged RECQ5 was produced in *E. coli* BL21-CodonPlus(DE3)-RIL cells (Stratagene) and bound to chitin beads (20 μl; NEB) in NET-150 buffer [10 mM Tris (pH 8.0), 1 mM EDTA, 150 mM NaCl and 0.1% (v/v) Triton X-100]. The beads were incubated with recombinant MRN proteins (0.5–2 μg) in 400 μl of NET-150 buffer supplemented with ethidium bromide (50 μg/ml) for 2 hour at 4°C. Bound proteins were analyzed by Western blotting.

Strand exchange assays

Strand-exchange assays with RECQ5 were performed essentially as described previously (17). Briefly, reactions were carried at 37°C in buffer containing 20 mM Tris–acetate (pH 7.9), 50 mM KOAc, 10 mM $Mg(OAc)_2$, 1 mM DTT and 50 mg/ml BSA. 1 nM DNA substrates (60-mer/30-mer partial duplex and complementary 60-mer oligonucleotide, of which the former 60-mer oligonucleotide was radiolabeled at 5' end) were preincubated with 40 nM RECQ5 for 10 minutes to form a forked duplex. RECQ5-mediated strand exchange between the arms of the fork was initiated by addition of ATP (2 mM). Where required, the annealing mixture was preincubated with 40 nM MRN complex for 5 minutes prior to addition of ATP. Aliquots (5 μl) from different reaction time points were subjected to electrophoresis in 10% non-denaturing polyacrylamide gel (acrylamide/bis-acrylamide 19:1) run in 1xTBE buffer at 140 V. Gels were dried and subjected to phosphor-imaging analysis using a Typhoon 9400 scanner.

Nuclease assays

The 3'-5' exonuclease activity of the MR(N) complex was measured using a 5'-tailed oligoduplex prepared by annealing of a 30-mer oligonucleotide (5'-ggagtaaagtactaggtatgtcgacattga-3') to the 3'-half of a 60-mer oligonucletide (5'-gaggtcactccagtgaattcgagctcgcagtcaatgtcgacatacctagtactttactcc-3'). The 30-mer oligonucleotide was radiolabeled at 5'-end prior to annealing. Reactions were conducted at 37°C in buffer containing 30 mM MOPS (pH 7.0), 25 mM KCl, 1 mM DTT, 2 mM $MnCl_2$, 2 mM ATP and 50 mg/ml BSA. Reaction mixtures contained 1 nM DNA substrate, 40 nM MR(N) and varying concentrations RECQ5 or *E.coli* RecQ, ranging from 0 to 80 nM. MR(N) and RECQ5 (RecQ) were pre-incubated for 5 minutes on ice before adding to the DNA substrate. Reactions were terminated after 30 minutes by adding an equal volume of stop solution [80% (v/v) formamide, 10 mM EDTA, 0.1% (w/v) bromophenol blue and 0.1% (w/v) xylene cyanol] and heating at 95°C for 5 minutes. Reaction aliquots were subjected to electrophoresis in 15% (w/v) polyacrylamide gel containing 8 M urea (acrylamide/bis-acrylamide 19:1) run in 1x TBE buffer at 300 V. Gels were dried and subjected to phosphor-imaging analysis using a Typhoon 9400 scanner.

RESULTS

Physical interaction between RECQ5 and the MRN complex

To explore the cellular role of the human RECQ5 helicase, we employed a proteomic approach to identify proteins associated with RECQ5 *in vivo*. Specifically, we immunoprecipitated RECQ5 from the total extract of human embryonic kidney cells (HEK 293T) using an affinity-purified rabbit polyclonal anti-RECQ5 antibody and analyzed the identity of co-precipitated proteins by mass spectrometry following their separation on a SDS polyacrylamide gel. The proteins revealed by this analysis included all three components of the MRE11/RAD50/NBS1 (MRN) complex, a nuclease that functions in many aspects of DNA metabolism including DNA DSBs. To confirm this finding, the RECQ5 immunoprecipitate from 293T cells was subjected to Western blot analysis using antibodies against the individual MRN subunits. We found that this immunoprecipitate contained a large fraction of the endogenous MRN proteins, whereas the control immunoprecipitate obtained with IgG isolated from a pre-immune rabbit serum was devoid of these proteins (Figure 1A, compare lanes 1-3). The concentration of MRN proteins in the RECQ5 immunoprecipitate did not significantly change if the cell extract was pre-treated with DNaseI or ethidium bromide, indicating that the association of RECQ5 with the MRN proteins is not mediated through independent DNA binding (Figure 1A; compare lanes 3, 4 and 5). We also

performed a reciprocal co-immunoprecipitation experiment using anti-MRE11 antibody. In agreement with the above data, we found that MRE11 immunoprecipitate contained a significant amount of the RECQ5 protein in addition to RAD50 and NBS1 (Figure 1B). Collectively, these data indicate that a fraction of MRN proteins exist as a stable complex with RECQ5 *in vivo*.

Next, we compared the levels of the MRE11 protein in RECQ5 immunoprecipitates from cells exposed to various genotoxic agents including hydroxyurea (HU), ionizing radiation (IR) and cisplatin in order to evaluate the effect of DNA damage on the formation of the RECQ5/MRN complex *in vivo*. The data from this experiment indicated that the cellular level of the RECQ5/MRN complex was not affected by exogenously-induced DNA damage except for a small reduction after IR (Figure 1C). Moreover, we examined the levels of RECQ5/MRN complex at different stages of the cell cycle. To do so, U2OS cells were synchronized at G1/S transition by HU treatment and then released into drug-free medium. Cells were collected at different time points after the removal of HU and subjected to immunoprecipitation with anti-RECQ5 antibody. In a parallel experiment, cell populations from the individual time points were subjected to FACS analysis to determine the stage of the cell cycle. We found that the level of the RECQ5/MRE11 complex remained constant throughout the cell cycle, suggesting a constitutive association (Figure 1D and Supplementary Figure S1).

To determine whether RECQ5 interacts with the MRN complex directly, we performed affinity pull-down assays with purified recombinant proteins. RECQ5 was expressed in bacteria as a fusion with a chitin-binding domain (CBD) and bound to chitin beads. The beads were subsequently incubated with recombinant MRN complex produced in insect cells by means of baculovirus system. We found that purified MRN complex was avidly bound to RECQ5 beads, but not to control beads coated with the *E. coli* McrA protein fused to CBD (Figure 2A, top panel). We also tested the individual MRN subunits as well as the MR complex for binding to RECQ5-CBD-beads in order to map more closely the interaction site for RECQ5 on the MRN complex. We found that except for RAD50, all these proteins were bound to RECQ5, suggesting that the interaction of RECQ5 with the MRN complex is mediated by the MRE11 and NBS1 proteins (Figure 2A, bottom panel, and 2B).

To confirm this finding, we performed immunoprecipitation experiments with total protein extracts from NBS (NBS1-deficient) and ATLD1 (MRE11-deficient) cells. We found that the RECQ5 immunoprecipitate from NBS cells contained both MRE11 and RAD50 proteins in similar concentrations as the RECQ5 immunoprecipitate from NBS cells complemented with the NBS1 cDNA, suggesting that the formation of the RECQ5/MRN complex in the cell does not rely on the

interaction between RECQ5 and NBS1 (Figure 2C, lanes 1, 2, 5 and 6). In ATLD1 cells lacking MRE11, the levels of NBS1 and RAD50 proteins were dramatically reduced as previously reported (34). However, a small amount of NBS1 could be detected in the RECQ5 immunoprecipitate from these cells, indicating that NBS1 could interact with RECQ5 even in the absence of MRE11 inside the cell (Figure 2C, lanes 3, 4, 7 and 8). In ATLD1 cells complemented by stable transfection of the MRE11 cDNA, expression of all three MRN proteins could be readily detected by Western blot (Figure 2C, lane 4). Accordingly, the RECQ5 immunoprecipitate from total extract of these cells was found to contain substantial amounts of all three MRN proteins (Figure 2C, lane 8).

RECQ5 inhibits the 3' - 5' exonuclease activity of MRN complex

Next, we investigated whether the interaction between RECQ5 and the MRN complex affects the biochemical activities of these proteins. First we tested the effect of the MRN complex on the helicases activity of RECQ5. Previous studies demonstrated that RECQ5 displays a poor helicase activity on oligonucleotide-based partial duplexes due to a strong strand-annealing activity residing in the C-terminal half of RECQ5 (13). However, RECQ5 could efficiently displace the lagging-strand oligonucleotide from synthetic forked structures with homologous arms where re-annealing of this oligonucleotide is prevented by annealing of the parental strands (17). Thus, we evaluated the effect of the MRN complex on this strand-exchange reaction. We found that the rate of RECQ5-mediated strand-exchange was not altered upon the addition of the MRN complex, suggesting that the MRN complex does not modulate the helicase activity of RECQ5 (Figure 3A).

The MRN complex was shown to possess a robust 3'-5' exonuclease activity residing in the MRE11 protein (28, 37). We tested the effect of RECQ5 on the MRN-mediated exonucleolytic processing of a 30-bp duplex with 30-nucleotide ssDNA tail. Our initial experiments showed that the MRN complex (40 nM) required manganese and ATP as cofactors to exhibit efficient 3'-5' exonuclease activity on this DNA substrate (1nM), which is consistent with previously published data (data not shown). Addition of increasing concentrations of RECQ5 (0 - 80 nM) to this reaction resulted in a gradual decrease in the exonuclease activity of MRN with complete inhibition seen at a RECQ5 : MRN ratio of 2 (Figure 3B, lanes 3-7). This effect was not observed with the *E. coli* RecQ helicase, excluding the possibility that the inhibition of the MRE11 nuclease by RECQ5 results from competition between these proteins for the DNA substrate (Figure 3C, lanes 3-7).

To investigate whether the inhibition of the exonuclease activity of MRN by RECQ5 is dependent on the presence of the NBS1 protein, we evaluated the effect of RECQ5 on the

exonuclease activity of the MR complex. The MR complex displayed a similar exonuclease activity as the MRN complex (Figure 3 B and C, compare lanes 3). Most importantly, RECQ5, but not RecQ, was found to dramatically inhibit the MR-mediated exonucleolytic processing (Figure 3A and B, lanes 8-12).

Collectively, these data suggest that RECQ5 negatively regulates the MRN complex by attenuating its exonuclease function through direct interaction with the MRE11 protein.

RECQ5 and the MRN complex co-localize at stalled replication forks and DNA double-strand breaks

To explore the role of the RECQ5/MRN complex in the maintenance of genomic stability, we analyzed the spatial relationship of these proteins in the nucleus in response to various types of DNA damage including stalled replication forks, DNA adducts and DSBs. In these experiments we used the human osteosarcoma cell line U2OS. After individual DNA-damaging treatments, cell were fixed with methanol and immunofluorescently stained to visualize the cellular distribution of RECQ5 and RAD50 proteins by fluorescence microscopy. As expected, in majority of unperturbed cells, both RECQ5 and RAD50 were uniformly distributed in the nucleus (Figure 4A). After hydroxyurea (HU) treatment that results in replication arrest due to depletion of deoxy-ribonucleotides, both RECQ5 and RAD50 formed bright nuclear foci that extensively co-localized in more than 70% of cells (Figure 4A). RECQ5 and RAD50 also largely co-localized at nuclear foci after exposure of cells to UV light (40 J/m^2) that can stall the progression of replication forks through induction of bulky DNA lesions (Figure 4A). Thus, it is possible that the RECQ5/MRN complex operates in the processing of stalled replication forks.

To generate DSBs, U2OS cells were pre-sensitized by incorporation of BrdU into genomic DNA and then locally exposed to UVA light (355 nm) using micro-laser technology, which results in linear tracks of DSBs across each irradiated nucleus (21). These tracks can be detected by immunofluorescence imaging of phosphorylated histone H2AX (γ-H2AX) that is rapidly generated in the DSB-flanking chromatin by the ATM kinase (2). We found that RECQ5 started to accumulate at DSB tracks as early as 15 minutes after irradiation, reaching maximal levels at about 30 minutes after irradiation, and persisted at those sites as long as 1 hour after irradiation (Figure 4B, top panel). Accumulation of RECQ5 at micro-irradiated areas was seen essentially in all γ-H2AX-positive cells (150 cells evaluated in two independent experiments), suggesting that the recruitment of RECQ5 to DSBs is not restricted to any particular phase of the cell cycle. Most importantly, the tracks of RECQ5 detected at 30 minutes after laser microirradiation completely

co-localized with the tracks of RAD50 protein, suggesting that the RECQ5/MRN complex plays a role in the cellular response to DSBs (Figure 4B, bottom panel)

The MRN complex is required for the recruitment of RECQ5 to sites of DNA damage

As the MRN complex is well known to function as a DNA damage sensor, we tested the possibility that it mediates the recruitment of RECQ5 to sites of DNA damage. First, we evaluated the effect of MRE11 deficiency on the focal distribution of RECQ5 after HU treatment. To do so, we silenced the expression of the *MRE11* gene in U2OS cells using two different shRNA constructs. With both constructs, we observed a dramatic reduction in the cellular level of MRE11 protein following puromycin selection for clones expressing shRNA, whereas no reduction in MRE11 levels was observed in cells harboring a control construct expressing a scrabbled shRNA (Figure 5A). Depletion of MRE11 by shRNA also dramatically reduced the cellular level of RAD50, which is consistent with low levels of RAD50 found in ATLD1 cells (compare Figure 5A, lane 2 and Figure 2C, lane 3). Importantly, we found that shRNA-mediated depletion of MRE11 in U2OS cells completely abolished the formation of RECQ5 foci in response to HU (Figure 5B, left panel). In contrast, U2OS cells expressing the control shRNA contained both RECQ5 and RAD50 foci that showed extensive co-localization (Figure 5B, right panel). Essentially the same results were obtained with ATLD1 and ATLD1-MRE11 cells (Figure 5C).

Further, the MRE11-proficient and deficient cells were doubly stained for RECQ5 and γ-H2AX. Histone H2AX is phosphorylated in response to replication arrest in ATR-dependent manner and forms nuclear foci that colocalize with PCNA and hence can serve as markers for stalled replication forks. (20, 38). As expected, in MRE11-proficient cells treated with HU, RECQ5 extensively co-localized with γ-H2AX at bright nuclear foci (Figure 5B and C, right panels). MRE11-deficient cells also displayed γ-H2AX foci in response to HU treatment (Figure 5B and C, left panels). However, RECQ5 foci co-localizing with γ-H2AX foci were not seen in these cells (Figure 5B and C, left panels).

To evaluate whether MRE11 is required for the recruitment of RECQ5 to DSBs, we microirradiated ATLD1 cells with UVA laser and stained them for RECQ5 and γ-H2AX at 30 minutes after irradiation. Interestingly, γ-H2AX tracks were detected only in a subset of irradiated ATLD1 cells. However, accumulation of RECQ5 at irradiated areas was not seen in any of these cells (Figure 6, top panel). In contrast, in ATLD-MRE11 cells, γ-H2AX and RECQ5 tracks were seen in all irradiated cells as in the case of U2OS cells (Figure 6; top panel). Moreover, co-localization of RECQ5 and RAD50 at laser-induced damage could also be detected in ATLD1-MRE11 cells (Figure 6, bottom panel).

Together, these data strongly suggested that MRE11 is required for the recruitment of RECQ5 to stalled replication forks and DSBs.

DISCUSSION

In this work, we present several lines of evidence suggesting a functional link between the human RECQ5 helicase and the MRN complex that plays a central role in many aspects of DNA metabolism involving DSBs. We found that these proteins formed a stable complex *in vivo* and *in vitro* through direct binding of RECQ5 to MRE11 and NBS1. At the biochemical level, RECQ5 strongly inhibited the 3'-5' exonuclease activity associated with the MRE11 protein, suggesting that RECQ5 interacts with the nuclease domain of MRE11 and hence prevents its access to the DNA substrate. At the cellular level, MRE11 was required for the accumulation of RECQ5 at sites of arrested replication forks and sites of laser-induced DSBs. Base on these findings, we propose that the MRN complex recruits RECQ5 to site of DNA damage and that these proteins work together to maintain genome stability.

Several lines of evidence suggest that the MRN complex promotes genomic integrity during DNA replication. The MRN complex is associated with replicating DNA throughout S-phase through its interaction with replication protein A, which is dependent on phosphorylation of both proteins by cyclin-dependent kinases (23, 25, 26). Depletion of MRN in *Xenopus* egg extracts results in accumulation DSBs during chromosomal DNA replication and a failure in restarting collapsed replication forks (6, 36). Moreover, it has been demonstrated that MRN is present in close proximity of restarting forks and that its relocalization to restarting forks is driven by ATR/ATM dependent phosphorylation (6, 36). These findings led to a model in which MRN, via its DNA tethering activity, promotes recapture of the broken DNA molecules at collapsed forks, favoring the reassembly of new functional forks through DNA recombination events (6, 36). Evidence also suggest that MRN acts in conjunction with CtIP to mediated resection of DSBs at collapsed forks to generate 3'-ssDNA tails for HR repair (30). Mouse Recql5-deficient cells accumulate RAD51/γ-H2AX foci in S-phase, which is clearly evident upon treatment of cells with camptothecin, a potent S-phase specific DSB inducer (16). Thus, it appears that also RECQ5 plays a role in the repair of collapsed replication forks, possibly as a part of the MRN complex. Our observation of rapid MRN-dependent accumulation of RECQ5 at laser-induced DSBs is consistent with this assumption. We have previously shown that RECQ5 could displace RAD51 from single-stranded (ss)DNA in a manner dependent on its ATPase activity (16). Moreover, RECQ5 deficiency was found to be associated with a significant increase in the level of DSB induced HR

(16). Therefore, RECQ5 could regulate HR repair at collapsed forks by preventing spurious HR events. It is also possible that RECQ5 prevents formation of RAD51 filaments on ssDNA regions at stalled forks that would hamper replication restart. In agreement with the later scenario, our preliminary experiments indicated that mouse *recql5*$^{-/-}$ cells are hypersensitive to hydroxyurea and aphidicolin that cause replication arrest (unpublished observations).

Previous studies demonstrated that other human RecQ helicases, namely BLM and WRN, are also linked functionally to the MRN complex. BLM was shown to be specifically required for the correct re-localization of the MRN complex at sites of replication arrest (11). As in the case of RECQ5, the re-localization of WRN to arrested replication forks and γ-radiation-induced DSBs requires a functional MRN complex (5, 12). WRN also forms a complex with MRN both *in vivo* and *in vitro*. However, WRN and RECQ5 differ in the nature of their interaction with MRN. WRN and MRN form a complex *in vivo* only in response to DNA damage or replication arrest (5, 12). In contrast, RECQ5 appears to associate with MRN constitutively *in vivo*. The interaction between WRN and the MRN complex is solely mediated by NBS1 (5), while RECQ5 can bind to both MRE11 and NBS1, and the absence of NBS1 does not affect the association of RECQ5 with the MR complex. At the functional level, MRN dramatically stimulates the helicase activity of WRN (5), whereas it has no effect on the helicase activity of RECQ5. Further studies will be needed to fully understand the molecular mechanisms by which the RecQ helicases and MRN proteins work together to maintain genomic stability.

ACKNOWLEDGEMENTS

We thank Dr. Vilhelm Bohr for providing us with baculoviruses expressing MRN proteins and Torsten Kleffmann for help with mass spectrometry analysis. This work was supported by grants from the Swiss National Science Foundation, Lidia Hochstrasser Stiftung and Cancer League of Kanton Zurich.

REFERENCES

1. Assenmacher, N., and K. P. Hopfner. 2004. MRE11/RAD50/NBS1: complex activities. Chromosoma 113:157-66.
2. Bekker-Jensen, S., C. Lukas, R. Kitagawa, F. Melander, M. B. Kastan, J. Bartek, and J. Lukas. 2006. Spatial organization of the mammalian genome surveillance machinery in response to DNA strand breaks. J Cell Biol 173:195-206.
3. Carney, J. P., R. S. Maser, H. Olivares, E. M. Davis, M. Le Beau, J. R. Yates, 3rd, L. Hays, W. F. Morgan, and J. H. Petrini. 1998. The hMre11/hRad50 protein

complex and Nijmegen breakage syndrome: linkage of double-strand break repair to the cellular DNA damage response. Cell 93:477-86.
4. Carson, C. T., R. A. Schwartz, T. H. Stracker, C. E. Lilley, D. V. Lee, and M. D. Weitzman. 2003. The Mre11 complex is required for ATM activation and the G2/M checkpoint. Embo J 22:6610-20.
5. Cheng, W. H., C. von Kobbe, P. L. Opresko, L. M. Arthur, K. Komatsu, M. M. Seidman, J. P. Carney, and V. A. Bohr. 2004. Linkage between Werner syndrome protein and the Mre11 complex via Nbs1. J Biol Chem 279:21169-76.
6. Costanzo, V., K. Robertson, M. Bibikova, E. Kim, D. Grieco, M. Gottesman, D. Carroll, and J. Gautier. 2001. Mre11 protein complex prevents double-strand break accumulation during chromosomal DNA replication. Mol Cell 8:137-47.
7. Crabbe, L., A. Jauch, C. M. Naeger, H. Holtgreve-Grez, and J. Karlseder. 2007. Telomere dysfunction as a cause of genomic instability in Werner syndrome. Proc Natl Acad Sci U S A 104:2205-10.
8. Crabbe, L., R. E. Verdun, C. I. Haggblom, and J. Karlseder. 2004. Defective telomere lagging strand synthesis in cells lacking WRN helicase activity. Science 306:1951-3.
9. D'Amours, D., and S. P. Jackson. 2002. The Mre11 complex: at the crossroads of dna repair and checkpoint signalling. Nat Rev Mol Cell Biol 3:317-27.
10. de Jager, M., J. van Noort, D. C. van Gent, C. Dekker, R. Kanaar, and C. Wyman. 2001. Human Rad50/Mre11 is a flexible complex that can tether DNA ends. Mol Cell 8:1129-35.
11. Franchitto, A., and P. Pichierri. 2002. Bloom's syndrome protein is required for correct relocalization of RAD50/MRE11/NBS1 complex after replication fork arrest. J Cell Biol 157:19-30.
12. Franchitto, A., and P. Pichierri. 2004. Werner syndrome protein and the MRE11 complex are involved in a common pathway of replication fork recovery. Cell Cycle 3:1331-9.
13. Garcia, P. L., Y. Liu, J. Jiricny, S. C. West, and P. Janscak. 2004. Human RECQ5beta, a protein with DNA helicase and strand-annealing activities in a single polypeptide. Embo J 23:2882-91.
14. Hanada, K., and I. D. Hickson. 2007. Molecular genetics of RecQ helicase disorders. Cell Mol Life Sci 64:2306-22.
15. Hu, Y., X. Lu, E. Barnes, M. Yan, H. Lou, and G. Luo. 2005. Recql5 and Blm RecQ DNA helicases have nonredundant roles in suppressing crossovers. Mol Cell Biol 25:3431-42.
16. Hu, Y., S. Raynard, M. G. Sehorn, X. Lu, W. Bussen, L. Zheng, J. M. Stark, E. L. Barnes, P. Chi, P. Janscak, M. Jasin, H. Vogel, P. Sung, and G. Luo. 2007. RECQL5/Recql5 helicase regulates homologous recombination and suppresses tumor formation via disruption of Rad51 presynaptic filaments. Genes Dev 21:3073-84.
17. Kanagaraj, R., N. Saydam, P. L. Garcia, L. Zheng, and P. Janscak. 2006. Human RECQ5beta helicase promotes strand exchange on synthetic DNA structures resembling a stalled replication fork. Nucleic Acids Res 34:5217-31.
18. Lavin, M. F., and S. Kozlov. 2007. ATM activation and DNA damage response. Cell Cycle 6:931-42.
19. Lee, J. H., and T. T. Paull. 2007. Activation and regulation of ATM kinase activity in response to DNA double-strand breaks. Oncogene 26:7741-8.
20. Limoli, C. L., E. Giedzinski, W. M. Bonner, and J. E. Cleaver. 2002. UV-induced replication arrest in the xeroderma pigmentosum variant leads to DNA double-

strand breaks, gamma -H2AX formation, and Mre11 relocalization. Proc Natl Acad Sci U S A 99:233-8.
21. Lukas, C., J. Bartek, and J. Lukas. 2005. Imaging of protein movement induced by chromosomal breakage: tiny 'local' lesions pose great 'global' challenges. Chromosoma 114:146-54.
22. Luo, G., M. S. Yao, C. F. Bender, M. Mills, A. R. Bladl, A. Bradley, and J. H. Petrini. 1999. Disruption of mRad50 causes embryonic stem cell lethality, abnormal embryonic development, and sensitivity to ionizing radiation. Proc Natl Acad Sci U S A 96:7376-81.
23. Maser, R. S., O. K. Mirzoeva, J. Wells, H. Olivares, B. R. Williams, R. A. Zinkel, P. J. Farnham, and J. H. Petrini. 2001. Mre11 complex and DNA replication: linkage to E2F and sites of DNA synthesis. Mol Cell Biol 21:6006-16.
24. Matsuura, S., H. Tauchi, A. Nakamura, N. Kondo, S. Sakamoto, S. Endo, D. Smeets, B. Solder, B. H. Belohradsky, V. M. Der Kaloustian, M. Oshimura, M. Isomura, Y. Nakamura, and K. Komatsu. 1998. Positional cloning of the gene for Nijmegen breakage syndrome. Nat Genet 19:179-81.
25. Mirzoeva, O. K., and J. H. Petrini. 2003. DNA replication-dependent nuclear dynamics of the Mre11 complex. Mol Cancer Res 1:207-18.
26. Olson, E., C. J. Nievera, E. Liu, A. Y. Lee, L. Chen, and X. Wu. 2007. The Mre11 complex mediates the S-phase checkpoint through an interaction with replication protein A. Mol Cell Biol 27:6053-67.
27. Paull, T. T., and M. Gellert. 1998. The 3' to 5' exonuclease activity of Mre 11 facilitates repair of DNA double-strand breaks. Mol Cell 1:969-79.
28. Paull, T. T., and M. Gellert. 1999. Nbs1 potentiates ATP-driven DNA unwinding and endonuclease cleavage by the Mre11/Rad50 complex. Genes Dev 13:1276-88.
29. Sangrithi, M. N., J. A. Bernal, M. Madine, A. Philpott, J. Lee, W. G. Dunphy, and A. R. Venkitaraman. 2005. Initiation of DNA replication requires the RECQL4 protein mutated in Rothmund-Thomson syndrome. Cell 121:887-98.
30. Sartori, A. A., C. Lukas, J. Coates, M. Mistrik, S. Fu, J. Bartek, R. Baer, J. Lukas, and S. P. Jackson. 2007. Human CtIP promotes DNA end resection. Nature 450:509-14.
31. Sekelsky, J. J., M. H. Brodsky, G. M. Rubin, and R. S. Hawley. 1999. Drosophila and human RecQ5 exist in different isoforms generated by alternative splicing. Nucleic Acids Res 27:3762-9.
32. Sharma, S., K. M. Doherty, and R. M. Brosh, Jr. 2006. Mechanisms of RecQ helicases in pathways of DNA metabolism and maintenance of genomic stability. Biochem J 398:319-37.
33. Shimamoto, A., K. Nishikawa, S. Kitao, and Y. Furuichi. 2000. Human RecQ5beta, a large isomer of RecQ5 DNA helicase, localizes in the nucleoplasm and interacts with topoisomerases 3alpha and 3beta. Nucleic Acids Res 28:1647-55.
34. Stewart, G. S., R. S. Maser, T. Stankovic, D. A. Bressan, M. I. Kaplan, N. G. Jaspers, A. Raams, P. J. Byrd, J. H. Petrini, and A. M. Taylor. 1999. The DNA double-strand break repair gene hMRE11 is mutated in individuals with an ataxia-telangiectasia-like disorder. Cell 99:577-87.
35. Tauchi, H., J. Kobayashi, K. Morishima, S. Matsuura, A. Nakamura, T. Shiraishi, E. Ito, D. Masnada, D. Delia, and K. Komatsu. 2001. The forkhead-associated domain of NBS1 is essential for nuclear foci formation after irradiation but not essential for hRAD50[middle dot]hMRE11[middle dot]NBS1 complex DNA repair activity. J Biol Chem 276:12-5.

36. Trenz, K., E. Smith, S. Smith, and V. Costanzo. 2006. ATM and ATR promote Mre11 dependent restart of collapsed replication forks and prevent accumulation of DNA breaks. Embo J 25:1764-74.
37. Trujillo, K. M., and P. Sung. 2001. DNA structure-specific nuclease activities in the Saccharomyces cerevisiae Rad50*Mre11 complex. J Biol Chem 276:35458-64.
38. Ward, I. M., and J. Chen. 2001. Histone H2AX is phosphorylated in an ATR-dependent manner in response to replicational stress. J Biol Chem 276:47759-62.
39. Wu, L., K. L. Chan, C. Ralf, D. A. Bernstein, P. L. Garcia, V. A. Bohr, A. Vindigni, P. Janscak, J. L. Keck, and I. D. Hickson. 2005. The HRDC domain of BLM is required for the dissolution of double Holliday junctions. Embo J 24:2679-87.
40. Wu, L., and I. D. Hickson. 2003. The Bloom's syndrome helicase suppresses crossing over during homologous recombination. Nature 426:870-4.
41. Yamaguchi-Iwai, Y., E. Sonoda, M. S. Sasaki, C. Morrison, T. Haraguchi, Y. Hiraoka, Y. M. Yamashita, T. Yagi, M. Takata, C. Price, N. Kakazu, and S. Takeda. 1999. Mre11 is essential for the maintenance of chromosomal DNA in vertebrate cells. Embo J 18:6619-29.
42. Zhu, J., S. Petersen, L. Tessarollo, and A. Nussenzweig. 2001. Targeted disruption of the Nijmegen breakage syndrome gene NBS1 leads to early embryonic lethality in mice. Curr Biol 11:105-9.

FIGURE LEGENDS

Figure 1. RECQ5 and MRN proteins form a complex *in vivo*. (A) Co-immunoprecipitation of the MRE11, RAD50 and NBS1 proteins with RECQ5 from a total extract of exponentially growing HEK293T cells (1 mg of protein). Lane 1, 5% of the input material; lane 2, immunoprecipitation using IgG (2 μg) isolated form a preimmune serum; lane 3, immunoprecipitation with affinity-purified rabbit anti-RECQ5 antibody (1 μg); lane 4, the same as lane 3, but the extract was pretreated with DNase I (50 U) for 30 minutes at 25°C; lane 5, the same as lane 3, but extract was supplemented with ethidium bromide (50 μg/ml). (B) Co-immunoprecipitation of RECQ5 with the MRE11 protein from total extract of HeLa cells. Lane 1, 5% of the input material; lane 2, immunoprecipitation using IgG (2 μg) isolated form a preimmune serum; lane 3, immunoprecipitation using mouse monoclonal anti-MRE11 antibody. (C) Effect of various genotoxic agents on the cellular association of RECQ5 with the MRN complex. RECQ5 immunoprecipitates from treated and untreated U2OS cells were subjected to Western blot analysis to determine the level of co-precipitated MRE11 protein. NT, non-treated cells; HU, cells treated with 2 mM hydroxyurea for 16 hours; IR, cells exposed to ionizing radiation (20 Gy) followed by incubation for 12 hours; CDDP, cells treated with 20 μM cis-diamminedichloroplatinum for 8 hours. (A-C) Immunoprecipitated proteins were separated by electrophoresis through 7.5 % (w/v) SDS-polyacrylamide gel followed by Western blotting. RECQ5 and MRN proteins were detected using antibodies described in Materials and Methods.

Figure 2. RECQ5 interacts with the MRN complex directly *via* its MRE11 and NBS1 subunits. (A) Binding of the MRN (top panel) and MR (bottom panel) complexes to chitin bead coated with RECQ5-CBD fusion. (B) Binding of individually purified RAD50 (top panel), NBS1 (middle panel) and MRE11 (bottom panel) proteins to chitin bead coated with RECQ5-CBD fusion. For (A) and (B): lanes 1, 30% of input material; lane 2, chitin beads coated with McrA-CBD; lane 3, chitin beads coated with RECQ5-CBD fusion protein (C) Western-blot analysis of RECQ5 immunoprecipitates from total extracts (1 mg of protein) of the following cells: NBS (NBS1 deficiency), NBS1+ (NBS complemented by stable transfection of the NBS1 cDNA), ATLD1 (MRE11 deficiency) and ATLD+ (ATLD complemented by stable transfection of the MRE11 cDNA). Lanes 1-4, 5% of the input material as indicated, lanes 5-8, RECQ5 immunoprecipitates from total extracts (1 mg of protein) of the indicated cells. Blots were probed for the presence of MRE11, RAD50 and NBS1 using antibodies described in Materials and Methods.

Figure 3. RECQ5 inhibits the 3'-5' exonuclease activity of MRE11. (A) Effect of the MRN complex on the strand-exchange activity of RECQ5 on a synthetic forked DNA structure with homologous arms lacking the leading strand. *Top panel*: Scheme of the assay. The lengths of the oligonucleotide substrate are indicated (nt, nucleotides; bp, base pairs). The 3'-end of the lagging oligonucleotide is indicated by an arrow and the position of the 5'-^{32}P label is marked by an asterisk. The homologous leading and lagging arms have a 5-nt heterology at the fork junction to prevent spontaneous strand exchange. *Bottom panel*: 1 nM ^{32}P-labeled 30-mer/60-mer duplex was incubated with 1 nM 60-mer complementary oligonucleotide in the presence of 40 nM RECQ5 to form forked DNA structure. After 10 minutes, ATP (2 mM) was added either alone (lanes 2-9) or together with the MRN complex (40 nM) (lanes 2 - 9). Aliquots from different reaction time points were analyzed by non-denaturing PAGE followed by phosphorimaging. Lanes 1 (marked by C), the 30-mer/60-mer duplex prior to annealing of the complementary oligonucleotide. (B) Effect of RECQ5 on the 3'-5' exonuclease activity of MRN (lanes 3 to 7) and MR (lanes 8 to 12). (C) Effect of *E.coli* RecQ on the 3'-5' exonuclease activity of MRN (lanes 3 to 7) and MR (lanes 8 to 12). In (B) and (C), reaction mixtures were incubated at 37°C for 30 minutes, and contained 1 nM 5'-tailed oligoduplex substrates (60-mer/30-mer with a 5'-^{32}P label on the shorter strand), 40 nM MRN or MR and various concentrations of RECQ5 or RecQ as indicated. Reaction products were analyzed by denaturing PAGE followed by phosphorimaging as described in Materials and Methods.

Figure 4. RECQ5 and RAD50 co-localize at sites of DNA damage. (A) Indirect immunofluorescence imaging of RECQ5 and RAD50 in U2OS cells prior to and after DNA replication arrest. Cells were either left untreated or incubated in the presence of hydroxyurea (HU) for 16 hours or exposed to UV light at a dose of 40 J/m^2 followed by incubation for 6 hours. After treatment, cells were fixed with methanol and triply stained for RECQ5 (green), RAD50 (red) and DNA (blue) as described in Materials and Methods. Images were captured by an Olympus IX81 fluorescence microscope. Overlap between the green and red signals in merged images appears yellow. (B) RECQ5 and RAD50 accumulate at laser-induced DNA double-strand breaks (DSBs). U2OS cells were sensitized with BrdU (10 μM; incubation for 24 hours) and subjected to microirradiation with pulsed UVA laser (λ =355 nm) to generate linear tracks of DSBs. At indicated time points after irradiation, cells were fixed with methanol and co-immunostained either with anti-RECQ5 (green) and anti-γ-H2AX (red) antibodies or with anti-

RECQ5 (green) and anti-RAD50 (red) antibodies as indicated. DAPI (blue) was used to stain nuclei. Images were captured and processed as in (A).

Figure 5. MRE11 is required for the recruitment of RECQ5 to stalled replication forks. (A) Western blot analysis of extracts of U2OS cells expressing indicated shRNAs. Cells were transfected with appropriate shRNA vector and subjected to puromycin selection for 3 days to enrich the population of transfected cells. Blots were probed for MRE11, RAD50, RECQ5, RAD51, ATM and TFIIH (loading control) using antibodies described in Materials and Methods. Lane 1, extract from cells expressing control shRNA (shRNActrl), lane 2 and 3, extracts from cells expressing shRNA#1 and shRNA#2, respectively, targeting different sequences of MRE11. (B) Effect of shRNA-mediated depletion of MRE11 in U2OS on nuclear distribution of RECQ5 in response to HU. Cells were transfected either with the plasmid expressing shRNActrl (right panel) or the plasmid expressing shRNA#1 (left panel), followed by puromycin selection. Two days after addition of puromycin, HU was added to a final concentration of 2 mM. After 16 hours, cells were fixed and co-immunostained either for RECQ5 (green) and RAD50 (red) [top row] or for RECQ5 (green) and γ–H2AX (red) [bottom row]. Images were captured and processed as in Figure 4. (C) Nuclear distribution of RECQ5 in ATLD1 (MRE11 deficient) [left panel] and ATLD1-MRE11 (complemented by stable transfection of the MRE11 cDNA) [right panel] cells after replication arrest by HU. Exponentially growing cells were treated with 2 mM HU for 16 hours and then fixed and co-stained either for RECQ5 (green) and RAD50 (red) [top row] or for RECQ5 (green) and γ–H2AX (red) [bottom row]. Images were captured and processed as in Figure 4.

Figure 6. MRE11 is required for the recruitment of RECQ5 to DNA DSBs. BrdU-sensitized ATLD1 and ATLD1-MRE11 cells were irradiated with UV-A laser, fixed at 30 minutes after the irradiation and co-immunostained to visualize either RECQ5 (green) and γ–H2AX (red) [top and middle panel] or RECQ5 (green) and RAD50 (red) [bottom panel]. DAPI (blue) was used to stain nuclei. Images were captured and processed as in Figure 4.

SUPPLEMENTARY INFORMATION

Supplementary Figure S1. Cell cycle status has no significant influence on the cellular level of RECQ5/MRN complex. (A) U2OS cells were synchronized at G1/S transition by treatment with hydroxyurea (HU) for 16 hours and then released to S phase by adding fresh medium without HU. At indicated time points, the level of RECQ5/MRN complex was analysed by immunoprecipitation under conditions described in the legend of Figure 1. (B) FACS analysis. The resultant cell cycle profiles for each time point (T0-9) are shown. AS, asynchronous cell population

Figure 1

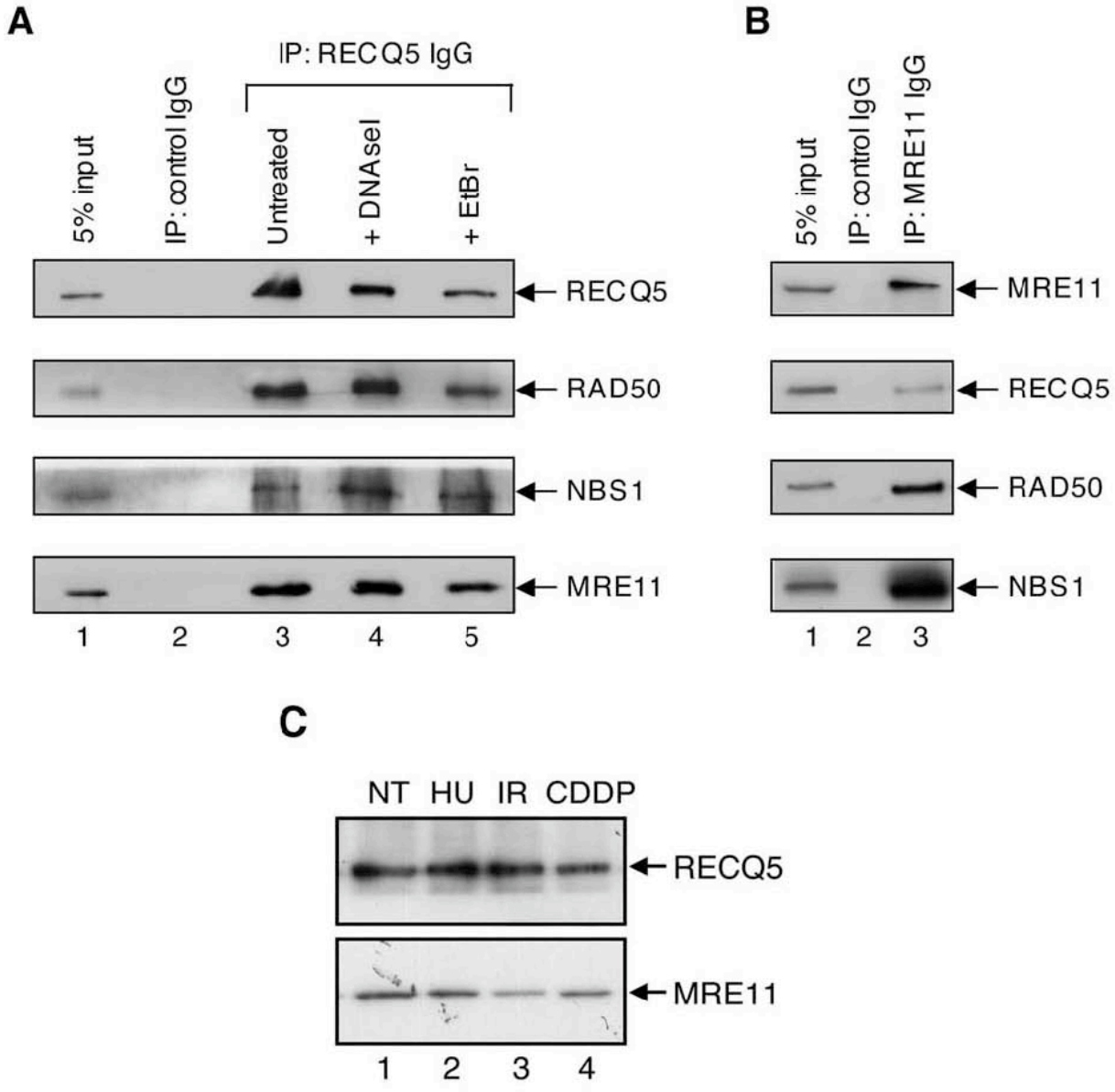
A
IP: RECQ5 IgG
5% input
IP: control IgG
Untreated
+ DNAseI
+ EtBr
RECQ5
RAD50
NBS1
MRE11
1 2 3 4 5
B
5% input
IP: control IgG
IP: MRE11 IgG
MRE11
RECQ5
RAD50
NBS1
1 2 3
C
NT HU IR CDDP
RECQ5
MRE11
1 2 3 4

Figure 2

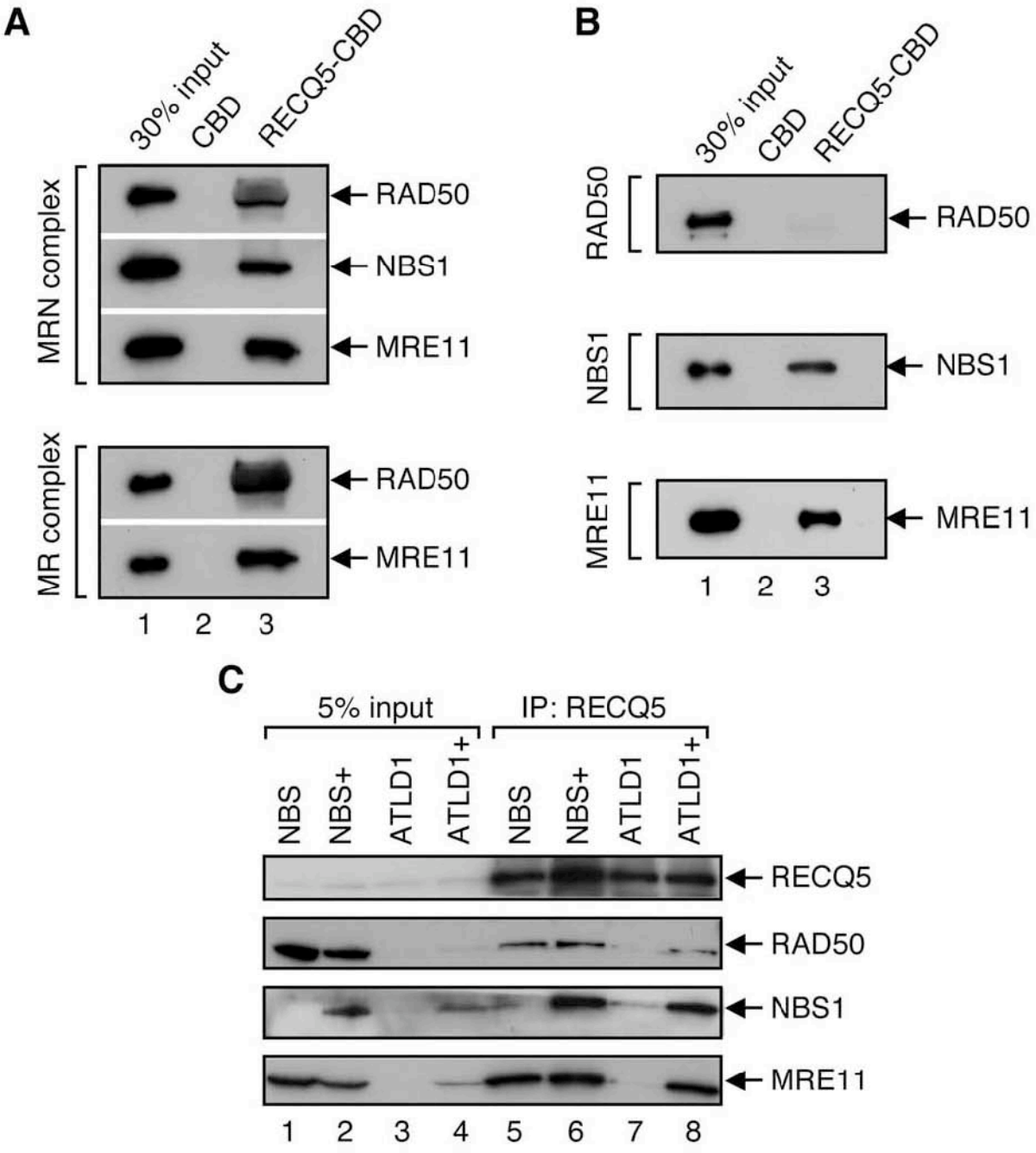
A
30% input
CBD
RECQ5-CBD
MRN complex
RAD50
NBS1
MRE11
MR complex
RAD50
MRE11
1 2 3
B
30% input
CBD
RECQ5-CBD
RAD50
RAD50
NBS1
NBS1
MRE11
MRE11
1 2 3
C
5% input
IP: RECQ5
NBS
NBS+
ATLD1
ATLD1+
NBS
NBS+
ATLD1
ATLD1+
RECQ5
RAD50
NBS1
MRE11
1 2 3 4 5 6 7 8

Figure 3

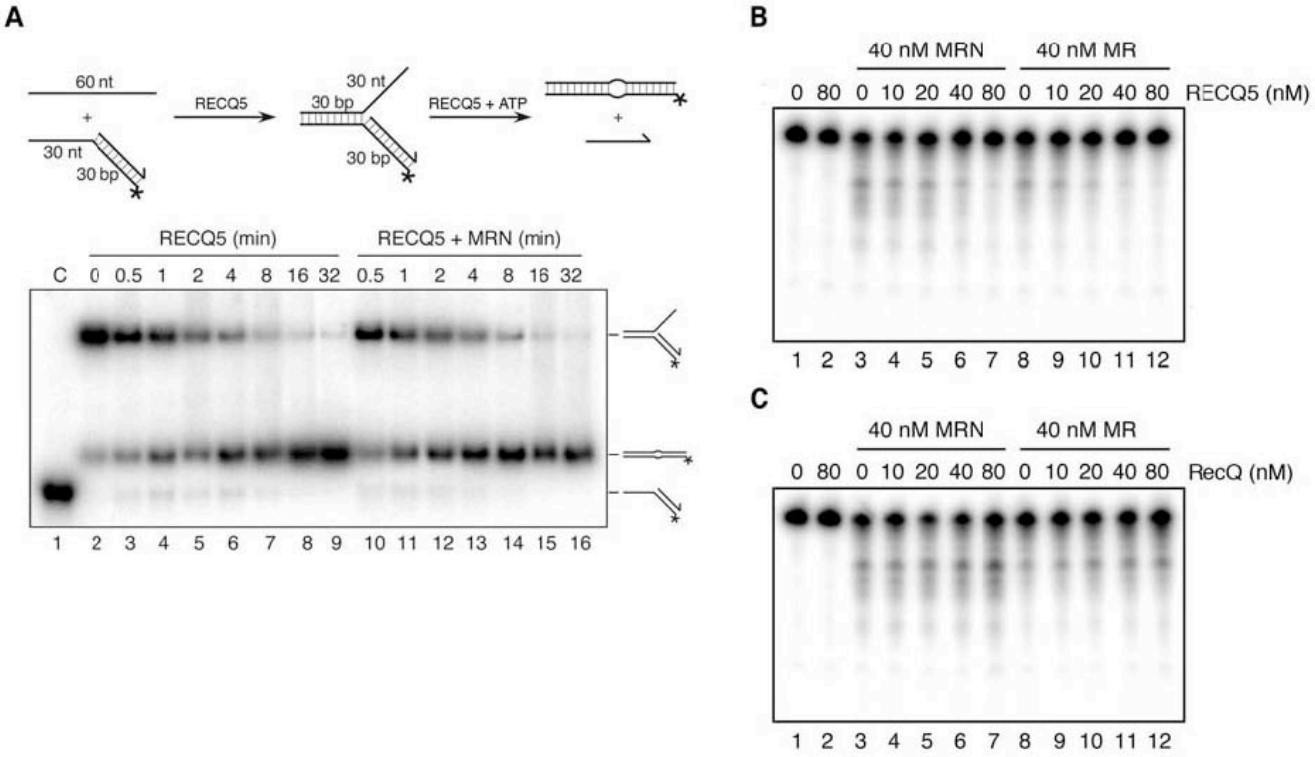
A
60 nt
30 nt
30 bp
RECQ5
30 nt
30 bp
30 bp
RECQ5 + ATP
RECQ5 (min)
RECQ5 + MRN (min)
C 0 0.5 1 2 4 8 16 32 0.5 1 2 4 8 16 32
1 2 3 4 5 6 7 8 9 10 11 12 13 14 15 16
B
40 nM MRN
40 nM MR
0 80 0 10 20 40 80 0 10 20 40 80 RECQ5 (nM)
1 2 3 4 5 6 7 8 9 10 11 12
C
40 nM MRN
40 nM MR
0 80 0 10 20 40 80 0 10 20 40 80 RecQ (nM)
1 2 3 4 5 6 7 8 9 10 11 12

Figure 4

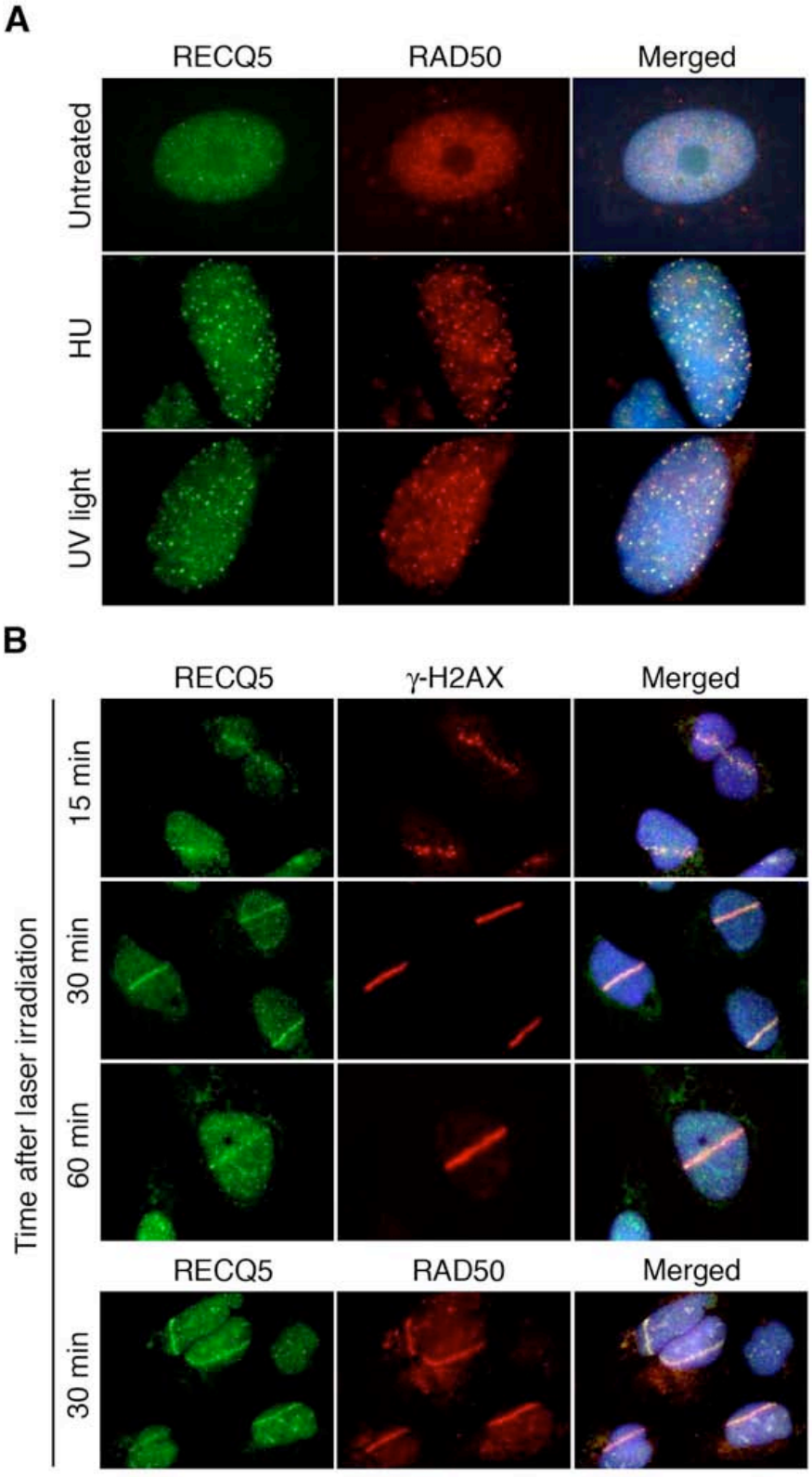
A
RECQ5
RAD50
Merged
Untreated
HU
UV light
B
RECQ5
γ-H2AX
Merged
Time after laser irradiation
15 min
30 min
60 min
RECQ5
RAD50
Merged
30 min

Figure 5

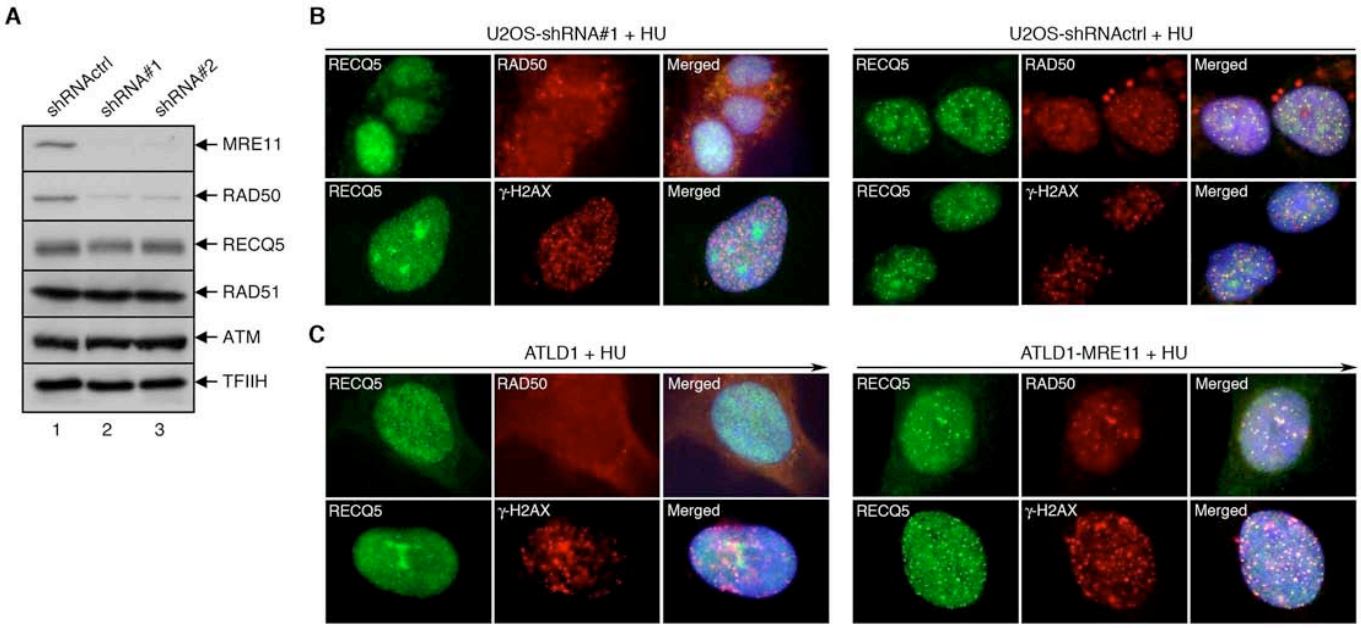

Figure 6

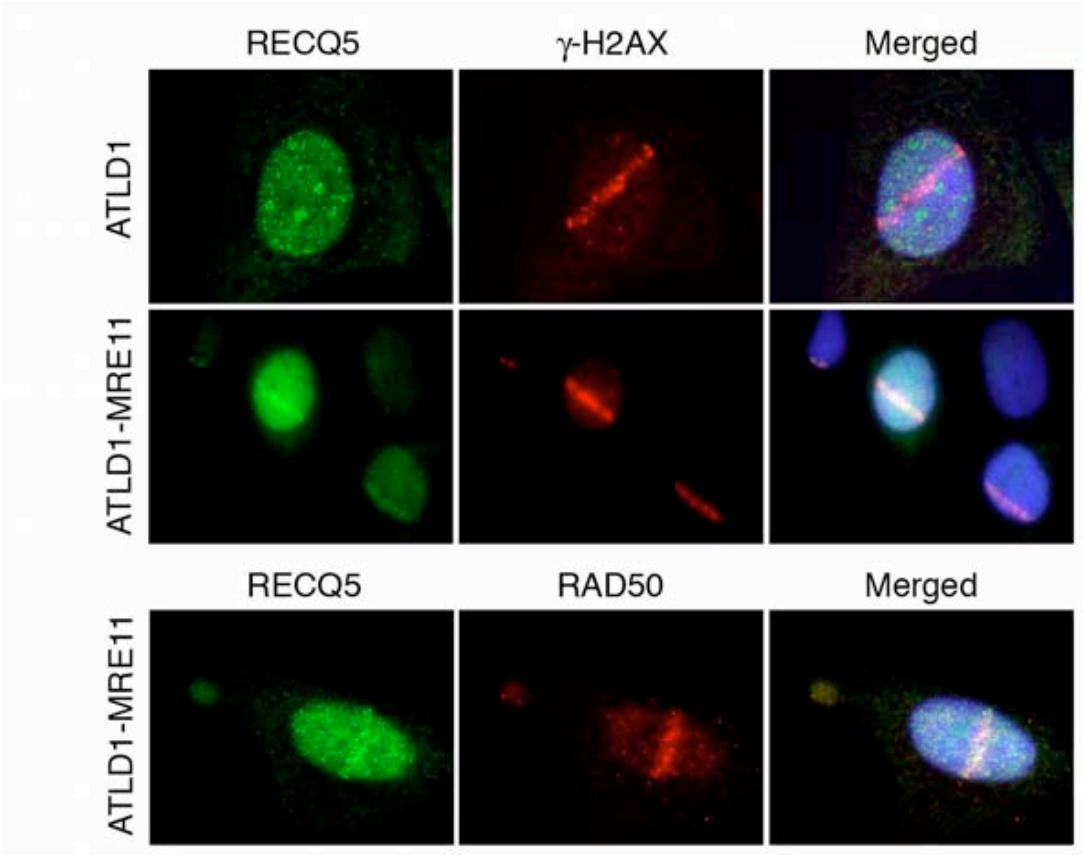

Figure S1

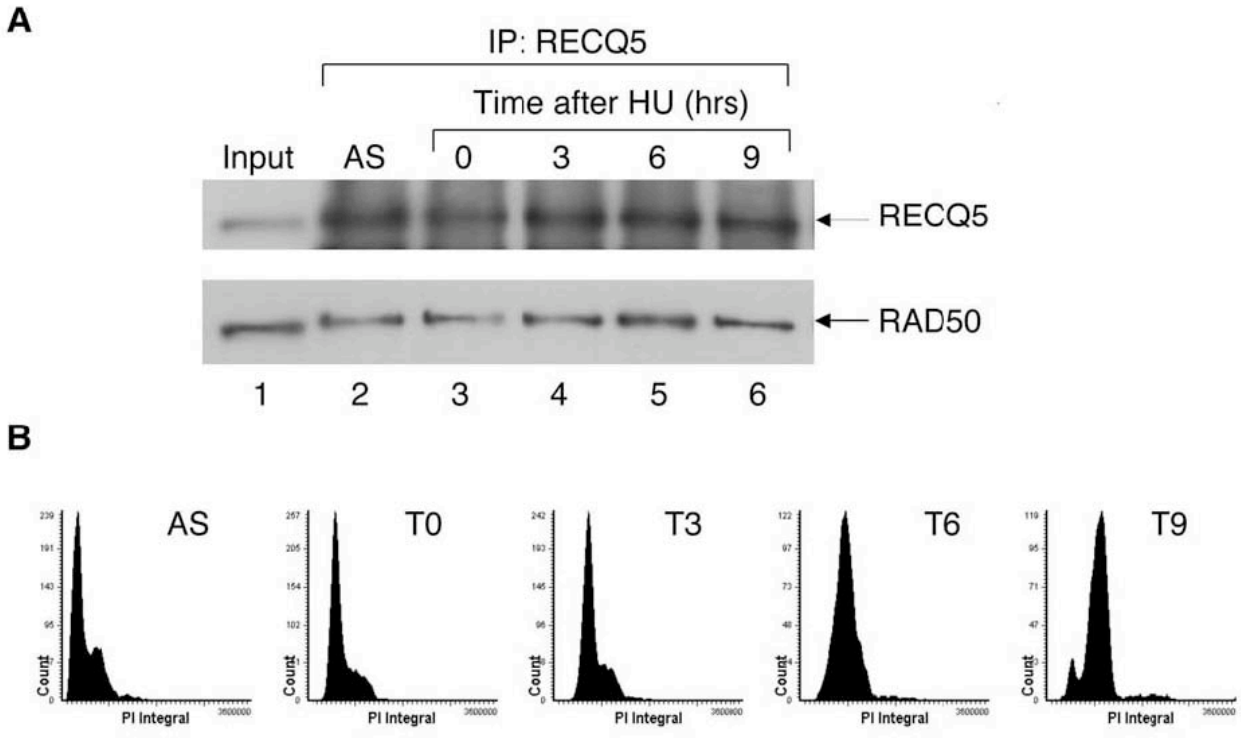
A
IP: RECQ5
Time after HU (hrs)
Input
AS
0
3
6
9
RECQ5
RAD50
1
2
3
4
5
6
B
AS
T0
T3
T6
T9
Count
PI Integral

Nucleic Acids Research Advance Access published August 22, 2007

Nucleic Acids Research, 2007, 1–11
doi:10.1093/nar/gkm500

Physical and functional interactions between Werner syndrome helicase and mismatch-repair initiation factors

Nurten Saydam[1] Radhakrishnan Kanagaraj[1], Tobias Dietschy[1,2,3], Patrick L. Garcia[1], Javier Peña-Diaz[1], Igor Shevelev[2,3], Igor Stagljar[2,3] and Pavel Janscak[1,*]

[1]Institute of Molecular Cancer Research of the University of Zurich, Switzerland and [2]Department of Biochemistry and [3]Department of Medical Genetics and Microbiology, Donnelly Centre for Cellular and Biomolecular Research, University of Toronto, Canada

Received April 26, 2007; Revised and Accepted June 7, 2007

ABSTRACT

Werner syndrome (WS) is a severe recessive disorder characterized by premature aging, cancer predisposition and genomic instability. The gene mutated in WS encodes a bi-functional enzyme called WRN that acts as a RecQ-type DNA helicase and a 3′-5′ exonuclease, but its exact role in DNA metabolism is poorly understood. Here we show that WRN physically interacts with the MSH2/MSH6 (MutSα), MSH2/MSH3 (MutSβ) and MLH1/PMS2 (MutLα) heterodimers that are involved in the initiation of mismatch repair (MMR) and the rejection of homeologous recombination. MutSα and MutSβ can strongly stimulate the helicase activity of WRN specifically on forked DNA structures with a 3′-single-stranded arm. The stimulatory effect of MutSα on WRN-mediated unwinding is enhanced by a G/T mismatch in the DNA duplex ahead of the fork. The MutLα protein known to bind to the MutSα–heteroduplex complexes has no effect on WRN-mediated DNA unwinding stimulated by MutSα, nor does it affect DNA unwinding by WRN alone. Our data are consistent with results of genetic experiments in yeast suggesting that MMR factors act in conjunction with a RecQ-type helicase to reject recombination between divergent sequences.

INTRODUCTION

Werner syndrome (WS) is an autosomal recessive disorder characterized by an early onset of age-related pathologies including graying hair, alopecia, arteriosclerosis, osteoporosis, diabetes mellitus and cancer (1). The gene mutated in WS, *WRN*, encodes a RecQ-type DNA helicase (2,3). WRN also possesses a 3′ - 5′ exonuclease activity residing in a separate domain located at the N-terminus of the protein (4,5). At the cellular level, WRN deficiency is associated with defects in DNA replication, homologous recombination (HR) and telomere maintenance (6–9). As a result, cells derived from WS patients display a high degree of genomic instability including elevated levels of chromosomal translocations and deletions (10–13). WS cells are hypersensitive to DNA-damaging agents such as 4-nitroquinoline 1-oxide, topoisomerase inhibitors and DNA cross-linkers, suggesting that WRN is actively involved in DNA repair (14–16). Several lines of evidence implicate WRN in the cellular response to DNA double-strand breaks (DSBs). WRN is rapidly recruited to the sites of ionizing radiation (IR)-induced damage (17). Moreover, it interacts physically and functionally with a number of proteins that are involved in the DSB-repair process including the MRE11-RAD50-NBS1 (MRN) complex (18), the Ku complex (19), RAD52 (20) and DNA-dependent protein kinase (21). However, the precise role for WRN in DNA repair remains to be elucidated.

The DNA mismatch-repair (MMR) system maintains genomic integrity by correcting DNA replication errors and preventing recombination between divergent sequences (22,23). Defects in a subset of MMR genes including *MSH2*, *MSH3*, *MSH6*, *MLH1* and *PMS2* are associated with hereditary non-polyposis colon cancer, highlighting the crucial role for MMR in genome maintenance (24). In the initiation step of the eukaryotic

*To whom correspondence should be addressed. Tel: +41(0)44 635 3470; Fax: +41(0)44 635 3484; Email: pjanscak@imcr.unizh.ch
Present address:
Nurten Saydam, Harvard School of Public Health, 667, Huntington Ave, Boston, USA

The authors wish it to be known that, in their opinion, the first three authors should be regarded as joint First Authors

MMR process, at least three heterodimers, namely MSH2/MSH6 (MutSα), MSH2/MSH3 (MutSβ) and MLH1/PMS2 (MutLα), are involved (22). MutSα binds to base-base mismatches and short insertion/deletion loops, while MutSβ can recognize only insertion/deletion loops containing up to 16 extra nucleotides in one strand (22). MutLα possesses an intrinsic endonuclease activity, which is activated upon mismatch recognition and introduces incisions in the discontinuous strand of the heteroduplex DNA, generating entry sites for the 5′-3′ exonuclease EXO1 (25).

Sgs1, the yeast ortholog of WRN, also contributes to the suppression of recombination between divergent DNA sequences (26). Heteroduplex rejection during repair of DSBs by the single-strand annealing pathway of HR in yeast requires the mismatch binding and ATPase functions of the Msh2p/Msh6p heterodimer and the helicase activity of Sgs1 (27,28). These findings led to the proposal that MMR proteins act in conjunction with Sgs1 to unwind DNA recombination intermediates containing mismatches (27,28).

Here we demonstrate that WRN directly interacts with MutSα, MutSβ and MutLα via distinct domains. MutSα and MutSβ are found to stimulate WRN-mediated unwinding of forked DNA duplexes with a 3′-single-stranded (ss) arm. The stimulatory effect of MutSα on WRN-mediated unwinding is enhanced by a single G/T mismatch located in the duplex ahead of the fork in a manner independent of MutLα. These data provide biochemical evidence suggesting that the rejection of homeologous recombination by MMR proteins occurs *via* helicase-mediated unwinding of recombination intermediates.

MATERIALS AND METHODS

Construction of plasmids

The bacterial expression vectors for the WRN fragments encompassing the amino acid residues 51–449, 949–1432, 500–946, 500–1149, 500–1236, respectively, fused to the C-terminus of glutathione *S*-transferase (GST) were constructed by PCR amplification of corresponding regions of the WRN cDNA and their insertion in pGEX-2TK (Amersham Biosciences) between the EcoRI and BamHI sites. The complete coding region of WRN was amplified by PCR and cloned in pACT2 (Clontech Palo Alto, CA) via SmaI site to construct a yeast two-hybrid (YTH) vector expressing WRN as a fusion with a Gal4 activation domain. MLH1 cDNA comprised of the codons 500–756 was cloned in a YTH vector pBTM116 (Clontech Palo Alto, CA) between the EcoRI and SalI sites, resulting in a fusion with a LexA DNA binding domain. The pBTM16 derivatives expressing other MLH1 variants as well as the full-length yMlh1 were previously described (29). The Gal4-hMSH2 (pLJR105), LexA-MSH3 and LexA-MSH6 bait plasmids were also described previously (30,31).

Proteins

Recombinant human WRN (3,32), MutSα (33), MutSβ (33) and MutLα (34) and *Escherichia coli* MutS (35) were produced and purified as previously described. An antibody against the N-terminal region of WRN encompassing amino acids 1–391 (ISEV-391) was raised in rabbit and purified on an antigen-coupled Sepharose 4A column (Amersham Biosciences). Control IgGs were purified from a rabbit preimmune serum on a 5 ml HiTrap protein G-Sepharose column (Amersham Biosciences).

Cell culture

The following human cell lines were used in this study: HEK 293 embryonic kidney cells and AG11395 SV40-transformed WS fibroblasts (Coriell Institute for Medical Research). The HEK 293 cells were maintained in DMEM (Gibco) supplemented with 10% fetal calf serum (Biochrome AG). The WS cells were maintained in MEM containing 15% fetal calf serum and 2 mM L-glutamine.

Immunoprecipitation assays

Cells were suspended in lysis buffer containing 20 mM Tris–HCl (pH 7.5), 150 mM NaCl, 2 mM EDTA, 0.1% (v/v) Triton X-100, 10% (v/v) glycerol and complete, EDTA-free protease inhibitor cocktail (Roche). After sonication, the suspension was centrifuged at 20 000 *g* for 30 min at 4°C. Aliquots containing 1.6 mg of protein were incubated overnight at 4°C with purified rabbit polyclonal anti-WRN IgGs (2 μg), which was followed by a 2-h incubation with protein A/G-agarose beads (Santa Cruz) at 4°C. Where required, extracts were treated with 50 U of DNaseI (Roche) for 30 min at 25°C prior to addition of antibody. After extensive washing with the lysis buffer, the immunoprecipitates were subjected to electrophoresis in a 7.5% polyacrylamide–SDS gel followed by western blotting. The blots were probed with mouse monoclonal antibodies against WRN (BD Biosciences, 611169), MSH6 (Pharmingen, clone 44), PMS2 (Pharmingen, clone 16-4), MLH1 (BD Biosciences, 554073), MSH2 (Calbiochem, clone NA 26) and MSH3 (Transduction Laboratories, clone 52). Immune complexes were detected using ECL-plus reagent (Amersham Biosciences), with horse anti-mouse IgG-horseradish peroxidase conjugate (Vector) used as a secondary antibody. In the control experiment, IgGs purified from a preimmune rabbit serum were used instead of the anti-WRN antibody.

GST pull-down assays

GST–WRN fusion proteins were produced in the *E. coli* BL21-CodonPlus(DE3)-RIL strain (Stratagene) using the expression vectors described above. The fusion proteins were bound to glutathione–sepharose beads (Amersham Biosciences) as previously described (36). The beads were incubated with 1 μg of purified MutSα, MutSβ or MutLα in 400 μl of NET-N 100 buffer [10 mM Tris HCl (pH 8.0), 1 mM EDTA, 100 mM NaCl, 0.5% (v/v) NP-40] for 2 h at 4°C. After extensive washing with NET-N 100 buffer, proteins bound to the beads were analyzed by western blotting. Membranes were probed with the monoclonal antibodies described above. MSH3 was detected with a rabbit polyclonal antibody (NTH3) raised against its first 200 amino acids (Eurogentec). In a control experiment, beads were coated with GST protein only.

ELISA-based protein binding assay

Purified recombinant WRN was diluted to a concentration of 20 nM in carbonate buffer [16 mM Na_2CO_3, 34 mM $NaHCO_3$ (pH 9.6)] and added to wells of a 96-well microtiter plate (50 µl/well). Plates were incubated overnight at 4°C. For control reactions, wells were pre-coated with an equivalent amount of bovine serum albumin (BSA). After aspiration of the samples, the wells were blocked with blocking buffer [phosphate-buffered saline, 0.5% (v/v) Tween-20 and 3% (w/v) BSA] for 2 h at 37°C (200 µl/well). Following blockage, the wells were incubated with increasing concentrations of purified recombinant MutSα, MutSβ and MutLα proteins for 1 h at 37°C. All samples were supplemented with ethidium bromide (EtBr) at a concentration of 50 µg/ml to prevent DNA-mediated interactions. Wells were washed four times with blocking buffer to eliminate unbound proteins, and incubated with the appropriate primary antibody diluted in blocking buffer (mouse monoclonal anti-MSH2 antibody for MutSα and MutSβ, and mouse monoclonal anti-MLH1 antibody for MutLα). Plates were incubated for 1 h at 37°C. After four washings with blocking buffer, horseradish peroxidase-conjugated anti-mouse secondary antibody (1:10 000 in blocking buffer) was added and the plates were incubated at 37°C for 30 min. After extensive washing with blocking buffer, the protein complexes were detected using o-Phenylenediamine dichloride (Sigma) dissolved in 0.1 M citrate-phosphate buffer (pH 5.0) containing 0.03% hydrogen peroxide (1 mg/ml). The reactions were terminated after 5 min by adding 50 µl of 2 M H_2SO_4. The plates were scanned in a microplate reader (Molecular Devices) for absorbance at 492 nm. The A_{492} values, corrected for background signal in the presence of BSA, were plotted as a function of the concentration of appropriate MMR protein using the GraphPad Prism software. To determine an apparent dissociation constant of each complex (K_d), the data points were fitted by the hyperbolic function $Y = B_{max}*X/(K_d + X)$ where B_{max} is the maximal binding and K_d is the concentration of ligand required to reach half-maximal binding.

YTH assay

YTH analysis was carried out using *Saccharomyces cerevisiae* strains L40 (*MAT*a *trp1 leu2 his3 LYS2::lexA-HIS3 URA3::lexA-lacZ*) and Y190 (*MAT*α, *ura3-52, his3-200*, *lys2-801, ade2-101, trp1-901, leu2-3, 112, gal4Δ*, *gal80Δ*, *cyh^{r}2*, *LYS2::GAL1$_{UAS}$-HIS3$_{TATA}$-HIS3*, *URA3::GAL1$_{UAS}$-GAL1$_{TATA}$-lacZ*). The former strain was used for LexA-bait vectors while the latter strain was used for Gal4-bait vectors. Clones carrying the bait and prey plasmids were tested for β-galactosidase activity using a pellet X-gal (PXG) assay as previously described (37).

Helicase assays

Schemes of DNA substrates as well as the sequences of the constituent oligonucleotides are summarized in Supplementary Table 1. The f11-20 oligonucleotide (50-mer) was labeled at the 5′-end using T4 polynucleotide kinase (NEB) and [γ-^{32}P]ATP (Amersham Biosciences), and annealed with appropriate oligonucleotides under previously described conditions (38). The helicase reaction mixtures (10 µl) contained 50 mM Tris–HCl (pH 7.5), 50 mM NaCl, 2 mM $MgCl_2$, 50 µg/ml of BSA, 2 mM ATP, 1 mM DTT, 1 nM DNA substrate and indicated concentrations of MMR proteins (MutSα, MutSβ, MutLα and MutS) and WRN. The MMR proteins were pre-incubated with the DNA substrate on ice for 1 min prior to the addition of WRN. The reactions were incubated at 37°C for 30 min and terminated by the addition of 0.5 reaction volume of buffer S [150 mM EDTA, 2% (w/v) SDS, 30% (v/v) glycerol, 0.1% (w/v) bromophenol blue] followed by treatment with proteinase K (0.1 mg/ml) at 37°C for 10 min. The reaction products were resolved on a non-denaturing 10% polyacrylamide gel [acrylamide to bis-acrylamide, 19:1 (w/w)] run in 1xTBE buffer at 140 V. Radiolabeled DNA species were visualized by a phosphorimager and quantified using ImageQuant software (Molecular Dynamics).

RESULTS

Physical association between WRN and MMR proteins

Based on genetic studies in yeast, it has been suggested that the proteins involved in the initiation of MMR act in conjunction with RecQ DNA helicases to eliminate DNA recombination intermediates containing mismatches, which can give rise to chromosomal rearrangements (27,28). We sought to test the validity of this model biochemically using the WRN helicase, one of the five RecQ homologs identified in human cells, whose dysfunction results in chromosomal translocations and deletions. First, we performed an ELISA-based protein-binding assay to investigate whether WRN and the MMR proteins interact physically. Increasing concentrations of purified MutSα (MSH2/MSH6), MutSβ (MSH2/MSH3) and MutLα (MLH1/PMS2) proteins (Figure 1A) ranging from 0 to 80 nM were incubated in wells that had been pre-coated with WRN at a concentration of 20 nM and subsequently blocked with BSA to prevent non-specific interactions. After extensive washing, the bound MMR proteins were incubated with specific antibodies followed by a colorimetric assay to quantify the binding. In control experiments, MMR proteins were incubated in wells pre-coated only with BSA. We found that all the three MMR heterodimers were specifically bound to WRN-coated wells in a dose dependent manner, indicating a direct interaction (Figure 1B–D). Interestingly, the apparent dissociation constant of the MutSβ–WRN complex (K_d = 8.8 nM) was much lower than that estimated for the MutSα–WRN complex (K_d = 38.5 nM). The dissociation constant of the MutLα–WRN complex (K_d = 34.9 nM) was similar to that of the MutSα–WRN complex.

To test whether WRN and MMR proteins form a stable complex *in vivo*, we immunoprecipitated WRN from extracts of exponentially growing human embryonic kidney cells (HEK 293) and subjected the resulting immunoprecipitate to western blot analysis.

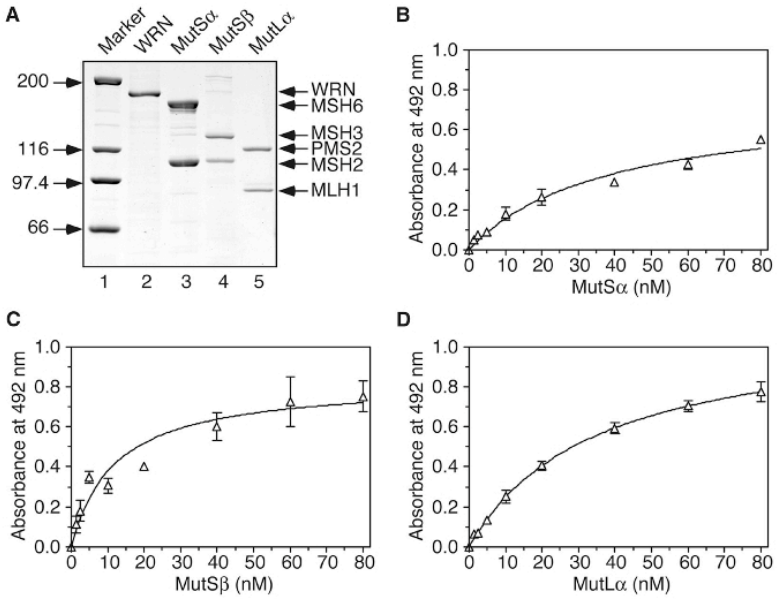

Figure 1. Direct physical interaction of WRN with MMR proteins. (**A**) SDS–PAGE analysis of purified recombinant MutSα, MutSβ, MutLα and WRN proteins produced in insect cells by means of the baculovirus system. (**B**) Binding of MutSα to WRN as a function of MutSα concentration. (**C**) Binding of MutSβ to WRN as a function of MutSβ concentration. (**D**) Binding of MutLα to WRN as a function of MutLα concentration. Increasing concentrations of MutSα, MutSβ and MutLα (0–80 nM) were incubated at 37°C for 1 h in the wells of an ELISA plate that were pre-coated with the WRN protein (20 nM) and subsequently blocked with 3% BSA. After extensive washing, the bound MMR proteins were detected by ELISA as described in Materials and Methods. The measured absorbance values were corrected by subtracting background values obtained with BSA-coated wells. The data points represent the mean of three independent experiments.

This immunoprecipitate was found to contain the MLH1 and PMS2 proteins, components of the MutLα complex, but not the MSH2 and MSH6 proteins, which form the MutSα heterodimer (Figure 2A, lanes 3 and 4). None of these MMR proteins were detected in the immunoprecipitate obtained with control IgGs (Figure 2A, lane 2). To exclude the possibility that the observed association of WRN with MLH1 and PMS2 results from independent binding of these proteins to DNA, we pre-treated the cell extracts with DNaseI. We found that this treatment did not alter the level of the MMR proteins in the WRN immunoprecipitate, suggesting that the WRN–MLH1–PMS2 complex is mediated by protein–protein interactions (Figure 2A, compare lanes 3 and 4). Furthermore, we did not detect PMS2 in an immunoprecipitate obtained with anti-WRN antibody from extracts of the WS cell line AG11395, excluding the possibility that the observed co-immunoprecipitation of MMR proteins with WRN is due to cross-reactivity of the antibody (Figure 2B).

Collectively, these data indicate that MutLα but not MutSα, forms a stable complex with WRN *in vivo*.

Mapping of protein–protein interaction domains

To identify the MutSα, MutSβ and MutLα-interaction sites on WRN, we performed affinity pull-down assays using a series of WRN fragments fused to GST. These fragments covered the entire WRN polypeptide except for the first 50 amino acids and the region spanning the amino acids 450–499 (Figure 3A and B). The GST pull-down experiments revealed that the MutSα interaction site on WRN was localized to the region between amino acids 500 and 946, which constitutes the helicase core of WRN composed of the DExH helicase and Zn-binding domains (Figure 3A and C). MutSβ was found to make contacts not only with the helicase core of WRN, but also with a region spanning amino acids 947–1149 that contains the winged-helix (WH) motif, a common interaction site for most of the WRN partners identified thus far (Figure 3A and C) (39). Notably, the binding affinity of MutSβ to the WH domain of WRN appeared to be much higher that its binding affinity to the helicase core of WRN (Figure 3C, compare lanes 4–7). The data also indicated that MutSβ binds to WRN more efficiently than MutSα (Figure 3C, top and middle panels; compare lane 1 with lanes 4–7), which is in agreement with the results of the ELISA assay (Figure 1).

MutLα was found to interact with the helicase core of WRN and with the N-terminal portion of WRN including the exonuclease domain, showing a higher binding affinity to the former domain (Figure 3A and C, bottom panel; compare lanes 3–7).

To identify the subunits of MutSα, MutSβ and MutLα that mediate the interaction with WRN, we performed a quantitative YTHassay with the full-length WRN as prey. The following interactions were examined: MSH2–WRN, MSH6–WRN, MSH3–WRN and MLH1–WRN.

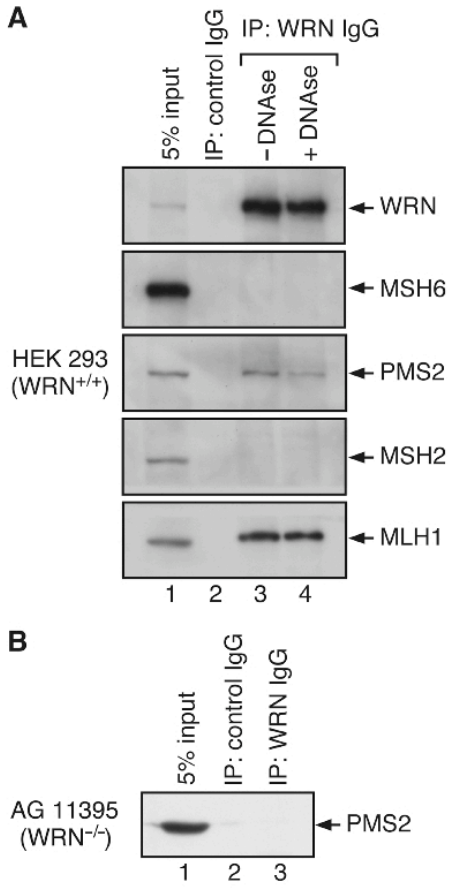

Figure 2. WRN forms a stable complex with MLH1 and PMS2 in human cells. (**A**) Western blot analysis of WRN immunoprecipitates from total extracts of HEK 293 cells (1.6 mg of protein) before (lane 3) and after (lane 4) treatment with DNaseI (50 U). Lane 1, 5% of input; lane 2, control immunoprecipitation experiment with a preimmune rabbit IgGs. Purified rabbit anti-WRN IgGs (2 μg) were used to immunoprecipitate WRN. Blots were probed with monoclonal antibodies against WRN, MSH2, MSH6, MLH1 and PMS2. (**B**) Western blot analysis of immunoprecipitate from extracts of AG11395 ($WRN^{-/-}$) cells obtained using an anti-WRN antibody. The immunoprecipitations were carried out under the same conditions as in (A). The blots were probed with a monoclonal antibody against PMS2.

We found WRN to interact with MLH1 and MSH2, but not with MSH3 and MSH6 (Figure 4A and B). This indicates that the MutSα–WRN and MutSβ–WRN interactions are mediated by MSH2, and the MutLα–WRN interaction is mediated by MLH1. However, the inability of MSH3 and MSH6 to interact with WRN in the YTH assay could be a consequence of the fact that these proteins are not soluble when expressed alone (33). This is also true for PMS2 (34). Therefore, the possibility still exists that these proteins could make additional contacts with WRN. This is particularly likely in the case of MSH3, since our GST pull-down experiments revealed that MutSβ interacts with both the helicase core and the WH domain of WRN, whereas MutSα interacts only with the helicase core of WRN (Figure 3).

In order to identify the WRN interaction domain on MLH1, we tested a series of MLH1 deletion variants for the ability to interact with the full-length WRN in YTH assay. We found that this domain is located at the C-terminus of the MLH1 polypeptide between amino acids 500 and 756 (Figure 4A and B). This is different from the location of the BLM-interaction site that was mapped to the region spanning amino acids 396–500 (29).

Stimulation of the helicase activity of WRN by MutSα and MutSβ

Next, we tested MutSα for the ability to affect the helicase activity of WRN on DNA substrates containing mismatches. In these experiments, we used a synthetic DNA duplex (49 bp) with a 3′-ss flap (19 nt) resembling a part of the structure that results from annealing of the resected arms of a broken chromosome at regions of homology. On such forked DNA structures, WRN preferentially translocates along the 3′-flap oligonucleotide to unwind the duplex ahead of the fork junction, generating a 3′-tailed duplex. This primary product can be further unwound by WRN into the component strands, as a consequence of loading of a second helicase molecule on the 3′-ssDNA tail (40). We prepared a fully matched substrate and a substrate containing a single G/T mismatch located 11 nt ahead of the ss/ds junction (Figure 5A and B, top panels). WRN alone displayed a very low helicase activity on both structures when present at the same concentration as the DNA substrate (1 nM). However, the helicase activity of WRN on these structures dramatically increased upon inclusion of an 8-fold molar excess of MutSα in the reaction (Figure 5A–D). Notably, the initial rate of the MutSα-stimulated unwinding reaction with G/T substrate was about 1.7 times higher than that measured with the G/C substrate (Supplementary Table 2).

Since MutLα is known to bind to MutSα–heteroduplex complexes (41), we investigated whether it can affect the WRN-mediated unwinding of G/T and G/C substrates induced by MutSα. We found that MutLα did not significantly alter the MutSα-dependent helicase activity of WRN on these DNA structures (Figure 5). Also, it had no effect on WRN-mediated unwinding in the absence of MutSα (Figure 7, lane 5).

To further assess the effect of MutSα on WRN-mediated unwinding of the 3′-flap duplex, we performed a protein titration experiment, in which we varied the concentration of MutSα while keeping WRN and DNA substrate at a fixed concentration of 1 nM. We found that MutSα stimulated the helicase activity of WRN in a concentration-dependent manner, exhibiting a significantly higher activity on the G/T substrate than on the homoduplex substrate (Figure 6).

To explore the specificity of the observed stimulatory effect, we tested human MutSβ as well as *E. coli* MutS for the ability to stimulate DNA unwinding by WRN. We found that MutSβ enhanced the WRN-mediated unwinding of the 3′-flap DNA duplex to a similar extent

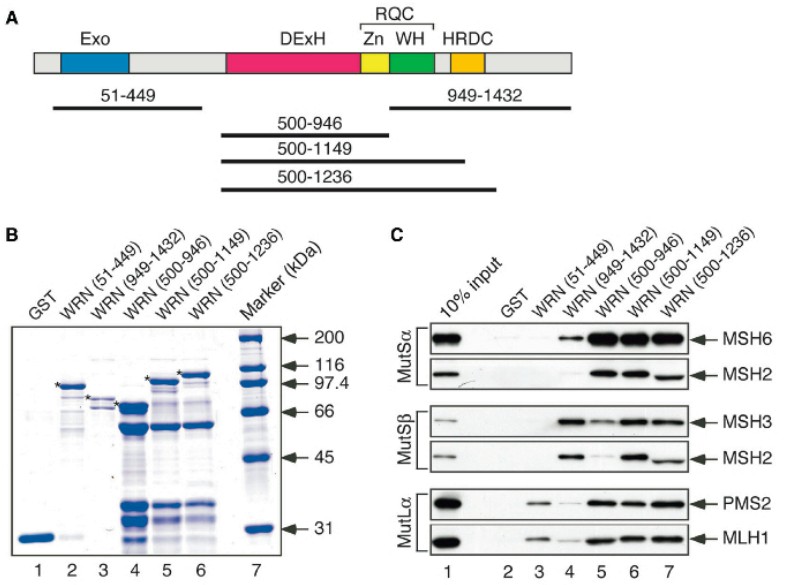

Figure 3. Mapping of MutSα, MutSβ and MutLα-interaction domains on WRN (**A**) Domain organization of the WRN protein. Exo, exonuclease domain; DExH, helicase domain; Zn, zinc-binding domain; WH, winged-helix domain; HRDC, helicase and RNaseD C-terminal domain; RQC, RecQ C-terminal region. The black lines indicate the boundaries of the various WRN fragments used in this study. (**B**) SDS–PAGE analysis of GST–WRN fragments expressed in *E. coli* and isolated using glutathione beads. Bands migrating below the WRN fragments (marked by an asterisks) were determined to be degradation products by western blot analysis using an anti-GST antibody. (**C**) GST pull-down assay. Glutathione beads coated with the indicated GST-tagged WRN fragments were incubated with purified MutSα, MutSβ or MutLα proteins expressed in insect cells using baculovirus system and the bound MMR proteins were analyzed by western blotting as described in Materials and Methods.

as seen with MutSα (Figure 7, compare lanes 2 and 3). In contrast, the *E. coli* MutS protein did not enhance the WRN-mediated DNA unwinding (Figure 7, lane 8), indicating that the observed stimulatory effect is specific to human MutS homologs. As in the case of MutSα, MutSβ-stimulated helicase activity of WRN was not influenced upon addition of MutLα (Figure 7, compare lanes 4 and 7) and it was dependent on MutSβ concentration (Supplementary Figure S1). We also found that in the presence of MutSβ, WRN unwound the G/T substrate with the same efficiency as the homoduplex substrate (Supplementary Figure S2). This is consistent with the fact that MutSβ does not bind to base–base mismatches (22) and supports the conclusion that the observed stimulatory effect of the G/T mismatch on MutSα-dependent unwinding of the 3′-flap duplex by WRN results from the specific binding of MutSα to the mismatch.

Together, the results described above indicate that MutSα and MutSβ, but not MutLα, can stimulate WRN to unwind DNA structures resembling recombination intermediates and that this stimulatory effect is enhanced by mismatches in the DNA substrate.

MutSα and MutSβ stimulate WRN helicase specifically on forked DNA duplexes with a 3′-ss arm

To gain further insights into the mechanism underlying the stimulation of the helicase activity of WRN by MutSα and MutSβ, we investigated the dependence of this reaction on the configuration of the arms of the fork. Using the same set of oligonucleotides, we prepared the following substrates: a forked duplex with both arms single stranded (splayed arm); a forked duplex with the 3′-arm single stranded and the 5′-arm double stranded (3′-flap duplex); a forked duplex with the 3′-arm double stranded and the 5′-arm single stranded (5′-flap duplex) and a forked duplex with both arms double stranded. Earlier studies revealed that WRN could unwind efficiently all these structures, indicating that it does not require the 3′-arm to be single stranded for loading at the fork (40). We found that MutSα and MutSβ strongly stimulated the WRN-mediated unwinding of the splayed arm and the 3′-flap duplex, but had no significant effect on the unwinding of the 5′-flap duplex and the fully double stranded fork (Figure 8). We also tested these proteins for the ability to stimulate the helicase activity of WRN on 3′-ssDNA-tailed duplex, which is normally a poor substrate for WRN (40). We found that neither MutSα nor MutSβ could activate WRN for unwinding of this partial DNA duplex (data not shown). Interestingly, the 3′-tail duplex resulting from unwinding of the 3′-flap structure was unwound by WRN efficiently. This discrepancy can result from the fact that WRN exists as an oligomeric structure, which would facilitate loading of a second molecule of WRN on the 3′-ssDNA generated by unwinding of the duplex ahead of the fork.

Collectively, these data indicate that MutSα and MutSβ require a forked DNA structure with 3′-ss DNA at the junction to stimulate WRN-mediated DNA unwinding.

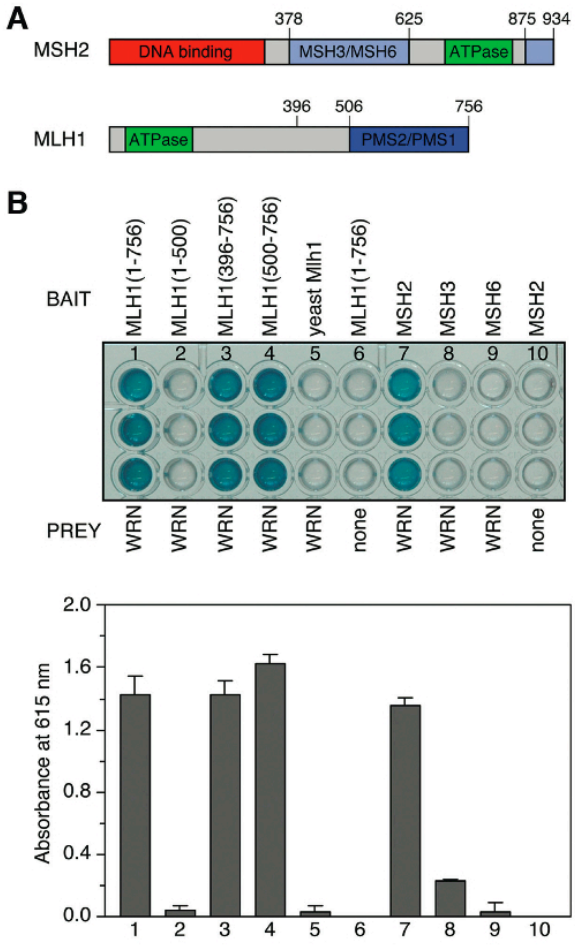

Figure 4. Interaction between WRN and MMR proteins in yeast two-hybrid system. (**A**) Domain organizations of the MSH2 and MLH1 proteins. The numbers refer to the amino acid sequence. (**B**) Quantitative yeast two-hybrid assay. The S. cerevisiae strain L40 harboring a pACT2 vector expressing the full-length WRN fused to the GAL4 activation domain was transformed with pBTM116 vectors encoding the indicated MMR proteins fused to LexA (MLH1 and its deletion derivatives, MSH3 and MSH6) or Gal4 (MSH2) DNA binding domains. Clones containing both plasmids were subjected to β-galactosidase assay on an ELISA micro-plate using 5-bromo-4-chloro-3-indolyl-β-D-galactopyranoside (X-gal) as a substrate. Top panel: An ELISA plate after a 30-min incubation at room temperature. Bottom panel: Graph showing absorbance at 615 nm measured in individual wells after 35 min, which is a measure of β-gal activity. The values represent the mean of three independent experiments.

DISCUSSION

Although WRN has been implicated in a number of DNA repair processes, the exact DNA transactions mediated by this helicase/exonuclease in the cell remain elusive. Here we show that WRN interacts physically with proteins that are involved in the initiation of MMR and the rejection of recombination between divergent sequences. Most importantly, our experiments revealed that MutSα and MutSβ can stimulate the helicase activity of WRN on forked DNA structures with a 3′-ss arm that resemble intermediates of single-strand annealing pathways of HR. In addition, we found that a single G/T mismatch located ahead of the fork junction increased the efficiency of the MutSα-dependent unwinding by WRN. These data are consistent with a model in which the MMR initiation factors prevent homeologous recombination by activating a DNA helicase for unwinding of recombination intermediates containing mismatches. This model was proposed earlier on the basis of results of *in vivo* heteroduplex rejection assays with yeast *msh2* and *sgs1* mutants (27,28). It is possible that MutSα and MutSβ bind to mismatches formed after pairing of sequences of imperfect homology and, following ATP binding, are converted into a DNA sliding clamp as proposed in the case of the MMR pathway (42). When the clamp encounters the junction between the heteroduplex and the non-homologous 3′-ss tail, it binds stably to it and recruits a DNA helicase to disrupt the joined DNA molecule. In agreement with this hypothesis, it has been demonstrated that yeast MutSβ specifically binds to forked DNA structures containing 3′- ssDNA making contacts with the sequences at the ds–ss junction (43). These studies also revealed that MutSβ holds the junction in an altered, perhaps more rigid, conformation (43). Such structural changes could facilitate the loading of the WRN helicase on the 3′- ssDNA at the junction, which is a prerequisite for duplex unwinding to occur. However, it should be noted that the MutSα-activated unwinding of a 3′-flap duplex by WRN displayed only a moderate dependence on mismatches. It is therefore possible that hereroduplex rejection *in vivo* involves some additional factors that ensure mismatch specificity of this transaction.

In our studies, we did not observe any significant modulation of WRN-mediated unwinding by MutLα, even in the presence of MutSα or MutSβ. In agreement with this finding, the yeast Mlh1 and Pms1 proteins have been shown to have only minor roles in the rejection of homeologous recombination relative to the contributions of Msh2 and Msh6 (27). Thus, it appears that the physical interaction between WRN and MutLα identified in this study has some other functional implication. Interestingly, MLH1 was shown to interact with various DNA repair factors including MRE11, BACH1, MBD4 and BLM (29,44–47). It is, therefore, possible that MLH1 plays a more general role in DNA repair processes.

A number of other functional implications for the observed interactions between WRN and the MMR factors can be discussed. Several lines of evidence suggest that WRN promotes replication of telomeric DNA by unwinding G-quadruplex structures that can readily form in G-rich telomeric DNA and impose a barrier for progression of DNA replication forks (9,48–50). Strikingly, human MutSα has been shown to bind efficiently to G-quadruplex DNA (51). Moreover, Msh2 deficiency in mice is associated with loss of telomeres and an elevated level of telomere end-to-end fusion, a phenotype similar to that manifested by WRN-deficient

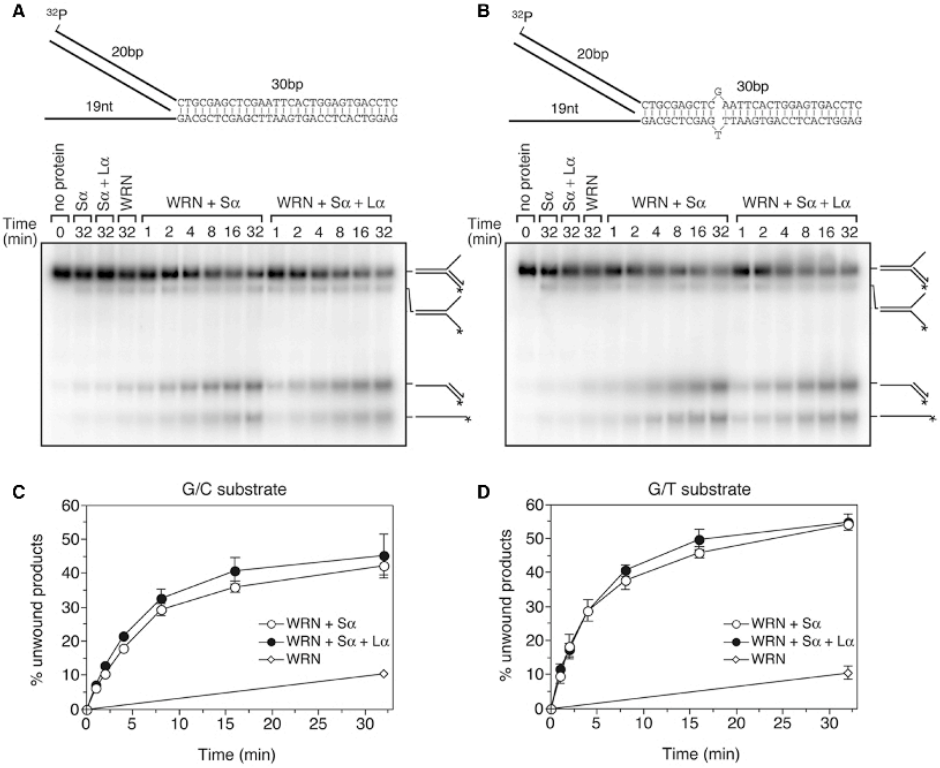

Figure 5. Kinetics of WRN-mediated unwinding of a 3′-flap DNA duplex in the presence of MutSα and MutLα. (**A**) Reactions with a homoduplex 3′ flap substrate. (**B**) Reactions with a 3′-flap duplex containing a G/T mismatch located 11 nucleotides ahead of the fork as indicated. (**C**) Quantification of the time course reactions in A. (**D**) Quantification of the time course reactions in B. All reactions contained 1 nM [^{32}P]DNA, 1 nM WRN and 8 nM MMR proteins as indicated. Aliquots at individual time points were analyzed by native PAGE followed by phosphorimaging and quantification as described in Materials and Methods section. Schemes of the substrate and the reaction products are shown on the right. The relative concentration of unwound products (3′-tailed duplex and free labeled oligonucleotide) is expressed as a percentage of total DNA.

cells (9,52). Thus, one can speculate that the MMR proteins can mediate recruitment of the WRN helicase to G-quadruplex structures formed at telomeres and hence facilitate their removal.

It has been shown that the human MutSβ and WRN are required along with PCNA, RPA and ERCC1-XPF for uncoupling of psoralen-induced inter-strand DNA crosslinks (ICLs) in cell-free extracts, suggesting a novel ICL-repair pathway in which MutSβ is essential for the recognition of ICLs, while the WRN helicase mediates unwinding of the DNA duplex adjacent to the lesion, which enables strand incision by ERCC1-XPF (53,54). Our finding that MutSβ physically interacts with WRN and stimulates its helicase activity brings further support for this model and suggests that MutSβ might recruit WRN to the ICL sites.

Earlier studies demonstrated that nuclear extracts from several fibroblastoid cell lines derived from WS patients were deficient in repair of base–base mismatches and insertion/deletion loops, suggesting that WRN could have a role in MMR (55). However, it is not certain that the MMR-deficiency of these extracts was caused solely by WRN deficiency because complementation experiments with recombinant WRN protein were not performed in this study. Moreover, in some cases, pairwise mixing of these extracts restored MMR proficiency, making the involvement of WRN in MMR rather questionable.

Recently, two other human RecQ homologs, namely RECQ1 and BLM, have been shown to interact physically and functionally with the MMR-initiation factors (29,31,47,56,57). As in the case of WRN, MutSα was found to stimulate RECQ1-mediated unwinding of a forked structure with a 3′-ss arm (56). In contrast, MutSα did not affect unwinding of forked DNA duplexes by BLM (31). Instead, MutSα was found to stimulate the ability of BLM to process Holliday junctions *in vitro* (57). Further studies will be needed to fully understand the molecular mechanisms by which the RecQ helicases and MMR factors work together to maintain genomic stability.

SUPPLEMENTARY DATA

Supplementary Data are available at NAR Online.

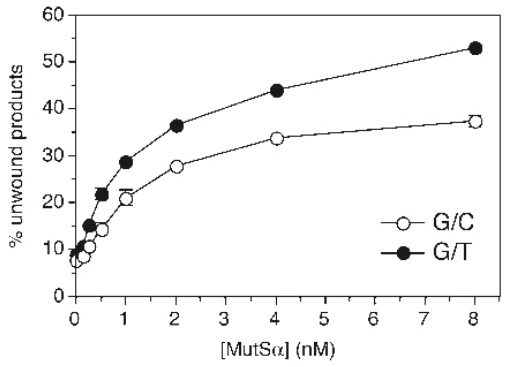

Figure 6. Helicase activity of WRN on 3′-flap duplexes with or without a G/T mismatch as a function of MutSα concentration. WRN and the DNA substrate were present at a concentration of 1 nM. The DNA substrates were the same as in Figure 5. Reactions were incubated for 30 min and analyzed by native PAGE followed by phosphorimaging as described in Materials and Methods section. The data points represent the mean of three independent experiments. The relative concentration of unwound products (3′-tailed duplex and free labeled oligonucleotide) is expressed as a percentage of total DNA.

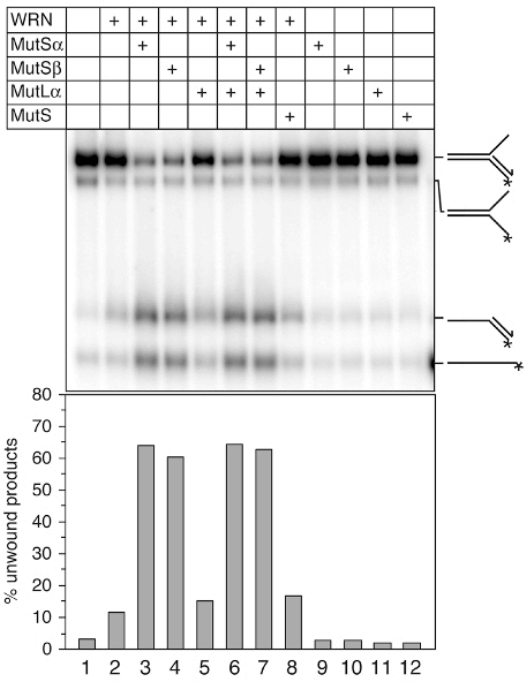

Figure 7. Effect of various MMR proteins on WRN-mediated unwinding of a 3′-flap DNA duplex. Helicase reactions contained 1 nM [^{32}P]DNA substrate and 2 nM WRN. The MMR proteins were present in a concentration of 8 nM as indicated. Reactions were incubated for 32 min and analyzed by native PAGE followed by phosphorimaging as described in Materials and Methods section (top panel). The relative concentration of unwound products (3′-tailed duplex and free labeled oligonucleotide) is expressed as a percentage of total DNA (bottom panel). Schemes of the substrate and the reaction products are shown on the right.

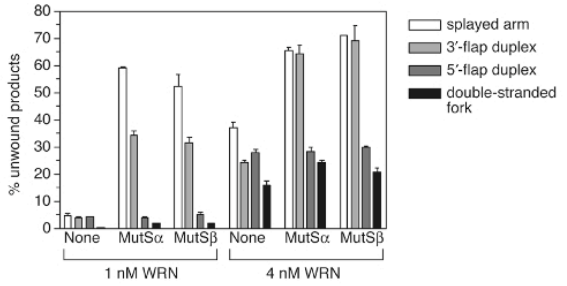

Figure 8. Stimulation of WRN-mediated unwinding of forked DNA structures by MutSα and MutSβ is dependent on the presence of 3′-single stranded DNA at the junction. Reactions with 1 nM splayed arm (white bars), 1 nM 3′-flap duplex (light gray bars), 1 nM 5′-flap duplex (dark gray bars) and 1 nM fully double-stranded fork duplex (black bars) contained 1 nM or 4 nM WRN and 8 nM MutSα or MutSβ as indicated. Reactions were incubated for 32 min and analyzed by native PAGE followed by phosphorimaging as described in Materials and Methods. The relative concentration of unwound products is expressed as a percentage of total DNA. The data points represent the mean of at least three independent experiments.

ACKNOWLEDGEMENTS

We thank Renjie Jiao for the construction of pACT2-WRN plasmid used in YTH assay, Peter Cejka for purified *E. coli* MutS protein and Lene Rasmussen for the plasmid pLJR105. We are also grateful to Josef Jiricny, Stefano Ferrari and David Lauterbach for comments on the manuscript. This work was supported by the Sassella and the Swiss National Science Foundations (Marie Heim-Vögtlin Grant Nr. PMPDA-102451 to N.S.). Funding to pay the Open Access publication charges for this article was provided by the Swiss National Science Foundation.

Conflict of interest statement. None declared.

REFERENCES

1. Martin,G.M. (1982) Syndromes of accelerated aging. *Natl. Cancer Inst. Monogr.*, **60**, 241–247.
2. Yu,C.E., Oshima,J., Fu,Y.H., Wijsman,E.M., Hisama,F., Alisch,R., Matthews,S., Nakura,J., Miki,T. *et al.* (1996) Positional cloning of the Werner's syndrome gene. *Science*, **272**, 258–262.
3. Gray,M.D., Shen,J.C., Kamath-Loeb,A.S., Blank,A., Sopher,B.L., Martin,G.M., Oshima,J. and Loeb,L.A. (1997) The Werner syndrome protein is a DNA helicase. *Nat. Genet.*, **17**, 100–103.
4. Huang,S., Li,B., Gray,M.D., Oshima,J., Mian,I.S. and Campisi,J. (1998) The premature ageing syndrome protein, WRN, is a 3′—>5′ exonuclease. *Nat. Genet.*, **20**, 114–116.
5. Kamath-Loeb,A.S., Shen,J.C., Loeb,L.A. and Fry,M. (1998) Werner syndrome protein. II. Characterization of the integral 3′ —> 5′ DNA exonuclease. *J. Biol. Chem.*, **273**, 34145–34150.
6. Fujiwara,Y., Higashikawa,T. and Tatsumi,M. (1977) A retarded rate of DNA replication and normal level of DNA repair in Werner's syndrome fibroblasts in culture. *J. Cell. Physiol.*, **92**, 365–374.
7. Rodriguez-Lopez,A.M., Jackson,D.A., Iborra,F. and Cox,L.S. (2002) Asymmetry of DNA replication fork progression in Werner's syndrome. *Aging Cell*, **1**, 30–39.
8. Saintigny,Y., Makienko,K., Swanson,C., Emond,M.J. and Monnat,R.J.Jr. (2002) Homologous recombination resolution defect in Werner syndrome. *Mol. Cell. Biol.*, **22**, 6971–6978.

9. Crabbe,L., Verdun,R.E., Haggblom,C.I. and Karlseder,J. (2004) Defective telomere lagging strand synthesis in cells lacking WRN helicase activity. *Science*, **306**, 1951–1953.
10. Fukuchi,K., Martin,G.M. and Monnat,R.J.Jr. (1989) Mutator phenotype of Werner syndrome is characterized by extensive deletions. *Proc. Natl Acad. Sci. USA*, **86**, 5893–5897.
11. Salk,D., Au,K., Hoehn,H. and Martin,G.M. (1985) Cytogenetic aspects of Werner syndrome. *Adv. Exp. Med. Biol.*, **190**, 541–546.
12. Salk,D., Au,K., Hoehn,H. and Martin,G.M. (1981) Cytogenetics of Werner's syndrome cultured skin fibroblasts: variegated translocation mosaicism. *Cytogenet. Cell. Genet.*, **30**, 92–107.
13. Crabbe,L., Jauch,A., Naeger,C.M., Holtgreve-Grez,H. and Karlseder,J. (2007) Telomere dysfunction as a cause of genomic instability in Werner syndrome. *Proc. Natl Acad. Sci. USA*, **104**, 2205–2210.
14. Poot,M., Gollahon,K.A., Emond,M.J., Silber,J.R. and Rabinovitch,P.S. (2002) Werner syndrome diploid fibroblasts are sensitive to 4-nitroquinoline-N-oxide and 8-methoxypsoralen: implications for the disease phenotype. *FASEB J.*, **16**, 757–758.
15. Poot,M., Yom,J.S., Whang,S.H., Kato,J.T., Gollahon,K.A. and Rabinovitch,P.S. (2001) Werner syndrome cells are sensitive to DNA cross-linking drugs. *FASEB J.*, **15**, 1224–1226.
16. Poot,M., Gollahon,K.A. and Rabinovitch,P.S. (1999) Werner syndrome lymphoblastoid cells are sensitive to camptothecin-induced apoptosis in S-phase. *Hum. Genet.*, **104**, 10–14.
17. Lan,L., Nakajima,S., Komatsu,K., Nussenzweig,A., Shimamoto,A., Oshima,J. and Yasui,A. (2005) Accumulation of Werner protein at DNA double-strand breaks in human cells. *J. Cell Sci.*, **118**, 4153–4162.
18. Cheng,W.H., von Kobbe,C., Opresko,P.L., Arthur,L.M., Komatsu,K., Seidman,M.M., Carney,J.P. and Bohr,V.A. (2004) Linkage between Werner syndrome protein and the Mre11 complex via Nbs1. *J. Biol. Chem.*, **279**, 21169–21176.
19. Cooper,M.P., Machwe,A., Orren,D.K., Brosh,R.M., Ramsden,D. and Bohr,V.A. (2000) Ku complex interacts with and stimulates the Werner protein. *Genes Dev.*, **14**, 907–912.
20. Baynton,K., Otterlei,M., Bjoras,M., von Kobbe,C., Bohr,V.A. and Seeberg,E. (2003) WRN interacts physically and functionally with the recombination mediator protein RAD52. *J. Biol. Chem.*, **278**, 36476–36486.
21. Karmakar,P., Piotrowski,J., Brosh,R.M.Jr, Sommers,J.A., Miller,S.P., Cheng,W.H., Snowden,C.M., Ramsden,D.A. and Bohr,V.A. (2002) Werner protein is a target of DNA-dependent protein kinase *in vivo* and *in vitro*, and its catalytic activities are regulated by phosphorylation. *J. Biol. Chem.*, **277**, 18291–18302.
22. Kunkel,T.A. and Erie,D.A. (2005) DNA mismatch repair. *Annu. Rev. Biochem.*, **74**, 681–710.
23. Jiricny,J. (2006) The multifaceted mismatch-repair system. *Nat. Rev. Mol. Cell. Biol.*, **7**, 335–346.
24. Jiricny,J. and Marra,G. (2003) DNA repair defects in colon cancer. *Curr. Opin. Genet. Dev.*, **13**, 61–69.
25. Kadyrov,F.A., Dzantiev,L., Constantin,N. and Modrich,P. (2006) Endonucleolytic function of MutLα in human mismatch repair. *Cell*, **126**, 297–308.
26. Myung,K., Datta,A., Chen,C. and Kolodner,R.D. (2001) SGS1, the *Saccharomyces cerevisiae* homologue of BLM and WRN, suppresses genome instability and homologous recombination. *Nat. Genet.*, **27**, 113–116.
27. Sugawara,N., Goldfarb,T., Studamire,B., Alani,E. and Haber,J.E. (2004) Heteroduplex rejection during single-strand annealing requires Sgs1 helicase and mismatch repair proteins Msh2 and Msh6 but not Pms1. *Proc. Natl Acad. Sci. USA*, **101**, 9315–9320.
28. Goldfarb,T. and Alani,E. (2005) Distinct roles for the *Saccharomyces cerevisiae* mismatch repair proteins in heteroduplex rejection, mismatch repair and nonhomologous tail removal. *Genetics*, **169**, 563–574.
29. Pedrazzi,G., Perrera,C., Blaser,H., Kuster,P., Marra,G., Davies,S.L., Ryu,G.H., Freire,R., Hickson,I.D. *et al.* (2001) Direct association of Bloom's syndrome gene product with the human mismatch repair protein MLH1. *Nucleic Acids Res.*, **29**, 4378–4386.
30. Rasmussen,L.J., Rasmussen,M., Lee,B., Rasmussen,A.K., Wilson,D.M.3rd, Nielsen,F.C. and Bisgaard,H.C. (2000) Identification of factors interacting with hMSH2 in the fetal liver utilizing the yeast two-hybrid system. *In vivo* interaction through the C-terminal domains of hEXO1 and hMSH2 and comparative expression analysis. *Mutat. Res.*, **460**, 41–52.
31. Pedrazzi,G., Bachrati,C.Z., Selak,N., Studer,I., Petkovic,M., Hickson,I.D., Jiricny,J. and Stagljar,I. (2003) The Bloom's syndrome helicase interacts directly with the human DNA mismatch repair protein hMSH6. *Biol Chem.*, **384**, 1155–1164.
32. Orren,D.K., Brosh,R.M.Jr, Nehlin,J.O., Machwe,A., Gray,M.D. and Bohr,V.A. (1999) Enzymatic and DNA binding properties of purified WRN protein: high affinity binding to single-stranded DNA but not to DNA damage induced by 4NQO. *Nucleic Acids Res.*, **27**, 3557–3566.
33. Palombo,F., Iaccarino,I., Nakajima,E., Ikejima,M., Shimada,T. and Jiricny,J. (1996) hMutSβ, a heterodimer of hMSH2 and hMSH3, binds to insertion/deletion loops in DNA. *Curr. Biol.*, **6**, 1181–1184.
34. Raschle,M., Marra,G., Nystrom-Lahti,M., Schar,P. and Jiricny,J. (1999) Identification of hMutLβ, a heterodimer of hMLH1 and hPMS1. *J. Biol. Chem.*, **274**, 32368–32375.
35. Lamers,M.H., Perrakis,A., Enzlin,J.H., Winterwerp,H.H., de Wind,N. and Sixma,T.K. (2000) The crystal structure of DNA mismatch repair protein MutS binding to a G x T mismatch. *Nature*, **407**, 711–717.
36. Brosh,R.M.Jr, von Kobbe,C., Sommers,J.A., Karmakar,P., Opresko,P.L., Piotrowski,J., Dianova,I., Dianov,G.L. and Bohr,V.A. (2001) Werner syndrome protein interacts with human flap endonuclease 1 and stimulates its cleavage activity. *EMBO J.*, **20**, 5791–5801.
37. Mockli,N. and Auerbach,D. (2004) Quantitative β-galactosidase assay suitable for high-throughput applications in the yeast two-hybrid system. *Biotechniques*, **36**, 872–876.
38. Janscak,P., Garcia,P.L., Hamburger,F., Makuta,Y., Shiraishi,K., Imai,Y., Ikeda,H. and Bickle,T.A. (2003) Caracterization and mutational analysis of the RecQ core of the bloom syndrome protein. *J. Mol. Biol.*, **330**, 29–42.
39. Lee,J.W., Harrigan,J., Opresko,P.L. and Bohr,V.A. (2005) Pathways and functions of the Werner syndrome protein. *Mech. Ageing Dev.*, **126**, 79–86.
40. Brosh,R.M.Jr, Waheed,J. and Sommers,J.A. (2002) Biochemical characterization of the DNA substrate specificity of Werner syndrome helicase. *J. Biol. Chem.*, **277**, 23236–23245.
41. Blackwell,L.J., Wang,S. and Modrich,P. (2001) DNA chain length dependence of formation and dynamics of hMutSα.hMutLα.heteroduplex complexes. *J. Biol. Chem.*, **276**, 33233–33240.
42. Gradia,S., Subramanian,D., Wilson,T., Acharya,S., Makhov,A., Griffith,J. and Fishel,R. (1999) hMSH2-hMSH6 forms a hydrolysis-independent sliding clamp on mismatched DNA. *Mol. Cell.*, **3**, 255–261.
43. Surtees,J.A. and Alani,E. (2006) Mismatch repair factor MSH2-MSH3 binds and alters the conformation of branched DNA structures predicted to form during genetic recombination. *J. Mol. Biol.*, **360**, 523–536.
44. Her,C., Vo,A.T. and Wu,X. (2002) Evidence for a direct association of hMRE11 with the human mismatch repair protein hMLH1. *DNA Repair (Amst.)*, **1**, 719–729.
45. Cannavo,E., Gerrits,B., Marra,G., Schlapbach,R. and Jiricny,J. (2007) Characterization of the interactome of the human MutL homologues MLH1, PMS1, and PMS2. *J. Biol. Chem.*, **282**, 2976–2986.
46. Bellacosa,A., Cicchillitti,L., Schepis,F., Riccio,A., Yeung,A.T., Matsumoto,Y., Golemis,E.A., Genuardi,M. and Neri,G. (1999) MED1, a novel human methyl-CpG-binding endonuclease, interacts with DNA mismatch repair protein MLH1. *Proc. Natl Acad. Sci. USA*, **96**, 3969–3974.
47. Langland,G., Kordich,J., Creaney,J., Goss,K.H., Lillard-Wetherell,K., Bebenek,K., Kunkel,T.A. and Groden,J. (2001) The Bloom's syndrome protein (BLM) interacts with MLH1 but is not required for DNA mismatch repair. *J. Biol. Chem.*, **276**, 30031–30035.
48. Kamath-Loeb,A.S., Loeb,L.A., Johansson,E., Burgers,P.M. and Fry,M. (2001) Interactions between the Werner syndrome helicase and DNA polymerase delta specifically facilitate copying of tetraplex and hairpin structures of the d(CGG)n trinucleotide repeat sequence. *J. Biol. Chem.*, **276**, 16439–16446.

49. Mohaghegh,P., Karow,J.K., Brosh,R.M.Jr, Bohr,V.A. and Hickson,I.D. (2001) The Bloom's and Werner's syndrome proteins are DNA structure-specific helicases. *Nucleic Acids Res.*, **29**, 2843–2849.
50. Vorlickova,M., Chladkova,J., Kejnovska,I., Fialova,M. and Kypr,J. (2005) Guanine tetraplex topology of human telomere DNA is governed by the number of (TTAGGG) repeats. *Nucleic Acids Res.*, **33**, 5851–5860.
51. Larson,E.D., Duquette,M.L., Cummings,W.J., Streiff,R.J. and Maizels,N. (2005) MutSα binds to and promotes synapsis of transcriptionally activated immunoglobulin switch regions. *Curr. Biol.*, **15**, 470–474.
52. Campbell,M.R., Wang,Y., Andrew,S.E. and Liu,Y. (2006) Msh2 deficiency leads to chromosomal abnormalities, centrosome amplification, and telomere capping defect. *Oncogene*, **25**, 2531–2536.
53. Zhang,N., Kaur,R., Lu,X., Shen,X., Li,L. and Legerski,R.J. (2005) The Pso4 mRNA splicing and DNA repair complex interacts with WRN for processing of DNA interstrand cross-links. *J. Biol. Chem.*, **280**, 40559–40567.
54. Zhang,N., Lu,X., Zhang,X., Peterson,C.A. and Legerski,R.J. (2002) hMutSbeta is required for the recognition and uncoupling of psoralen interstrand cross-links *in vitro*. *Mol. Cell. Biol.*, **22**, 2388–2397.
55. Bennett,S.E., Umar,A., Oshima,J., Monnat,R.J.Jr. and Kunkel,T.A. (1997) Mismatch repair in extracts of Werner syndrome cell lines. *Cancer Res.*, **57**, 2956–2960.
56. Doherty,K.M., Sharma,S., Uzdilla,L.A., Wilson,T.M., Cui,S., Vindigni,A. and Brosh,R.M.Jr. (2005) RECQ1 helicase interacts with human mismatch repair factors that regulate genetic recombination. *J. Biol. Chem.*, **280**, 28085–28094.
57. Yang,Q., Zhang,R., Wang,X.W., Linke,S.P., Sengupta,S., Hickson,I.D., Pedrazzi,G., Perrera,C., Stagljar,I. *et al.* (2004) The mismatch DNA repair heterodimer, hMSH2/6, regulates BLM helicase. *Oncogene*, **23**, 3749–3756.

Supplementary Figure S1

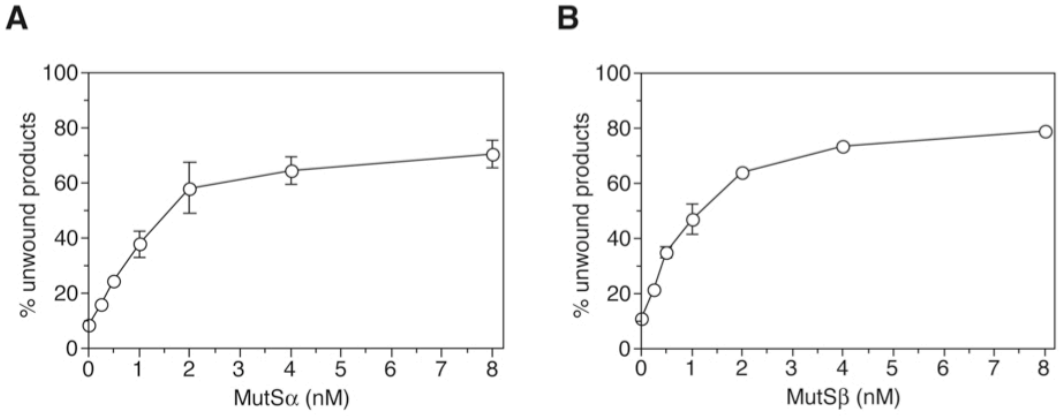

Figure S1. Dependence of WRN-mediated unwinding of a 3'-flap DNA duplex on MutSα (A) and MutSβ concentration. WRN and the DNA substrate were present at a concentration of 2 nM and 1 nM, respectively. Reactions were incubated for 30 minutes and analyzed by native PAGE followed by phosphorimaging as described in Materials and Methods. The data points represent the mean of three independent experiments. The relative concentration of unwound products (3'-tailed duplex and free labeled oligonucleotide) is expressed as a percentage of total DNA.

Supplementary Figure S2

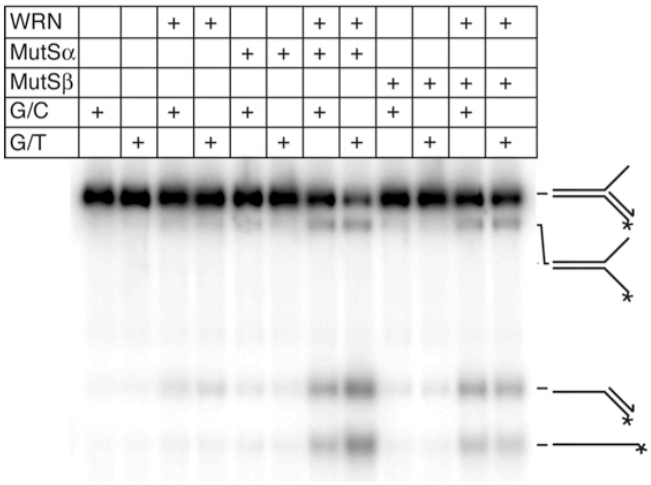

Figure S1. WRN-mediated unwinding of a 3'-flap DNA duplex, without or with a G/T mismatch, in the presence of 2 nM MutSα or 2 nM MutSβ. WRN and DNA substrates were present at a concentration of 1 nM.

Supplementary Table 1. Oligonucleotides and schemes of DNA substrates

f11-20 (50mer)	TCAAAGTCACGACCTAGACACTGCGAGCTCGAATTCACTGGAGTGACCTC
f12 (49mer)	GAGGTCACTCCAGTGAATTCGAGCTCGCAGCAATGAGCACATACCTAGT
f13 (19mer)	ACTAGGTATGTGCTCATTG
f14 (20mer)	TGTCTAGGTCGTGACTTTGA
f12(G/T) (49mer)	GAGGTCACTCCAGTGAATT**T**GAGCTCGCAGCAATGAGCACATACCTAGT
Splayed arm	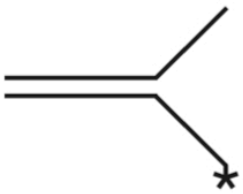 f11-20 + f12
3'-flap duplex	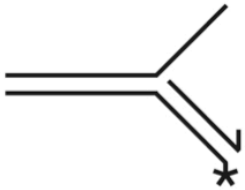 f11-20 + f12 + f14
3'-flap duplex	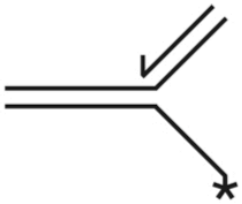 f11-20 + f12 + f13
Fully double-stranded Duplex	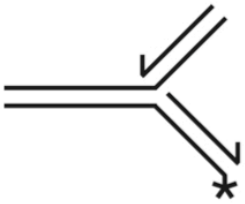 f11-20 + f12 + f13 + f14

f11-20 is complementary to the 5'-half of f12 or f12(G/T). f13 is fully complementary to the 3'-half of f12. f14 is fully complementary to the 5'-half of f11-20. The position of the T residue introducing a G/T mismatch after annealing of f12(G/T) to f11-20 is highlighted. The polarity of the leading and lagging oligonucleotides is indicated by arrows (5' – 3'). The position of ^{32}P-label at the 5'-end of f11-20 is indicated by asterisk.

Supplementary Table 2 . Initial rates and the extent of unwinding of reactions in Figure 5

Reaction Composition	Unwinding velocity	Extent of unwinding (%)
WRN + MutSα	1.0	42.2
WRN + MutSα + MutLα	1.2	45.2
WRN + MutSα	1.7	54.3
WRN + MutSα + MutLα	1.7	54.8

The data points collected within the first two minutes of the reaction were used for calculation of the initial unwinding velocity. The data were analyzed by linear regression method using GraphPad Prism software. The slope values were divided by the value obtained for the reaction of G/C substrate with WRN and MutSα. Extent of unwinding represents data from the 32-minute time point.

8. Acknowledgements

First, I thank my advisor and supervisor Dr. Pavel Janscak, for his continuous support during my doctorate studies. Also a special thanks goes to him for getting me to IMCR. He showed me different ways to approach a research problem and the need to be persistent to accomplish any goal.

Next, I would like to convey my sincere gratitude to Prof. Dr. Josef Jiricny for being the doctor father of my PhD. I always feel that I am lucky to do my PhD in his institute. And I am very very proud of his trust on me.

Besides my advisors, I would like to thank Prof. Dr. Michael Hengartner and Prof. Dr. Silvio Hemmi for the recognition of my master's degree that is required for the admission of the PhD at the University of Zürich.

I also thank Prof. Dr. Ueli Hübscher and Prof. Dr. Primo Schär for their presence in my thesis committee.

I would like to thank all the past and present members of Pavel's lab (Patrick, Nurten, Tracy, Sybille, Tobi, Dani, Javier, Boris and Igor), for their friendship, encouragement and constructive scientific discussions. My special thanks to Patrick, who helped me survive the initial bad phase in the lab, and for accompanying me frequently for a dinner to my favourite Indian restaurant. Nurten and Tracy, thanks for all the good times that we spent together. Sybille, Tobi and Dani, danke vielmal for the German translations. Javi, thanks for your creative scientific inputs. Boris, thanks for the chocolates and for your help with laser irradiation.

I would also like to thank all the past and present members of IMCR. My special thanks and love to Ludovic, Petr Cejka, Elda, Jacob, Nina, Betta, Vinh, Stefano, Mahmoud and Jawad.

And, many many thanks to all my Indian friends (past and present) here in Switzerland (Ajit, Sarath, Srini, Praveen, Mami, Isai, Mini, Naresh, Payal, Prasanna, Annu, Anshu, Gopi, Amit, Partho, Farooq, Arnab, Sabari, Sunil, Sashi, Shravan, Pawani, Alok and Ashok) for all the good times that we spent together. I would also like to specially thank Bala, Ilavarasi and Aishu for the good times that we spent together.

Last, but not least, I thank all my family people for supporting me throughout my PhD. Very very special thanks to my in-laws for always being a great moral support to

9. *Curriculum Vitae*

Personal Information

First name	Kanagaraj
Last name	Radhakrishnan
Address	Oerlikonerstrasse 37, 8057 Zürich
Date of birth	30th May 1979
Place of birth	Tamilnadu, India
Nationality	Indian
E-mail	rajsss@imcr.uzh.ch
Contact number	+41-(0)78-6043762

Scientific Education and Research Experiences

Since April 2004 -	Doctoral thesis in the research group of Dr. Pavel Janscak at the Institute of Molecular of Cancer Research (IMCR) at the University of Zürich, Switzerland on the roles of the human RECQ DNA helicases in DNA repair. Responsible member of faculty: Prof. Dr. Josef Jiricny.
July 2002 – March 2004	Junior Research Fellow in the research group of Prof. Dr. Valakunja Nagaraja at the Department of Microbiology and Cell Biology at the Indian Institute of Science, Bangalore, India. Worked on the research project – Kinetic studies on the KpnI restriction endonuclease, an HNH superfamily REase.
September 2001 – March 2002	Junior Research Fellow in the research group of Dr. Sumantra Chattarji at the National Institute of Biological Sciences, Bangalore, India. Worked on the research project – Stress induces cell loss in hippocampus.
March 2001 – August 2001	Postgraduate thesis under the guidance of Prof. Dr. S. Shanmugasundaram at the Madurai Kamaraj Univeristy, India on the cloning, overexpression and purification of the *E.coli* exonuclease III.

Education

1999-2001	Postgraduate course, Master of Science in Microbial Gene Technology at the Madurai Kamaraj University, Madurai, India.
1996-1999	Undergraduate course, Bachelor of Science in Microbiology at the Madras University, Chennai, India.
1992-1996	Higher Secondary Education, Kanchipuram, Tamilnadu, India.
1984-1992	Primary and Secondary Education, Kanchipuram, Tamilnadu, India.

10. List of publications

Kanagaraj R, Saydam N, Garcia PL, Zheng L, Janscak P. "Human RECQ5β helicase promotes strand exchange on synthetic DNA structures resembling a stalled replication fork" *Nucleic Acids Res*. 2006; 34(18): 5217-31.

Saravanan M, Vasu K, **Kanagaraj R**, Rao DN, Nagaraja V. "R.KpnI, an HNH superfamily REase, exhibits differential discrimination at non-canonical sequences in the presence of Ca2+ and Mg2+" *Nucleic Acids Res*. 2007; 35 (8): 2777-86.

Saydam N*, **Kanagaraj R***, Dietschy T*, Garcia PL, Peña-Diaz J, Shevelev I, Stagljar I, Janscak P. "Physical and functional interactions between Werner syndrome helicase and mismatch-repair initiation factors" *Nucleic Acids Res*. 2007; 35 (17): 5706-16. * - Joint first authors.

Ren H, Dou SX, Zhang XD, Wang PY, **Kanagaraj R**, Liu JL, Janscak P, Hu JS, Xi XG. "The zinc-binding motif of human RECQ5beta suppresses the intrinsic strand-annealing activity of its DExH helicase domain and is essential for the helicase activity of the enzyme" *Biochem J*. 2008; 412 (3): 425-33.

Yodh JG, Stevens BC, **Kanagaraj R**, Janscak P, Ha T. "Single-molecule study of Bloom syndrome helicase reveals repetitive unwinding via strand-switching" Manuscript submitted.

Zheng L, **Kanagaraj R**, Mihaljevic B, Schwendener S, Janscak P. "The MRE11/RAD50/NBS1 complex links RECQ5 helicase to sites of DNA damage" Manuscript to be submitted.

11. Abstracts presented in scientific meetings

"***Characterization of the helicase activity of Human RECQ5β protein***", 7th Charles Rodolphe Brupbacher Symposium – Advances in Oncology: From Model Systems to the Clinic, 16-19 March 2005, Zürich, Switzerland. Radhakrishnan Kanagaraj, Patrick L. Garcia, Lu Zheng and Pavel Janscak. **Poster presented by Radhakrishnan Kanagaraj.**

"***Role of human RECQ5β protein in the maintenance of genomic stability***" Benzon Symposium No. 52 - Cellular responses to DNA damage, 22-25 August 2005, Copenhagen, Denmark. Radhakrishnan Kanagaraj, Patrick L. Garcia, Lu Zheng and Pavel Janscak. **Poster presented by Radhakrishnan Kanagaraj.**

"***Human RECQ5β helicase localizes to sites of DNA replication and promotes fork regression***" 2nd Swiss Meeting on Genome Stability - DNA Dynamics and Epigenetics, 12-14 October 2005, Zentenhaus, Uetendorf, Switzerland. Radhakrishnan Kanagaraj, Nurten Saydam, Patrick L. Garcia, Lu Zheng and Pavel Janscak. **Poster presented by Radhakrishnan Kanagaraj.**

"***Role of RECQ5β in the maintenance of genomic stability***" RRR (*R*eplication, *R*ecombination and *R*epair) Club, 20th October 2005, IMCR, Zürich, Switzerland. **Talk presented by Radhakrishnan Kanagaraj**.

"***RecQ helicases: Caretakers of the genome***" 3rd CALZONE meeting ("Colloquium for Ambitious Life Scientists in Zurich: Opportunities for Networking and Exchanges") conducted by Young European Biotech Network, 6th June 2006, Zürich, Switzerland. **Talk presented by Radhakrishnan Kanagaraj.**

"***RECQ5β helicase and maintenance of genomic stability***" 2nd Cancer Research Retreat conducted by Cancer Network Zurich, 01-03 September 2006, Monte Verita, Ascona, Switzerland. **Talk presented by Radhakrishnan Kanagaraj.**

"***Genomic Instability and Cancer: Insights from Analysis of the Human RECQ5β Helicase***", 8th Charles Rodolphe Brupbacher Symposium – Cancer Immunosurveillance & Immunotherapy, 14-16 March 2007, Zürich, Switzerland. Radhakrishnan Kanagaraj, Lu Zheng, Sybille Schwendener, Daniela Huehn and Pavel Janscak. **Poster presented by Radhakrishnan Kanagaraj.**

"***Exploring the role of human RECQ5β helicase upon replication fork arrest***" Gordon Research conference – Genetic Toxicology meeting, 29th July - 03 August 2007, Oxford, United Kingdom.

Radhakrishnan Kanagaraj, Lu Zheng, Sybille Schwendener, Daniela Huehn and Pavel Janscak. **Poster presented by Radhakrishnan Kanagaraj.**

"***Functional Interplay between Werner syndrome helicase and Mismatch repair proteins***" 3rd Swiss Meeting on Genome Stability - DNA Dynamics and Epigenetics, 03-05 October 2005, Zentenhaus, Uetendorf, Switzerland. **Talk presented by Radhakrishnan Kanagaraj.**